

University of Windsor

Scholarship at UWindor

Electronic Theses and Dissertations

Theses, Dissertations, and Major Papers

10-5-2017

Development of Mg Alloy AM60-based Hybrid Nano-Composites Reinforced with Nano Al₂O₃ or AlN Particles and Micron Al₂O₃ Fibres

Junxiang Zhou
University of Windsor

Follow this and additional works at: <https://scholar.uwindsor.ca/etd>

Recommended Citation

Zhou, Junxiang, "Development of Mg Alloy AM60-based Hybrid Nano-Composites Reinforced with Nano Al₂O₃ or AlN Particles and Micron Al₂O₃ Fibres" (2017). *Electronic Theses and Dissertations*. 7312. <https://scholar.uwindsor.ca/etd/7312>

This online database contains the full-text of PhD dissertations and Masters' theses of University of Windsor students from 1954 forward. These documents are made available for personal study and research purposes only, in accordance with the Canadian Copyright Act and the Creative Commons license—CC BY-NC-ND (Attribution, Non-Commercial, No Derivative Works). Under this license, works must always be attributed to the copyright holder (original author), cannot be used for any commercial purposes, and may not be altered. Any other use would require the permission of the copyright holder. Students may inquire about withdrawing their dissertation and/or thesis from this database. For additional inquiries, please contact the repository administrator via email (scholarship@uwindsor.ca) or by telephone at 519-253-3000ext. 3208.

**Development of Mg Alloy AM60-based Hybrid Nano-Composites Reinforced
with Nano Al₂O₃ or AlN Particles and Micron Al₂O₃ Fibres**

By

Junxiang Zhou

A Thesis

Submitted to the Faculty of Graduate Studies

Through the Department of Mechanical, Automotive and Materials Engineering

In Partial Fulfillment of the Requirements for

The Degree of Master of Applied Science

At the University of Windsor

Windsor, Ontario, Canada

2017

© 2017 Junxiang Zhou

**Development of Mg Alloy AM60-based Hybrid Nano-Composites Reinforced
with Nano Al₂O₃ or AlN Particles and Micron Al₂O₃ Fibres**

By

Junxiang Zhou

APPROVED BY:

T. Bolisetti

Department of Civil and Environmental Engineering

R. Riahi

Department of Mechanical, Automotive and Materials Engineering

H. Hu, Advisor

Department of Mechanical, Automotive and Materials Engineering

September 12, 2017

DECLARATION OF CO-AUTHORSHIP / PREVIOUS PUBLICATION

I. Co-Authorship

I hereby declare that this thesis incorporates material that is result of joint research. In all cases, the key ideas, primary contributions, experimental designs, data analysis and interpretation, were performed by the author and Dr. H. Hu as advisor. Chapter 3 was co-authored with Xuezhi Zhang, Li Fang. Xuezhi Zhang and Li Fang both contributed in bulk samples preparations. Chapter 4 and 5 were co-authored with Luyang Ren, Xingyu Geng, and Li Fang. Luyang Ren, Xingyu Geng, and Li Fang all contributed to bulk samples preparations. I certify that, with the above qualification, this dissertation, and the research to which it refers, is the product of my own work.

I am aware of the University of Windsor Senate Policy on Authorship and I certify that I have properly acknowledged the contribution of other researchers to my thesis, and have obtained written permission from each of the co-author(s) to include the above material(s) in my thesis.

I certify that, with the above qualification, this thesis, and the research to which it refers, is the product of my own work.

II. Previous Publication

This thesis includes 3 original papers that have been previously published/submitted for publication in peer reviewed journals, as follows:

Thesis Chapter	Publication title/full citation	Publication status*
Chapter 3	Junxiang Zhou, Xuezhi Zhang, Li Fang, Henry Hu, Processing and properties of as-cast magnesium AM60-based composite containing alumina nano particles and micron fibres, Magnesium Technology 2017, Part of the series The Minerals, Metals & Materials Series, 573-578, 2017 Annual Meeting & Exhibition, February 26- March 2, 2017, San Diego, CA, USA.	Published
Chapter 4	Junxiang Zhou, Luyang Ren, Xinyu Geng, Li Fang and Henry Hu, As-cast Magnesium AM60-Based Hybrid Nanocomposite Containing Alumina Fibres and Nanoparticles: Microstructure and Tensile Behavior, Materials Science & Engineering A, August, 2017	Revision Requested
Chapter 5	Junxiang Zhou, Luyang Ren, Xinyu Geng, Li Fang and Henry Hu, Microstructure and Tensile Properties of Cast Magnesium AM60-Based Hybrid Nanocomposites Reinforced With Al ₂ O ₃ Fibres and Al ₂ O ₃ or AlN Nanoparticles	Prepared

I certify that I have obtained a written permission from the copyright owner(s) to include the above published material(s) in my thesis. I certify that the above material describes work completed during my registration as a graduate student at the University of Windsor.

III. General

I declare that, to the best of my knowledge, my thesis does not infringe upon anyone's copyright nor violate any proprietary rights and that any ideas, techniques, quotations, or any other material from the work of other people included in my thesis, published or otherwise, are fully acknowledged in accordance with the standard referencing practices. Furthermore, to the extent that I have included copyrighted material that surpasses the bounds of fair dealing within the meaning of the Canada Copyright Act, I certify that I have obtained a written permission from the copyright owner(s) to include such material(s) in my thesis.

I declare that this is a true copy of my thesis, including any final revisions, as approved by my thesis committee and the Graduate Studies office, and that this thesis has not been submitted for a higher degree to any other University or Institution.

ABSTRACT

Mg-based hybrid nano composites (MHNC) reinforced with alumina (Al_2O_3) fibre and/or micron-sized/nano-sized Al_2O_3 or AlN particles were successfully prepared by a perform-squeeze casting technique under an applied pressure of 90 MPa. Mechanical properties of unreinforced AM60 alloy, Al_2O_3 fibre/AM60 composite, hybrid composite containing both Al_2O_3 fibres and micron-sized Al_2O_3 particles, as well as hybrid composite containing both Al_2O_3 fibres and nano-sized Al_2O_3 or AlN particles (MHNC) were determined by tensile testing. The addition of fibres and micron-sized particle considerably increases the ultimate tensile and yield strengths of the matrix alloy, despite that a substantial reduction in ductility. Microstructure analyses by optical (OM) and scanning electron (SEM) microscopes show that the homogeneous distribution of reinforcements, clean interfacial structure and grain refinement lead to the high strengths of the composites. The addition of nano-sized Al_2O_3 or AlN ceramics particles (3 vol.%) into the hybrid composite restores their ductility. The microstructure observation of transmission electron microscopy (TEM) indicates that the presence of a relatively low dislocation density in the matrix grains of the Mg-based hybrid nano composites (MHNCs). The SEM fractography reveals that the fracture of the composites is caused primarily by localized damages, such as particles and fibres damage and cracking, matrix fracture, and interface debonding. The determined tensile properties support the fractographic features.

DEDICATION

To My Parents,

Lixin Zhou and Xue Yi

For their endless love and devotion

ACKNOWLEDGEMENT

I would like to express to Dr. Henry Hu, for providing me with the opportunity to work on this project in the engineering materials program of the University of Windsor, and for his kindly suggestion, encouragement and excellent supervision of this research work.

Great thanks to Dr. Reza Riahi and Dr. Tirupati Bolisetti for the time given for my research thesis and presentations as my committee members, and providing valuable suggestions for this project.

I am very grateful to Mr. Andy Jenner, Mr. Steve Budinsky, Ms. Sharon Lackie, and other technicians for the technical support, Dr. Xuezhi Zhang, Mr. Li Fang, and all other group members for their technical assistance in the experimental analysis, tests, informative and valuable discussion in this research.

Most of all I would like to express my deepest gratitude to my family: my parents for their love, understanding, encouragement and support.

TABLE OF CONTENTS

DECLARATION OF CO-AUTHORSHIP / PREVIOUS PUBLICATION	III
ABSTRACT.....	VI
DEDICATION.....	VII
ACKNOWLEDGEMENT	VIII
LIST OF TABLES.....	XII
LIST OF FIGURES	XIII
CHAPTER 1 Introduction	1
1.1. Background.....	1
1.1.1. Introduction.....	1
1.2. Objectives of this study.....	3
CHAPTER 2 Literature Review	5
2.1. Introduction.....	6
2.2. Fibers Reinforced Magnesium Alloys	7
2.2.1. Solidification process.....	7
2.2.2. Microstructure and Mechanical Properties	8
2.2.2.1. Alumina Fiber Reinforced Magnesium Alloys.....	8
2.2.2.2. Carbon Fiber Reinforced Magnesium Alloys (Processing).....	13
2.3. Micro-particles Reinforced Magnesium Alloys.....	14
2.3.1. Solidification process.....	14
2.3.2. Microstructure and Mechanical Properties	15
2.3.2.1. SiC Particle Reinforced Magnesium Alloy AZ91D	15
2.3.2.2. Titanium Particle Reinforced Magnesium Alloy AZ91.....	19
2.4. Nano Particle Reinforced Magnesium.....	20
2.4.1. Solidification process.....	20
2.4.2. Microstructure and Mechanical Properties	23
2.4.2.1. Nano-sized SiC Particles Reinforced AZ31B Magnesium Composites	23
2.4.2.2. Nano-sized AlN Particles Reinforced AZ91/ZK60A Hybrid Magnesium Composite	25
2.4.2.3. Nano-sized Alumina Particles Reinforced AZ31 Magnesium Composite	29
2.4.2.4. Nano-sized Aluminum Particle Reinforced Pure Magnesium Composite	32
2.4.2.5. Nano-sized Silicon Carbide Particles and Carbon Nano Tube Reinforced Pure Magnesium Composite	35
2.4.2.6. Nano-sized Alumina Particles and Carbon Nano Tube Reinforced Pure Magnesium Composite	36
2.5. Hybrid Composite Magnesium.....	40
2.5.1. Solidification process.....	40
2.5.2. Microstructure and Mechanical Properties	40
2.5.2.1. Hybrid Reinforced AM60 Magnesium Composites	40
2.6. Other Fabrication Methods for Magnesium-Based Composites.....	43

2.6.1. In-situ Synthesis.....	43
2.6.2. Pressure-less Infiltration	44
2.6.3. Gas Injection	46
2.6.4. Spray Forming	47
2.7. Summary	47
2.8. References.....	49
CHAPTER 3 Processing and Properties of As-cast Magnesium AM60-Based Composite Containing Alumina Nano Particles and Micron Fibres.....	56
3.1. Introduction.....	56
3.2. Experimental Procedures	57
3.2.1. Materials	57
3.2.2. Fabrication of hybrid preform.....	59
3.2.3. Fabrication of composites	59
3.2.4. Microstructure analysis.....	60
3.2.5. Tensile testing	60
3.3. Results and Discussion	61
3.3.1. Characterization of hybrid preform composite.....	61
3.3.2. Tensile properties.....	69
3.4. Conclusions.....	71
3.5. Acknowledgments.....	71
3.6. References.....	72
CHAPTER 4 As-cast Magnesium AM60-Based Hybrid Nanocomposite Containing Alumina Fibres and Nanoparticles: Microstructure and Tensile Behavior	74
4.1. Introduction.....	74
4.2. Experimental Procedures	76
4.2.1. Materials	76
4.2.2. Fabrication of hybrid preform.....	77
4.2.3. Fabrication of composites	78
4.2.4. Microstructure analysis.....	79
4.2.5. Tensile testing	79
4.3. Results and Discussion	80
4.3.1. Microstructure.....	80
4.3.2. Tensile properties.....	93
4.3.3. Strain hardening	97
4.3.4. Fractography	100
4.4. Conclusions.....	103
4.5. Acknowledgments.....	104
4.6. References.....	104
CHAPTER 5 Microstructure and Tensile Properties of Cast Magnesium AM60-Based Hybrid Nanocomposites Reinforced With Al₂O₃ Fibres and Al₂O₃ or AlN Nanoparticles	107
5.1. Introduction.....	107

5.2. Experimental Procedures	109
5.2.1. Materials	109
5.2.2. Fabrication of hybrid preform.....	111
5.2.3. Fabrication of composites	112
5.2.4. Microstructure analysis.....	112
5.2.5. Tensile testing	113
5.3. Results and Discussion	114
5.3.1. Microstructure.....	114
5.3.2. Tensile properties.....	128
5.3.3. Strain hardening.....	131
5.3.4. Fractography	134
5.4. Conclusions.....	137
5.5. Acknowledgments.....	138
5.6. References.....	138
CHAPTER 6 Conclusions	142
CHAPTER 7 Future Work	145
APPENDIX A	146
COPYRIGHT RELEASES FROM PUBLICATIONS	146
APPENDIX B	148
Microstructure Analysis Figures.....	148
AM60 (3 vol% micron Al ₂ O ₃ particle +5 vol% fibre).....	148
AM60 (3 vol% nano AlN particle +5 vol% fibre)	154
AM60 (3 vol% nano Al ₂ O ₃ particle +5 vol% fibre)	159
AM60 Alloy	168
VITA AUCTORIS	172

LIST OF TABLES

Table 2.1 Tensile Properties of 35 and 55 Volume Fraction Alumina Fiber Reinforced Magnesium [12].....	10
Table 2.2 Tensile Properties of Ac-cast AZ91 alloy and AZ91/SiC particles (10 volume percentage) [20]	18
Table 2.3 Results of grain characteristics and micro-hardness of AZ91/ZK60A and AZ91/ZK60A/AlN nanocomposite [37].....	26
Table 2.4 Results of tensile testing of AZ91/ZK60A and AZ91/ZK60A/AlN nanocomposite [37]	27
Table 2.5 Results of compressive testing of AZ91/ZK60A and AZ91/ZK60A/AlN nanocomposite [37].....	28
Table 2.6 Results of grain and intermetallic particle characteristics and microhardness of AZ31 and AZ31/Al ₂ O ₃ nanocomposite [42].....	30
Table 2.7 Results of tensile testing of AZ31 and AZ31/Al ₂ O ₃ nanocomposite [42]	30
Table 2.8 Results of compressive testing of AZ31 and AZ31/Al ₂ O ₃ nanocomposite [42].....	30
Table 2.9 Results of density and grain size measurements [36]	33
Table 2.10 Results of the room temperature mechanical properties of Mg and Mg/Alp samples [36].....	33
Table 2.11 Results of density and porosity measurements [43].....	36
Table 2.12 Results of CTE determination and image analysis [43].....	36
Table 2.13 Results of micro-hardness and tensile properties [43]	36
Table 2.14 Results of porosity and density measurements Mg/CNT/alumina [45]	38
Table 2.15 Results of hardness tests Mg/CNT/alumina [44]	38
Table 2.16 Results of tensile tests Mg/CNT/alumina [44].....	38
Table 3.1 Thermo-physical properties of the ceramic Al ₂ O ₃ nano particle, Al ₂ O ₃ fibre and matrix alloy AM60; Physical chemistry of property of ceramic grain and fibre Al ₂ O ₃ and magnesium alloy	59
Table 3.2 Grain sizes of AM60 alloy, 5 vol.% Fibre/ AM60, and (3 vol.% nano-Particle +5 vol. % Fibre)/ AM60 composites.....	67
Table 3.3 UTS, YS, ef and E of the matrix alloy AM60, the composites of 5 vol. % Fibre/AM60, and (5 vol.% Fibre+3 vol.% nano-Particle)/AM60.....	70
Table 4.1 UTS, YS, ef and E of the Matrix Alloy AM60, the Composites of 5 vol. % Fibre/AM60, and (5 vol.% Fibre+3 vol.% nano-Particle)/AM60.....	95
Table 4.2 Best fit parameters of power equation	100
Table 5.1 Mechanical properties of nano-sized ceramics particles.....	110
Table 5.2 UTS, YS, ef and E of the Matrix Alloy AM60, the Composites of 5 vol. % Fibre/AM60, (5 vol.% Fibre+3 vol.% nano Al ₂ O ₃ particles)/AM60, (5 vol.% Fibre+3 vol.% nano AlN particles)/AM60	129
Table 5.3 Best fit parameters of power equation	133

LIST OF FIGURES

Figure 2.1. Fatigue Properties of 35 and 55 Volume Fraction Alumina Fiber Reinforced Magnesium [12]	10
Figure 2.2. Microstructure of Axial Specimens of Alumina Fiber Reinforced Magnesium (1. transverse fibers; 2. Clumps of alumina grains) [12].....	11
Figure 2.3. Microstructure of Axial Specimens of Alumina Fiber Reinforced Magnesium Failure (a. tensile overload; b. fatigue failure) [12]	11
Figure 2.4. Minimum Creep Rate of AZ91 and QE22 alloys with 20% Alumina Fibers compared with AZ91 and Pure Magnesium [13]	12
Figure 2.6. Schematic diagram showing ITM liquid mixing and casting process for magnesium MMCs [20].....	14
Figure 2.7. Optical Micro-graphs Showing the As-cast Microstructures of AZ91/SiC Composites under Different Conditions (A. agglomerate, B. oxide, C. porosity) [20]	16
Figure 2.8. Optical Micro-graphs Showing the As-cast Microstructures of Pure Magnesium/SiC Composites under Different Conditions (A. agglomerate, B. oxide, C. porosity) [20]	17
Figure 2.9. Optical Micro-graphs Showing the As-cast Microstructures of (a) AZ91 alloy (b)AZ91/SiC Composites [20].....	17
Figure 2.10. Grain Size Comparison of As-cast AZ91 alloy and AZ91/10vol.% SiC [20].....	18
Figure 2.11. True stress–true strain curves of Mg–10 Vol.%Ti composite in the 25–300 °C temperature range [27].....	20
Figure 2.12. Arrangement of raw materials in crucible before casting for AZ91/ZK60A/AlN nanocomposite [37].....	22
Figure 2.13. SEM Micrographs of As-cast SiCp/AZ31B Nanocomposites: (a) 1 vol.% SiCp/AZ31B Nanocomposite, (b) 2 vol.% SiCp/AZ31B Nanocomposite, (c) 3 vol.% SiCp/AZ31B Nanocomposite, (d) High Magnification of (c) [33].....	23
Figure 2.14. Grain Sizes of As-cast SiCp/AZ31B Nano-composites [33].....	24
Figure 2.15. The Mechanical Properties of SiCp/AZ31B Nanocomposite after Hot Extrusion. (a) Tensile Stain–Stress Curves, (b) Ultimate Tensile Strength, Yield Strength and Elongation [33].....	25
Figure 2.16. Representative FESEM micrographs showing grain size in monolithic AZ91/ZK60A and AZ91/ZK60A/AlN nanocomposite: (a) lower magnification and (b) higher magnification. (c) Representative TEM micrograph (including SAED pattern) showing the presence of individual nitride nanoparticles and fine intermetallic particles in AZ91/ZK60A/AlN nanocomposite. (d) Representative TEM micrograph (including SAED pattern) showing the presence of individual Mg-Zn rod-shaped nanoparticles in AZ91/ZK60A/AlN nanocomposite. Phases present but not labeled in the SAED patterns include Mg and Mg-Al phases only [37]	28
Figure 2.17. Representative micrographs showing grain and intermetallic particle sizes in: (a) monolithic AZ31 and (b) AZ31/Al ₂ O ₃ nanocomposite. Representative micrographs showing	

Al ₂ O ₃ reinforcement distribution (location) in the AZ31/Al ₂ O ₃ nanocomposite at: (c) grain boundary and (d) within the grain [42]	31
Figure 2.18. Representative tensile fractographs of: (a) monolithic AZ31 and (b) AZ31/Al ₂ O ₃ nanocomposite [42].....	32
Figure 2.19. Representative FESEM micrograph showing the distribution of aluminum particulates (represented by white spots) in Mg/1.00Alp composite [36]	34
Figure 2.20. TEM micrograph showing good interfacial integrity between Mg matrix and nano-Al particulates. The EDX spectrum verifies the presence of nano-aluminum particulate [36]	34
Figure 2.21. SEM micrograph showing cleavage step like features in the magnesium matrix of the Mg+1%CNT composite [44]	39
Figure 2.22. SEM micrograph showing intrinsic features on the fracture surface of the Mg+0.3%CNT + 0.7%Al ₂ O ₃ composite sample deformed in uniaxial tension [44].....	39
Figure 2.23. SEM Micrograph of (a) Pure Fibre Perform, arrow1—fibre and arrow2—empty cell, (b) Hybrid Preforms, arrow1—fibre, arrow2—particle and arrow3—empty cell [45]	41
Figure 2.24. Optical Photograph Showing the Microstructures of Matrix Alloy and Composites, (a) AM60, (b) 9%Fibres/AM60, and (c) (4% particles +9%Fibres)/AM60 [45].....	41
Figure 2.25. Grain Size of the Matrix Alloy, F/AM60 and (F+P)/AM60 Composites [45]	42
Figure 2.26. Hardness Measurements for the Matrix Alloy and Composites [45]	42
Figure 2.27. Typical Engineering Stress vs. Strain Curves for AM60 alloy, F/AM60, and (P+F)/AM60 Composites [45]	43
Figure 2.28. Experiment Set-up for Pressure-less Infiltration SiC/Mg [48].....	45
Figure 2.29. The Microstructure of the Infiltrated SiC/Mg Composites [48].....	46
Figure 3.1. Flowchart showing the procedure for fabricating hybrid (a) preform and (b) composites.....	58
Figure 3.2. SEM micrograph of composite matrix alloy and composites (3% nano-particles + 5% Fibres) /AM60. a) overall dispersion of nano-particles and fibres; b) nano particles dispersion: Arrow 1-nano particles; Arrow 2-fibres	62
Figure 3.3. SEM micrograph of composite matrix alloy and composites (5% Fibres) /AM60. a) overall dispersion of fibres; b) enlarged fibres: Arrow 1-fibres	64
Figure 3.4. Fractures of preform fibres : Arrow 1-fibres crush	66
Figure 3.5. Optical micrographs showing grain structure of (a) unreinforced AM60 matrix alloy, (b) 5 vol.% Fibre/ AM60 and (c) (3 vol. % nano-Particle +5 vol. %Fibre)/ AM60. All are under as-cast condition	68
Figure 3.6. Typical engineering stress vs. strain curves for the matrix alloy AM60, the composites of 5 vol. % Fibre/AM60, and (5 vol.% Fibre+3 vol.% nano-Particle)/AM60... ..	70
Figure 4.1. Flowchart showing the procedure for fabricating hybrid (a) preform and (b) composites.....	77
Figure 4.2. Optical photograph showing the microstructures of unetched as-cast matrix alloy and composites, (a) unreinforced matrix alloy AM60, (b) 5 vol% Fibre/ AM60, (c) (3 vol% micron particle +5 vol% Fibre)/ AM60. (d) (3 vol% nanoparticle +5 vol% Fibre)/ AM60. 83	

Figure 4.3. Optical micrographs showing grain structures of etched (a) unreinforced matrix alloy AM60, (b) 5 vol% fibre/ AM60, (c) (3 vol% micron particle +5 vol% fibre)/ AM60, and (d) (3 vol% nano particle +5 vol% fibre)/ AM60.....	86
Figure 4.4. Measured grain sizes of the unreinforced matrix alloy AM60, 5 vol% fibre/ AM60, (3 vol% micron particle +5 vol% fibre)/ AM60, and (3 vol% nano particle +5 vol% fibre)/ AM60.....	86
Figure 4.5. SEM micrographs in BSE mode showing the reinforcement distribution in (a) 5 vol% fibre/ AM60, (b) (3 vol% micron-particle +5 vol% fibre)/ AM60, and (c) (3 vol. % nano-particle +5 vol% fibre)/ AM60.....	88
Figure 4.6. TEM and EDS results showing the particle presence and the interface between the particle and matrix, (a) a micron Al ₂ O ₃ particle in the (3 vol% micron Al ₂ O ₃ particles + 5 vol% Fibres) /AM60, (b) line scans and the corresponding line scanning pattern for the cross-section area of the micron particle, (c) a nano Al ₂ O ₃ particle in the (3 vol% micron Al ₂ O ₃ particles + 5 vol% Fibres) /AM60 MHNC, and (d) line scans and the corresponding line scanning pattern for the cross-section area of the nano particle. The gray lines denote the approximate scanning path.....	90
Figure 4.7. TEM micrographs showing dislocations in the composites with Al ₂ O ₃ particles: (a) micron and (b) nano.....	93
Figure 4.8. Engineering stress vs. strain curves for the matrix alloy AM60, 5 vol% Fibre/AM60, (5 vol.% Fibre+3 vol% micron Al ₂ O ₃ particle)/AM60, and (5 vol.% fibre+3 vol.% nano Al ₂ O ₃ particle)/AM60.....	95
Figure 4.9. True stress vs. strain curves for the matrix alloy AM60, 5 vol% Fibre/AM60, (5 vol.% Fibre+3 vol% micron Al ₂ O ₃ particle)/AM60, and (5 vol.% fibre+3 vol.% nano Al ₂ O ₃ particle)/AM60.....	97
Figure 4.10. Strain hardening curves for the matrix alloy AM60, 5 vol% Fibre/AM60, (5 vol.% Fibre+3 vol% micron Al ₂ O ₃ particle)/AM60, and (5 vol.% fibre+3 vol.% nano Al ₂ O ₃ particle)/AM60, upon the commencement of plastic deformation.....	98
Figure 4.11. Fractures of AM60, AM60 composites with Al ₂ O ₃ fibres particles (a) AM60 alloy (b) AM60 alloy with 5% fibre (c) AM60 alloy with 5% fibre/ 3% micron size particles (d) AM60 alloy with 5% fibre/ 3% nano size particles (arrow 1- matrix crack; arrow 2- fibre crack; arrow 3- debonding; arrow 4- micron-particle crack; arrow).	102
Figure 5.1. Flowchart showing the procedure for fabricating hybrid (a) preform and (b) composites.....	111
Figure 5.2. Optical photograph showing the microstructures of unetched as-cast matrix alloy and composites, (a) unreinforced matrix alloy AM60, (b) 5 vol% Fibre/ AM60, (c) (3 vol% nano Al ₂ O ₃ particle +5 vol% fibre)/ AM60, and (d) (3 vol. % nano AlN particle +5 vol% fibre)/ AM60.....	116
Figure 5.3. Optical micrographs showing grain structures of etched (a) unreinforced matrix alloy AM60, (b) 5 vol.% fibre/ AM60, (c) (3 vol% nano Al ₂ O ₃ particle +5 vol.% fibre)/ AM60, and (d) (3 vol. % nano AlN particle +5 vol.% fibre)/ AM60.....	119

Figure 5.4. Measured grain sizes of the unreinforced matrix alloy AM60, 5 vol% fibre/ AM60, (3 vol% nano Al ₂ O ₃ particle +5 vol% fibre)/ AM60, and (d) (3 vol. % nano AlN particle +5 vol% fibre)/ AM60.....	120
Figure 5.5. SEM micrographs in BSE mode showing the reinforcement distribution in (a) 5 vol% fibre/ AM60, (b) (3 vol% nano Al ₂ O ₃ particle +5 vol% fibre)/ AM60, and (c) (3 vol. % nano AlN particle +5 vol% fibre)/ AM60.	121
Figure 5.6. TEM micrographs (a) a nano Al ₂ O ₃ particle in the (3 vol% nano Al ₂ O ₃ particles + 5 vol% Fibres) /AM60 MHNC line scans and the corresponding line scanning pattern for the nano particle cross-section area (b) EDS pattern for the nano Al ₂ O ₃ particle line scan (c) a nano AlN particle in the (3 vol% nano AlN particles + 5 vol% Fibres) /AM60 MHNC line scans and the corresponding line scanning pattern for the particle cross-section area (d) EDS and EELS patterns for the nano AlN particle line scan.	124
Figure 5.7. TEM micrographs showing (a) the micron fibre-only composites with dislocations, (b) the MHNC- Al ₂ O ₃ with almost no dislocations, and MHNC-AlN with (c) AlN particle and (d) nano pores and dislocations ((c)zoomed out).....	127
Figure 5.8. Engineering stress vs. strain curves for the matrix alloy AM60, 5 vol% Fibre/AM60, (5 vol.% Fibre+3 vol% nano Al ₂ O ₃ particles)/AM60, and (5 vol.% fibre+3 vol.% nano AlN particles)/AM60.	130
Figure 5.9. True stress vs. strain curves for the matrix alloy AM60, 5 vol% Fibre/AM60, (5 vol.% Fibre+3 vol% nano Al ₂ O ₃ particles)/AM60, and (5 vol.% fibre+3 vol.% nano AlN particles)/AM60.	131
Figure 5.10. Strain hardening curves for the matrix alloy AM60, 5 vol% Fibre/AM60, (5 vol.% Fibre+3 vol% nano Al ₂ O ₃ particles)/AM60, and (5 vol.% fibre+3 vol.% nano AlN particles)/AM60, upon the commencement of plastic deformation.....	132
Figure 5.11. Fractures of AM60, AM60 composites with Al ₂ O ₃ fibres particles (a) AM60 alloy (b) AM60 alloy with 5% fibre (c) AM60 alloy with 5% fibre/ 3% nano Al ₂ O ₃ particles, and (d) AM60 alloy with 5% fibre/ 3% nano AlN particles (arrow 1- matrix crack; arrow 2- fibre crack; arrow 3- debonding).....	136

CHAPTER 1 Introduction

1.1. Background

1.1.1. Introduction

The requirement for high-performance and lightweight materials in the automotive industry has led to extensive research and development efforts in the development of magnesium matrix composites and their cost-effective fabrication technologies. Composite materials are versatile in terms of constituent selection so that the properties of the materials can be tailored. The major disadvantage of metal matrix composites usually lies in the relatively high cost of fabrication and of the reinforcement materials. The cost-effective processing of composite materials is, therefore, an essential element for expanding their applications. The availability of a wide variety of reinforcing techniques is attracting interest in composite materials. This is especially true for the high-performance and lightweight magnesium-based materials due to certain unique characteristics of composites which offer effective approaches to strengthen magnesium.

Hybrid composites are fabricated by adding two or more reinforcements into matrix materials so that excellent properties can be achieved through the combined advantages of short fibres, and different size particles, which provide a high degree of design freedom. Hybrid metal matrix composites are reinforced with hybrid reinforcement in which both particles and short fibres are employed. As a result they can provide large opportunities to optimize the engineering performance of metal matrix composites for potential applications in the automotive industry, where different volumes, especially the relatively low volume, and selective reinforced areas of reinforcements are required.

The hybrid metal-based composites could be fabricated by preform-squeeze casting, in which a two-step process is involved. First, a preform is made and then the squeeze casting pressurizes molten alloy to infiltrate into the preform. The advantages of preform-squeeze cast hybrid composites are the following: both the particles and short fibres can be employed to facilitate microstructure design and mechanical property optimization; reasonable low cost raw materials and wide volume percentage range of reinforcements can be selected; mass production becomes feasible; and improvements in the wettability of reinforcements enable selected regions of parts to be reinforced only with no wetting agent.

In the open literature, there are a few studies on hybrid magnesium-based composites which are fabricated by the preform-squeeze casting technique with micron-fibre skeleton and/or micron-sized particles. The micron-particle introduction increases the efficiency of reinforcement in wear resistance and strength of resultant composites. However, the addition of micron-sized particles into the magnesium matrix leads to a significant decrease in ductility.

The inferior ductility of micron-sized particle reinforced magnesium composites limits its expansion. For the improvement of the ductility of the resultant composite, studies on the introduction of nano-sized particles to the magnesium composites have been carried out. However, the nano-sized particles introduction was limited in the volume-fraction of the reinforcement in the matrix alloy. The agglomeration of the nano-sized particles with high volume fractions was inevitable with the traditional stirring casting method even with the pre-mixed matrix alloy and nano-sized particles. There were studies in successful fabrication with higher volume fraction nano-sized particles magnesium composite by the evaporation of magnesium in an environment of high vacuum. But, the evaporation method was costly and not

suitable for larger components in high volume production. Moreover, the low volume fraction of nano-particles introduction limits the design freedom of magnesium-based composite materials.

Therefore, the stirring problem faced by nano-sized particles could be resolved by the hybrid preform fabrication with nano-sized particles. No detailed research reports on processing, solidification and characterization of Mg-based hybrid nano-composites (MHNC) have been found, although Mg-based composites reinforced with only nano-sized particles possess not only the enhanced strengths but also reasonable ductilities.

1.2. Objectives of this study

The objectives of this work are outlined as follows:

- Develop a process for preform fabrication with introduction of nano-sized particles;
- Develop a process for manufacturing magnesium-based hybrid nano composites with no agglomerated nano-sized particles and micron-sized reinforcements;
- Analyze the microstructures of the developed magnesium-based hybrid nano composites in comparison with the composites containing micron fibres and/or particles;
- Evaluate the mechanical properties of the fabricated composites; and
- Determine the fracture mechanisms of the developed magnesium-based hybrid composites.

1.3. Organization of the thesis

In this study, the fabrication method for producing the Mg/AM60-based hybrid nano composites by using the preform and squeeze casting technology has been developed. The microstructures of the fabricated MHNCs were analyzed with the optical (OM), Scanning (SEM) and Transmission (TEM) electron microscopes. The mechanical properties of the MHNCs were

evaluated by tensile testing. The obtained results were compared with those of the composites containing micron fibres and particles as well as the matrix alloy (AM60).

To effectively and concisely present the completed work, this thesis contains seven chapters. Chapter 1 provides a general background of metal-based composites and the advantages of nano-sized particles-reinforced hybrid metal matrix composites fabricated by preform-squeeze casting technique. Chapter 2 reviews recent studies on the processing, microstructure, and mechanical properties of magnesium-matrix composites. Chapter 3, Chapter 4, Chapter 5 reports the detailed fabrication method, comparisons, results and discussion with respect to the effects of nano-sized particles in magnesium alloy AM60-based hybrid nano composite (MHNC) on microstructures, tensile properties, and fracture mechanism of the developed magnesium-based hybrid composites. The conclusions of the present study are summarized in Chapter 6. Finally, Chapter 7 gives some recommendations for future work.

CHAPTER 2 Literature Review

In this chapter, progresses upon magnesium-based metal matrix composite technologies in recent decades are reviewed. Different reinforcement systems are discussed, including fiber, micron-sized particles, nano-sized particles, and hybrid fiber/particles reinforcements. Several reinforcement categories and combinations for magnesium composites have been introduced, especially in nano-particle reinforcement and its composites. The superior hardness, tensile and compressive properties of the composites should be attributed to not only the addition of reinforcements themselves, but also the reinforcement distribution in the matrix, the bonding between the reinforcement and matrix, and the grain structure refinement caused by reinforcements. Typical methods for fabrication of composites are discussed and compared. Squeeze Casting, Stir-casting, Powder Metallurgy, and Hot Extrusion are considered as the common process techniques for the preparation of Mg-based composites. The formation of intermetallic phases due to the reaction between the reinforcement and matrix alloy also plays an important role in enhancing the mechanical properties of the composite. As the reinforcement content increases, the composite with micron-sized reinforcements shows a significant decrease in ductility. However, the addition of nano-particles to magnesium alloys causes no significant reduction in the ductility of the resultant composites. The hybrid and nano-particles reinforced magnesium composites are considered as the most promising and emerging high strength light-weight materials owing to their unique engineering performance.

2.1. Introduction

Automakers are being subjected to increased strict fuel economy requirements, while consumers are demanding improved interior comforts and advanced electronic systems for safety, navigation, and entertainment, all of which add otherwise unnecessary weight. Automotive manufacturers are turning to light-weight metals as one of the solutions to meet the demands [1-3]. Aluminum alloys components such as engine blocks, body panels, and frame members. In recent decades, magnesium alloys, as lighter alloys choice to aluminum ones, are being researched and successfully subjected to certain types of components for mass production such as instrument panels, valve covers, transmission housings, and steering column components. The major current area of growth for the use of magnesium alloys in the high volume commercial automotive sector enable an incentive for weight savings to maximize fuel economy and minimize emissions [4]. BMW Company even achieves mass production of the whole 3.0-liter six-cylinder gasoline engine with only 161 kilograms by magnesium Mg-Al-Sr alloys system [5]. Moreover, combining or replacing these efforts with the use of advanced metal-matrix micro- and nano-composites (MMCs) not only reduce the mass of components, but also improve reliability and efficiency [6,7]. Metal-matrix composites are metals or alloys that incorporate particles, whiskers, fibers, or hollow micro-balloons made of a different material, and offer unique features to tailor materials to specific design needs.

2.2. Fibers Reinforced Magnesium Alloys

2.2.1. Solidification process

Short Fiber and whisker reinforced metal-matrix-composites (MMCs) are manufactured with various reinforcement distributions. Castings of magnesium matrix composites are most commonly presented by liquid metal or preform infiltration method. The preform method presents majority of short fibers randomly aligned in 2D planar architecture that normal to applied pressing direction compared with the liquid or powder-metallurgy method, in which substantial fibers alignment is parallel to the processing direction.

For preform method, the most common fabrication route is squeeze casting with pressure infiltration. During squeeze casting, the reinforcement fibers is usually made into a preform and placed into a permanent mold. The molten magnesium alloys are then poured into the mold and solidified under high pressures. During the solidification period, the high pressure applied forced the liquid magnesium infiltrate into the gaps in the preform that forms bonds between reinforcement fibers with magnesium alloys. The pressure is the primary parameters that influence the quality of castings. The pressure is supposed to be as high as possible; however, for manufacturing magnesium composite, excessive high pressure may produce a turbulent flow of molten magnesium causing gas entrapment and magnesium oxidation [8]. The advantage of this method is allowing the superior types and volume fractions of reinforcement to incorporate with magnesium alloys.

For powder-metallurgy method, magnesium alloy and reinforcement are mixed, pressed, degased and sintered at a certain temperature under controlled atmosphere or in a vacuum [9]. Compared to squeeze casting with pressure infiltration method, this method requires powder

alloy instead of bulk material, and the conditions required are more critical; therefore, the cost for fabrication is not ideal for mass production.

The varied reinforcement types of fibers, such as Al_2O_3 fibers, enable to meet majority of requirement of demands. In general, carbon fibers and alumina fibers are considered as the most popular reinforcement fibers for commercial usage as those relatively cheap features. Magnesium composites reinforced by alumina fibers are the most common combination; for squeeze casting with pressure infiltration method, alumina fibers preform is made and placed in the mold for squeeze casting. Then the liquid magnesium alloy is poured into the mold with certain degree of pressure applied during solidification period. The carbon fibers reinforced magnesium alloys are more complicated to fabricate with this method. It is reported by Kuo et al [10] that if without proper treatment, the APC-2 prepreg (AS-4 carbon fibers) and magnesium alloy delaminate after solidification as a result of surface energies difference and large thermal expansion coefficient difference [11]. Kuo et al [10] treat the composites with a combination of HNO_3 and H_2SO_4 with transition-metal ions instead of binder to resolve delamination problem, which is effective.

2.2.2. Microstructure and Mechanical Properties

2.2.2.1. Alumina Fiber Reinforced Magnesium Alloys

There are bulk of studies on this type of reinforcement in magnesium and its alloys. The very first study to be discussed is reported by Hack et al[12]. They chose pure magnesium for the matrix as its microstructural simplicity and batch-to-batch reproducibility. The alumina fibers chosen were in 20 μm diameters with 35 and 55 percent volume fraction respectively. The fibers

were laid in unidirectional manner. Specimens were cut into 15.2 cm long with 1.27 cm x 0.25 cm rectangular for tensile and fatigue testing. As the prior-known information that the mechanical properties of composites with hard alumina fibers is better than pure magnesium, this report only contained the comparison of the results for difference volume fraction of reinforcement and fibers orientation. Table 2.1 gives the results for the tensile test results. It showed the longitude direction fibers provide superior tensile yield strength (YS) and ultimate tensile strength (UTS) as those bears more loads than other orientations. It is interesting that even the alumina fiber is brittle than magnesium fibers, with higher volume fraction 55% fibers, it showed better elongation percentage. Figure 2.1 shows the fatigue data for the tests; similar to tensile test, the axial direction provided superior properties under same level of loads applied. Figure 2.2 shows the microstructure of the axial specimens containing defects attributed to crack initiations, which are transverse (normal direction) fibers and clumps of alumina grains. Figure 2.3 shows the tensile failure and fatigue failure microstructure of axial specimens. It could be observed that the tensile overload was identical to those of the off-axis tensile failure, while the fatigue was by a combination of delamination of fiber/matrix interface and cracking of the magnesium matrix.

Table 2.1 Tensile Properties of 35 and 55 Volume Fraction Alumina Fiber Reinforced Magnesium [12]

Vol Pct Al ₂ O ₃	Orientation, Deg.	YS, MPa	UTS, MPa	E, GPa	e_f , Pct
35	0 (axial)	213	383 (396)	149 (162)	0.26
35	22.5	34	207	116	0.52
35	45	23	108	90	0.45
35	90 (transverse)	21	104	85	0.42
55	0 (axial)	321*	567* (571)	197 (229)	0.30*
55	22.5	27	196	155	0.81
55	45	30	157	124	0.58
55	90 (transverse)	18	67	90	0.24

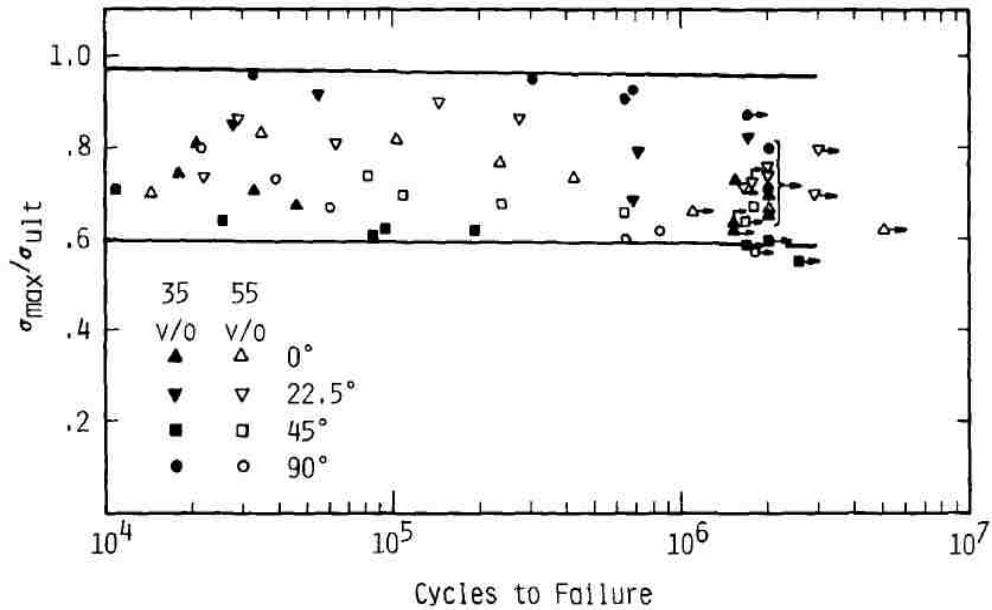


Figure 2.1. Fatigue Properties of 35 and 55 Volume Fraction Alumina Fiber Reinforced Magnesium [12].

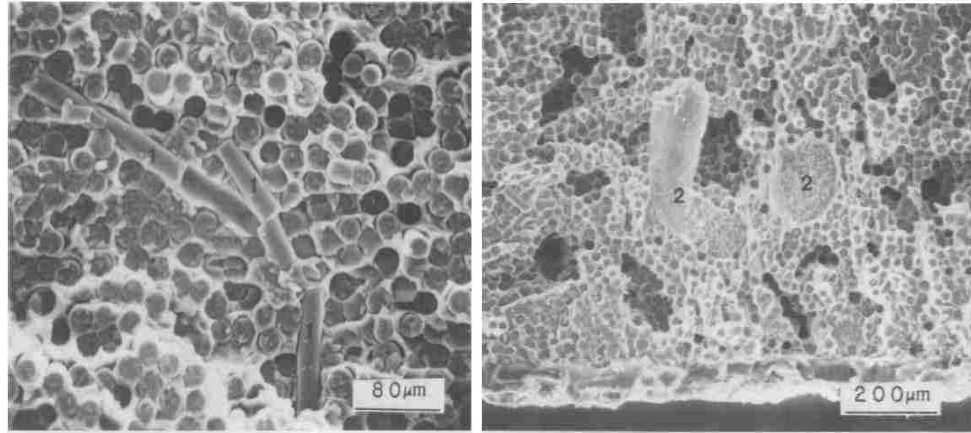


Figure 2.2. Microstructure of Axial Specimens of Alumina Fiber Reinforced Magnesium (1. transverse fibers; 2. Clumps of alumina grains) [12].

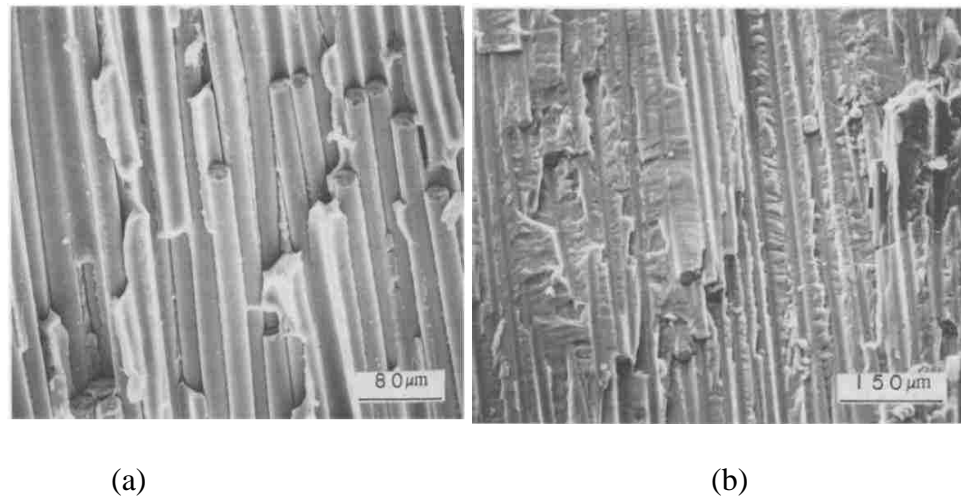


Figure 2.3. Microstructure of Axial Specimens of Alumina Fiber Reinforced Magnesium Failure (a. tensile overload; b. fatigue failure) [12].

Creep resistance of aluminum fiber reinforced magnesium alloys was reported by Sklenicka et al[13] with AZ91 and QE22 magnesium alloy. Low Creep resistance of magnesium alloy was not suitable for applications in automotive power-train. Pure AZ91D magnesium alloy also showed poor creep resistance above 125 °C [14]. They added 20 volume fraction Saffil fibers (97 pct Al₂O₃, 3pct SiO₂) in AZ91 alloy and QE22 alloy. Their results shown in Figure 2.4

and 2.5 demonstrated the second stage minimum creep rate and the creep fracture time. There was apparent improvement with alumina fiber reinforcement.

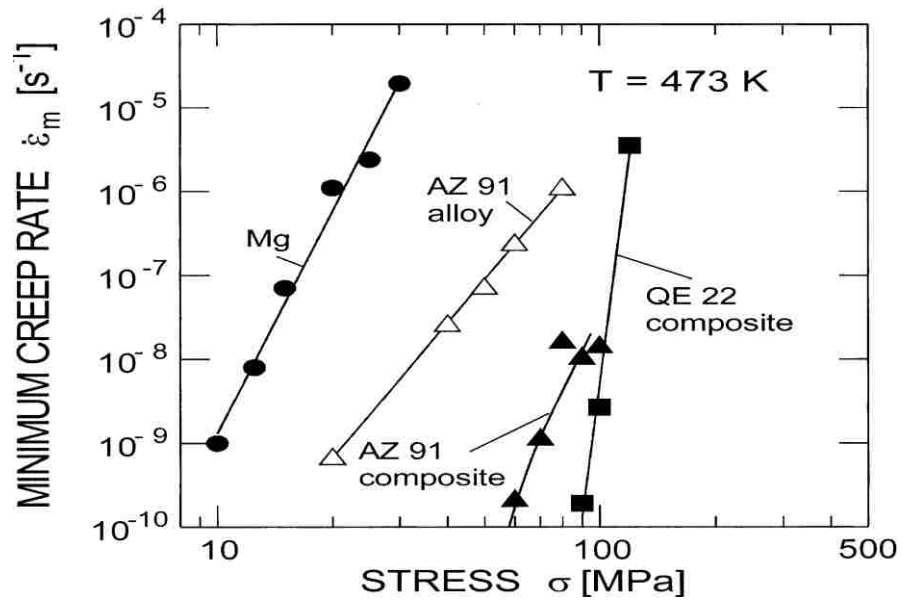


Figure 2.4. Minimum Creep Rate of AZ91 and QE22 alloys with 20% Alumina Fibers compared with AZ91 and Pure Magnesium [13].

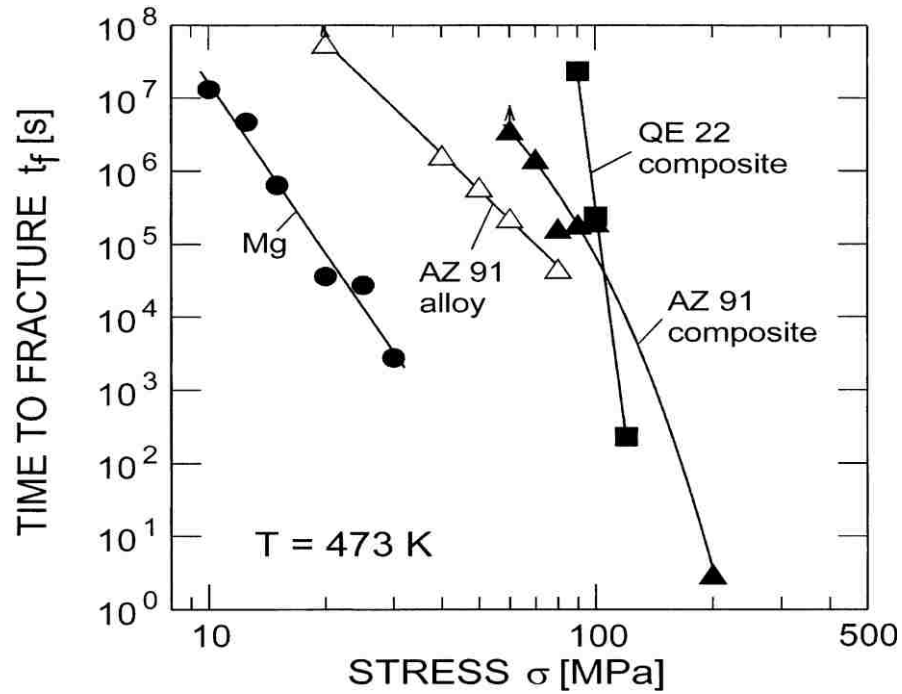


Figure 2.5. Time for Creep Failure of AZ91 and QE22 alloys with 20% Alumina Fibers compared with AZ91 and Pure Magnesium [13].

2.2.2.2. Carbon Fiber Reinforced Magnesium Alloys (Processing)

Carbon fibers have been popular in the past several decades. This reinforcement into magnesium is considered as a feasible and cheap route to improve magnesium and its alloys properties. As the carbon fibers have excellent mechanical properties, it is no doubt that the addition of carbon fiber into magnesium alloy matrix provides superior mechanical properties. However, compared to metal based reinforcement, the bonding between carbon fibers and magnesium alloys are critical during the fabrication. A solution was provided by Huang et al[10]. There are another method provided by Katzman [15] that silicon dioxide coating is deposited on the fiber surfaces from an organometallic precursor solution after the fibers passing the solution. Hydrolysis or pyrolysis of the organometallic compound is used to form silicon dioxide on the fiber surfaces that generates wetting and bonding when the fibers are immersed in molten magnesium. In Katzman's report[15], graphite fibers are prior-processed by using alkoxides, a class of organometallic compounds to bond hydrocarbon groups with metal atoms by bridging oxygen atoms [16] as precursors for ceramics and glasses [17,18], to form thin, uniform oxide coatings.

Although carbon fibers are expensive in North America compared to those in Asia, the features of carbon fibers into magnesium alloys reinforcement are remarkable.

2.3. Micro-particles Reinforced Magnesium Alloys

2.3.1. Solidification process

Instead of fibers reinforcement, micro-particles reinforcement is another popular route to reinforce magnesium alloys. As there is no direction concern in particles reinforcement, the dispersion of particles is the key for this type of reinforcement. One of the popular particles involved in magnesium alloy reinforcement is SiC particles. The general processing method for particle reinforced magnesium composites is the mixing and casting process developed by Institute of Magnesium Technology (ITM) [19]. A schematic diagram showing ITM liquid mixing and casting process for magnesium MMCs is provided in Figure 2.6. It should be noted that the furnace used should be under protective atmosphere such as SF₆/CO₂ [20].

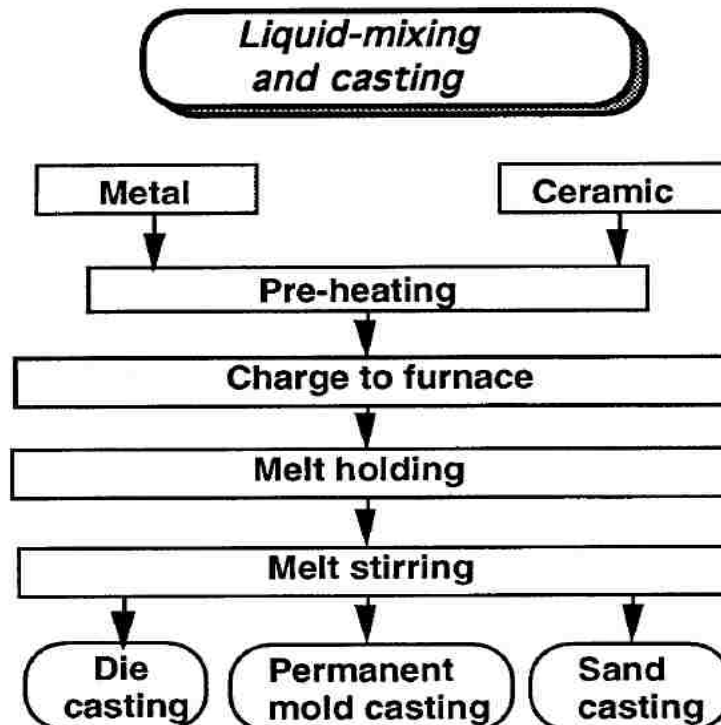


Figure 2.6. Schematic diagram showing ITM liquid mixing and casting process for magnesium MMCs [20].

The fabrication for this type of composite can be achieved also by pressure infiltration technique. It is reported that AZ91D magnesium alloy matrix with 40 volume percentage SiC particles were made by Lo et al [21] in MTL/Canmet Canada et al in ITM. The preform held SiC together by alumina binder to form a rigid three-dimensional network of inter-connecting particulates. The infiltration stage at 600 °C (100 °C superheat for AZ91D alloy) and 40 MPa.

2.3.2. Microstructure and Mechanical Properties

2.3.2.1. SiC Particle Reinforced Magnesium Alloy AZ91D

By using different process parameters of the mixing and casting method, Luo et al[20] prepared several pure Mg-based and AZ91D-based SiC-reinforced composites. He investigated their microstructures and mechanical behavior.

Figure 2.7 compares the microstructures of the AZ91D-based SiC-reinforced composites under different casting conditions. T_m , t_m , and t_s stand for melting temperature, melting time, solidification temperature. The microstructure of pure magnesium-based reinforce also with SiC particles under the same casting conditions in Figure 2.8 showed a success incorporation of SiC particles in the AZ91 alloy as well as pure magnesium. The AZ91-based composite gave a better dispersion of SiC particles compared to pure magnesium composites, which provides superior mechanical properties improvement.

Figure 2.9 compares AZ91 alloys with/without reinforcement microstructures. The apparent grain refinement was observed in the particles reinforcement AZ91 alloy reported in Figure 2.10. Therefore, a conclusion could be made that particles reinforcement refined grain

size to improve the mechanical properties as well as the properties provided by particles materials. A same conclusion was made by Hu [22] with the casting of AM50A/SiC composites.

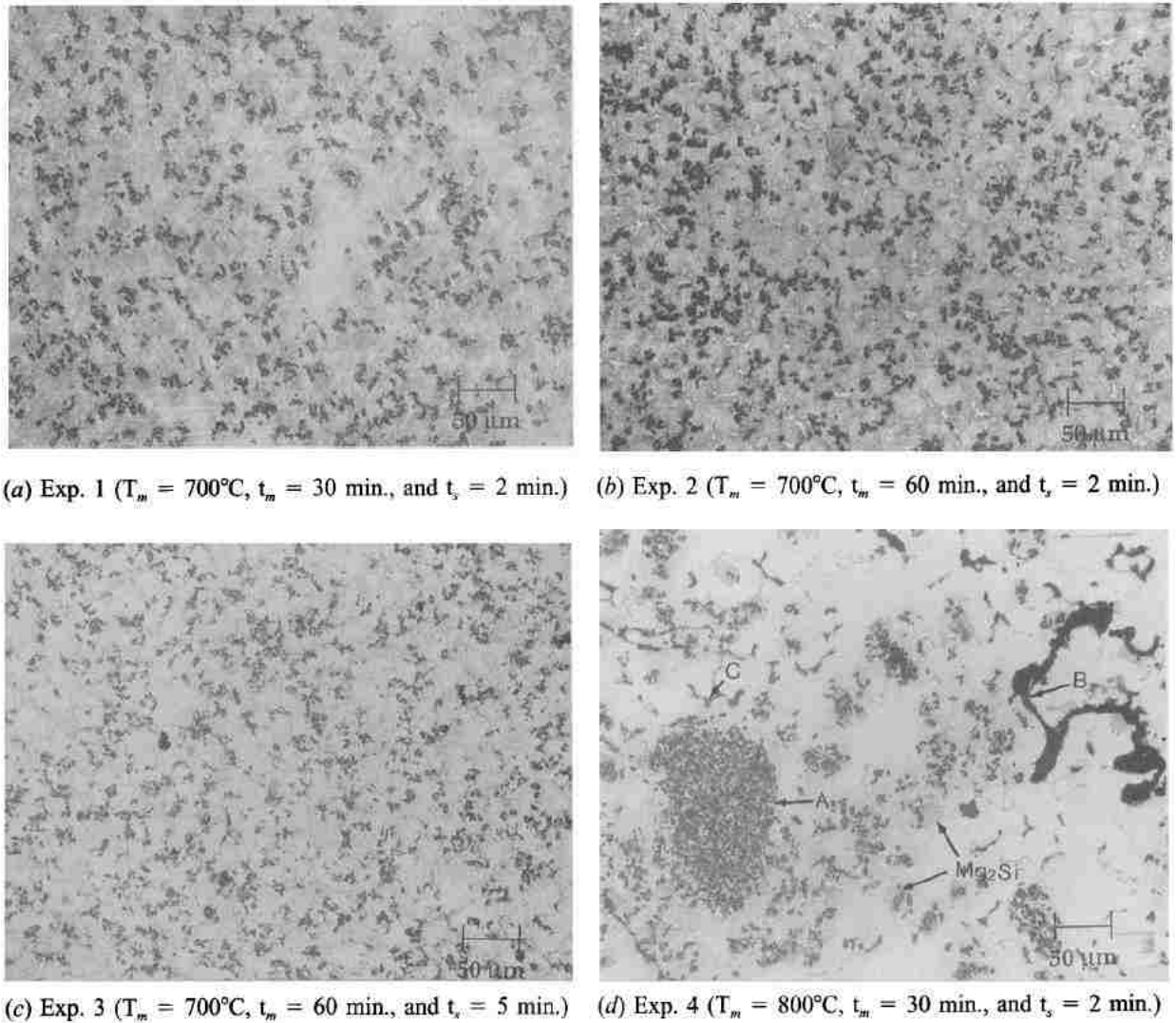
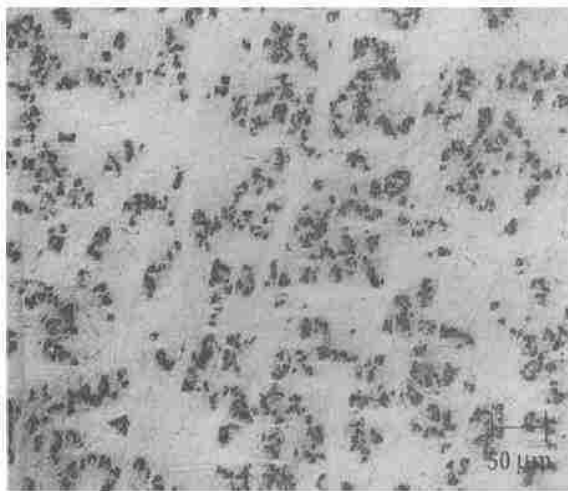
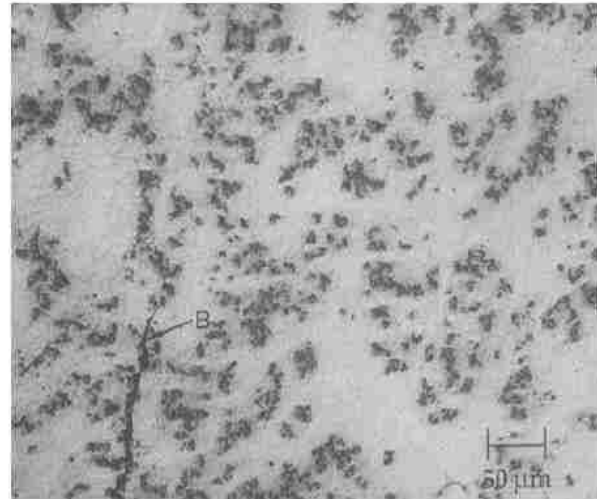


Figure 2.7. Optical Micro-graphs Showing the As-cast Microstructures of AZ91/SiC Composites under Different Conditions (A. agglomerate, B. oxide, C. porosity) [20].

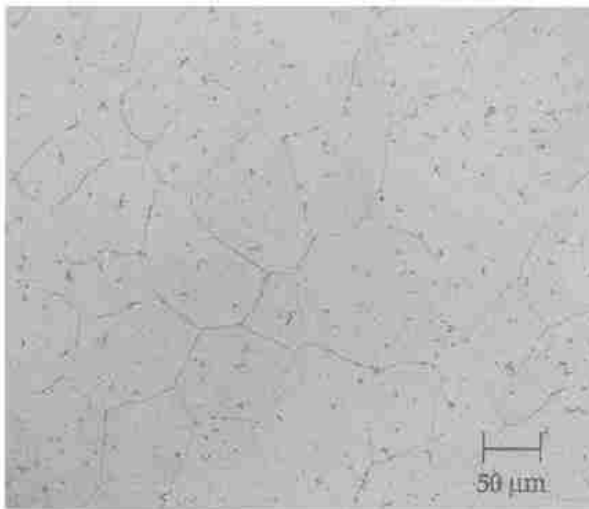


(a) Exp. 5 ($T_m = 700^\circ\text{C}$, $t_m = 60$ min., and $t_c = 2$ min.)

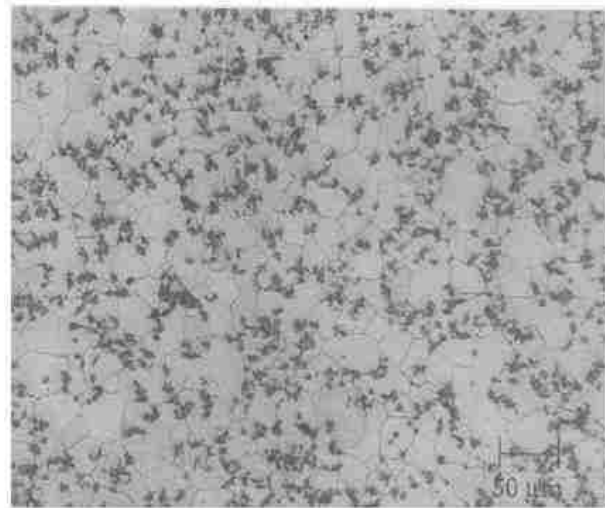


(b) Exp. 6 ($T_m = 800^\circ\text{C}$, $t_m = 30$ min., and $t_c = 2$ min.)

Figure 2.8. Optical Micro-graphs Showing the As-cast Microstructures of Pure Magnesium/SiC Composites under Different Conditions (A. agglomerate, B. oxide, C. porosity) [20].



(a)



(b)

Figure 2.9. Optical Micro-graphs Showing the As-cast Microstructures of (a) AZ91 alloy (b)AZ91/SiC Composites [20].

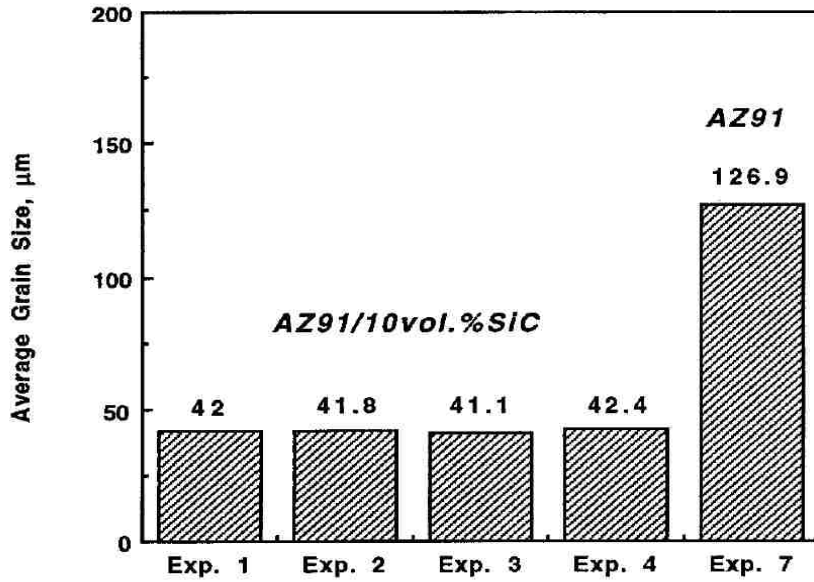


Figure 2.10. Grain Size Comparison of As-cast AZ91 alloy and AZ91/10vol.% SiC [20].

Table 2.2 shows the mechanical properties comparison of non-reinforcement AZ91 alloy and AZ91/SiC particles (10 volume percentage); improvement can be apparently observed in the Table 2.2.

Table 2.2 Tensile Properties of Ac-cast AZ91 alloy and AZ91/SiC particles (10 volume percentage) [20]

Material	Elastic Modulus (EM, GPa)	0.2 Pct Yield Strength (YS, MPa)	Ultimate Tensile Strength (UTS, MPa)	Elongation (E_f , Pct)
AZ91	42.6	86.7	203	7.1
AZ91/SiC	44.7	135	152	0.8

2.3.2.2. Titanium Particle Reinforced Magnesium Alloy AZ91

Improvement in the mechanical properties can be achieved through an adequate control of the microstructure of the alloy such as grain size, texture, size and precipitates). Among those, the most effective for improving strength magnesium is grain size refinement [21, 23, 24]. The micron size reinforcements, usually ceramics such as SiC, results in an increase in the yield strength with a considerable decrease in the elongation to failure [25-27]. Titanium particles are popular in the micron-sized reinforcement technology in magnesium composites for its low density and no reaction among elements to form brittle phases at magnesium and titanium interface.

The processing method titanium as reinforcement is powder metallurgical route [28]. According to the research by Perez et al [28], magnesium powder particles were smaller than 300 μm mixed with titanium powder for 1 hour at 100 rpm with planetary mill. After the mixing, the powder degased at 150 $^{\circ}\text{C}$ and hot extruded at 400 $^{\circ}\text{C}$ with a ratio of 18/1. The resulting product was Mg/10 vol.% Ti. A true stress and strain curve of the magnesium/Ti composite is shown in Figure 2.11. At room temperature, the magnesium/Ti composite has a yield stress of 160 MPa, which is a remarkable improvement. However, due to its high cost, the method is not recommended for mass production.

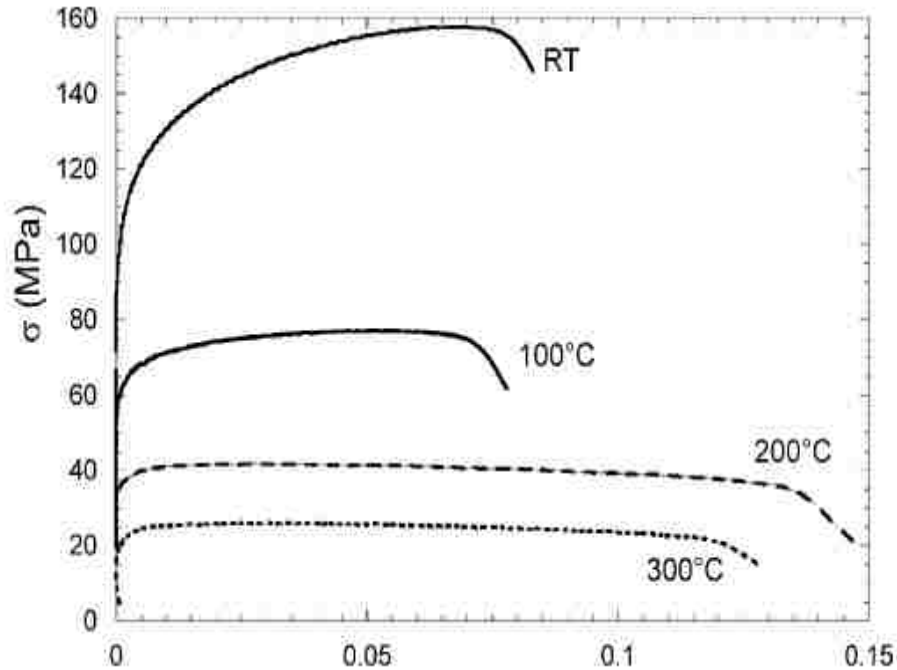


Figure 2.11. True stress–true strain curves of Mg–10 Vol.%Ti composite in the 25–300 °C temperature range [28].

2.4. Nano Particle Reinforced Magnesium

2.4.1. Solidification process

Among different reinforcement reinforced magnesium matrix composites, the reinforcements with low cost and practicability are usually silicon carbide and alumina particles [29, 30]. The micron particle-reinforced magnesium alloy processes higher tensile strength and elastic modulus compared to unreinforced magnesium alloy. However, there is a remarkable reduction in ductility. According to the study of Wans et al [31], the AZ91D alloy with micron SiC particles reinforcement decreases elongation to 3% from non-reinforced AZ91D with 18%. From the study of Hassan and Gupta [32], the compared to the AZ91 magnesium alloy reinforced with much higher content of micron sized SiCp, the 0.2% yield strength, ultimate

tensile strength, and ductility of the magnesium matrix nano-composites containing 1.11 vol.% of alumina particle were remain higher. Nie et al[33] has carried out nano-SiCp/AZ91D alloy composites prepared as semi-solid slurry by by hot extrusion under 2000 kN load. However, by exceeding 1% volume fraction of nano SiC particles in the composites, the tensile properties appeared decreases obviously. The basic idea to reinforce magnesium composites is to increase the volume fraction of reinforcement and decrease particles size. With the limitation given above, compromise should be carried out for fabrication of nano-sized magnesium composites.

The general processing method for nano-sized reinforced magnesium composites is by using the semisolid stirring assisted ultrasonic vibration technique. In the study of Shen at al[34] study, by using the above method, different compositions of reinforcement nano SiC particles in AZ31B magnesium alloy were compared and discussed. In 2011, Tham et al [35] and Gupta et al [36], used the DMD method for the fabrication of Mg-based nano composites. They employed AlN nano-particle powder in 10-20 nm as reinforcement. The matrix was AZ91 and ZK60A hybrid alloy with 2wt.% decreased aluminum content in AZ91. The hybrid alloys were heated in a graphite crucible to 750 °C under Ar gas atmosphere. The crucible was equipped with bottom pouring. Upon the set superheat temperature, the slurry liquid metal was stirred by a mild steel impeller with Zirtex 25 coating to avoid iron contamination before pouring. The pouring liquid metal was first disintegrated by two jets of argon gas normal to the liquid metal stream. The disintegrated melt was subsequently deposited onto a metallic substrate located 500 mm from the pouring point to obtain an ingot with 40 mm in diameter. After forming the mixture hybrid alloy ingot, arrange the alloy and nano particles powder in a crucible. In the crucible, the arrangement of alloys and particles powder was important. Figure 2.12 shows the arrangement in the crucible. To form the AZ91/AK60A/1.5vol.% AlN nanocpmposite, AlN nanoparticles powder was

isolated by wrapping in Al foil with minimal weight, which is the reason to decrease the aluminum content in the AZ91. The wrap was arranged on the top of hybrid alloy block. The resulting composite was fabricated by hot extrusion by 150 ton hydraulic press; the ratio is 20.25:1. Hot extrusion is carried out at 350 degree °C with holding at 400 °C for 1 hour. The lubrication used was Colloidal graphite. The resulting product was 8 mm rods. Heat treatment for the composites was mentioned in 200 °C for 1 hour in order to relax the monolithic AZ91/ZK60A hybrid alloy without recrystallization softening. Prior to heat treatment, ingot warped with aluminum foil was needed to avoid minimize reaction with oxygen in the heat treatment furnace. A same DMD fabrication method by Zhong et al [37] using AZ31 matrix with alumina nanoparticles powder warped by Al foil was under same pressure, temperature, and extrusion ratio.

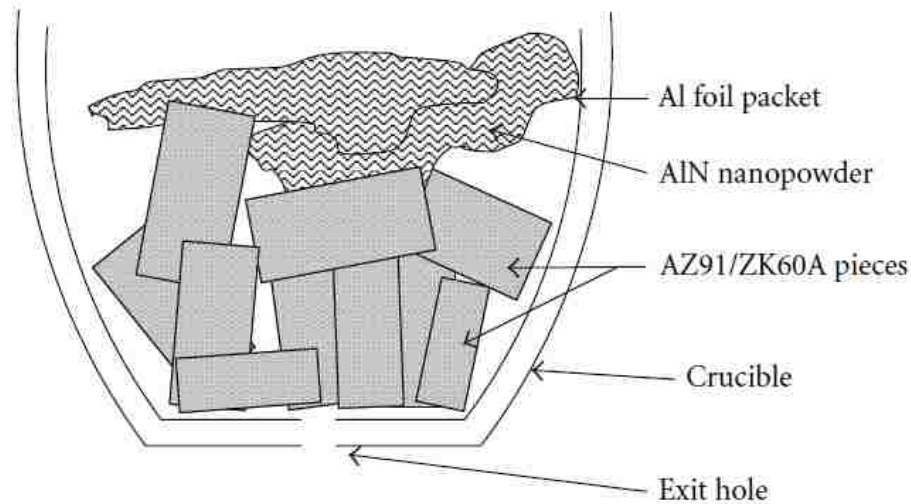


Figure 2.12. Arrangement of raw materials in crucible before casting for AZ91/ZK60A/AlN nanocomposite [38].

2.4.2. Microstructure and Mechanical Properties

2.4.2.1. Nano-sized SiC Particles Reinforced AZ31B Magnesium Composites

Shen et al[34] has made several groups of nano-sized SiC particles reinforced AZ31B composite. The SEM analysis shows the microstructures of different compositions of reinforcement is demonstrated in Figure 2.13, while the measured grain sizes are reported in Figure 2.14.

Figure 2.15 shows the tensile test results for composites of those three compositions. The results suggest the higher amount of composition of nano-particles reinforcement in AZ31B provides the higher tensile properties, which is not consistent with the situation with AZ91D. Reasons for the increase of tensile properties are attributed to grain refinement and uniform distribution of nano SiC particles that act as ductility enhancer [39, 40].

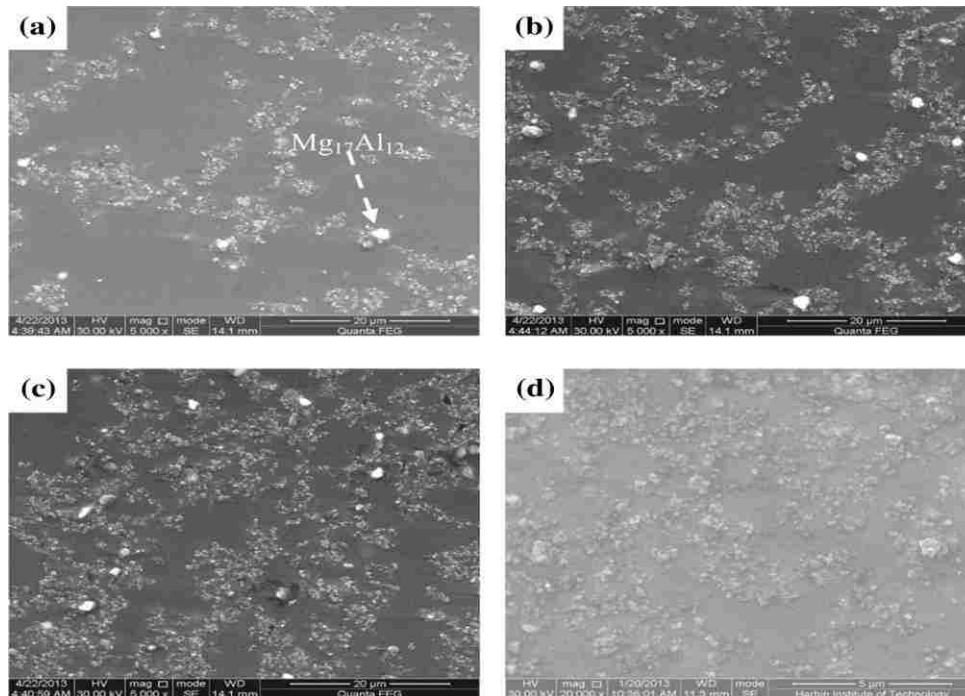


Figure 2.13. SEM Micrographs of As-cast SiCp/AZ31B Nanocomposites: (a) 1 vol.% SiCp/AZ31B Nanocomposite, (b) 2 vol.% SiCp/AZ31B Nanocomposite, (c) 3 vol.% SiCp/AZ31B Nanocomposite, (d) High Magnification of (c) [34].

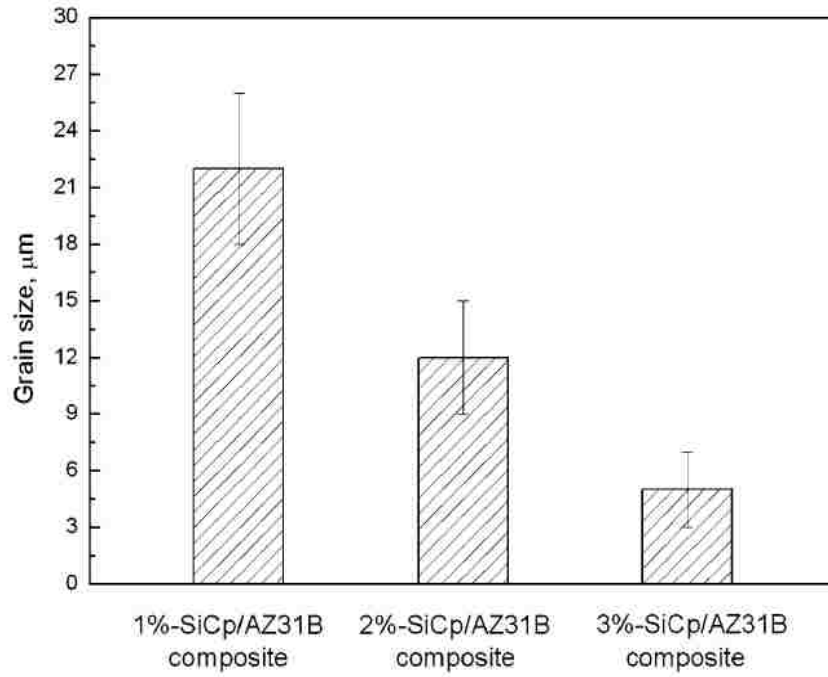
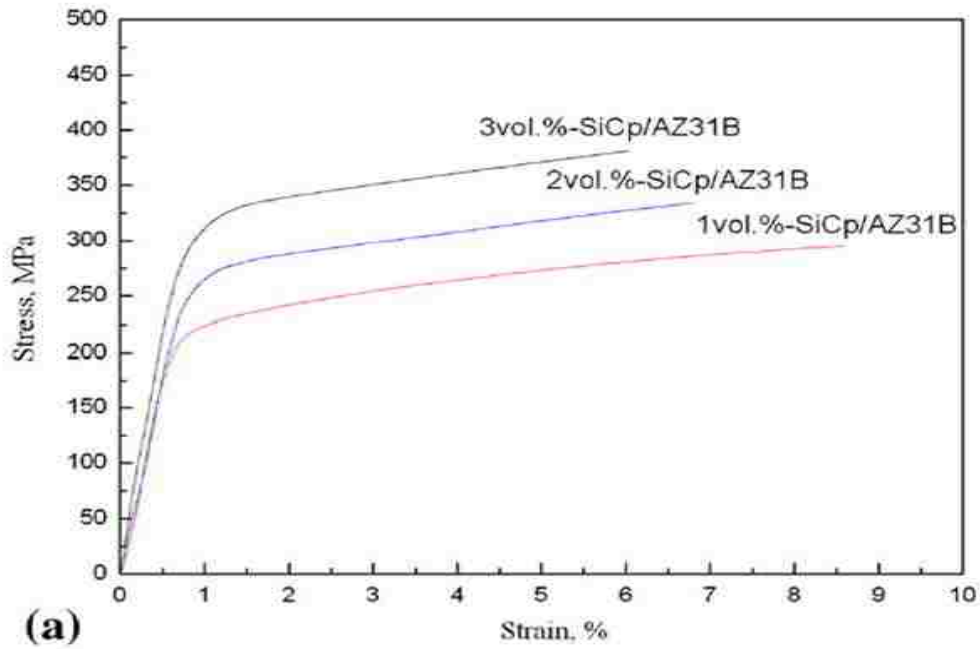


Figure 2.14. Grain Sizes of As-cast SiCp/AZ31B Nano-composites [34].



(a)

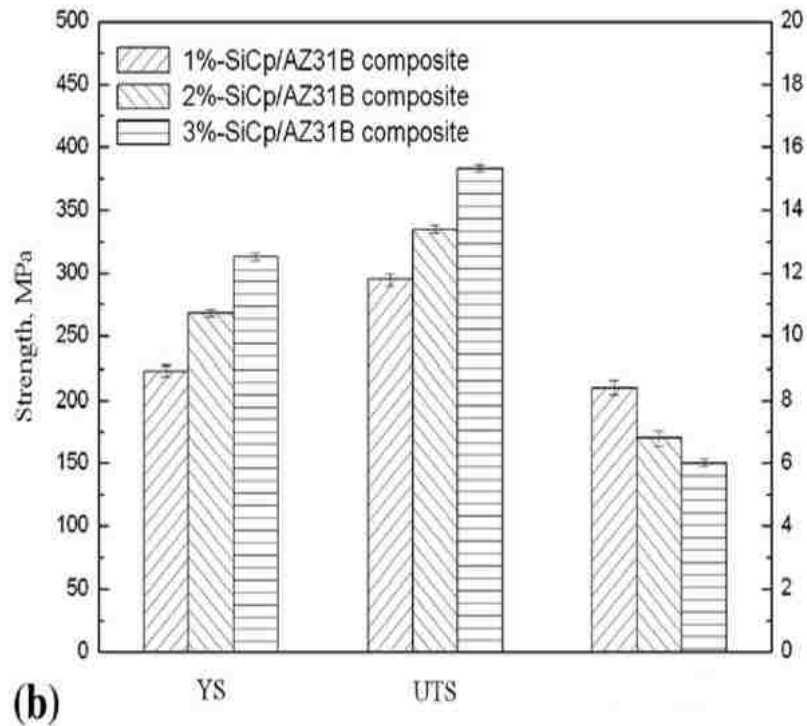


Figure 2.15. The Mechanical Properties of SiCp/AZ31B Nanocomposite after Hot Extrusion. (a) Tensile Stain–Stress Curves, (b) Ultimate Tensile Strength, Yield Strength and Elongation [34].

2.4.2.2. Nano-sized AlN Particles Reinforced AZ91/ZK60A Hybrid Magnesium Composite

AZ91 and ZK60A hybrid AlN nanoparticle (10-20 nm) composites prepared by Paramoathy et al [38] has achieved higher yield strength and ultimate tensile strengths without significantly decreasing the ductility of the alloys. The microstructure analysis was carried out by FESEM (Field Emission Scanning Electron Microscopy) and TEM showing the intermetallic phases in Figure 2.16. There were no macro-pores or shrinkage cavities observed, and the intermetallic particles were distributed uniformly. The results of grain size measurements are given in Table 2.3, with the nano particles addition, the grain size refinement was not significant, and the grain aspect ratio was not changed. But, the hardness has been increased. The reason for hardness improvement should be attributed to the uniform distribution of AlN particles in the matrix and

the higher constraint to localized matrix deformation during indentation due to the presence of nano particles [41,42].

As the tensile and compression data carried out in Tables 2.4 and 2.5, the nano reinforced alloys showed higher tensile and compressive strengths than those of monolithic alloys. The 0.2% yield stress improvement was observed in tensile and not that significantly in compression. The tensile failure strain was not significantly decreased, because the nano-sized particles had the effect to decrease the ductility drop phenomenon compared to micron-sized particles. It was noted that in compressive test, the failure strain for composites was higher than the monolithic alloy. The reason in this case was the presence of the Mg-Zn nano rods reported in Figure 2.16. The brittle Mg-Zn nano rod is prone to buckling followed by fracture with the hybrid alloy matrix during compressive deformation unlike during tensile deformation.

Table 2.3 Results of grain characteristics and micro-hardness of AZ91/ZK60A and AZ91/ZK60A/AlN nanocomposite [38]

Material	AlN (vol.%)	Grain characteristics ^a		Microhardness (HV)
		Size (μm)	Aspect ratio	
AZ91/ZK60A	—	4.5 ± 0.9	1.4	137 ± 4
AZ91/ZK60A/ 1.5 vol% AlN	1.50	4.2 ± 0.8	1.4	$160 \pm 8 (+17)$

^a Based on approximately 100 grains.

() Brackets indicate % change with respect to corresponding result of AZ91/ZK60A.

Table 2.4 Results of tensile testing of AZ91/ZK60A and AZ91/ZK60A/AlN nanocomposite [38]

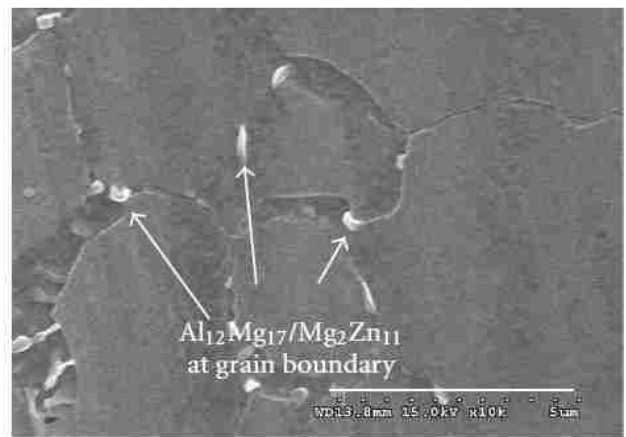
Material	0.2% TYS (MPa)	UTS (MPa)	Failure Strain (%)	Energy absorbed, EA (MJ/m ³) ^a
AZ91/ZK60A	225 ± 4	321 ± 4	16.1 ± 0.3	49 ± 1
AZ91/ZK60A/ 1.5 vol% AlN	236 ± 6 (+5)	336 ± 4 (+5)	13.8 ± 1.0 (-14)	44 ± 4 (-10)

^a Energy absorbed until fracture, that is, area under the engineering stress-strain curve until the point of fracture (obtained using EXCEL software).

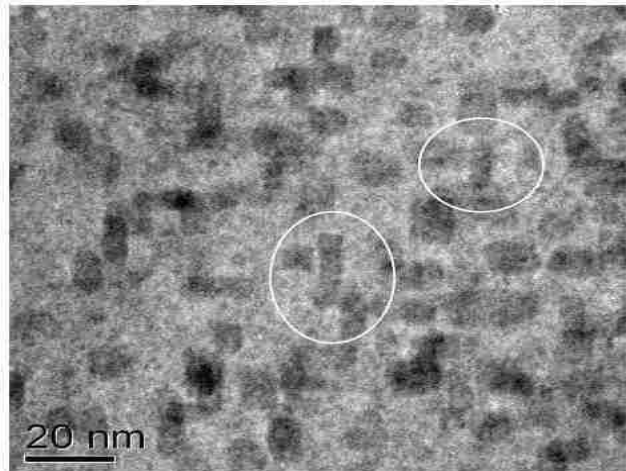
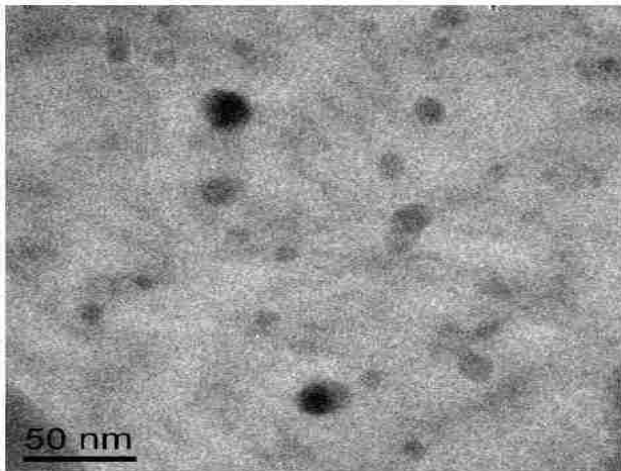
() Brackets indicate % change with respect to corresponding result of AZ91/ZK60A.



(a)



(b)



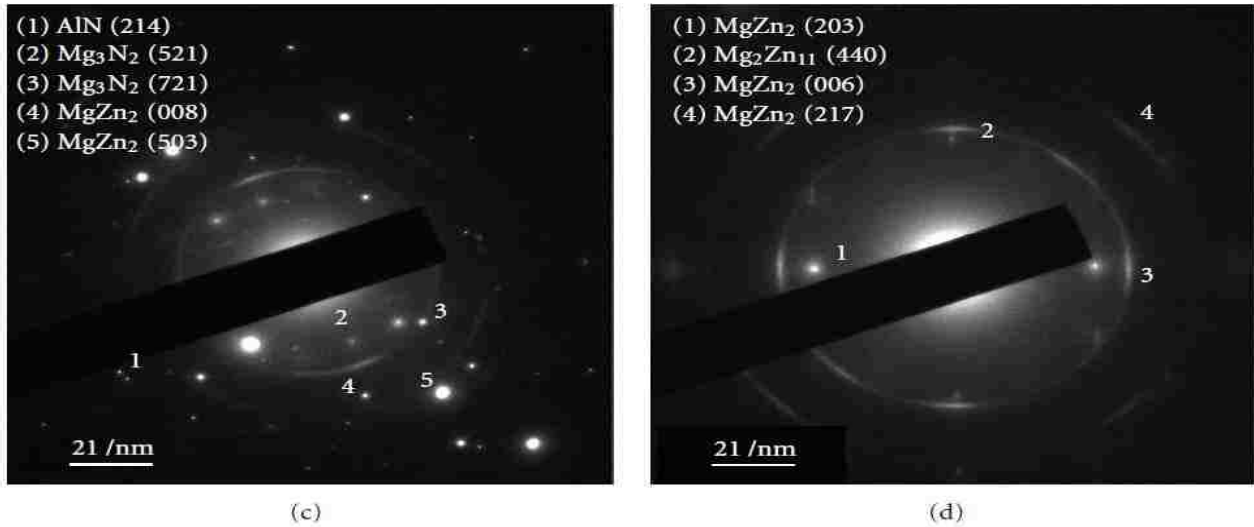


Figure 2.16. Representative FESEM micrographs showing grain size in monolithic AZ91/ZK60A and AZ91/ZK60A/AlN nanocomposite: (a) lower magnification and (b) higher magnification. (c) Representative TEM micrograph (including SAED pattern) showing the presence of individual nitride nanoparticles and fine intermetallic particles in AZ91/ZK60A/AlN nanocomposite. (d) Representative TEM micrograph (including SAED pattern) showing the presence of individual Mg-Zn rod-shaped nanoparticles in AZ91/ZK60A/AlN nanocomposite. Phases present but not labeled in the SAED patterns include Mg and Mg-Al phases only [38].

Table 2.5 Results of compressive testing of AZ91/ZK60A and AZ91/ZK60A/AlN nanocomposite [38]

Material	0.2% CYS (MPa)	UCS (MPa)	Failure Strain (%)	Energy absorbed, EA (MJ/m ³) ^a
AZ91/ZK60A	106 ± 5	508 ± 17	19.5 ± 1.7	83 ± 9
AZ91/ZK60A/ 1.5 vol% AlN	107 ± 12 (+1)	541 ± 19 (+6)	24.1 ± 6.5 (+24)	88 ± 7 (+6)

^a Energy absorbed until fracture, that is, area under the engineering stress-strain curve until the point of fracture (obtained using EXCEL software).
() Brackets indicate % change with respect to corresponding result of AZ91/ZK60A.

2.4.2.3. Nano-sized Alumina Particles Reinforced AZ31 Magnesium Composite

The DMD method [35, 36] was also applied to produce AZ31 with nano alumina particles (50 nm size) [43]. Because of using the aluminum foil warping method for reinforcement particles powder, AZ31 was not degraded its aluminum content prior to hot extrusion. AZ31 was provided by Alfa Aesar in USA; and alumina nanoparticles powder was supplied by Baikowski in Japan.

The microstructure of AZ31/nano alumina particles composite was observed under FESEM. No macro pores, defects or shrinkages were observed in the nano composites. The XRD diffraction found that the beta phase $Al_{12}Mg_{17}$ presented in the composite. The alumina reinforcement distribution was uniform in Figure 2.17 (c) and (d), which appeared at grain boundaries as well as inside grains.

Compared to AZ91/ZK60A hybrid alloys with AlN nano particles composites, AZ31 with the same volume fraction of reinforcement (1.5 vol.% alumina) showed the significant grain refinement over that of the monolithic alloy (Table 2.6). The grain size was reduced from 4.0 micron to 2.3 micron. With the addition of brittle alumina nano particles, the hardness of the composite was superior compared with that of the monolithic alloy (30%). With the alumina nano particles addition, the tensile UTS, 0.2% YS, the compressive UCS, and 0.2% CYS were determined, showing significant improvements (Tables 2.7 and 2.8). The nano size particles alumina additions resolved the problem of significant ductility reduction in micron size alumina reinforcement, since there was an increment of failure strain in composites. The solution should be attributed to that nano particles provide sites where cleavage cracks are opened ahead of the advancing crack front that dissipates stress concentration from crack front and alters local effective stress state from plane strain to plane stress in the neighborhood crack tip. However,

with the SEM observation of fracture in tensile deformation (Figure 2.18), the AZ31/1.5 vol.% nano alumina composites demonstrated micro-crack, while the tensile fracture in monolithic AZ31 alloy had no micro-cracks. The work of fracture absorbed energy was also tested and reported in Tables 2.7 and 2.8. It showed there were improvements for both tensile and compressive deformation and a significant increase in tensile deformation was tested with 162% increase.

Table 2.6 Results of grain and intermetallic particle characteristics and microhardness of AZ31 and AZ31/Al₂O₃ nanocomposite [43]

Material	Al ₂ O ₃ (vol%)	Grain characteristics ^a		Intermetallic particle characteristics ^b		Microhardness (HV)
		Size (μm)	Aspect ratio ^c	Size (μm)	Roundness ^d ratio	
AZ31	–	4.0 ± 0.9	1.4	3.3 ± 1.1	1.9	64 ± 4
AZ31/1.5 vol%Al ₂ O ₃	1.50	2.3 ± 0.7	1.6	1.0 ± 0.4	1.1	83 ± 5 (+30)

() Brackets indicate %change with respect to corresponding result of AZ31.

^a Based on approximately 100 grains.

^b Based on approximately 100 particles.

^c Aspect ratio = major length/minor length.

^d Roundness measures the sharpness of a particle's edges and corners expressed by $(\text{perimeter})^2/4\pi(\text{area})$ [26].

Table 2.7 Results of tensile testing of AZ31 and AZ31/Al₂O₃ nanocomposite [43]

Material	0.2%TYS (MPa)	UTS (MPa)	Failure strain/elongation (%)	WOF (MJ/m ³) ^a
AZ31	172 ± 15	263 ± 12	10.4 ± 3.9	26 ± 9
AZ31/1.5 vol%Al ₂ O ₃	204 ± 8 (+19)	317 ± 5 (+21)	22.2 ± 2.4 (+113)	68 ± 7 (+162)

Table 2.8 Results of compressive testing of AZ31 and AZ31/Al₂O₃ nanocomposite [43]

Material	0.2%CVS (MPa)	UCS (MPa)	Failure strain/ductility (%)	WOF (MJ/m ³) ^a
AZ31	93 ± 9	486 ± 4	19.7 ± 7.2	76 ± 14
AZ31/1.5 vol%Al ₂ O ₃	98 ± 2 (+5)	509 ± 12 (+5)	19.0 ± 2.7 (-4)	84 ± 15 (+11)

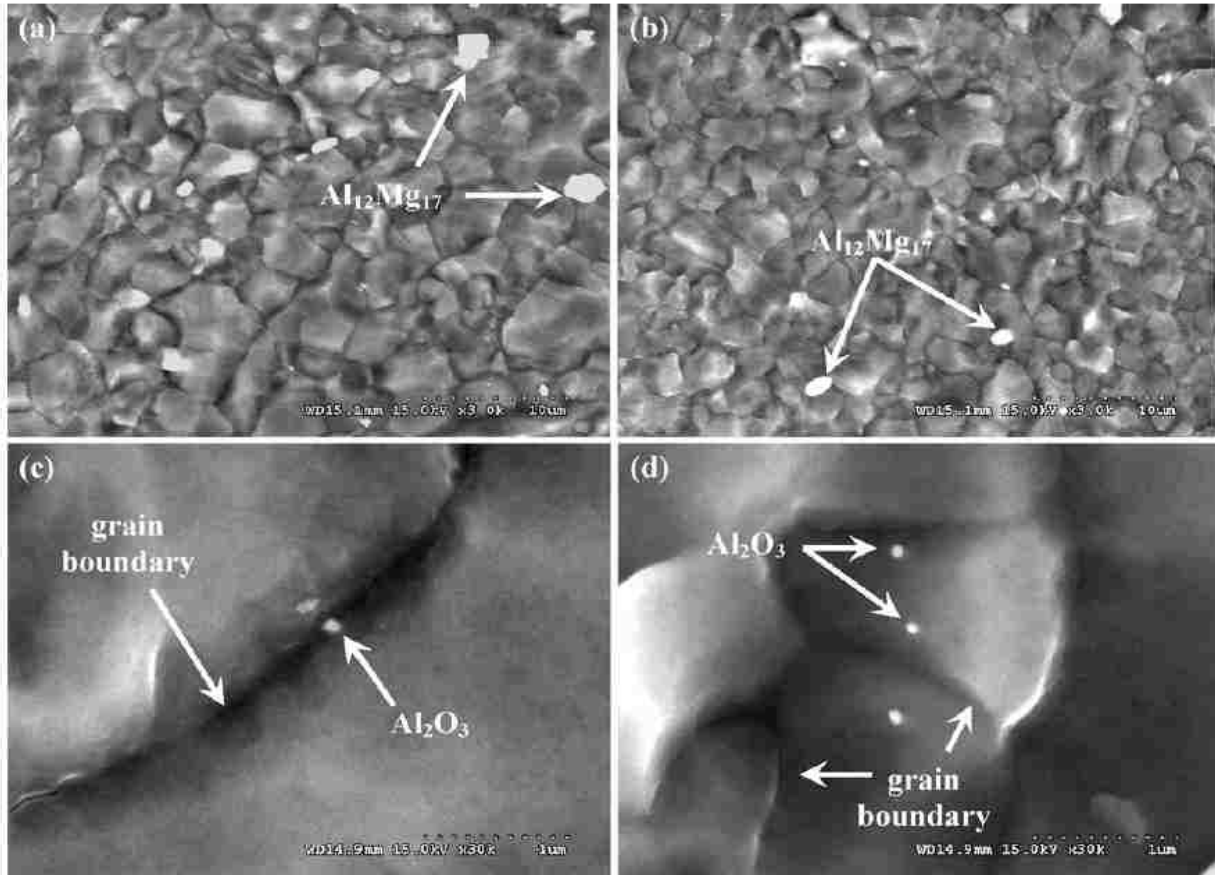


Figure 2.17. Representative micrographs showing grain and intermetallic particle sizes in: (a) monolithic AZ31 and (b) AZ31/ Al_2O_3 nanocomposite. Representative micrographs showing Al_2O_3 reinforcement distribution (location) in the AZ31/ Al_2O_3 nanocomposite at: (c) grain boundary and (d) within the grain [43].

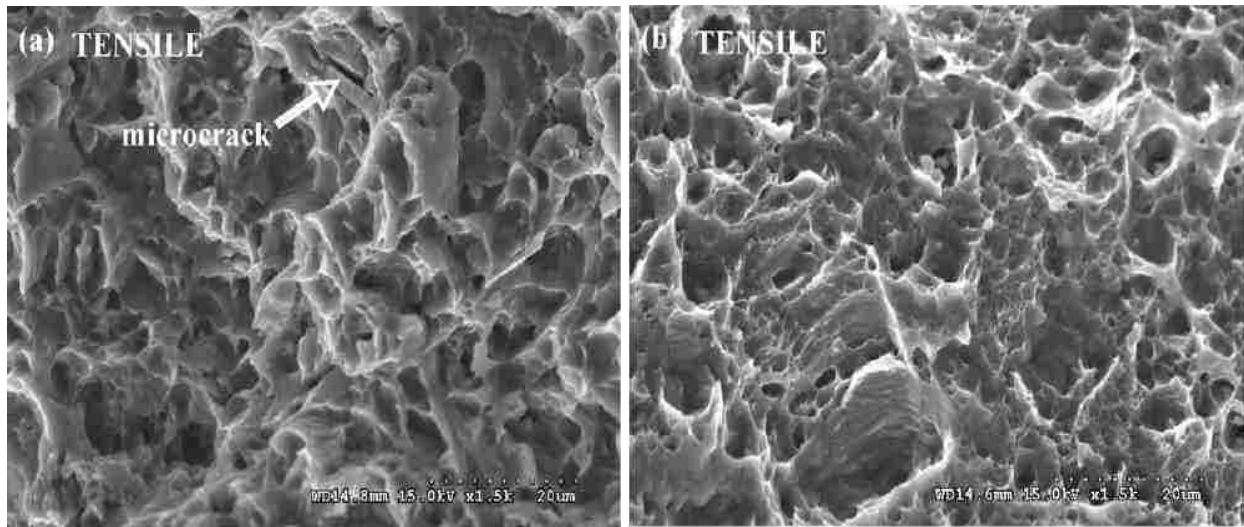


Figure 2.18. Representative tensile fractographs of: (a) monolithic AZ31 and (b) AZ31/Al₂O₃ nanocomposite [43].

2.4.2.4. Nano-sized Aluminum Particle Reinforced Pure Magnesium Composite

The monolithic magnesium with aluminum nano particle composite was made by Gupta et al [37] et al in 2007. Magnesium was supplied by Merck (Germany) in powder phase (60-300 micron-meter). The aluminum powder was in 18 nm provided by Nanostructured & Amorphous Materials Inc. (USA) The magnesium powder and aluminum power were blended in aV-blender for 5h at 50 rpm. The mixture powder was pressed under 97 bar to ingot. The ingot was sintered at 500 °C for 2 hours in an inert Ar gas atmosphere. The sintered ingot was soaked at 400 °C for 1 hour, and then hot extrude at 350 °C in an 150 tons hydraulic press. The extrusion ratio was 25:1 to obtain a 7 mm diameter. 4 volume percentages of aluminum were produced (0.25, 0.5, 0.75, 1) in the process for comparison.

The grain refinement was observed in the nano-particles composite. The most effective refinement was the highest 1% vol fraction aluminum composite, which was reported in the Table 2.9.

The microstructures analyses (Figure 2.19 and 2.20) by FESEM and TEM with EDX, showed that nano-Al particulates were uniformly distributed.

With the content of aluminum particles increased, the tensile mechanical properties were indeed improved. However, with the content of volume fraction exceeding 0.5%, the 0.2% yield stress and ultimate tensile stress decreased. This phenomenon was applied to the ductility improvement, hardness, and work of fracture, which was reported in Table 2.10. This decrease may be due to the agglomeration of aluminum nano particulates with increasing volume fraction.

Table 2.9 Results of density and grain size measurements [37]

Material	Al _p (wt.%)	Experimental density (g cm ⁻³)	Theoretical density (g cm ⁻³)	Porosity (%)	Grain size (μm)	Aspect ratio
Mg/0.00Al _p	0.00	1.731 ± 0.012	1.74	0.5	23 ± 6	1.3 ± 0.5
Mg/0.25Al _p	0.38	1.738 ± 0.004	1.74	0.2	17 ± 5	1.3 ± 0.6
Mg/0.50Al _p	0.76	1.746 ± 0.009	1.75	0.4	17 ± 8	1.5 ± 0.3
Mg/0.75Al _p	1.16	1.751 ± 0.003	1.75	0	16 ± 7	1.2 ± 0.2
Mg/1.00Al _p	1.52	1.755 ± 0.011	1.75	0	16 ± 6	1.4 ± 0.6

Table 2.10 Results of the room temperature mechanical properties of Mg and Mg/Al_p samples [37]

Materials	Hardness (15HRT)	0.2% YS (MPa)	UTS (MPa)	Failure strain (%)	WOF (MJ m ⁻³)
Mg/0.00Al _p	46 ± 3	134 ± 11	190 ± 10	4.6 ± 0.6	7.6 ± 1.6
Mg/0.25Al _p	54 ± 1	181 ± 14	221 ± 15	4.8 ± 0.4	10.5 ± 1.9
Mg/0.50Al _p	57 ± 1	218 ± 16	271 ± 11	6.2 ± 0.9	15.9 ± 2.1
Mg/0.75Al _p	60 ± 1	202 ± 7	261 ± 10	5.0 ± 1.6	13.1 ± 2.9
Mg/1.00Al _p	61 ± 1	185 ± 9	226 ± 12	3.3 ± 1.0	7.9 ± 1.8

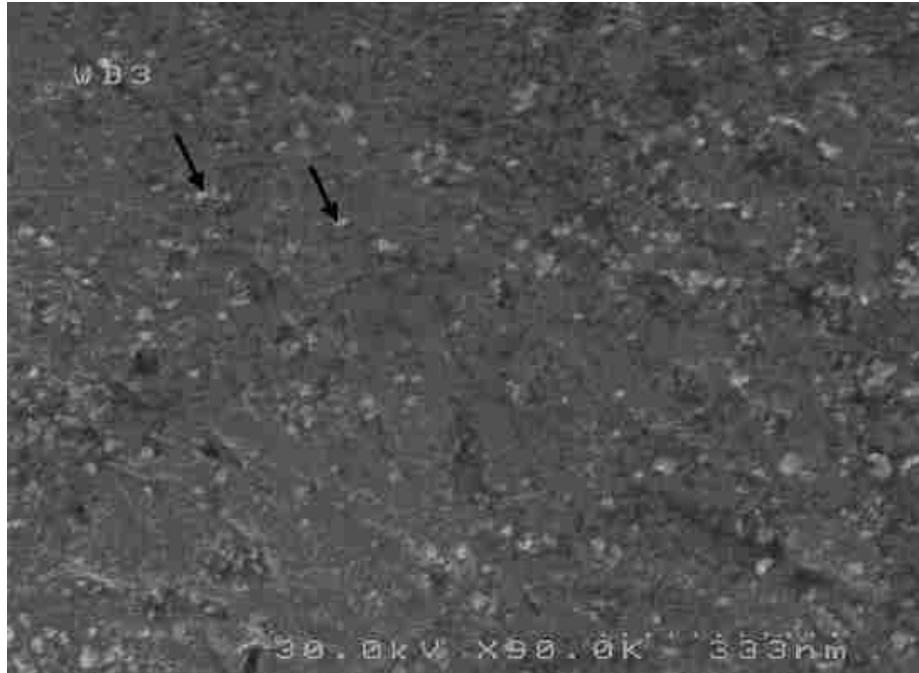


Figure 2.19. Representative FESEM micrograph showing the distribution of aluminum particulates (represented by white spots) in Mg/1.00Alp composite [37].

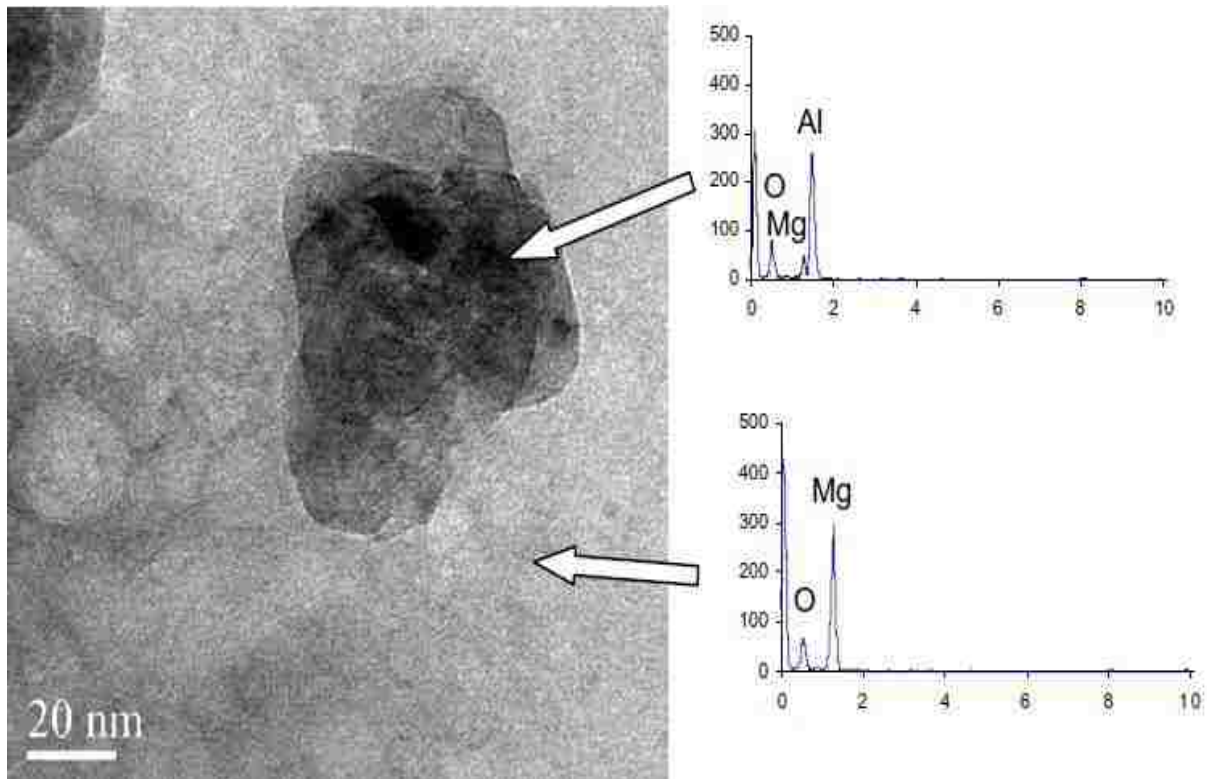


Figure 2.20. TEM micrograph showing good interfacial integrity between Mg matrix and nano-Al particulates. The EDX spectrum verifies the presence of nano-aluminum particulate [37].

2.4.2.5. Nano-sized Silicon Carbide Particles and Carbon Nano Tube Reinforced Pure Magnesium Composite

In 2007, Thakur et al[44] et al carried out silicon carbide and carbon nano tube reinforced pure magnesium composite. The processing method was blending the mixture particles and alloys powder followed by sintering. Silicon carbide powder in 50 nm and multi-walled nanotube in 40-70 nm were prepared as reinforcement. The sintering process is carried out by micro-wave quick method at 640 °C near the melting temperature of magnesium for 25 minutes to remain the original grain size in order to protect the effect of grain refinement by reinforcements. The following hot extrusion was under 400 °C 1 hour holding and 350 °C extrusion temperature. The ratio was 25:1.

The resulting test for the products with 1% volume fraction in total derived that by increasing the SiC volume fraction, the grain size was decreasing; and with the increasing the SiC volume fraction, the porosity was decreasing. The results were reported in Tables 2.11 and 2.12.

Table 2.13 shows the tensile deformation and hardness data for the resulting product. With higher volume fractions of SiC particles, hardness, UTS, and 0.2% YS showed improvement compared to low volume fraction composites. However, with even high volume fraction SiC particles, although the tensile 0.2% YS, UTS, and hardness were improved, the ductility was not as good as those of pure magnesium.

The properties improvement and porosity were superior with nano SiC particles than carbon nano-tube, which should be attributed to the poor bonding between the magnesium matrix and carbon nano-tubes.

Table 2.11 Results of density and porosity measurements [44]

Material	Theoretical density (g/cm ³)	Experimental density (g/cm ³)	Porosity (%)
Mg	1.74	1.737 ± 0.002	0.17 ± 0.11
Mg+0.3%CNT+0.7%SiC	1.746	1.742 ± 0.003	0.23 ± 0.15
Mg+0.5%CNT+0.5%SiC	1.744	1.740 ± 0.001	0.24 ± 0.04
Mg+0.7%CNT+0.3%SiC	1.743	1.739 ± 0.002	0.23 ± 0.09
Mg+1%CNT	1.741	1.736 ± 0.002	0.29 ± 0.10

Table 2.12 Results of CTE determination and image analysis [44]

Material	Average CTE (×10 ⁻⁶ /°C)	Grain size (µm)	Aspect ratio	Roundness
Mg	29.04 ± 1.05	25.9 ± 4.0	1.5 ± 0.2	1.5 ± 0.4
Mg+0.3%CNT+0.7%SiC	28.03 ± 0.38	21.8 ± 1.4	1.5 ± 0.1	1.4 ± 0.3
Mg+0.5%CNT+0.5%SiC	28.13 ± 0.53	21.9 ± 1.3	1.4 ± 0.2	1.4 ± 0.3
Mg+0.7%CNT+0.3%SiC	28.25 ± 0.63	22.1 ± 2.7	1.5 ± 0.2	1.5 ± 0.4
Mg+1%CNT	28.67 ± 0.29	22.3 ± 2.0	1.5 ± 0.3	1.6 ± 0.5

Table 2.13 Results of micro-hardness and tensile properties [44]

Materials	Micro-hardness (HV)	0.2% YS (MPa)	UTS (MPa)	Failure strain (%)
Mg	41 ± 1	111.9 ± 7.7	155.8 ± 2.1	5.9 ± 1.2
Mg+0.3%CNT+0.7%SiC	46 ± 1	152.9 ± 4.1	195.4 ± 4.7	3.3 ± 0.7
Mg+0.5%CNT+0.5%SiC	45 ± 1	152.1 ± 1.2	188.5 ± 2.7	2.3 ± 0.6
Mg+0.7%CNT+0.3%SiC	44 ± 1	139.5 ± 6.5	182.9 ± 7.5	2.1 ± 0.5
Mg+1%CNT	43 ± 1	117 ± 6.2	153.8 ± 2.8	1.5 ± 0.3

2.4.2.6. Nano-sized Alumina Particles and Carbon Nano Tube Reinforced Pure Magnesium

Composite

Alumina powder in 50nm and multi-walled nanotube in 40-70nm size were used as reinforcement for pure magnesium matrix by Thakur et al [45]. The fabrication method was by

powder metallurgy and hot extrusion. The magnesium powders, alumina particles, carbon nano-tube were mixed by blender and sintered between 630 and 640 °C, which was close to pure magnesium melting temperature, to promote better binding between the particulates. The sintering was processed in a microwave instead of furnace for advantage of retention of original microstructure without grain growth to help grain refinement. After the sintering method, a hot extrusion method was carried out at 350 °C with 25:1 extrusion rate under an 150 tons hydraulic press. The holding was at 400 °C for 1 hour.

As shown in Table 2.14, higher volume fractions of alumina resulted in higher porosity. The tendency of hardness was very similar. But, the increment was slight with the addition of nano Al₂O₃ particles (Table 2.15). This phenomenon should be attributed to the combination of hindrance to the motion of mobile dislocations by the presence of the reinforcing alumina particles, grain refinement resulting from alumina particulates presence, and the low level of porosity that helps improving the hardness of composite.

With increasing the aluminum volume fraction, the 0.2% yield strength, ultimate tensile strength, and the failure strain were improved that represented in Table 2.16. The 1% CNT reinforcement composite had inferior properties, which might be due to the following two points:

- 1) Poor interfacial bonding between CNT particulates and magnesium matrix for ineffective load transfer from matrix to CNT particulates, and
- 2) Uneven distribution of CNT particulates in the magnesium matrix.

Figures 2.21 and 2.22 showed the tensile failure microstructure of the Mg-1 vol.% CNT composite and Mg-0.7 vol.%CNT-0.3 vol.%Al₂O₃. With the decreasing in CNT volume fraction, the macro cracks decreased. The Mg-1% CNT composite failed in a cleavage like features; while the Mg-0.7%CNT-0.3%Al₂O₃ composite failed for overall of its content.

Table 2.14 Results of porosity and density measurements Mg/CNT/alumina [45]

Materials	Reinforcement (vol. %)		Theoretical density (g/cm ³)	Experimental density (g/cm ³)	Porosity (%)
	CNT	Al ₂ O ₃			
Mg+1%CNT	0.7	-	1.746	1.735 ± 0.008	0.611 ± 0.460
Mg+0.7%CNT+0.3%Al ₂ O ₃	0.5	0.1	1.747	1.737 ± 0.005	0.592 ± 0.258
Mg+0.5%CNT+0.5%Al ₂ O ₃	0.3	0.2	1.748	1.745 ± 0.002	0.191 ± 0.119
Mg+0.3%CNT+0.7%Al ₂ O ₃	0.2	0.3	1.749	1.730 ± 0.001	1.068 ± 0.066

Table 2.15 Results of hardness tests Mg/CNT/alumina [45]

Materials	Macrohardness (Rockwell superficial 15T)	Vickers microhardness (HV)
Mg+1%CNT	47.9 ± 2.6	43.2 ± 1.6
Mg+0.7%CNT+0.3%Al ₂ O ₃	48.0 ± 0.8	43.5 ± 1.4
Mg+0.5%CNT+0.5%Al ₂ O ₃	48.2 ± 1.5	43.7 ± 2.3
Mg+0.3%CNT+0.7%Al ₂ O ₃	48.3 ± 1.5	44.2 ± 1.8

Table 2.16 Results of tensile tests Mg/CNT/alumina [45]

Materials	0.2% Yield strength (MPa)	UTS (MPa)	Failure strain (%)
Mg+1%CNT	112.9 ± 2.8	146.5 ± 6.5	1.9 ± 0.9
Mg+0.7%CNT+0.3%Al ₂ O ₃	131.4 ± 6.2	164.3 ± 11.2	2.6 ± 1.3
Mg+0.5%CNT+0.5%Al ₂ O ₃	136.5 ± 5.8	181.0 ± 8.6	2.5 ± 0.4
Mg+0.3%CNT+0.7%Al ₂ O ₃	153.5 ± 2.1	196.0 ± 3.3	2.5 ± 0.8

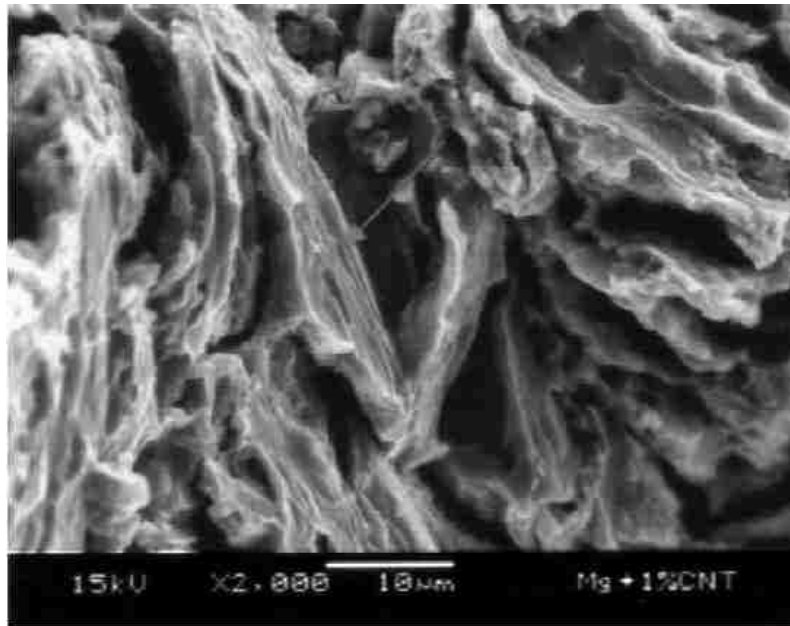


Figure 2.21. SEM micrograph showing cleavage step like features in the magnesium matrix of the Mg+1%CNT composite [45].

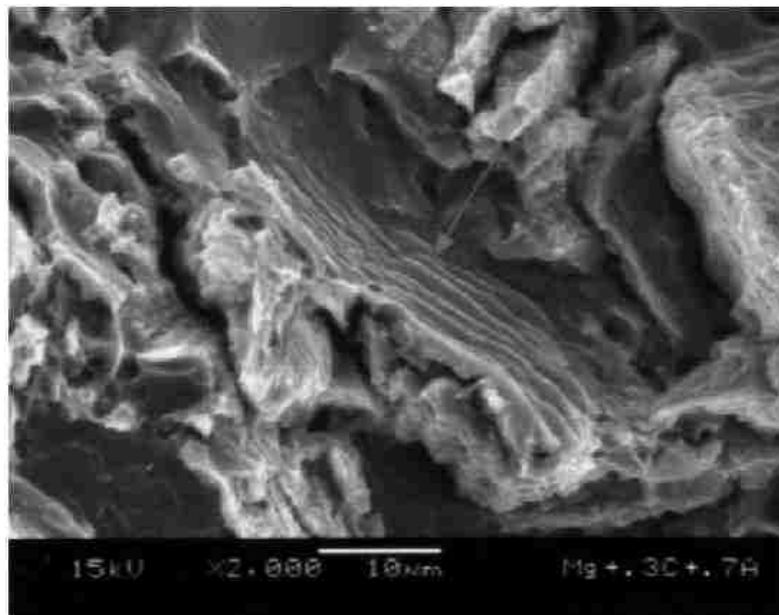


Figure 2.22. SEM micrograph showing intrinsic features on the fracture surface of the Mg+ 0.3%CNT + 0.7%Al₂O₃ composite sample deformed in uniaxial tension [45].

2.5. Hybrid Composite Magnesium

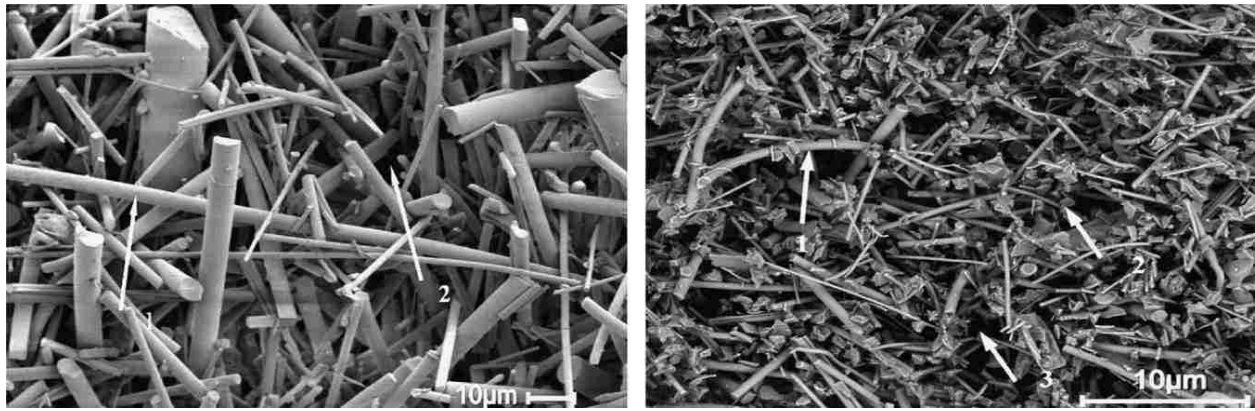
2.5.1. Solidification process

Hybrid reinforcements in magnesium alloy are considered as a comprehensive method for mass and inexpensive production. The combination of fibers and particles provides wide range of modifications for demand of mechanical properties. The processing method is generally similar to fibers reinforced magnesium composites with a difference in preform fabrication. The hybrid preform is fabricated by introducing binding compounds, forming the shape of preforms under certain pressure, drying and sintering. The direction of fibers is not required as in the unidirectional as the fiber reinforced composites [46].

2.5.2. Microstructure and Mechanical Properties

2.5.2.1. Hybrid Reinforced AM60 Magnesium Composites

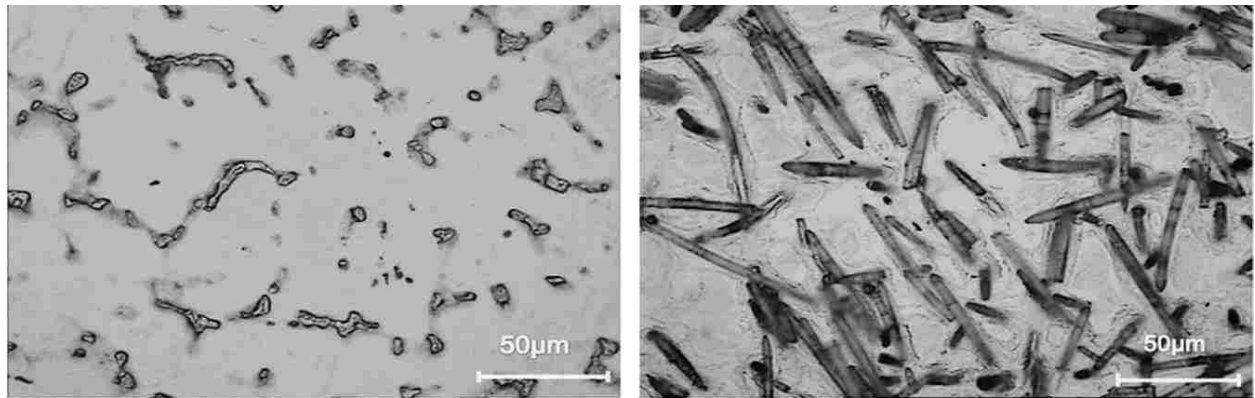
AM60-based hybrid composites were made with alumina fibers with/without particles. Figure 2.23 shows the SEM analysis microstructure of the preforms by Zhang et al][46],. Figure 2.24 shows the microstructures of AM60 and its composites with fibers and hybrid reinforcement with same composition of fibers. Figure 2.25 shows the measured grain sizes. The results indicates that fibers refine the grain size of the fibre-only composite. With the addition of micron particles, the combination of two types of reinforcement refines the grain structure significantly. Figures 2.26 and 2.27 present the hardness and stress-strain curves. The additions of particles improve the mechanical properties of the AM60-based hybrid composites.



(a)

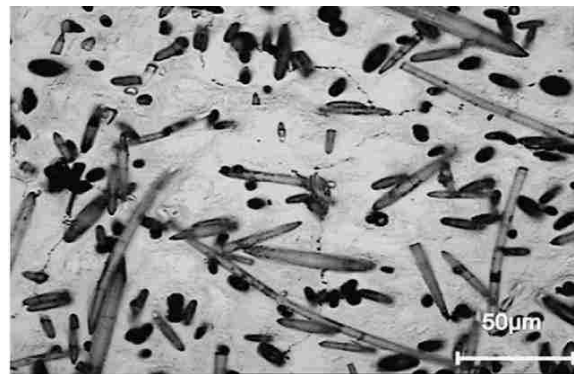
(b)

Figure 2.23. SEM Micrograph of (a) Pure Fibre Perform, arrow1—fibre and arrow2—empty cell, (b) Hybrid Preforms, arrow1—fibre, arrow2—particle and arrow3—empty cell [46]



(a)

(b)



(c)

Figure 2.24. Optical Photograph Showing the Microstructures of Matrix Alloy and Composites, (a) AM60, (b) 9%Fibres/AM60, and (c) (4% particles +9%Fibres)/AM60 [46].

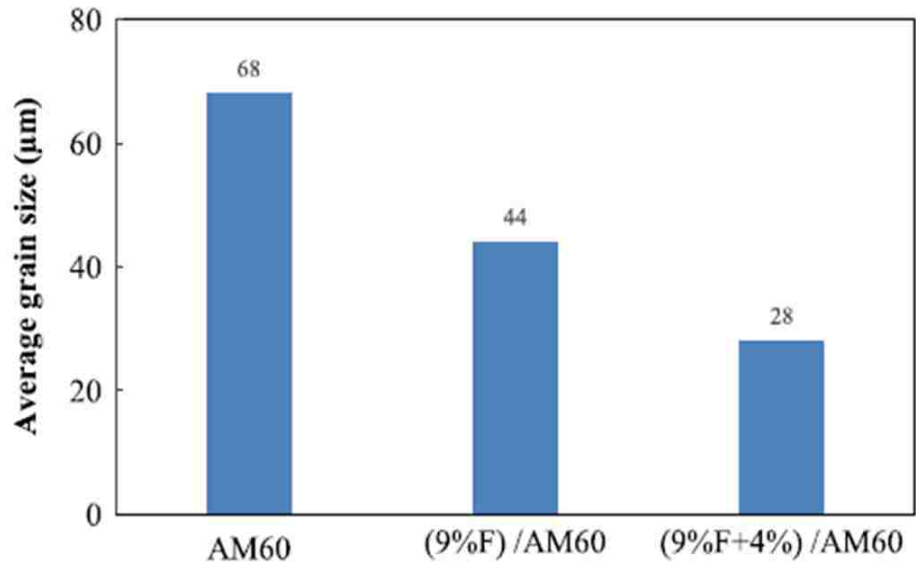


Figure 2.25. Grain Size of the Matrix Alloy, F/AM60 and (F+P)/AM60 Composites [46].

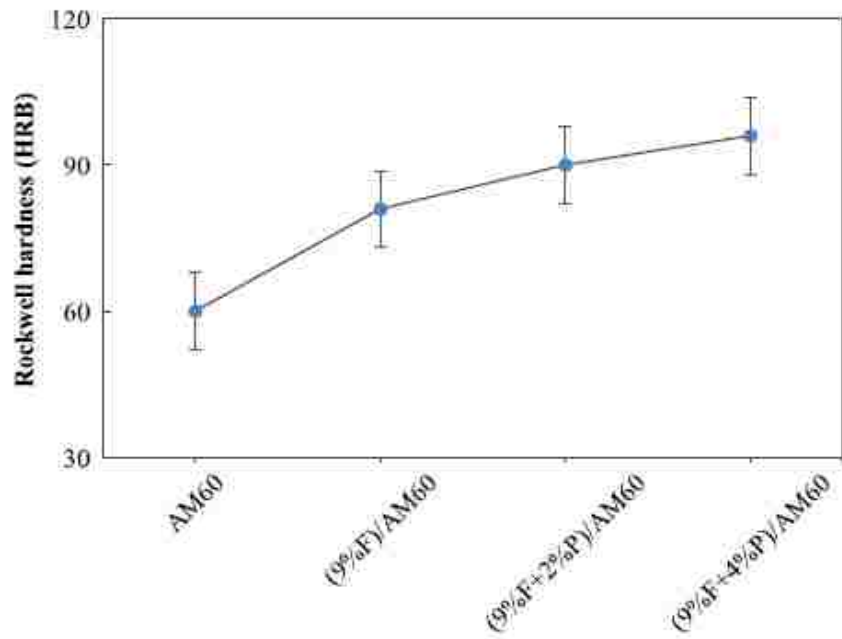


Figure 2.26. Hardness Measurements for the Matrix Alloy and Composites [46].

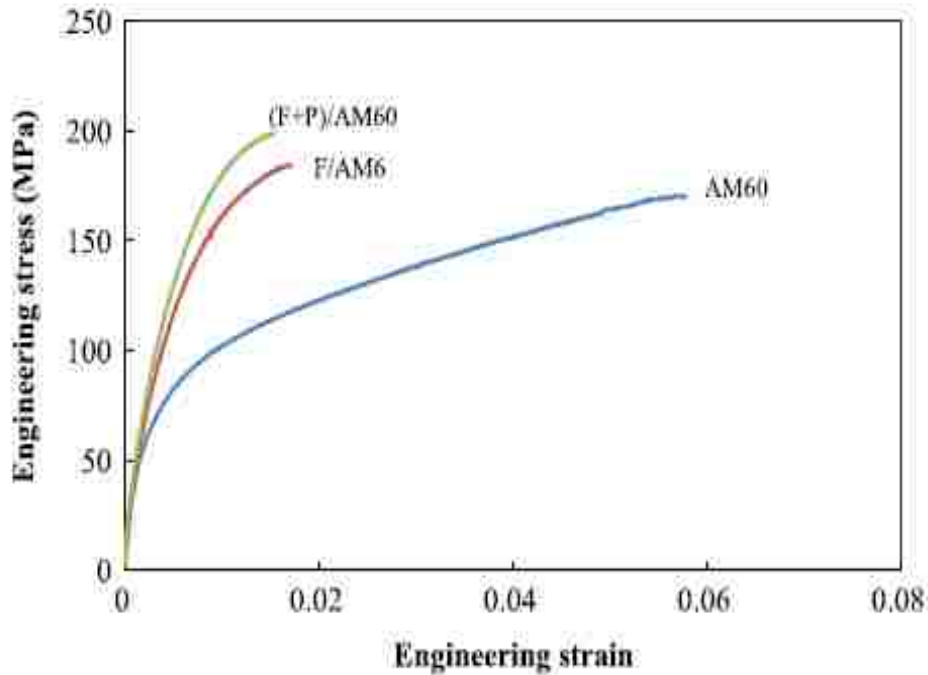


Figure 2.27. Typical Engineering Stress vs. Strain Curves for AM60 alloy, F/AM60, and (P+F)/AM60 Composites [46].

2.6. Other Fabrication Methods for Magnesium-Based Composites

Although the powder metallurgy, squeeze casting, and stirring followed by hot extrusion methods, which are demonstrated to be the effective processes for fabricating magnesium-based composites according to reinforcements types, have been introduced in previous sections, there are still other methods reported for magnesium-based composites.

2.6.1. In-situ Synthesis

In-situ synthesis is a fabrication process differed from casting. Casting, as its process feature, can be described as ex-situ synthesis. For magnesium-based casting, casting (hot extrusion included) adds external reinforcement into the bulk magnesium-based material. In in-situ synthesis, the reinforcement is generated inside the bulk material by controlling and take

advantage of reactions between compositions of bulk material. As this feature, especially for magnesium-based composite fabrication, very limited systems have been studied.

Mg-Si system is one of the systems studied to fabrication of Mg-based composites reinforced by Mg_2Si . The Si added to magnesium alloy can either readily react with the magnesium during the melting process or can precipitate from the matrix during the cooling process in the form of an intermetallic Mg_2Si phase. The low-cost and abundance explains the reason why Mg-Si alloy has been studied for in-situ synthesis of a magnesium-based matrix composite. The Mg-Si phase has excellent hardness, but imposes serious difficulties in casting Mg- Mg_2Si with a high content of Mg_2Si [9, 47]. The tendency of Mg_2Si to form coarse needle-shape Mg_2Si phase at high concentration of Si can reduce the mechanical properties of the final product.

The other system Mg-Ti-C was studied by Hwang et al [48] for nano-particle reinforcement magnesium-based alloy. Milling was the preparation of material for this in-situ process. The Mg, Ti, C powders were milled for 24 hours for the complete reaction of Ti and C followed by sintering at 350 °C.

2.6.2. Pressure-less Infiltration

The pressure-less infiltration is relatively new compared to pressure infiltration (squeeze casting). During the infiltration process, molten alloys flow through the channels of the reinforcement bed or preform under the capillary action. For spontaneous infiltration, certain infiltration agents are required for each unique system.

SiC/Mg composite has been studied by Hiromitsu and Takoo [49] for pressure-less infiltration. The experiment set-up is shown schematically in Figure 2.28. SiC micron particles and infiltration agent SiO_2 powders were mixed and placed in the bottom crucible. The upper

crucible containing pure magnesium ingot that was placed on the top of the powder mixture. When the system was heated, the magnesium was melted, and spontaneously infiltrated the powder mixture. The reaction between SiO_2 and magnesium to form MgO and Si provided the localized heat to resist solidification of Mg liquid and localized route for Mg liquid to penetration the SiC powders. The resulting composite microstructure is shown in Figure 2.29. The reinforcement distribution is evenly in the magnesium matrix.

The key of this pressure-less infiltration was the reaction of infiltration agent SiO_2 and matrix magnesium. The infiltration behaviors depended mainly on the SiO_2 content and powder size. Without SiO_2 , there was no infiltration. To acquire decreased size SiC , the minimum SiO_2 content needed to start the infiltration process.

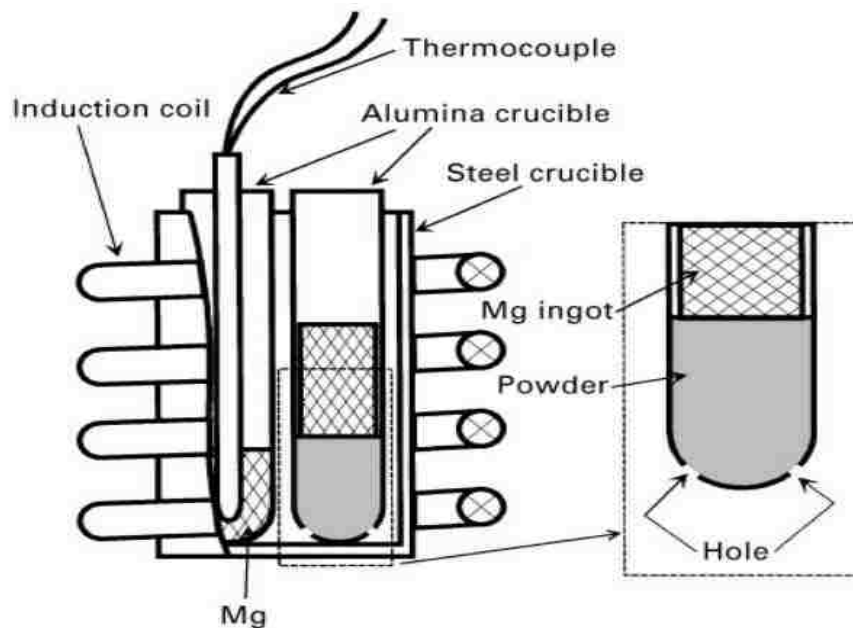


Figure 2.28. Experiment Set-up for Pressure-less Infiltration SiC/Mg [49].

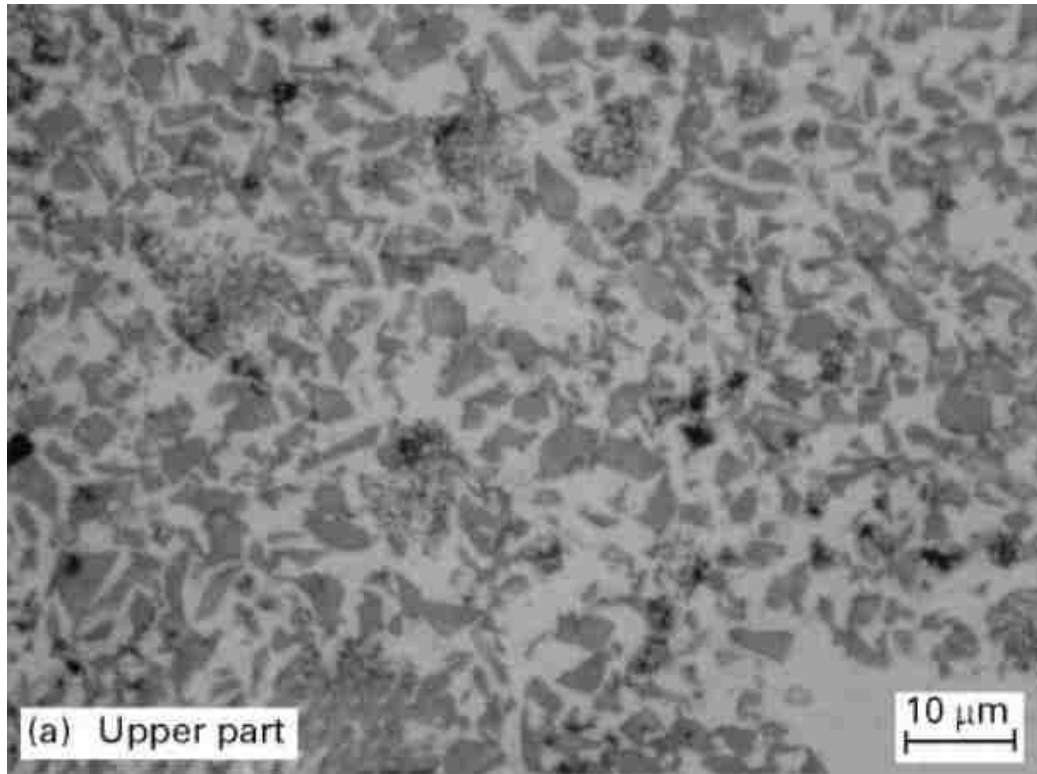


Figure 2.29. The Microstructure of the Infiltrated SiC/Mg Composites [49].

2.6.3. Gas Injection

The Gas injection is a process that reinforcement carried by gases is blown into the liquid phase matrix metal. The study carried out by Hansen et al [50] showed the fabrication of AZ91 alloy magnesium based composite reinforced by SiC and Al₂O₃ particles by the gas injection. Particles were transported through a tube below the bath surface of molten AZ91 alloy at 720-730 °C with the carrier gas of Ar or N₂. The resulting composite contained evenly distributed reinforcement in AZ91 matrix. However, the presence of a number of clusters and agglomerates of the particulates and the limitation of volume fractions of reinforcement made this process less attractive.

2.6.4. Spray Forming

The spray forming directs the molten materials droplets onto a substrate to build up bulk metallic materials. For magnesium composite fabrication, the reinforcement particles are injected into the stream of the atomized matrix materials. SiC in 8 to 12 micron-meters reinforced QE22 magnesium alloy has found the process parameters exerts considerable influence on the resulting microstructure [51]. As the rapid solidification during the spray forming process, the fine grains, porosity, and absence of brittle phase at the SiC/matrix has been proved [9]

2.7. Summary

Significant research efforts have been made in the recent decades for improving mechanical properties of magnesium alloys by introducing reinforcement addition. Several improvements are made in not only just mechanical property enhancement but also economic fabrication technologies. Powder metallurgy is an effective process method for fabrication of Mg-based composite. However, due to its requirement of powder metals and reinforcement, its high cost seems not acceptable. In-situ methods, which control the reaction of forming reinforcement inside the matrix, require strict metallurgy system as well as ambient condition. Only few systems have been tried such like Mg-Si with Mg_2Si reinforcement. Despite its economy of the in-situ process, the presence the needle-shaped Mg_2Si phase reduces the mechanical properties of the composite. Pressure-less infiltration needs a minimum size of powder and infiltration agents such as SiO_2 with strict content. The gas injection method, which requires support from inert gas to inject reinforcement into matrix, limits the volume fraction of the reinforcement. Spray forming is not ideal for the fabrication of composites as the

homogeneous reinforcement distribution is hard to achieve. For nano-sized particle-reinforced magnesium composites, due to the introduction of tiny powder reinforcement, quick sintering to prevent grain coarsen and hot extrusion to densify materials, which are considered as the effective processes, must be applied for the mixture of reinforcement and magnesium-based matrix after blending or stirring. As such, strict material preparation procedures of nano particle-reinforced Mg-based composites are required. Duplicated thermal processes in the DMD technique significantly increase the manufacturing cost and prevent the nano composite from applications with complex geometries in large sizes. Those drawbacks limit the nano-sized reinforcement Mg-based composites to be applied for large scale industrial fabrication. On the other hand, the advantage of nano-sized reinforcement Mg-based composites is that the composite brittleness caused by increased volume fractions of reinforcement in micron size has been significantly reduced by the substitution of ceramic nano particles. The introduction of metallic nano particles such as aluminum into magnesium nano composites can make the composite even more ductile than the matrix itself with improved tensile and compressive properties. Despite the fineness of particles influences the refinement of matrix grain structure, the key to the success in the full engagement of particles in the magnesium composites is the bonding between matrix and reinforcement. Squeeze casting with preform infiltration has been demonstrated that the most effective and economic method for fabrication of micron-sized fiber or particle-reinforced only, and hybrid fiber and particles reinforced magnesium composites in relatively large sizes. Hence, the preform and squeeze casting technology could enable the Mg-based hybrid nano composites to be applied cost-effectively for complex geometries with various sizes in the highly competitive automotive industry.

2.8. References

- [1] S.B. Singh, Metal Matrix Composites: A potential Material for Futuristic Automotive, SAE Technical Paper, (26) (2003) 38.
- [2] M. Kim, T. Lim, K. Yoon, and Y. Ko, Development of Cast-Forged Knuckle using High Strength Aluminum Alloy, SAE Technical Paper, 01 (2011) 537.
- [3] A. Sherman and P. Sklad, Collaborative Development of Lightweight Metal and Alloys for Automotive Applications, SAE Technical Paper, 01 (2002) 1938.
- [4] H. Friedrich and S. Schumann, The Second Edge of Magnesium: Research Strategies to Bring the Automotive Industry's Vision to Reality, Magnesium 2000: Second International Conference on Magnesium Science & Technology. (2000) 9-18.
- [5] Bavarian Motor Works (2007) Magnesium fosters rebirth of an automotive engine. International Magnesium Association: The global voice for magnesium (May):1–3, = Retrieved 4 December, 2015, from <http://www.intlmag.org/showcase/mg001.pdf>.
- [6] P.K. Rohatgi, Use of Lightweight Metal-Matrix Composites for Transportation Applications in India, In Proceedings of the third International Conference on Automotive and Fuel Technology (453). Allied Publishers.
- [7] W.H. Hunt and D.B. Miracle, Automotive Applications of Metal Matrix Composites, ASM hand book: Composites, ASM International, Materials Park, Ohio, (21) (2001) 1029-1032.
- [8] L. X. Hu and E. D. Wang, Materials Science and Engineering: A, 278 (2000) 267.
- [9] H.Z. Ye, X.Y. Liu, Review of Recent Studies in Magnesium Matrix Composites, Journal of Materials Science, 39 (2004) 6153-6171.

- [10] M.C. Kuo, J.C. Huang, M. Chen, and M.H. Jen, Fabrication of High Performance Magnesium/Carbon-Fiber/PEEK Laminated Composites, *Materials Transactions*, 44, (8) (2003) 1613-1619.
- [11] L. Broutman and R. Krock, *Metal-Matrix Composites*, Academic Press, Inc., New York, (1974).
- [12] J.E. Hack, R.A. Page, g. R. Leverant, Tensile and Fatigue Behavior of Aluminum Oxide Fiber Reinforced Magnesium Composites: Part I. Fiber Fraction and Orientation, *Metallurgical Transactions A*, 15 (7) (1984) 1389-1396.
- [13] V. Skylenicka, M. Pahutova , K. Kucharova , M. Svoboda, and T.G. Langdon, Creep Processes in Magnesium Alloys and their Composites, *Metallurgical and Materials Transactions A*, March 2002, 33 (3) 883–889.
- [14] C. Suman, Creep of Diecast Magnesium Alloys AZ91D and AM60B, SAE Technical Paper, 910416, (1991).
- [15] H.A. Katzman, Fibre Coatings for the Fabrication of Graphite-reinforced Magnesium Composites, *Journal of Materials Science* 22 (1987) 144-148.
- [16] D.C. Bradley, R.C. Mehrotra and D.P. Gaur, *Metal Alkoxides*, Academic Press, New York, (1978).
- [17] L.L. Hench and D.R. Ulrich , *Ultrastructure Processing of Ceramics, Glasses and Composites*, Wiley, New York, (1984).
- [18] C.J. Brinker, D.E. Clark and D. R. Ulrich, *Better Ceramics Through Chemistry*, North-Holland, New York, (1984).
- [19] Data Sheet, Die Casting Magnesium Alloys, Norsk Hydro Magnesium, (1995).

- [19] A. Luo, Processing, Magnesium, Microstructure, and Mechanical Metal Matrix Composites Behavior of Cast, Metallurgical and Materials Transactions A, September 1995, 26 (9) 2445–2455.
- [21] J. Lo, Microstructural and Interfacial Characteristics of SiC Reinforced AZ91D Magnesium based Composite. Metallographic Techniques and the Characterization of Composites, Stainless Steels, and Other Engineering Materials, Microstructural Science, 22 (1994) 237-248.
- [22] H. Hu, Grain microstructure evolution of Mg (AM50A)/SiC p metal matrix composites, Scripta Materialia 39 (8) (1998) 1015-1022.
- [23] M. Mabuchi, Y. Chino, H. Iwasaki, T. Aizawa, K. Higashi. The Grain Size and Texture Dependence of Tensile Properties in Extruded Mg–9Al–1Zn. Materials Transactions, JIM 42 (9) (2001) 1182.
- [24] H. Watanabe, T. Mukai, M. Mabuchi, K. Higashi. Superplastic Deformation Mechanism in Powder Metallurgy Magnesium Alloys and Composites. Acta Materialia, 49 (37) (2001) 2027.
- [25] H. Lianxi, W. Erde, Fabrication and Mechanical Properties of SiCw/ZK51Amagnesium Matrix Composite by Two-step Squeeze Casting, Materials Science and Engineering: A, 278 (1–2) (2000) 267-271
- [26] M. Gupta, L. Lu, M.O. Lai, K.H. Lee. Microstructure and Mechanical Properties of Elemental and Reinforced Magnesium Synthesized Using a Fluxless Liquid-phase Process, Mrs Bulletin, 34 (14) (1999) 1201.
- [27] H. Ferkel, B.L. Mordike. Magnesium Strengthened by SiC Nanoparticles. Materials Science and Engineering: A, 298 (2001) 193–199.

- [28] P. Perez, G. Garces, P. Adeva, Mechanical Properties of a Mg–10 (vol.%)Ti Composite, *Composites Science and Technology* 64 (2004) 145–151
- [29] C.R. Dandekar and Y.C. Shin, Effect of Porosity on the Interface Behavior of an Al₂O₃-Aluminum Composite: A Molecular Dynamics Study, *Compos. Sci. Technol.*, 71 (2011) 350–356
- [30] X.J. Wang, K. Wu, W.X. Huang, H.F. Zhang, M.Y. Zheng, and D.L. Peng, Study on Fracture Behavior of Particulate Reinforced Magnesium Matrix Composite Using In Situ SEM, *Compos. Sci. Technol.*, 67 (2007) 2253–2260
- [31] X.J. Wang, L. Xu, X.S. Hu, K.B. Nie, K.K. Deng, K. Wu, and M.Y. Zheng, Influences of Extrusion Parameters on Microstructure and Mechanical Properties of Particulate Reinforced Magnesium Matrix Composites, *Materials Science and Engineering: A*, 528 (2011) 6387–6392
- [32] S.F. Hassan and M. Gupta, Development of High Performance Magnesium Nanocomposites Using Nano-Al₂O₃ as Reinforcement, *Materials Science and Engineering: A*, 392 (2005) 163–168
- [33] K.B. Nie, X.J. Wang, L. Xu, K. Wu, X.S. Hu, and M.Y. Zheng, Effect of Hot Extrusion on Microstructures and Mechanical Properties of SiC Nanoparticles Reinforced Magnesium Matrix Composite, *Journal of Alloys and Compounds.*, 512 (2012) 355–360
- [34] M.J. Shen, W.F. Ying, X.J. Wang, M.F. Zhang, and K. Wu, Development of High Performance Magnesium Matrix Nanocomposites Using Nano-SiC Particulates as Reinforcement, *The Journal of Materials Engineering and Performance*, 24 (2015) 3798–3807

- [35] L.M. Tham, M. Gupta, and L. Cheng, Influence of processing parameters during disintegrated melt deposition processing on near net shape synthesis of aluminum based metal matrix composites, *Materials Science and Technology*, 15 (10) (1999) 1139–1146.
- [36] M. Gupta, M.O. Lai, and S.C. Lim, Regarding the processing associated microstructure and mechanical properties improvement of an Al-4.5 Cu alloy, *Journal of Alloys and Compounds*, 260 (1-2) (1997) 250–255,
- [37] X.L. Zhong, W.L.E. Wong, M. Gupta, Enhancing Strength and Ductility of Magnesium by Integrating it with Aluminum Nanoparticles, *Acta Materialia*, 55 (2007) 6338–6344
- [38] M. Paramsothy, J. Chan, R. Kwok, M. Gupta, The Overall Effects of AlN Nanoparticle Addition to Hybrid Magnesium Alloy AZ91/ZK60A Hybrid Magnesium Alloy AZ91/ZK60A, *Journal of Nanotechnology*, (2012) Article ID 687306
- [39] S. Sankaranarayanan, R.K. Sabat, S. Jayalakshmi, S. Suwas, and M. Gupta, Effect of Nanoscale Boron Carbide Particle Addition on the Microstructural Evolution and Mechanical Response of Pure Magnesium, *Materials & Design*, 56 (2014) 428–436
- [40] M.C. Zhao, T. Hanamura, H. Qiu, and K. Yang, Low Absorbed Energy Ductile Dimple Fracture in Lower Shelf Region in an Ultrafine Grained Ferrite/Cementite Steel, *Metallurgical and Materials Transactions A*, 37 (2006) 2897–2990
- [41] S.F. Hassan and M. Gupta, Effect of Particulate Size of Al₂O₃ Reinforcement on Microstructure and Mechanical Behavior of Solidification Processed Elemental Mg, *Journal of Alloys and Compounds*, 419 (1-2) (2006) 84–90.
- [42] S.F. Hassan and M. Gupta, Effect of different types of nanosize oxide participates on microstructural and mechanical properties of elemental Mg, *Journal of Materials Science*, 41 (8) (2006) 2229–2236.

- [43] M. Paramsothy, S.F. Hassan, N. Srikanth, M. Gupta, Enhancing tensile/compressive response of magnesium alloy AZ31 by integrating with Al₂O₃ nanoparticles, *Materials Science and Engineering A*, 527 (2009) 162–168
- [44] S.K. Thakur, G.T. Kwee, M. Gupta, Development and Characterization of Magnesium Composites Containing Nano-sized Silicon Carbide and Carbon Nanotubes as Hybrid reinforcements, *Journal Materials Science*, 42 (2007) 10040–10046
- [45] S.K. Thakur, T.S. Srivatsan, M. Gupta, Synthesis and Mechanical Behavior of Carbon Nanotube–magnesium Composites Hybridized with Nanoparticles of Alumina, *Materials Science and Engineering A*, 466 (2007) 32–37
- [46] X. Zhang, Q. Zhang, H. Hu, Tensile Behavior and Microstructure of Magnesium AM60-based Hybrid Composite Containing Al₂O₃ Fibres and Particles, *Materials Science & Engineering, A*, 607 (2014) 269–276
- [47] S. Beer, G. Frommeyer, E. Schmid, *Magnesium Alloys and Their Applications*, 317-324, (1998) Frankfurt, Germany, DGM Informationsgesellschaft.
- [48] S. Hwang, C. Nishimura, P.G. McCormick, Compressive Mechanical Properties of Mg-Ti-C Nanocomposite Synthesised by Mechanical Milling, *Scripta Materialia*, 44 (2001) 2457–2462
- [49] K. Hiromitsu, C. Takao, Fabrication of Particulate Reinforced Magnesium Composites by Applying a Spontaneous Infiltration Phenomenon, *Journal of Materials Science*, 32 (1997) 47-56
- [50] N. L. Hansen, T.A. Engh, O. Lohne, *The Minerals, Metals & Materials Society*, 1990, 241

[51] T. Ebert, F. Moll, K.U. Kainer, Spray Forming of Magnesium Alloys and Composites, Power Metallurgy, 40 (2) (1997) 126-130.

CHAPTER 3 Processing and Properties of As-cast Magnesium AM60-Based Composite Containing Alumina Nano Particles and Micron Fibres

3.1. Introduction

The need for high-performance and lightweight materials in automobile and aerospace industries has led to extensive research and development efforts generating metal matrix composites (MMCs) and cost-effective fabrication technologies. The major disadvantage of MMCs usually lies in the relatively high cost of fabrication and reinforcement materials. The cost-effective processing of composite materials is, therefore, an essential element for expanding their applications. This is especially true for the high performance magnesium-based materials due to their high material and processing costs [1-4]. Since hybrid composites are fabricated by adding two or more reinforcements into matrix materials, excellent properties and a high degree of design freedom combinations including short fibres and different size particles become achievable. As magnesium matrix composites are reinforced with hybrid reinforcement in which both of the particles and short fibres are employed, large opportunities are provided to optimize the engineering performance of magnesium based composites for potential applications in automobile and aerospace industries [5]. The fabrication process for the hybrid preform with cellular structure made by micron-sized ceramic Al_2O_3 particles and Al_2O_3 fibres was described by Zhang [6]. Although the micron particle-reinforced magnesium alloy processes higher tensile strength and elastic modulus compared to the unreinforced magnesium alloy, a remarkable reduction in ductility is somewhat disappointing. To minimize ductility reduction recently, nano-sized particles were introduced into magnesium alloys by substituting micron-sized particles [7, 8]. However, high cost of nanoparticles and manufacturing processes make them

less attractive to the highly competitive automotive industry than conventional approaches, i.e., stir casting and/or preform and squeeze casting.

In this article, the on-going work on the development of the preform-squeeze casting process, which is capable of infiltrating liquid magnesium alloy into the hybrid preform containing nano particles and micron fibres under an applied pressure, was presented. Both of the optical microscopy (OM) and scanning electron microscopy (SEM) were employed for the microstructural analysis of the composite. The informative results of tensile testing on the hybrid composites are compared with those of the unreinforced matrix alloy.

3.2. Experimental Procedures

3.2.1. Materials

Al_2O_3 ceramic particles sized as 200 nm and Al_2O_3 short fibres with an average diameter of 3 μm and height of 50 μm were employed as the raw materials for preparation of the hybrid reinforcements since they are relatively inexpensive and possess adequate properties. The matrix alloy AM60, with a chemical composition (wt.%) of 6.0Al-0.22Zn-0.4Mn-0.1Si-0.01Cu-0.004Fe-0.002Ni-Mg, was chosen for its widespread use in the automotive industry with high ductility and moderate strengths. The thermo-physical properties of the ceramic Al_2O_3 nano particle, Al_2O_3 fibre and matrix alloy AM60 are given in Table 3.1.

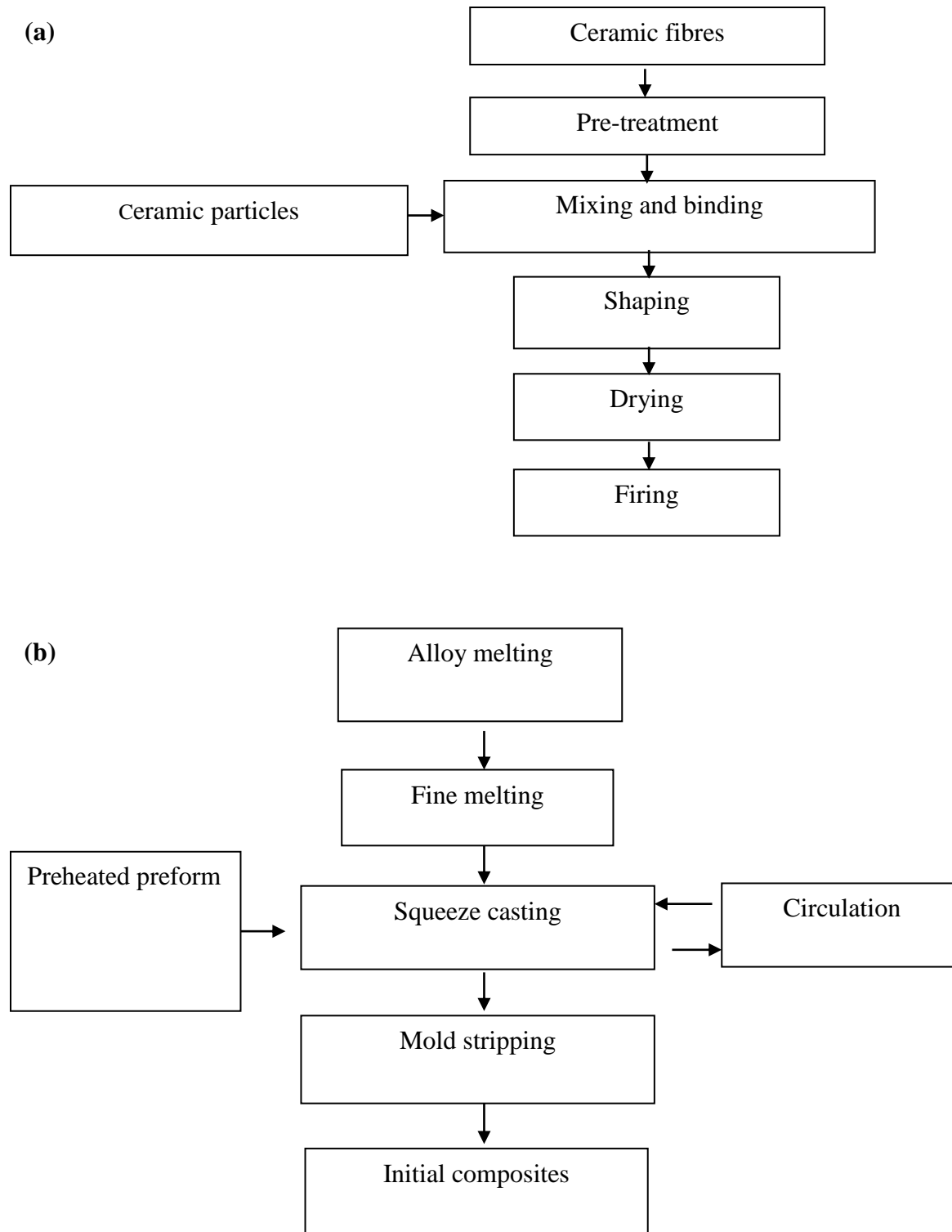


Figure 3.1. Flowchart showing the procedure for fabricating hybrid (a) preform and (b) composites.

Table 3.1 Thermo-physical properties of the ceramic Al₂O₃ nano particle, Al₂O₃ fibre and matrix alloy AM60; Physical chemistry of property of ceramic grain and fibre Al₂O₃ and magnesium alloy

Material	Al ₂ O ₃ particle	Al ₂ O ₃ fibre	AM60
APS size	200 nm		
Density g/cm ³	3.97	3.40	

3.2.2. Fabrication of hybrid preform

The preparation steps for fabrication of the hybrid preforms (Figure 3.1, a) involve mixing the ceramic short fibres and particles, introducing the binding compounds, forming the preform shape under pressure, drying and sintering. In the hybrid preform, the fibres serve as the skeleton for a cellular structure. The content level of the fibre was pre-determined based on the desired amount of porosity in the cellular solid. The particulate reinforcements were dispersed in the pores present in the cellular solid. The content, size and type of the ceramic reinforcements were adjusted to yield the required quantity, and shape of preform. In addition, for the purpose of a comparative study of the hybrid preform characteristics; a pure fibre preform was also fabricated using the same process without adding particulate reinforcements.

3.2.3. Fabrication of composites

Figure 3.1 (b) shows the fabrication process for the composites in which a squeeze casting process was adopted. During fabrication, a hybrid preform was first preheated to 300 0C. Then, molten matrix alloy AM60 at 750 0C infiltrated into the preheated preform under an applied

pressure of 90 MPa. The pressure was maintained at the desired level for 25 seconds. After squeeze casting, a cylindrical disk of dual-phase reinforced composite with 3 vol.% Al₂O₃ nano-sized particles and 5 vol.% Al₂O₃ fibres, named (F+P)/AM60, was obtained. In the hybrid composite, the particles constituted the primary reinforcement phase, and short fibres served as the secondary reinforcement phase. For the purpose of comparison, a composite (F/AM60) with only 5vol. % Al₂O₃ fibre reinforcement was also prepared.

3.2.4. Microstructure analysis

All specimens were cut from the center of the casting coupon. The samples were then polished and etched for the microstructural analysis. The primary characteristics of the prepared samples were investigated under an optical microscopy (Buehler image analyzer 2002). A scanning electron microscope (SEM) was employed for the detailed analysis of the microstructure. The maximum resolution used was up to 100 nm, which was in a backscattered mode. To further analyze the composition of the material, the energy dispersive spectroscopy (EDS) was used during the microstructure analysis.

3.2.5. Tensile testing

The INSTRON machine was employed for the tensile test and the test rate was set as 0.05mm/min. The mechanical properties for both of the composites and unreinforced matrix alloy were evaluated by tensile tests, by following ASTM B557. The tensile tests were performed at ambient temperature. Based on the average of three tests, the mechanical

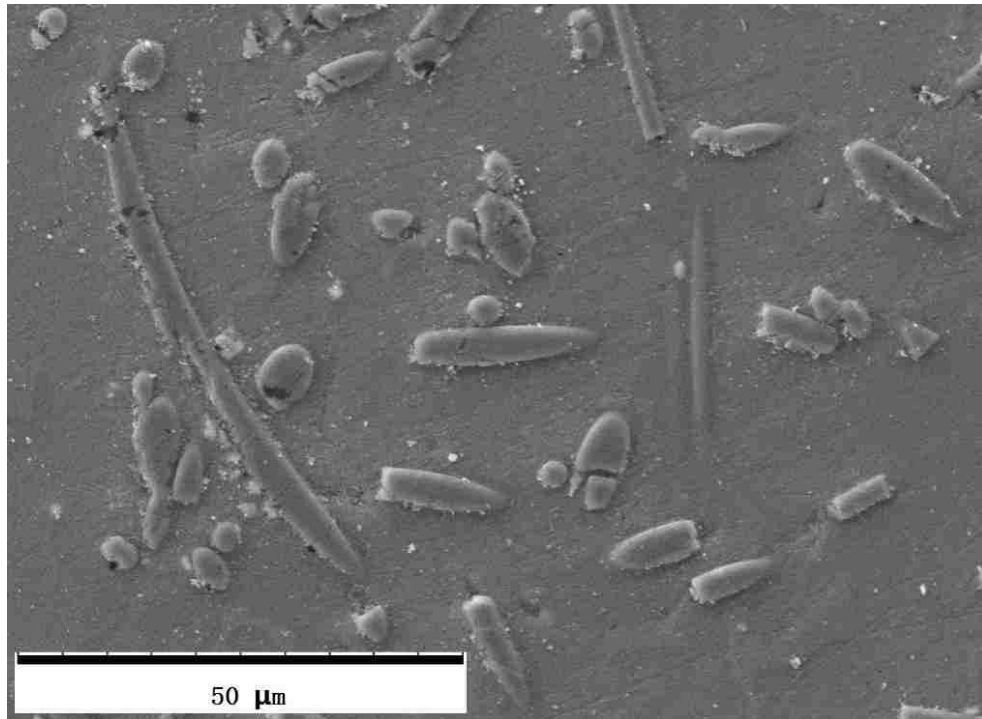
properties, such as elastic modulus (E), ultimate tensile strength (UTS), yield strength (YS) and elongation (ϵ_f) were obtained.

3.3. Results and Discussion

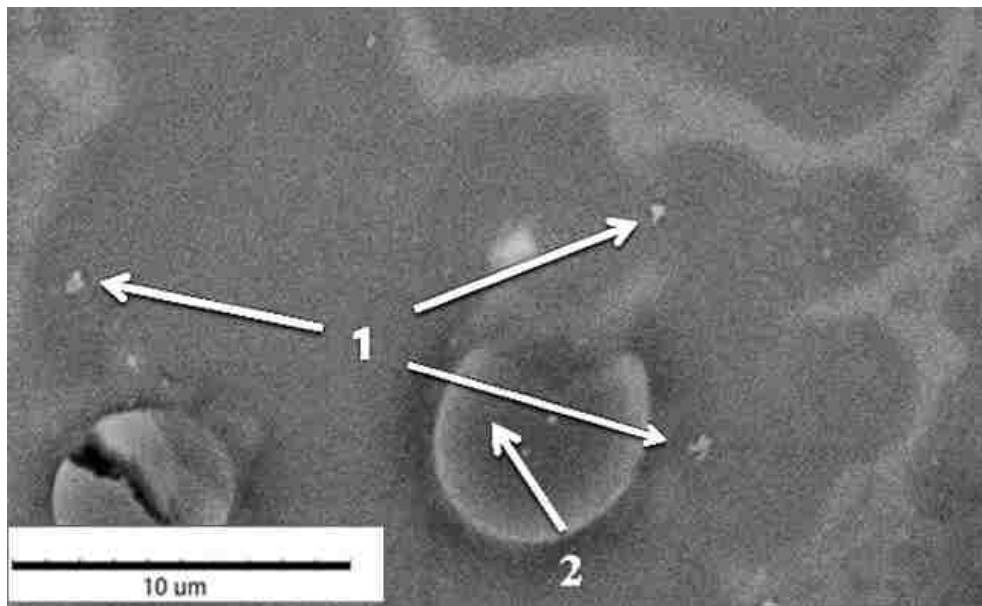
3.3.1. Characterization of hybrid preform composite

Prior to liquid metal pressure infiltration of preform, during the preform fabricating process, a three-dimensional skeleton is constructed. The fibres constitute a solid supporting frame with homogeneously dispersed ceramic particles in this three-dimensional structure. A novel fabrication process with high-frequency and long-term stirring ensures the reinforcements, both fibres and particles, disperse uniformly with acceptable little agglomeration. Consequently, it ensures AM60 alloy can be easily infiltrated into the preform. As well, the space of each cell provided by fibres skeleton in the preform represents a channel in which the molten magnesium alloy can flow through that preventing the deformation of the preforms to ensure efficient infiltration. The developed process for the fabrication of hybrid preforms is flexible to combine different kinds of discontinuous ceramic reinforcements and matrices for a wide range of engineering applications.

The preform eventual properties are critical in determining the properties of the magnesium composites. The SEM micrograph (Figure 3.2) depicts the microstructure of as-cast composite. It can be seen from Figure 3.2 that the reinforced particles were dispersed and placed individually with acceptable little agglomeration; a comparison is given as Figure 3.3 showing the distribution of only 5% vol/fibres reinforced composite.



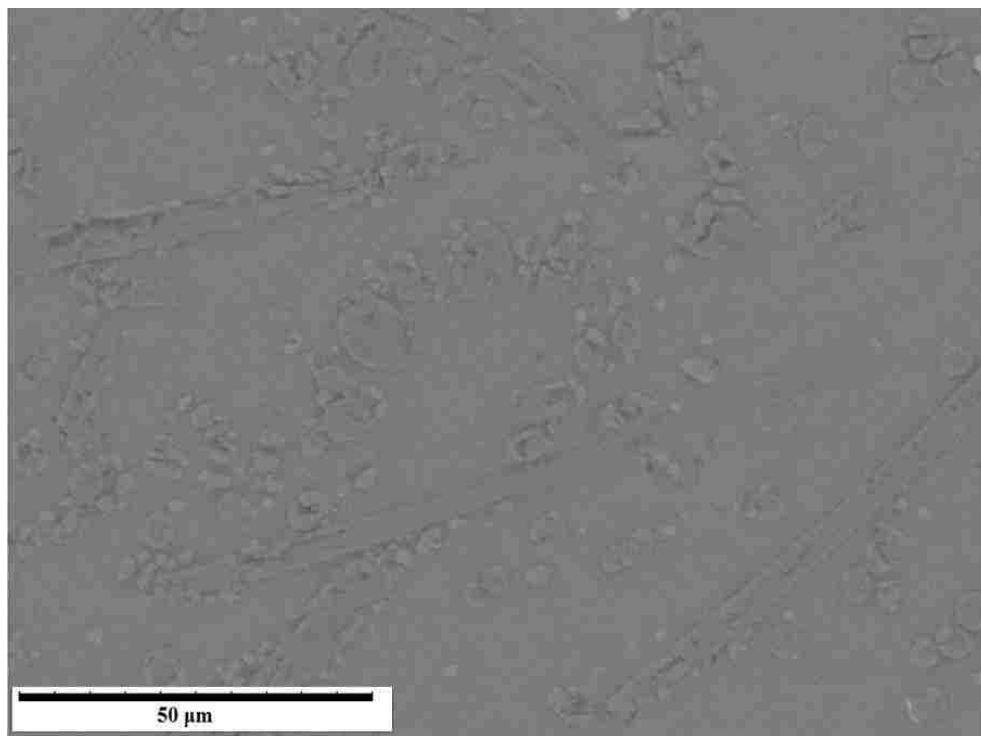
(a)



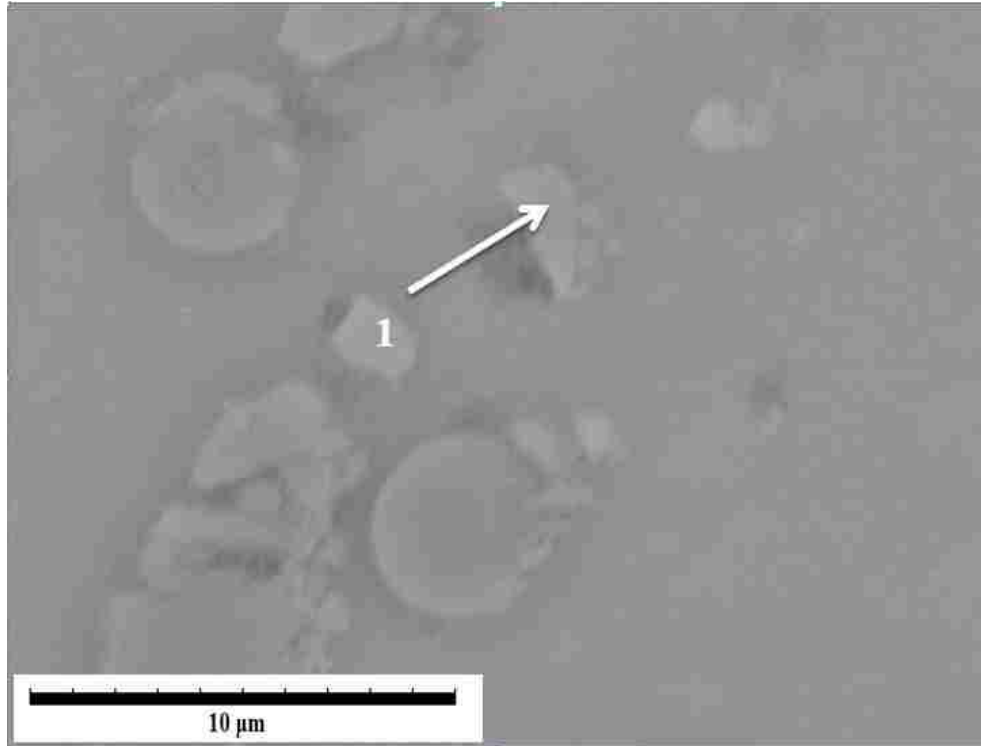
(b)

Figure 3.2. SEM micrograph of composite matrix alloy and composites (3% nano-particles + 5% Fibres) /AM60. a) overall dispersion of nano-particles and fibres; b) nano particles dispersion: Arrow 1-nano particles; Arrow 2-fibres.

Molten matrix alloy was infiltrated into a preheated preform under pressure during the squeeze casting process. The previous studies [6, 9] have demonstrated that the quality of the preform and the processing parameters, such as the preform preheated temperature, the matrix alloy pouring temperature, and the applied pressure level in the preform plus squeeze casting process, influence the quality and performance of the composites significantly.



(a)



(b)

Figure 3.3. SEM micrograph of composite matrix alloy and composites (5% Fibres) /AM60. a) overall dispersion of fibres; b) enlarged fibres: Arrow 1-fibres.

Nishida [10] described the threshold infiltration pressure, P_o , using the following equation during squeeze casting:

$$P_o = -[4V_f \gamma \cos\theta] / [d_f (1-V_f)]$$

where γ is the surface energy of the melt; θ is the contact angle between reinforcement and melt, V_f is the reinforcement volume fraction of the preform and d_f is the diameter of fibre or particle. If it is under ideal conditions, when $V_f = 5\% \text{ vol}$ and $d_f = 5\mu\text{m}$, for the magnesium alloy which can improve the wetting and decrease the surface energy of the melt, the contact angle between reinforcement and magnesium alloy is less than 90° , the molten metal infiltrates the hybrid preform spontaneously. Generally, when modeling the infiltration, it is assumed that there is no

deformation on the preform. However, in practice pressure applied to the molten matrix to overcome capillary forces and other space resistance forces. As a result, residual porosity can be formed during infiltration. In fact, to achieve high quality and density in composites, the applied high pressure can transmit to the preform, the pressure can be reached to 90 MPa. This high pressure may deform the preform and led to undesired defects in the composites.

To optimize the applied pressure and prevent deformation of the hybrid preform, the compressive strengths of hybrid preform were evaluated by compressive tests at room temperature. From the data analysis, the critical stress P_0 of the hybrid preform is as low as 0.6 MPa [9]. Above this pressure, the deformation in the hybrid preform begins to localize, the cellular structure of preform suffer progressive crushing, and fractures propagate catastrophically. As shown in Figure 3.4, fractures of the fibres occur in a typical brittle manner, i.e., crush and cut. To avoid the premature fracture of the preform, the pressure applied in the squeeze casting was increased gradually from a value below the critical stress. The gradual increase in the applied pressure could effectively prevent the deformation of preform during squeeze casting. The applied pressure during casting and infiltration enabled the superheated molten matrix alloy in the preheated die to flow into the preform and wet reinforcement although no wetting agents was employed. Also, because the contacting time between the molten alloy and reinforcement at relatively high casting temperature was very short with the help of the applied pressure, the microstructure of the composites is homogeneous without the porosity and reactants.

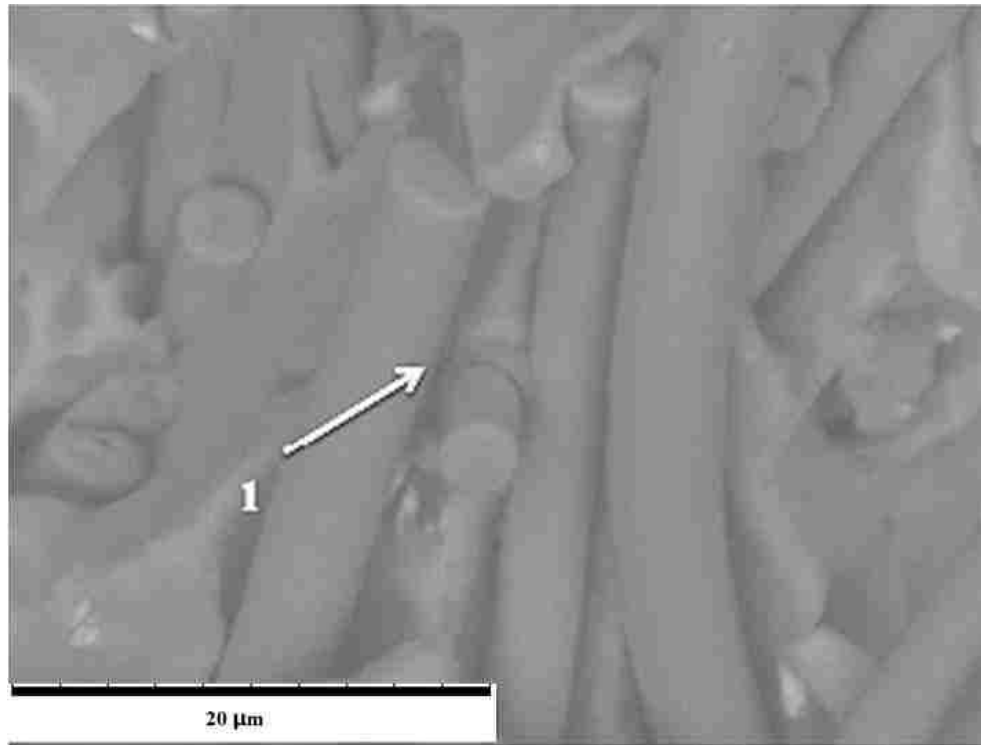
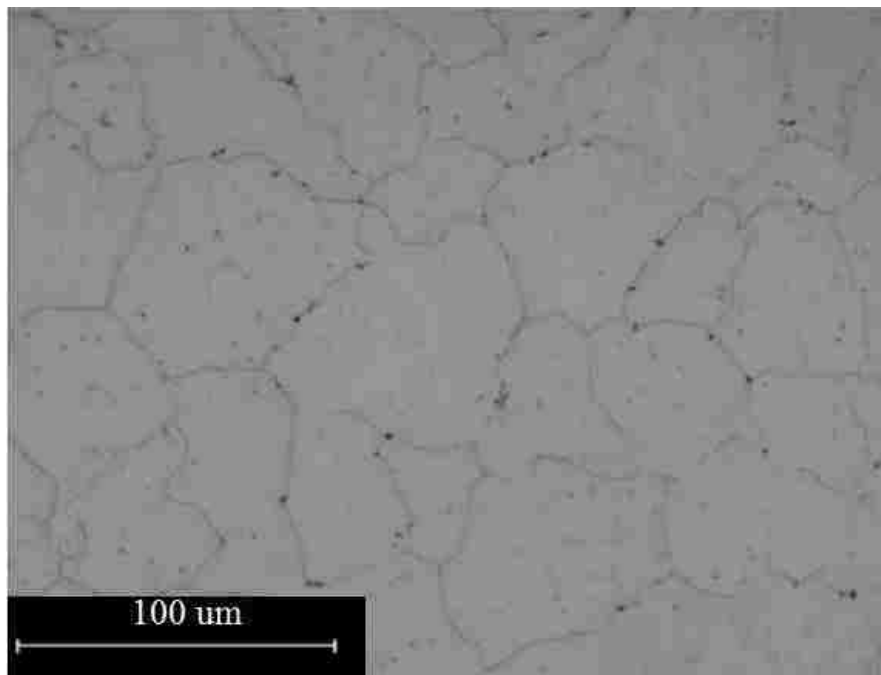


Figure 3.4. Fractures of preform fibres : Arrow 1-fibres crush.

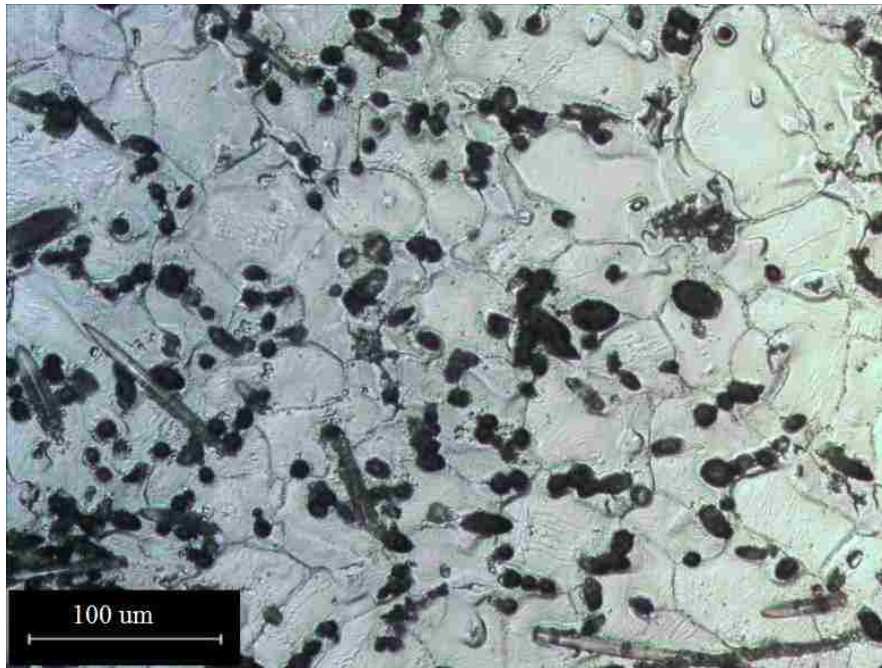
Figure 3.5 gives the grain structures of the matrix alloy and the composites. The grain size measurements for the composites and unreinforced AM60 matrix alloy are presented in Table 3.2. With 5 vol.% of micron fibres, the grain size of the matrix alloy decreases from 68 to 45 μm by 34%. It was reported [11] that the addition of micron particles resulted in a grain refinement of Mg alloy AM50. The microstructural analysis of the composite reveals the similar effect of grain refinement by Al_2O_3 nano particles. The addition of 3 vol.% Al_2O_3 nano particles further reduces the grain size of the matrix alloy from 45 to 20 μm by 56%. The observed grain refinement might be primarily due to the combined effect of heterogeneous nucleation of primary magnesium on Al_2O_3 particles, restricted growth of magnesium grains, and heterogeneous nucleation of eutectic magnesium ($\text{Mg}_{12}\text{Al}_{17}$) on Al_2O_3 particles and fibres[12].

Table 3.2 Grain sizes of AM60 alloy, 5 vol.% Fibre/ AM60, and (3 vol.% nano-Particle +5 vol. % Fibre)/ AM60 composites

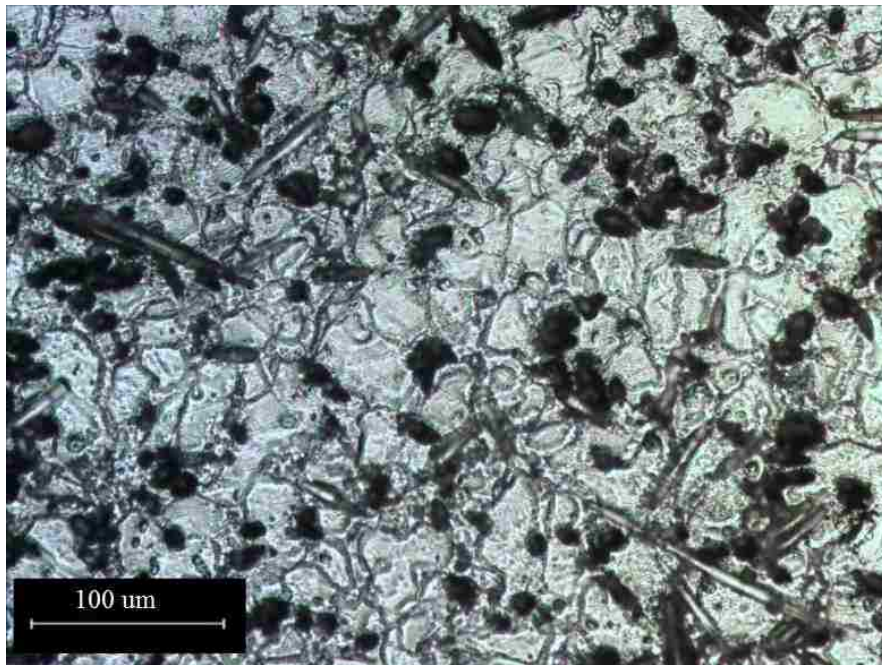
	AM60	5% Fibre /AM60	(5%Fibre + 3% nano-Particle) /AM60
Average grain size (μm)	68	45	20



(a)



(b)



(c)

Figure 3.5. Optical micrographs showing grain structure of (a) unreinforced AM60 matrix alloy, (b) 5 vol.% Fibre/ AM60 and (c) (3 vol. % nano-Particle +5 vol. %Fibre)/ AM60. All are under as-cast condition.

3.3.2. Tensile properties

The typical engineering stress-strain curves for AM60, 5 vol. % Fibre/AM60, and (5 vol.% Fibre+3 vol.% nano-Particle)/AM60 composites are shown in Figure 3.6 and the mechanical properties data are given in Table 3.2. It is observed from the results that the addition of micron-sized reinforcements leads to a significant improvement in the elastic modulus and the strengths, but results in a marked diminishment in elongation. However, the addition of nano-sized particles results in a significant improvement in the elastic modulus and the strengths as well as a restoration of ductility. From Table 3.3, it can be seen that the yield strength (YS) of the composites, of 5 vol.% Fibre/ AM60, and (5 vol.% Fibre+3 vol.% nano-Particle)/AM60 are 120 and 140 MPa, which increase by 48% and 73% over that of the unreinforced matrix alloy, respectively. According to the tensile curve showing in Figure 3.5, the elastic moduli (E) of the composites of 5 vol.% Fibre/ AM60, and (5 vol.% Fibre+3 vol.% nano-Particle)/AM60 are 50 and 53 GPa, which are 25% and 33% higher than that of the unreinforced matrix alloy, respectively. The UTS of the 5 vol.% Fibre/ AM60, and (5 vol.% Fibre+3 vol.% nano-Particle)/AM60 composites is 189 MPa and 216 MPa, which represents 11% AND 26% over that of the matrix alloy, respectively. Compared to that (6%) of the matrix AM60 alloy, the elongation to failure (ϵ_f) of the composites are 2.2% and 3.5% for the 5 vol.% Fibre/ AM60, and (5 vol.% Fibre+3 vol.% nano-Particle)/AM60 composites, respectively. The elongation is restored after 3 vol.% of nano-sized alumina particles by 1.3% is added to the composite. This might be because the sites provided by nano-particles where cleavage cracks are opened ahead of the advancing crack front are capable of dissipating stress concentration from crack tips and altering local effective stress state from plane strain to plane stress in the neighborhood crack tip [7].

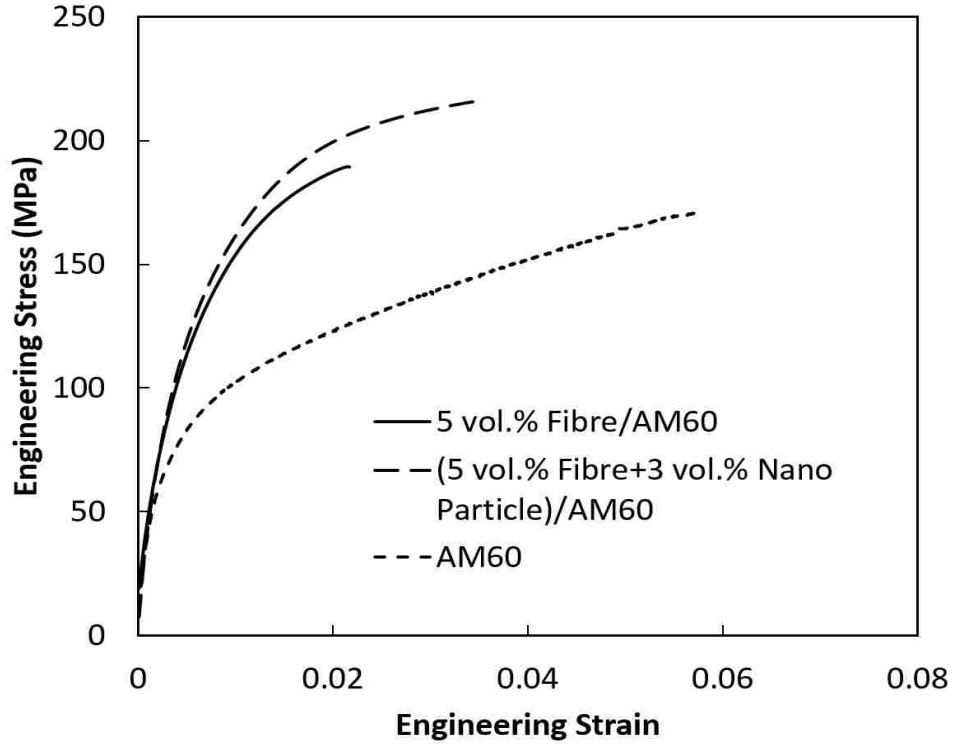


Figure 3.6. Typical engineering stress vs. strain curves for the matrix alloy AM60, the composites of 5 vol. % Fibre/AM60, and (5 vol.% Fibre+3 vol.% nano-Particle)/AM60.

Table 3.3 UTS, YS, ϵ_f and E of the matrix alloy AM60, the composites of 5 vol. % Fibre/AM60, and (5 vol.% Fibre+3 vol.% nano-Particle)/AM60.

	UTS (MPa)	YS (MPa)	ϵ_f (%)	E (GPa)
AM60	171	81	6.0	40
(5 vol.% F)/AM60	189	120	2.2	50
(3 vol. % nano-Particle +5 vol. % Fibre)/AM60	216	140	3.5	53

3.4. Conclusions

A hybrid preform-squeeze casting process for fabricating magnesium alloy AM60-based hybrid composites reinforced by nano-sized particles and micron-sized fibres has been developed. The SEM observation on the microstructure reveals that the nano-sized particles dispersed homogenously in the matrix alloy without large agglomeration. The optical microstructure analysis of the composites indicates that fibres orientate randomly in the matrix. The hybrid composite reinforced with 3 vol. % nano-sized Al_2O_3 particles and 5 vol. % Al_2O_3 fibres exhibits improved tensile strengths over those of the matrix alloy. In particular, the yield strength (140 MPa) of the hybrid composite is 73% higher than that of the matrix alloy. The elastic modulus of the hybrid composite (53 GPa) shows 33 % improvement over the matrix alloy (40 GPa). Compared with the 6% elongation of the matrix alloy, the composite reinforced by 5 vol.% of the Al_2O_3 micron fibre exhibits only the elongation of 2.2%. The addition of 3 vol.% of the Al_2O_3 nano particles restores the elongation of the composite by 1.3% to 3.5%.

3.5. Acknowledgments

The author would like to take this opportunity to thank the Natural Sciences and Engineering Research Council of Canada and the University of Windsor for supporting this work.

3.6. References

- [1] S. R. Bansal and S. Ray, Microstructure and Mechanical Properties of Cast Composite of Steel Wool Infiltrated by Magnesium and AZ91 Alloy, *Materials and Manufacturing Processes*, 26 (2011) 1173-1178.
- [2] E. Hajjari, M. Divandari and H. Arabi, Effect of Applied Pressure and Nickel Coating on Microstructural Development in Continuous Carbon Fibre-reinforced Aluminum Composites Fabricated by squeeze Casting, *Materials and Manufacturing Processes*, 26 (2011) 599-603.
- [3] A. Banerji, H. Hu and A.T. Alpas, Ultra-mild Wear of Al₂O₃ Fibre and Particle Reinforced Magnesium Matrix Composites, *Advanced Materials Research*, 445 (2012) 503-508.
- [4] J. Lo, and R. Santos, Magnesium Matrix Composites for Elevated Temperature Applications, 2007 Society of Automotive Engineers World Congress, Detroit, MI, 01 (2007) 1028.
- [5] Q. Zhang, and H. Hu, Development of Hybrid Magnesium-based Composites, *Advances in Light Weight Materials-Aluminum, Casting Materials, Magnesium Technologies*, Society of Automotive Engineers World Congress, (2010) 107-114.
- [6] X. Zhang, Q. Zhang and H. Hu, Tensile Behavior and Microstructure of Magnesium AM60-based Hybrid Composite Containing Al₂O₃ Fibres and Particles, *Materials Science Engineering A*. 607 (2014) 269-276.
- [7] S.F. Hassan and M. Gupta, Development of High Performace Magnesium Nano-composites Using Nano-Al₂O₃ As Reinforcement, *Material Science Engineering. A*, 392 (2005) 163-168
- [8] L. Chen, J. Xu, H. Choi, M. Pozuelo, X. Ma, S. Bhowmick, J. Yang, S. Mathaudhu and X. Li., Processing and Properties of Magnesium Containing a Dense Uniform Dispersion of Nanoparticles, *Nature*, 528 (2015) 539-543.

- [9] X. Zhang, L. Fang, Q. Zhang, H. Hu and X. Nie, Fabrication and Tensile Properties of Al₂O₃ Particle and Fibre Hybrid Magnesium-based Composites. *Journal of the Chinese Ceramic Society*, 1(2) (2014) 122-128.
- [10] Y.Nishida, and G.Ohira, Modelling of Infiltration of Molten Metal in Fibrous Preform by Centrifugal Force, *Acta Materialia*, 47(3) (1999) 841-852.
- [11] H. Hu, Grain Microstructure Evolution of Mg (AM50A)/ SiCp Metal Matrix Composites, *Scripta Materialia*, 39(8) (1998) 1015-1022.
- [12] Q. Zhang, H. Hu, and J. Lo, Solidification of Discontinuous Al₂O₃ Fiber Reinforced Magnesium (AM60) Matrix Composite. *Defect and Diffusion Forum*. 312-315 (2011) 277-282.

CHAPTER 4 As-cast Magnesium AM60-Based Hybrid Nanocomposite Containing Alumina Fibres and Nanoparticles: Microstructure and Tensile Behavior

4.1. Introduction

Magnesium as the lightest structural metal possesses high specific strengths and low density over other metallic metals. In the past two decades, the use of magnesium-based engineering applications in the automotive industry has risen significantly owing to the increased demand for fuel economy, light-weighting, and performance. From the viewpoint of engineering performance, magnesium alloys are not very competitive owing to their inferior mechanical and high-temperature and corrosion and wear properties in comparison with aluminum alloys and steels. When one or more reinforcements are added to a monolithic alloy to form a metal matrix composite (MMC), a novel material with considerably improved properties such as high strengths, high moduli and high-wear resistance, low coefficients of thermal expansion, becomes available. MMCs accompanying with their superior mechanical properties over non-reinforced monolithic alloys offers a large variety of engineering designs. Therefore, magnesium-based composites have been receiving attention in recent years as an attractive choice for automotive applications because of their low density and superior specific properties due to the need for lightweight materials with high-performance in the automotive industry [1-3].

The major disadvantage of MMCs usually lies in the relatively high cost of fabrication and reinforcement materials. The cost-effective processes for the preparation of composite materials are an essential element for expanding their applications. This is especially true for the high-performance Mg-base MMCs due to their high material and processing costs [4-7]. Recently,

Zhang et al [8] and Zhou et al [9] demonstrated the success in the introduction of two or more reinforcements including short fibres and particles with different sizes into magnesium matrix alloy AM60 by using a preform-squeeze casting process. The fabricated Mg-based hybrid composites exhibited excellent properties, and made a high degree of material design freedom available for magnesium [8, 9]. As Mg-based hybrid composites employed hybrid reinforcements such as particles and short fibres, opportunities emerges to optimize the engineering performance of magnesium-based composites for various potential applications [10]. The study by Zhang et al [11] indicated that, although the micron-sized particle and fibres-reinforced magnesium hybrid composites had high tensile strengths and elastic modulus compared to the unreinforced matrix alloy, it was disappointed to observe a remarkable reduction in ductility. To minimize ductility reduction recently, nano-sized particles were introduced into magnesium alloys by substituting micron-sized particles [1, 12-14]. However, high costs of nanoparticles and manufacturing processes such as evaporation, spray processing and ball milling make them less attractive to the highly competitive automotive industry than conventional approaches, i.e., stir casting and/or preform and squeeze casting.

In this article, the on-going work on the development of the preform-squeeze casting process, which was capable of infiltrating liquid magnesium alloy AM60 into the hybrid preform containing nano-sized Al_2O_3 particles and micron-sized Al_2O_3 fibres under an applied pressure, was presented. The tensile properties of the Mg-based hybrid nanocomposite (MHNC) were evaluated. The informative results of tensile testing on the MHNC were compared with those of the unreinforced matrix alloy and the composites reinforced with micron-sized Al_2O_3 fibres and/or Al_2O_3 particles. The Transmission Electron Microscopy (TEM), Scanning Electron

Microscopy (SEM), and Optical Microscopy (OM) were employed for the microstructural and fractural analyses of the MHNC.

4.2. Experimental Procedures

4.2.1. Materials

Magnesium alloy AM60 with a chemical composition (wt %) of 6.0Al-0.22Zn-0.4Mn-0.1Si-0.01Cu-0.004Fe-0.002Ni-Mg was chosen as matrix alloy. Nano-sized Al₂O₃ ceramic particles with an average particulate size of 100 nm (US Research Nanomaterials, Inc., USA), micron-sized Al₂O₃ ceramic particles with an average particulate size of 5 μm (Inframat Corporation, USA), and Al₂O₃ short fibres (Morgan Advanced Materials, United Kingdom) with an average diameter of 4 μm and length of 50 μm were employed as raw materials for the preparation of hybrid reinforcements since they are relatively inexpensive and possess adequate properties.

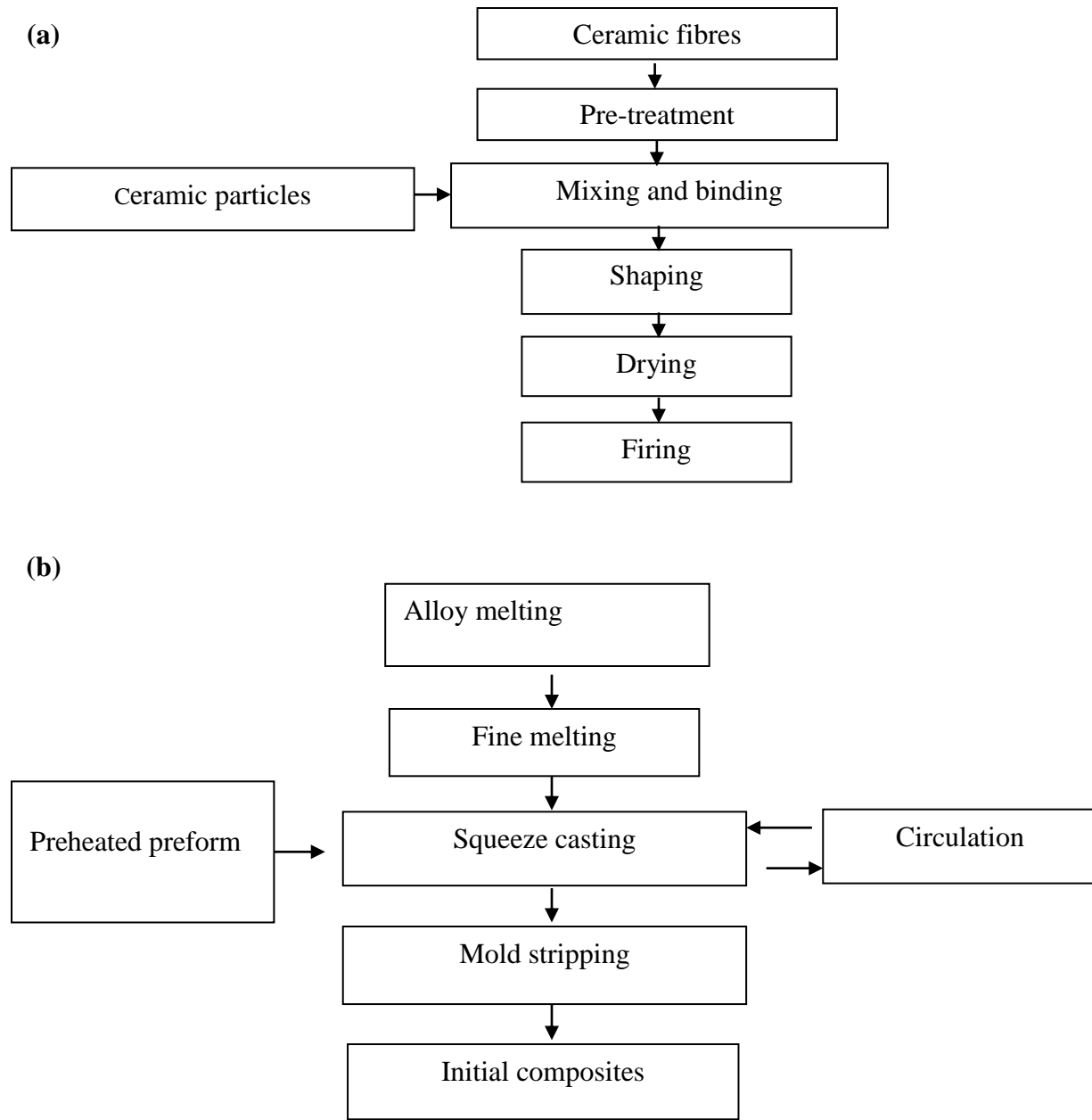


Figure 4.1. Flowchart showing the procedure for fabricating hybrid (a) preform and (b) composites.

4.2.2. Fabrication of hybrid preform

The preparation steps for fabrication of the hybrid preforms (Figure 4.1, a) involve: mixing the ceramic short fibres and particles, introducing the binding compounds, forming the preform

shape under pressure, drying, and sintering. In the hybrid preform, the fibres serve as the skeleton for a cellular structure. The content level of the fibre was pre-determined based on the desired amount of porosity in the cellular solid. The particulate reinforcements were dispersed in the pores present in the cellular solid. The content, size and type of the ceramic reinforcements were adjusted to yield the required quantity, and shape of preform. In addition, for the purpose of a comparative study of the hybrid preform characteristics; a pure fibre preform was also fabricated using the same process without adding particulate reinforcements.

4.2.3. Fabrication of composites

Figure 4.1 (b) shows the fabrication process for the composites in which a squeeze casting process was adopted. During fabrication, a hybrid preform was first preheated to 700 °C. Then, molten matrix alloy AM60 at 750 °C infiltrated into the preheated preform under an applied pressure of 90 MPa. The pressure was maintained at the desired level for 30 seconds. After squeeze casting, a cylindrical disk of single or dual-phase reinforced composite with 3 vol.% Al₂O₃ nano-sized or micron-sized particles and 5 vol.% Al₂O₃ fibres, was obtained. In the hybrid composite, the particles constituted the primary reinforcement phase, and the short fibres served as the secondary reinforcement phase. For the purpose of comparisons, three different types of 5 vol% Fibre/AM60, (5 vol.% Fibre + 3 vol% micron-Particle)/AM60, and (5 vol.% Fibre+3 vol.% nano-Particle)/AM60 composites were prepared, which were named the fibre-only composite, the micron hybrid composite, and the MHNC, respectively. More details on the process for fabricating the composites are given in references 8, 9 and 11.

4.2.4. Microstructure analysis

All specimens were cut from the center of the casting coupon. The type of heat treatment, T4, was conducted on both of the unreinforced alloy AM60 and fiber-reinforced composites to reveal the grain structure. Following the standard metallographic procedures, as-cast and T4-treated specimens were mounted and polished. To disclose the microstructural characteristics of the composites and alloys, samples were then polished and etched in a solution (60 ml 99% ethanol solution, 20 ml acetic acid, 19 ml dilute water, and 1 ml nitric acid) for microstructural analyses. The primary morphologic grain characteristics of the polished and etched samples were investigated under optical microscopy (OM) (Buehler image analyzer 2002). The existence and distribution of the reinforcements were investigated by a JEOL JSM-5800LV scanning electron microscope (SEM) with an energy dispersive X-ray spectrometer (EDS). Samples for TEM (JOEL 2010F) analyses were prepared by focus ion beam (FIB) (Zeiss NVision 40) using STEM modulus for investigation. To prevent the fall-off of the tiny nanoparticle, a tungsten coating was applied to the cross-section surface of the MHNC foil prepared by the FIB before the TEM observation.

4.2.5. Tensile testing

Mechanical properties were evaluated via tensile testing (ASTM B557) at ambient temperature using specimens of 25 mm × 6 mm × 6 mm (gauge length×width×thickness) on an Instron (Grove City, PA, USA) machine equipped with a computer data acquisition system. The

tensile specimens were machined from the center of as-cast coupons. The tensile tests were performed at an initial strain rate of $5 \times 10^{-3} \text{ s}^{-1}$. The tensile properties, including 0.2% yield strength (YS), ultimate tensile strength (UTS), elongation to failure (ϵ_f), and elastic modulus (E) were obtained based on the average of three tests.

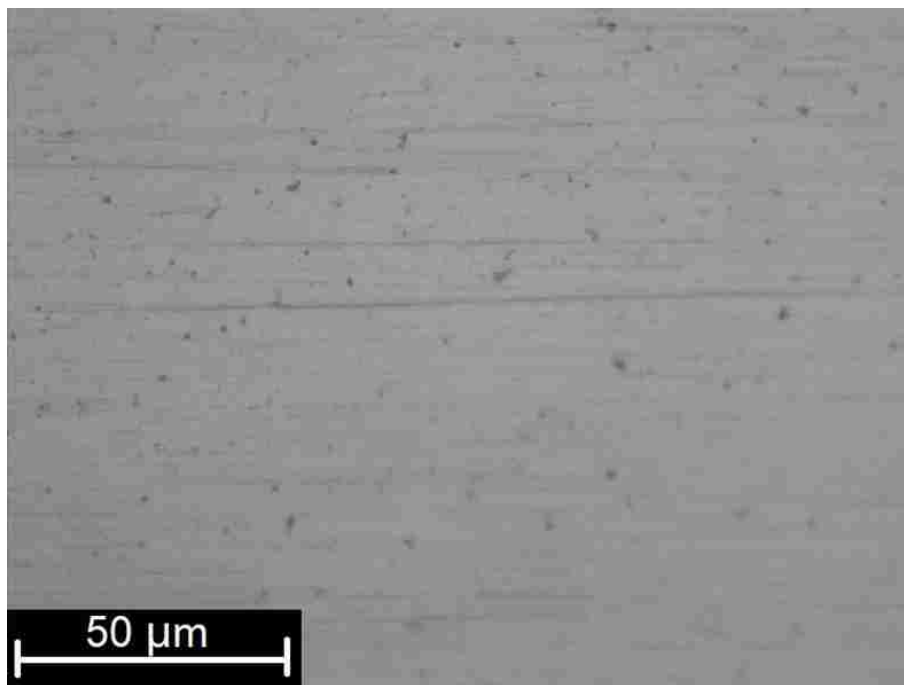
4.3. Results and Discussion

4.3.1. Microstructure

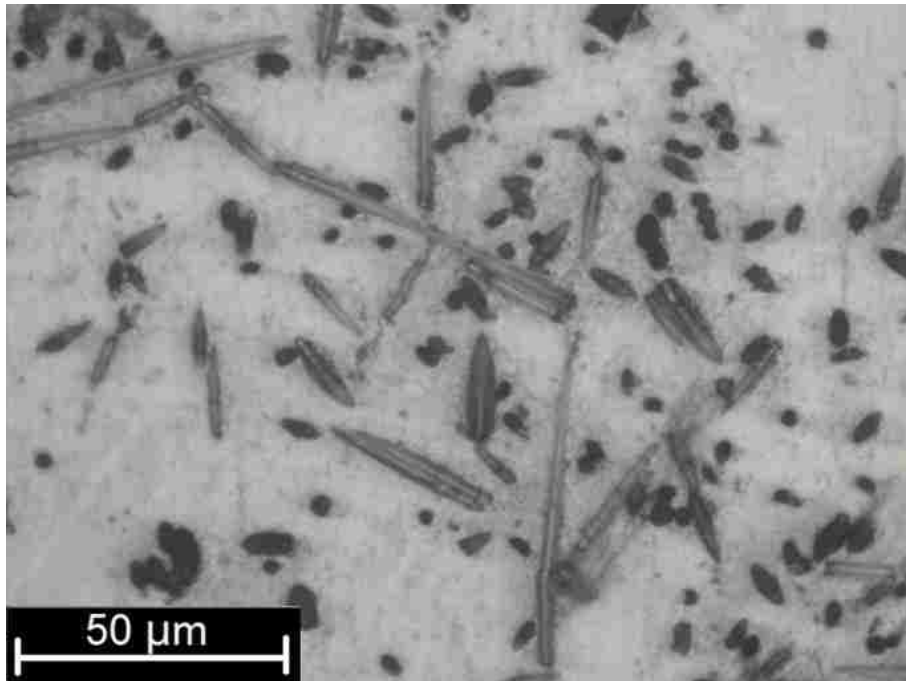
Figure 4.2 presents optical micrographs showing the unetched matrix alloy and the composites. As shown in Figure 4.2(a) by the OM, the divorced eutectic phases ($\beta\text{-Mg}_{17}\text{Al}_{12}$) is present along the grain boundaries of the unreinforced alloy. Figure 4.2(b) depicts that the short fibres are distributed in a random and isotropic orientation in the fibre-reinforced composite. The microstructures of the hybrid magnesium composites reinforced with micron-sized and nanosized particles are given in Figure 4.2(c) and (d), respectively. It can be seen that the fibres and particles are uniformly distributed throughout the matrices in the fibre-only composite and the hybrid composites. The introduction of either micron or nano particles up to 3 vol% has little effect on the uniformity of fibres. Pores are barely found in the microstructure, implying the hybrid composites were well densified during fabrication due to a gradual application of the infiltration pressure. The pore-free microstructure of the composites also suggests the success in the infiltration of the matrix alloy into the hybrid preform.

A non-uniform distribution of reinforcements could result in the degradation of mechanical properties of the composites, a non-uniform grain structure and defect formation of the composites. Although the large difference in size between the particles and the fibres is

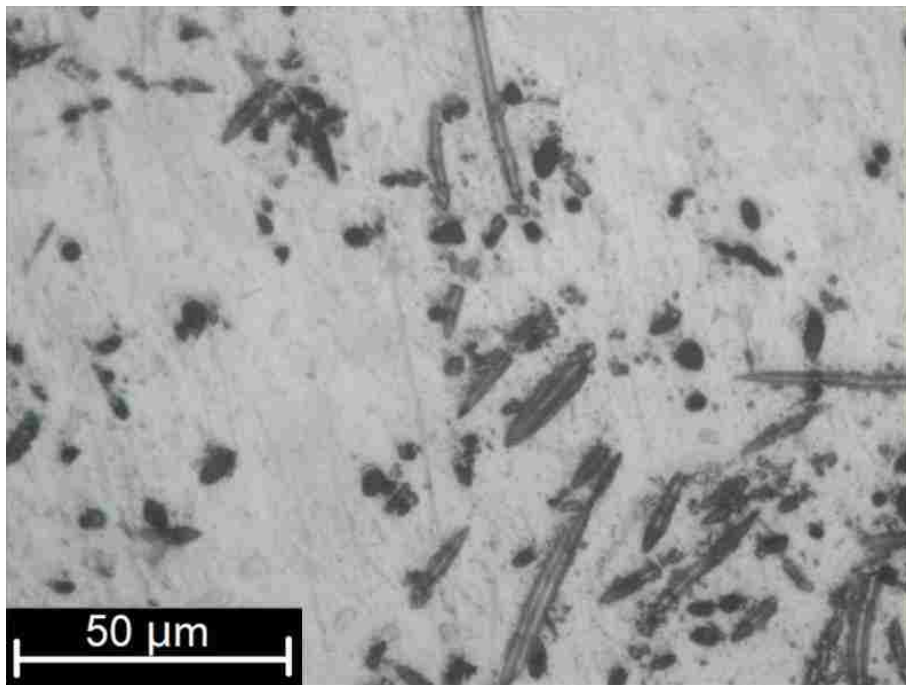
present, it can be seen from Figures. 4.2(c) and (d) that the micron or nanoparticles and fibres are dispersed uniformly without agglomeration and cave in the matrix alloy. The microstructure of the composites reinforced with both the Al_2O_3 micron and nanoparticles and micron fibres distributed homogeneously in the matrix satisfies the materials design requirements by using ceramic particles as the main reinforcement to enhance the mechanical and wear properties of the composites, with the fibres helping improve their toughness. The overall properties of the composites can be improved and tailored via optimization.



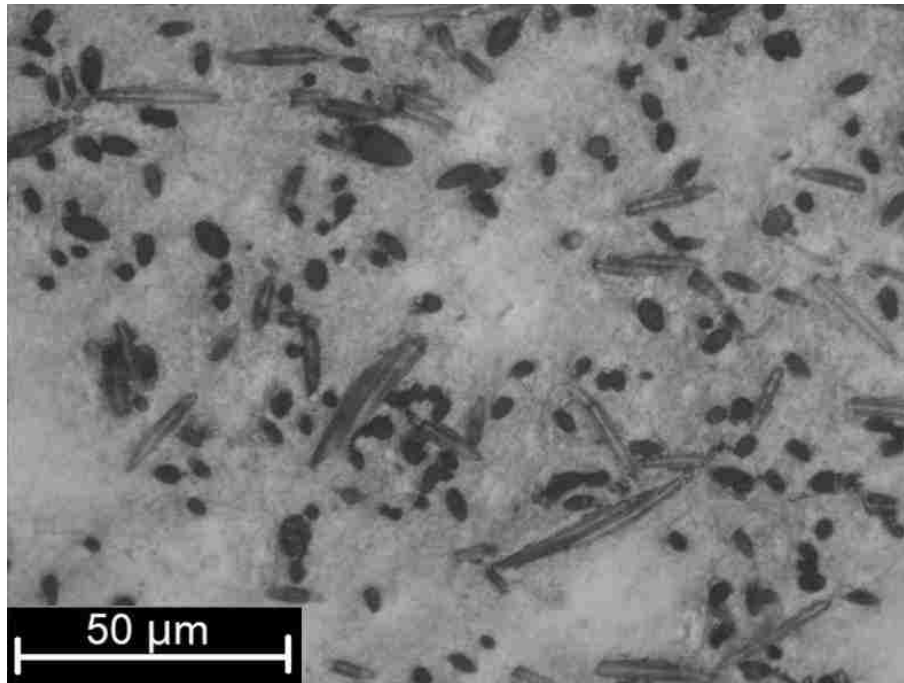
(a)



(b)



(c)

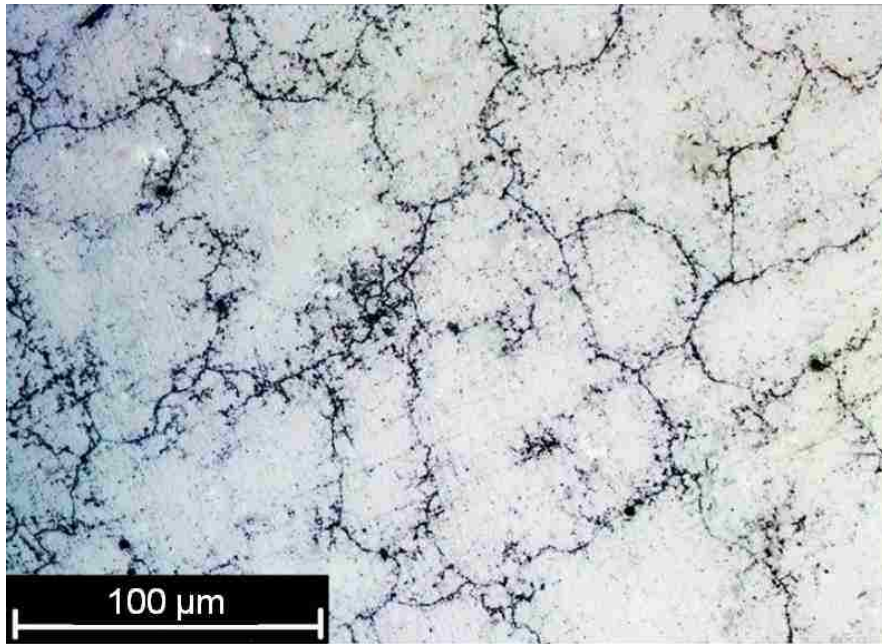


(d)

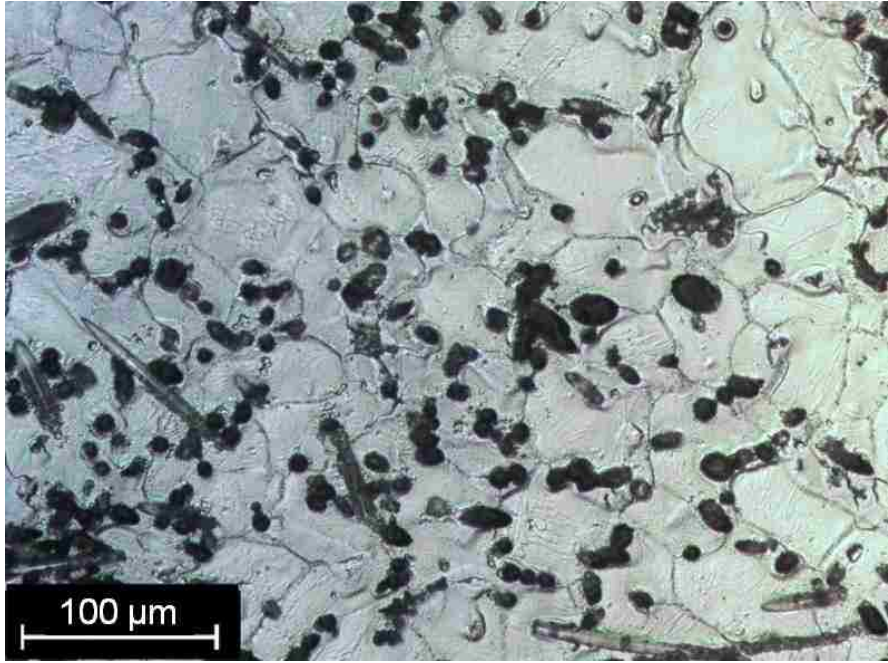
Figure 4.2. Optical photograph showing the microstructures of unetched as-cast matrix alloy and composites, (a) unreinforced matrix alloy AM60, (b) 5 vol% Fibre/ AM60, (c) (3 vol% micron particle +5 vol% Fibre)/ AM60. (d) (3 vol% nanoparticle +5 vol% Fibre)/ AM60.

Figure 4.3 presents the grain structures of the etched matrix alloy and the composites. The grain size measurements for the composites and unreinforced AM60 matrix alloy are presented in Figure 4.4. With 5 vol% of micron-sized fibres, the grain size of the matrix alloy decreases from 68 to 45 μm by 34%. The refinement of grain structure in the fibre-only composite should be primarily attributed to the restriction of grain growth by the limited cellular space formed in the skeleton of the fiber preform structure[15]. The addition of 3 vol.% Al_2O_3 micron particles to the hybrid composite further reduces the grain size of the matrix alloy from 45 to 28 μm by 38%. It was reported [16] that the coupled effect of the heterogeneous nucleation of the primary magnesium phase on micron particles and the restricted growth of magnesium crystals should be

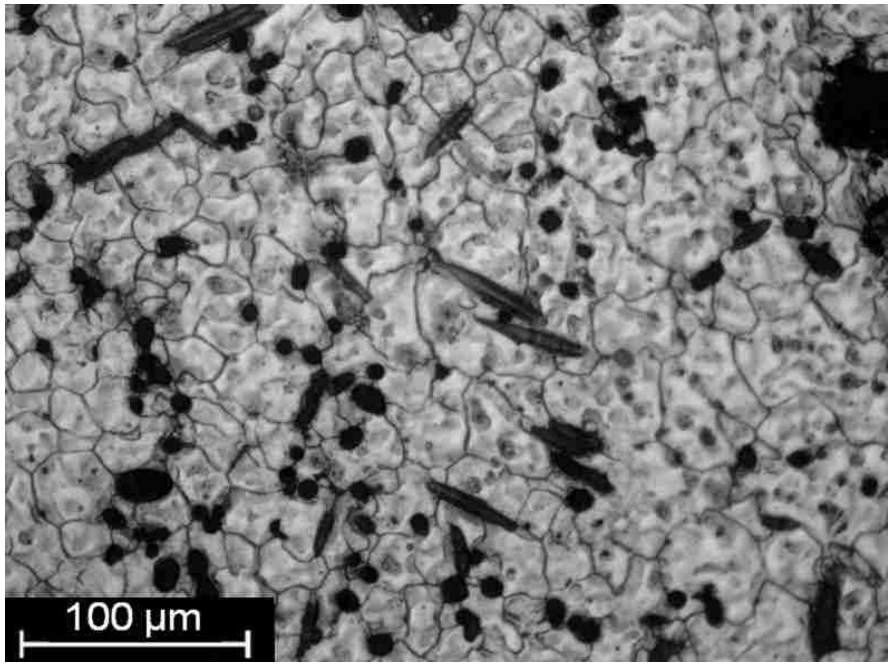
responsible for the grain refinement of as-cast Mg alloy AM50 with 5 vol% micron particles. The microstructural analysis of the nanocomposite reveals the similar effect of grain refinement. The substitution of the Al_2O_3 nano particles for the micron ones further reduces the grain size of the matrix in the MHNC from 28 to 20 μm by 40%.



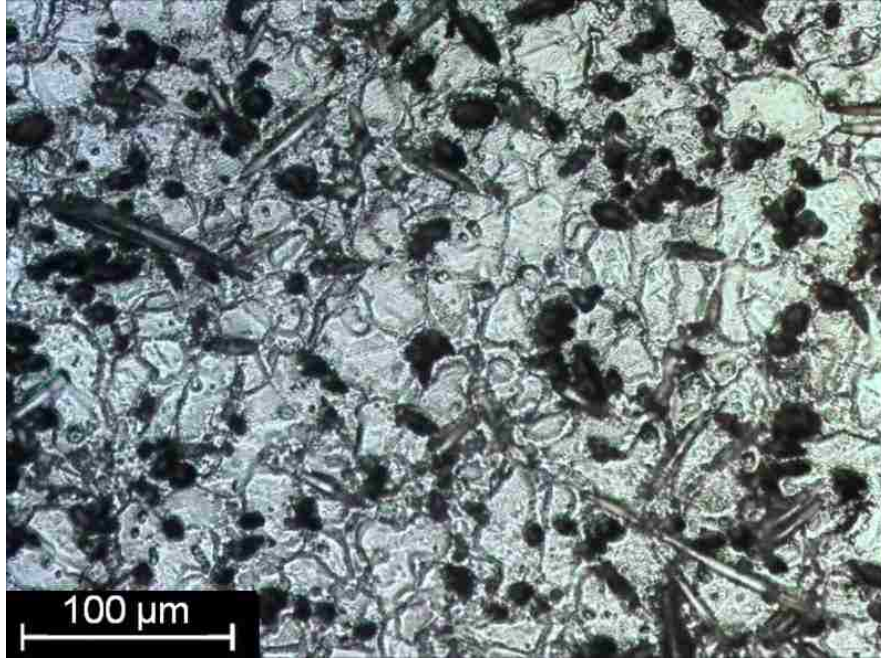
(a)



(b)



(c)



(d)

Figure 4.3. Optical micrographs showing grain structures of etched (a) unreinforced matrix alloy AM60, (b) 5 vol% fibre/ AM60, (c) (3 vol% micron particle +5 vol% fibre)/ AM60, and (d) (3 vol% nano particle +5 vol% fibre)/ AM60.

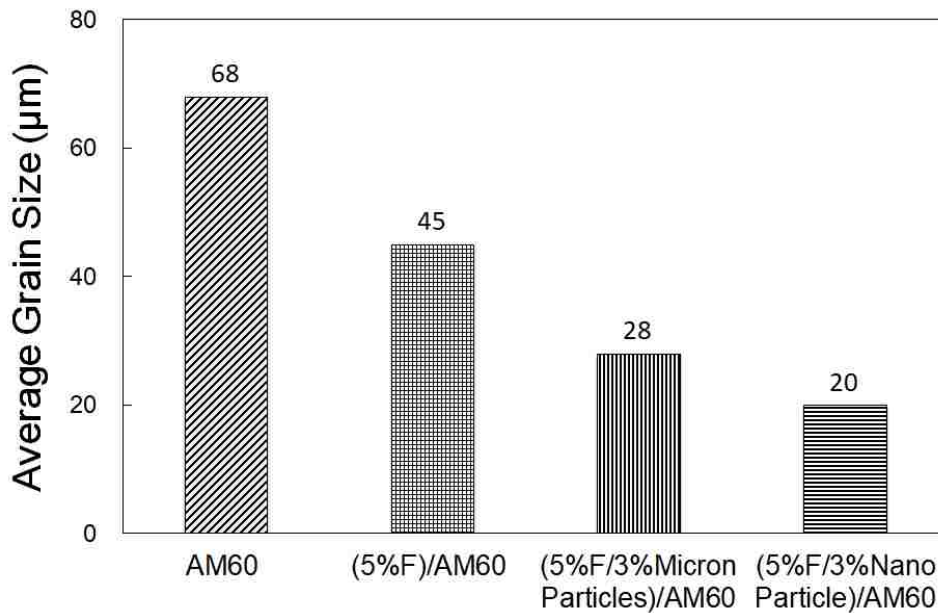
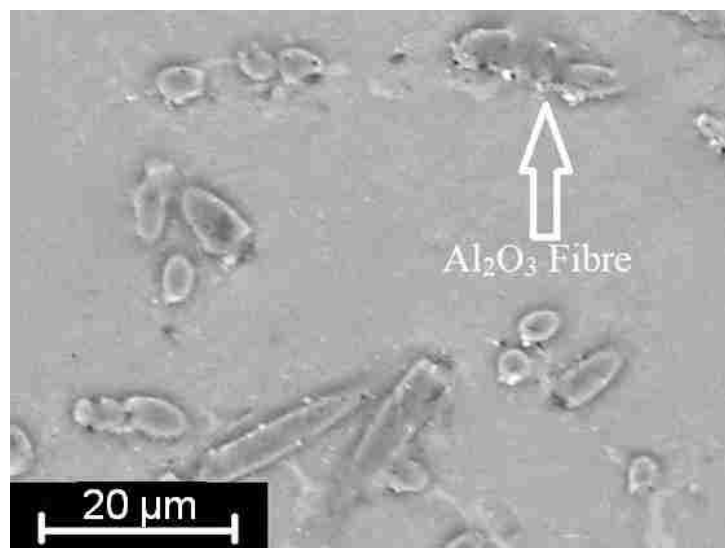
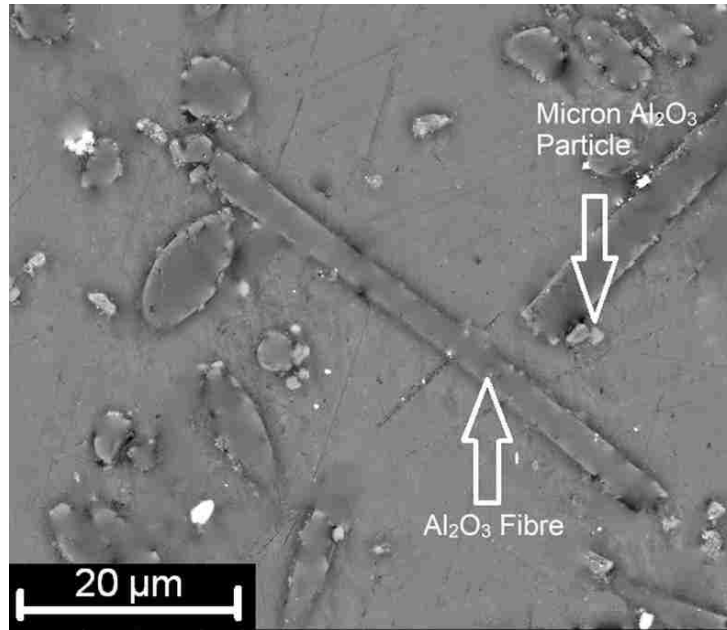


Figure 4.4. Measured grain sizes of the unreinforced matrix alloy AM60, 5 vol% fibre/ AM60, (3 vol% micron particle +5 vol% fibre)/ AM60, and (3 vol% nano particle +5 vol% fibre)/ AM60.

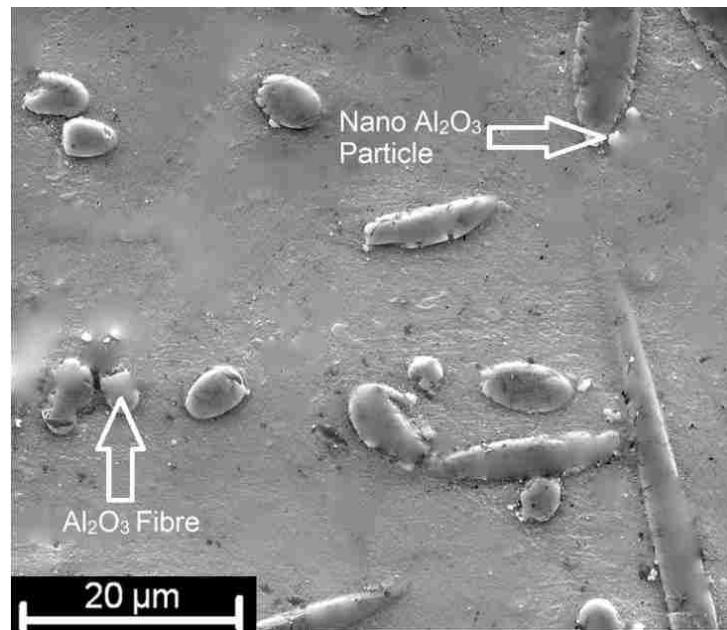
Figure 4.5 shows the reinforcement distribution in the microstructure of the unreinforced matrix alloy, the fibre-only composite and the hybrid composites by SEM micrographs in a backscattered electron (BSE) mode. It can be seen from Figure 4.5 that the reinforced fibres and micron/nano particles were dispersed and placed individually with little agglomeration. As illustrated in Figure 4.6, the TEM and EDS analyses confirms the presence of the micron particles in the hybrid composite (Figure 4.6(a)), and the nanoparticles in the MHNC which further evidences the successful introduction of the nanoparticles in the composites (Figure 4.6(c)). The probe crossed the alumina micron and nano particles along the white line in Figure 4.6(b) and (d). When the probe went from the matrix to the particles, a large sharp decrease in magnesium, and a rapid increase in aluminum and oxygen were found. This observation was consistent with the compositions of the matrix and particle reinforcements. Examination of the interfacial structure revealed a relatively clean interface of both the micron and nano particles. No particle/matrix reaction products were detected in the hybrid composite and MHNC by TEM. This should be primarily due to the presence of inadequate reaction time between the particles and matrix alloy as a result of fast pressurized infiltration implemented during squeeze casting.



(a)

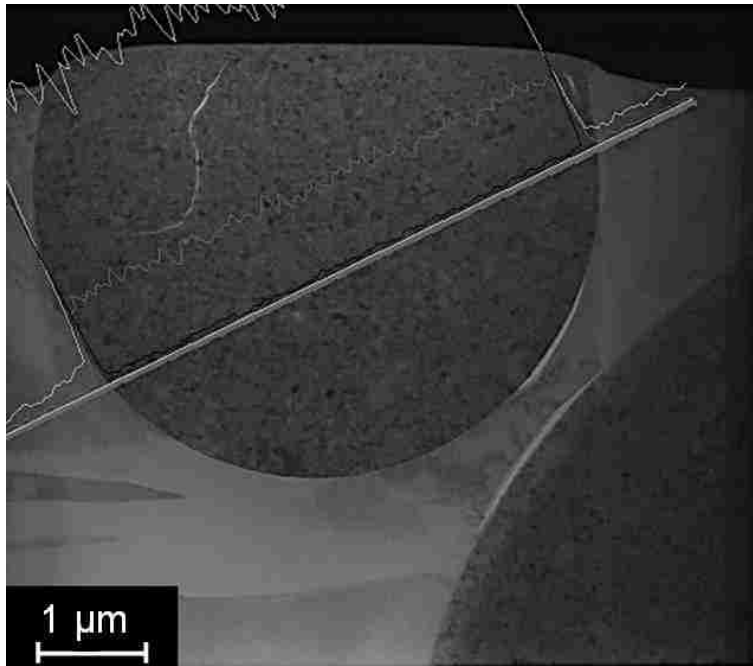


(b)

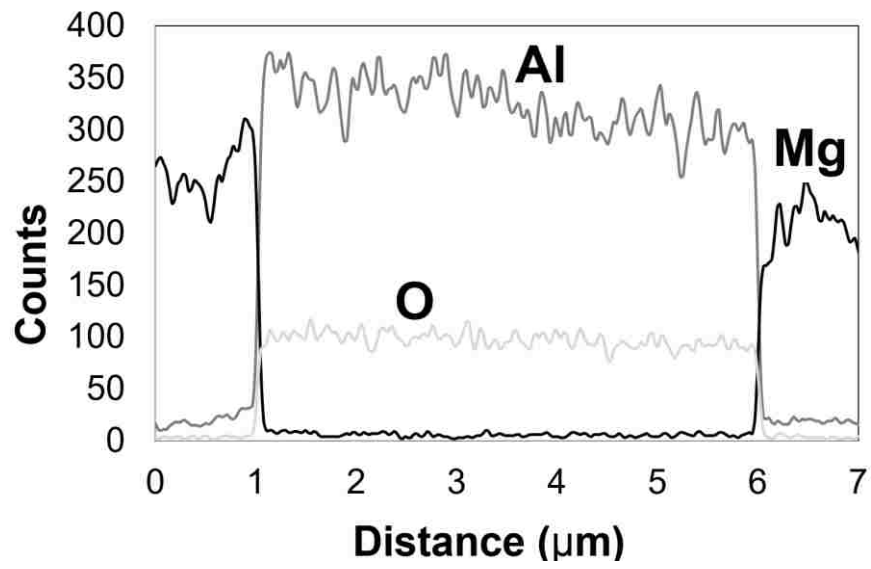


(c)

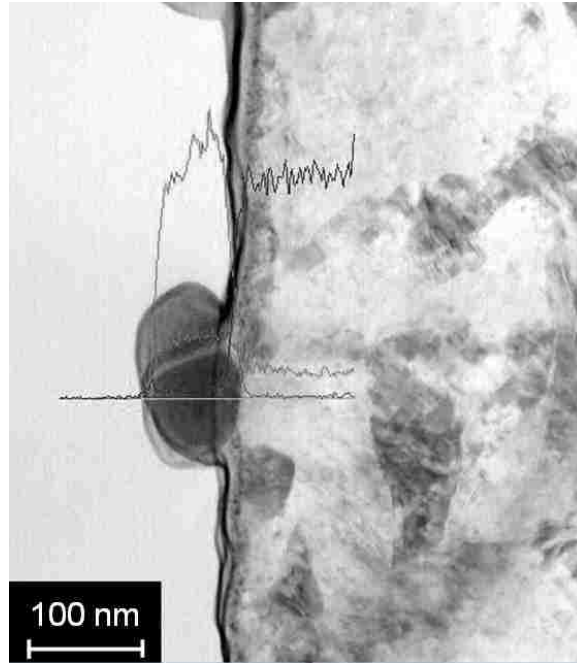
Figure 4.5. SEM micrographs in BSE mode showing the reinforcement distribution in (a) 5 vol% fibre/ AM60, (b) (3 vol% micron-particle +5 vol% fibre)/ AM60, and (c) (3 vol. % nano-particle +5 vol% fibre)/ AM60.



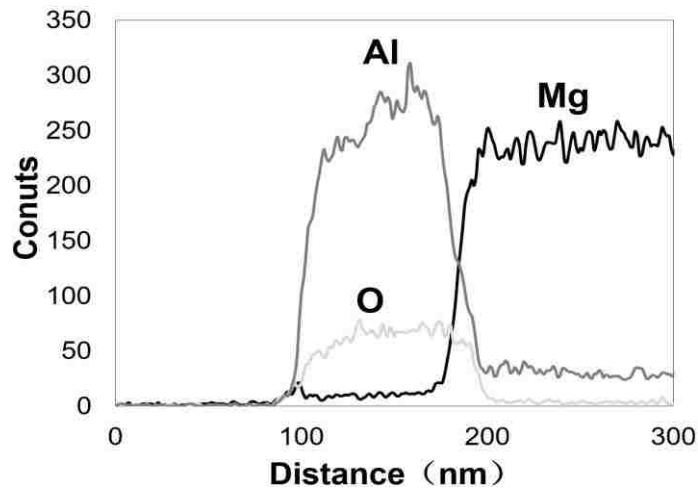
(a)



(b)



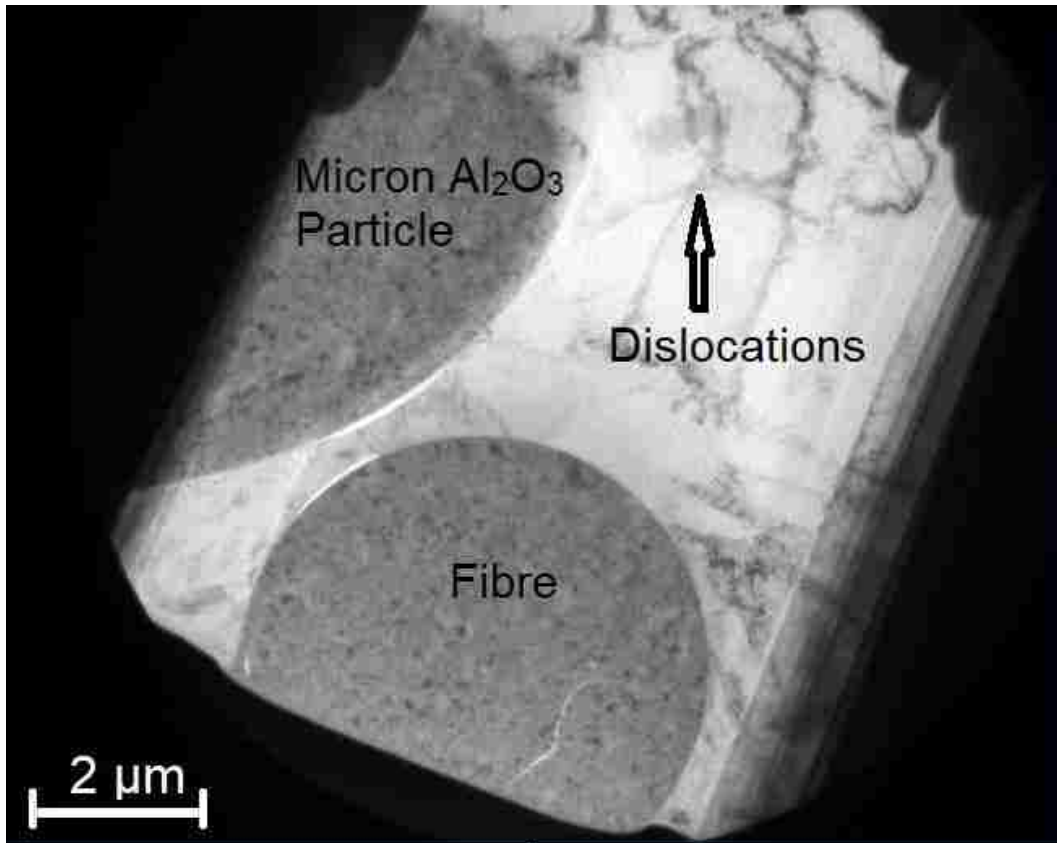
(c)



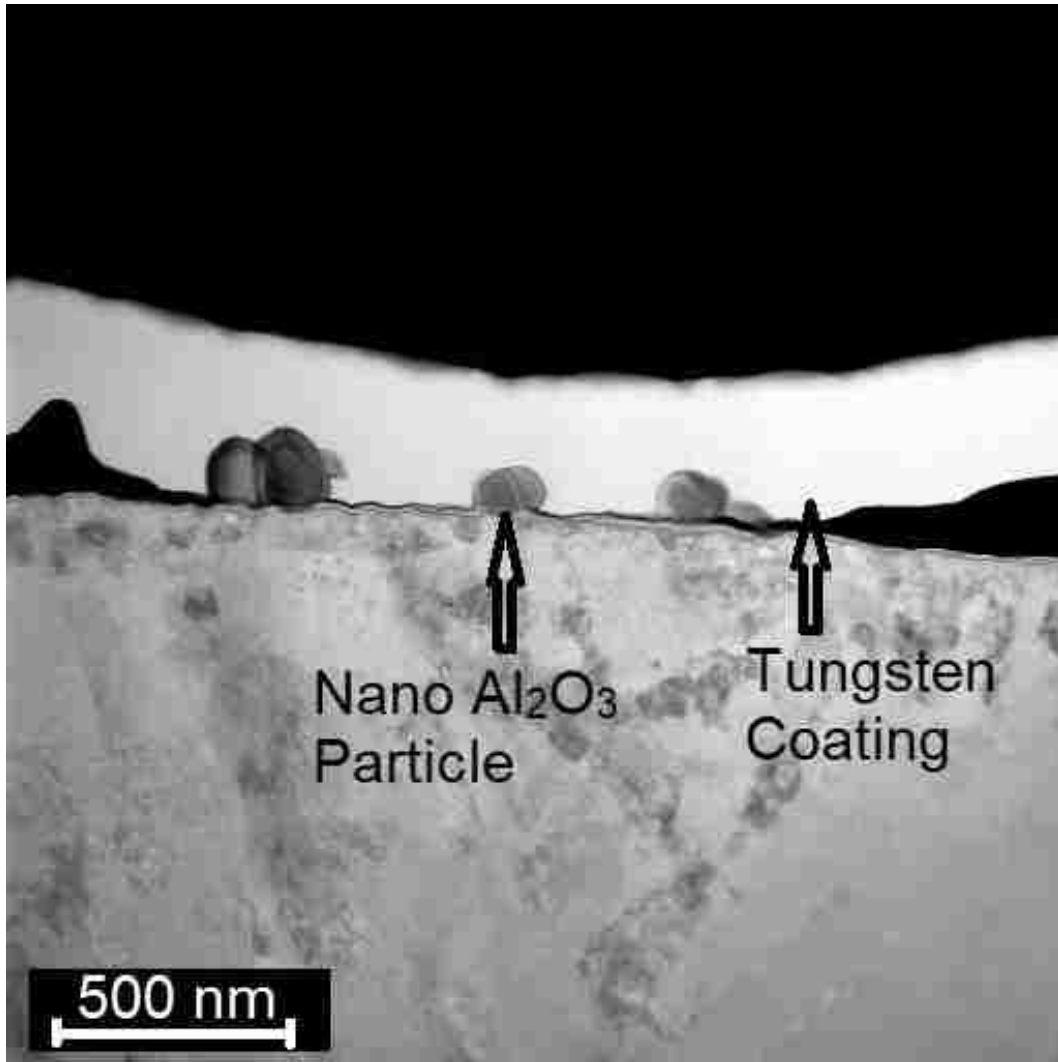
(d)

Figure 4.6. TEM and EDS results showing the particle presence and the interface between the particle and matrix, (a) a micron Al_2O_3 particle in the (3 vol% micron Al_2O_3 particles + 5 vol% Fibres) /AM60, (b) line scans and the corresponding line scanning pattern for the cross-section area of the micron particle, (c) a nano Al_2O_3 particle in the (3 vol% micron Al_2O_3 particles + 5 vol% Fibres) /AM60 MHNC, and (d) line scans and the corresponding line scanning pattern for the cross-section area of the nano particle. The gray lines denote the approximate scanning path.

Figure 4.7 shows the TEM images of the composites reinforced with the two different sizes of Al_2O_3 particles. Examination of microstructure revealed by TEM manifests the difference between the two composites in the presence of defects. Relatively high dislocation density exists in the composites reinforced by the micron size particles (Figure 4.7(a)). The inherent difference in thermal expansion coefficients should be responsible for the formation of mismatch stress of the Al_2O_3 particles and matrix alloy, which results in high dislocation density. This observation is consistent with the results disclosed in references [12, 17]. However, when the particle size decreases to the nano level, despite the presence of the distinctive difference in their thermal expansion coefficients between the Al_2O_3 particles and the matrix alloy, no evident dislocations around the nano particle are observed in the matrix alloy under the applied condition of the electron diffraction pattern, as shown in Figure 4.7(b). The low dislocation density in the MHNC might be due to the fact that the nano particles are extremely tiny, which are hard to generate sufficient strain by the thermal mismatch to induce dislocations during solidification.



(a)



(b)

Figure 4.7. TEM micrographs showing dislocations in the composites with Al_2O_3 particles: (a) micron and (b) nano.

4.3.2. Tensile properties

The representative engineering stress-strain curves for AM60, the fibre-only composite (AM60 5%F), the micron hybrid composite (AM60 5%F-3%P micron Al_2O_3), and the MHNC (AM60 5%F-3%P nano Al_2O_3) are shown in Figure 4.8. The curves for the matrix alloy and the composites have a similar pattern, in which the materials deform elastically first. Once the yield

point is reached, the plastic deformation sets in. The addition of fibers and/or particles pushes the yield points of the composites to high stress levels. Finally, the composites fractured at much higher stress and lower strain levels than that of the matrix alloy AM60. It can be seen from Figure 4.7 that, although the introduction of the reinforcements leads to an increase in the strengths and modulus, there is a significant reduction in elongation when micron fibres and particles are added. But, the placement of the nano particles in the MHNC, which replace the micron ones, offsets the elongation reduction.

The tensile properties data given in Table 4.1 show that the as-cast matrix alloy exhibits 171 MPa of its UTS, 81 MPa of its YS, 40 GPa of its elastic modulus and 6.0% failure elongation. The introduction of the micron fibre reinforcement, increases the UTS, YS and E to 189 MPa, 120 MPa and 50 GPa, by 11%, 48%, and 25%, respectively. Although additional 3 vol% of micron particles further enhances the UTS, YS and E only by 2%, 18%, 6%, respectively, the elongation is reduced considerably from 6.0% to 1.6% by 73%. Meanwhile, the MHNC gives the UTS of 216 MPa showing an increase of 13% in UTS over the hybrid composite as the YS (140 MPa) and the E (53 GPa) are maintained. The determined tensile strengths are in line with the grain size measurements since the grain refinement enhances the materials strengths. Moreover, it is worthwhile noting that the e_f of the MHNC is 3.5%, which represents an increase of 119% over that of the hybrid composites. The replacement of the micron particles with the nano particles in the Mg-based hybrid composite effectively recovers the ductility of the composite by 2% .

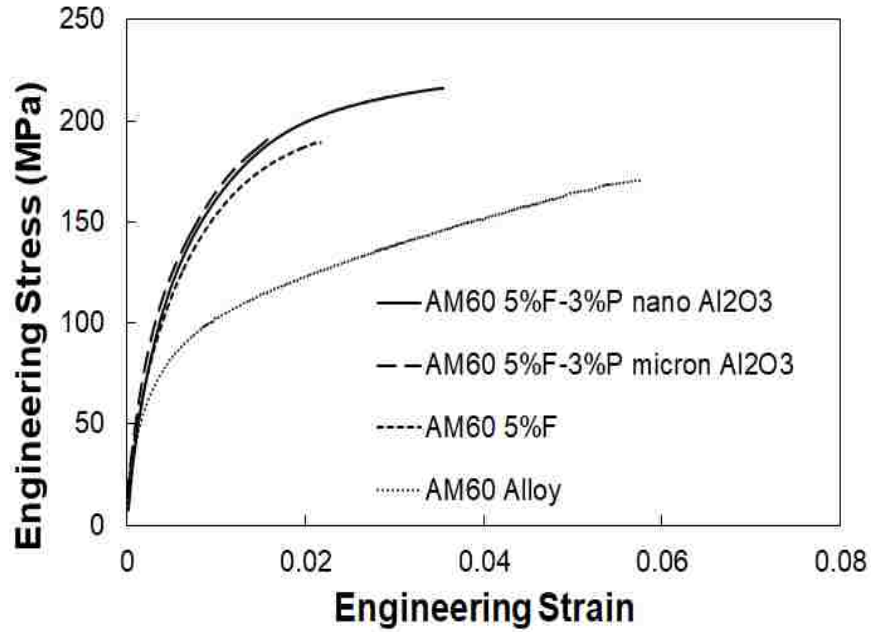


Figure 4.8. Engineering stress vs. strain curves for the matrix alloy AM60, 5 vol% Fibre/AM60, (5 vol.% Fibre+3 vol% micron Al₂O₃ particle)/AM60, and (5 vol.% fibre+3 vol.% nano Al₂O₃ particle)/AM60.

Table 4.1 UTS, YS, ef and E of the Matrix Alloy AM60, the Composites of 5 vol. % Fibre/AM60, and (5 vol.% Fibre+3 vol.% nano-Particle)/AM60.

	YS	UTS	ef	E
	(MPa)	(MPa)	(%)	(GPa)
AM60	81±6	171±8	6.0±1.3	40±4
Fibre-only	120±5	189±12	2.2±1.7	50±2
Micron Hybrid	142±7	192±15	1.6±1.1	54±5
MHNC	140±14	216±5	3.5±1.2	53±3

The observed ductility restoration is evidently supported by the results of the TEM analysis. A high dislocation density provides more tough obstacles to overcome, which increases the strength and toughness of materials. With a low dislocation density, however, materials are capable of carrying more strain during deformation. Also, Hassan and Gupta[12] have also observed that the addition of micron-sized reinforcements leads to an improvement in the elastic modulus and the strengths, but results in a marked diminishment in elongation. However, the addition of nano-sized particles results in a significant improvement in the elastic modulus and the strengths as well as a restoration of ductility. This is because the sites provided by nano-particles where cleavage cracks are opened ahead of the advancing crack front are capable of dissipating stress concentration from crack tips and altering local effective stress state from plane strain to plane stress in the neighborhood of the crack tip. Overall, the high strengths and moderate elongation of the MHNC should result from the combined strengthening effect: homogeneous distribution of nano particles, matrix grain structure refinement, good interfacial bonding between the matrix and the nano particles and micron fibres[13].

4.3.3. Strain hardening

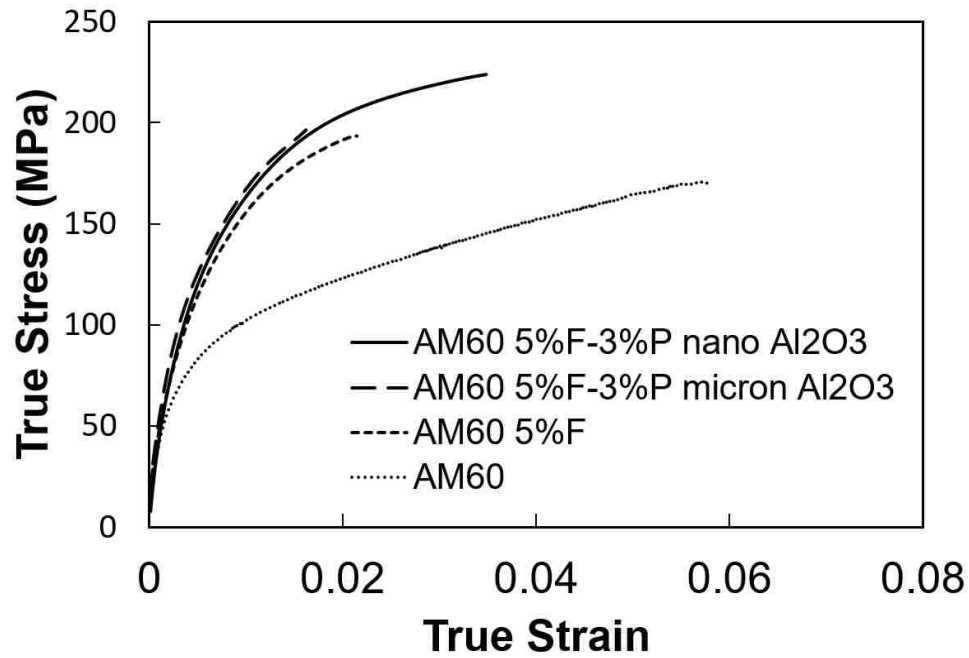


Figure 4.9. True stress vs. strain curves for the matrix alloy AM60, 5 vol% Fibre/AM60, (5 vol.% Fibre+3 vol% micron Al₂O₃ particle)/AM60, and (5 vol.% fibre+3 vol.% nano Al₂O₃ particle)/AM60.

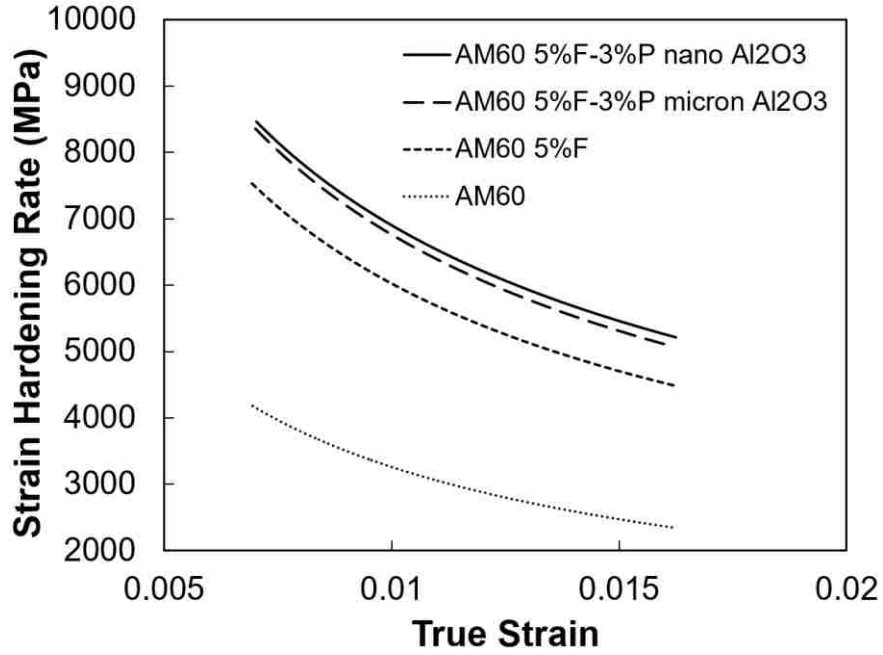


Figure 4.10. Strain hardening curves for the matrix alloy AM60, 5 vol% Fibre/AM60, (5 vol.% Fibre+3 vol.% micron Al_2O_3 particle)/AM60, and (5 vol.% fibre+3 vol.% nano Al_2O_3 particle)/AM60, upon the commencement of plastic deformation.

The true stress and strain could be determined from the engineering stress and strain by applying the following equations:

$$\sigma_t = \sigma_e (1 + \epsilon_e) \quad (\text{Eq. 4.1})$$

$$\epsilon_t = \ln (1 + \epsilon_e) \quad (\text{Eq. 4.2})$$

where σ_t is the true stress, ϵ_t is the true strain, σ_e is the engineering stress, and ϵ_e is the engineering strain. Figure 4.9 shows the true stress vs. strain curves for the matrix alloy AM60, 5 vol% Fibre/AM60, (5 vol.% Fibre+3 vol.% micron Al_2O_3 particle)/AM60, and (5 vol.% fibre+3 vol.% nano Al_2O_3 particle)/AM60.

The true stress-strain curve for engineering materials can be described by the power law relationship for plastic deformation [11]:

$$\sigma = K \epsilon^n \quad (\text{Eq. 4.3})$$

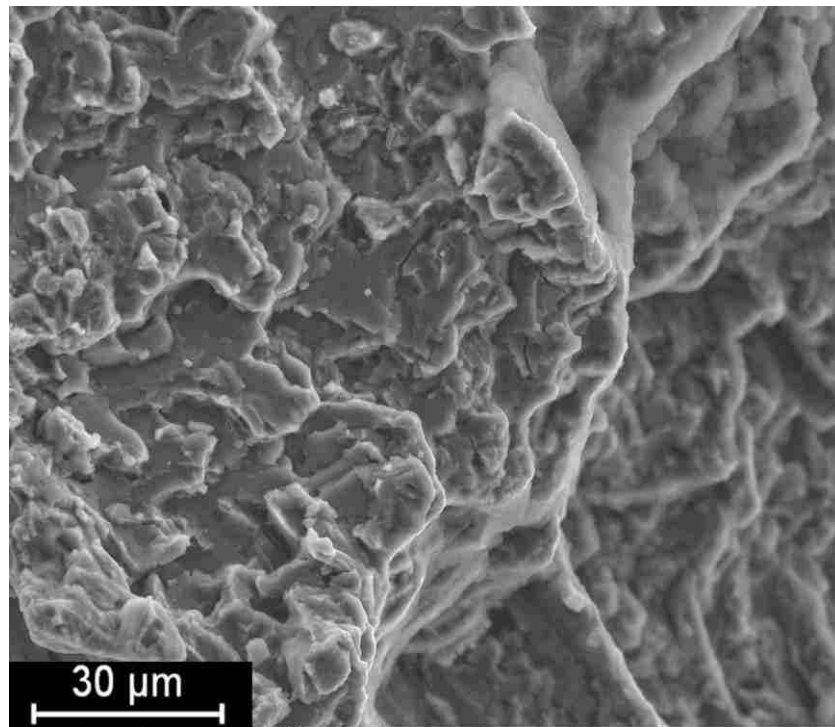
where K is the strength index, ε is the plastic strain and n is the strain hardening exponent.

Table 4.2 lists the numerical values of the constants in Eq. 4.3 with the regression coefficients. The strain hardening rate ($d\sigma/d\varepsilon$) can be obtained from the differentiation of the Eq. 4.3. The strain hardening behaviors of the alloy and composites are shown in Figure 4.10, which was derived from Figure 4.9. Figure 4.10 presents the strain hardening rates at the beginning of the plastic deformation for the matrix alloy AM60, 5 vol% Fibre/AM60, (5 vol.% Fibre + 3 vol% micron Al_2O_3 particle)/AM60, and (5 vol.% fibre + 3 vol.% nano Al_2O_3 particle)/AM60. All the tested materials revealed the similar trend, in which the strain hardening rates decrease with increasing the true strain. At the beginning of the plastic deformation, the matrix alloy shows a strain hardening rate of only 4085.2 MPa. The ceramics fibre introduction increases the strain hardening rate to 7453.5 MPa. The strain hardening rate rises to 8360.9 MPa after the addition of the micron particles to the hybrid composite. The substitution of the nano particles for the micron ones leads to an increase in the strain hardening rate to 8418.6 MPa. The effect of the particle size on the strain hardening rate of the hybrid composite and the MHNC seems limited. Among all the tested materials, the MHNC has the highest strain hardening rate, which implies that the MHNC are able to spontaneously strengthen itself increasingly to a large extent, in response to plastic deformation before the final fracture.

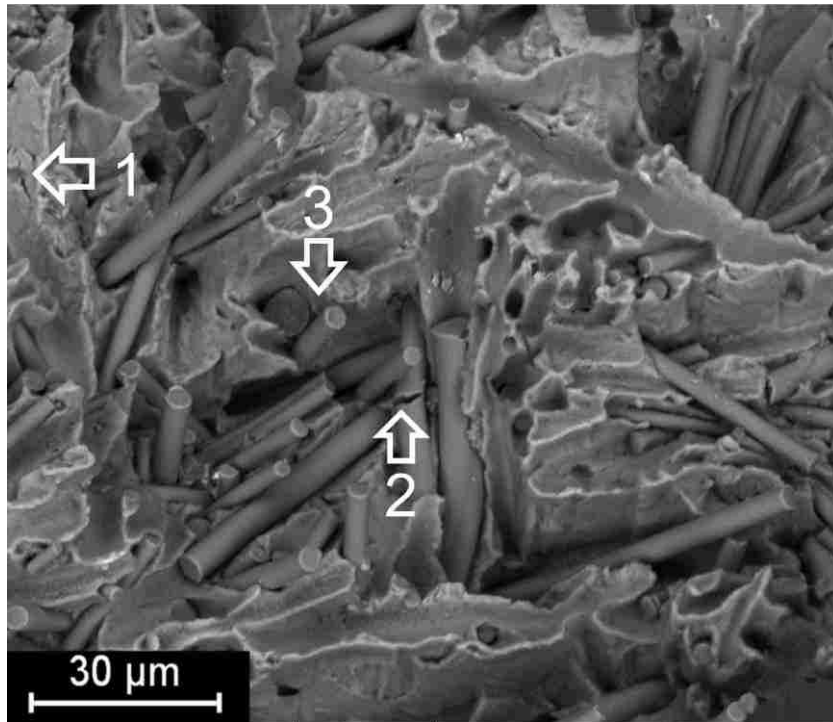
Table 4.2 Best fit parameters of power equation

Materials	K (MPa)	n	R ²
AM60	444±10	0.3187±0.0074	0.9957±0.0019
AM60 5%F	932±11	0.3908±0.0052	0.9946±0.0021
AM60 5%F-3%P- micron Al ₂ O ₃	1077±12	0.4045±0.0070	0.9998±0.0001
AM60 5%F-3%P nano Al ₂ O ₃	1143±15	0.4223±0.0098	0.9992±0.007

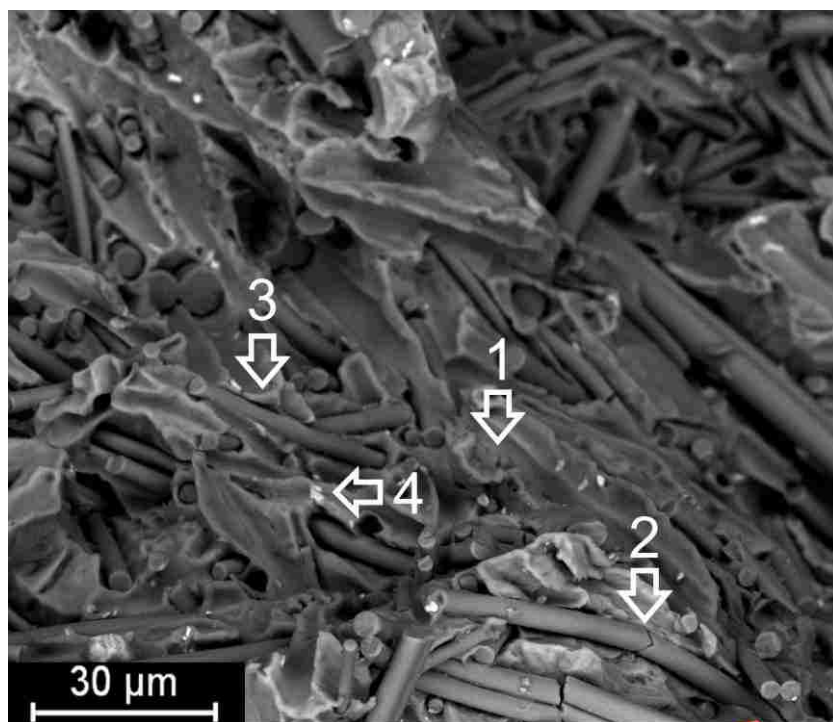
4.3.4. Fractography



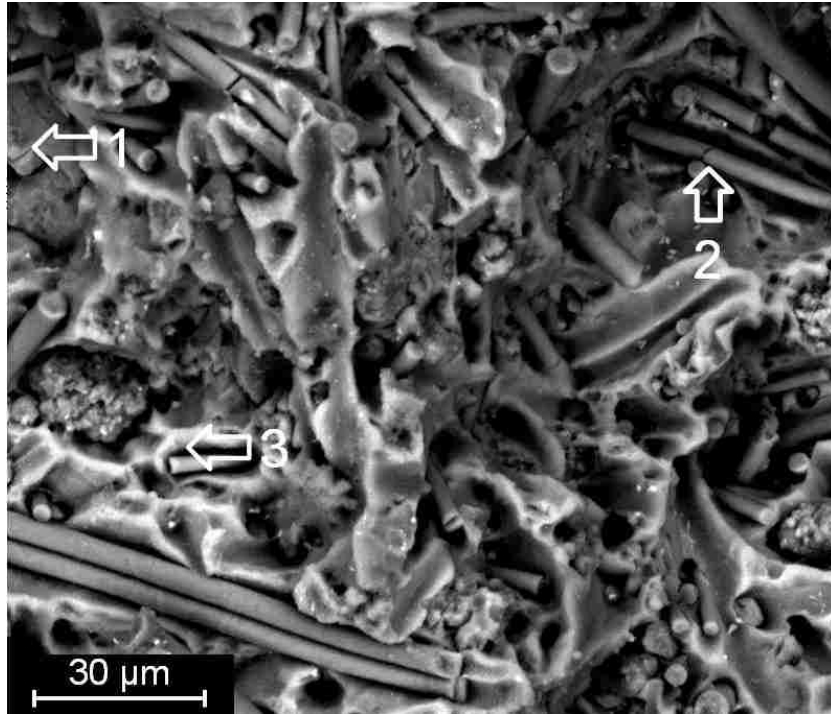
(a)



(b)



(c)



(d)

Figure 4.11. Fractures of AM60, AM60 composites with Al_2O_3 fibres particles (a) AM60 alloy (b) AM60 alloy with 5% fibre (c) AM60 alloy with 5% fibre/ 3% micron size particles (d) AM60 alloy with 5% fibre/ 3% nano size particles (arrow 1- matrix crack; arrow 2- fibre crack; arrow 3- debonding; arrow 4- micron-particle crack; arrow).

As shown in SEM fractography in Figure 4.11, the specimens were observed under high magnifications in attempt to reveal detailed features of the fracture surfaces and determine the fracture behaviors with reference to the mechanical properties of the composites reinforced with the different volume fraction, sizes and types of fibre and particles. Figure 4.11 (a) shows a typical fracture surface with a unreinforced AM60 alloy. There were shallow dimples on the surface and generally displayed ductile behavior. A considerable amount of energy was consumed in the process of the formation of micronvoids, eventually leading to the formation of cracks. This type of cracks resulted from the coalescence of microvoids under tensile stress. As the reinforcement introduction of fibre and micron/nano-sized particles, significant amount of

loads were transferred to fibre and micron/nano-sized particles. The composite broke in a brittle mode much different from that of the unreinforced alloy. The final tensile fracture primarily results from fibre and particles cracks, as shown in Figure 4.11, due to the inherent nature of the high strength and brittleness of the ceramic fibres and particles. The debonding at the interface between the fibre and matrix as well as the particle and matrix could be another crack initiation area of the composite, which might be attributed to the insufficient infiltration of the molten metal into the close packed network of fibres and particles. Few dimples are found on the fracture surfaces of the fibre-only and the micro hybrid composites in Figure 4.11 (b) and (c). However, certain deformation of the matrix alloy is evidently present on the fracture surface of the MHNC. Overall, the SEM fractography results were in consistent with the tensile data as reinforcement addition into the particles.

4.4. Conclusions

A hybrid preform-squeeze casting process for fabricating magnesium alloy AM60-based hybrid nanocomposites reinforced by nano-sized particles and micron-sized fibres has been developed. The SEM observation on the microstructure reveals that the nano-sized particles disperse homogenously in the matrix alloy without large agglomeration. The optical and SEM microstructure analyses of the composites indicate that fibres orientate randomly in the matrix and grain structure is well refined. The TEM analyses reveal the presence of a low dislocation density in the MHNC resulting from the deficiency of thermal strains due to the introduction of nano-sized particles. The MHNC reinforced with 3 vol% nano-sized Al_2O_3 particles and 5 vol% Al_2O_3 fibres exhibits an balance on tensile strengths and elongation compared with the fibre-only and hybrid composites and the matrix alloy. Among the three types of the tested composites, the

MHNC gives the highest UTS (216 MPa), ϵ_f (3.5%) and the strain hardening rate (8418.6 MPa). The YS (140 MPa) and E (53 GPa) of the MHNC are very comparable to those of the hybrid composite. The addition of the 3 vol% Al_2O_3 nano particles restores the elongation of the hybrid composite from 1.6% to 3.5%. The replacement of the micron particles with the nano particles in the Mg-based hybrid composite effectively recovers the ductility of the composite by 118%. The presence of the low dislocation density in the matrix of the MHNC should be responsible for the ductility restoration.

4.5. Acknowledgments

The author would like to take this opportunity to thank the Natural Sciences and Engineering Research Council of Canada and the University of Windsor for supporting this work.

4.6. References

- [1] H. Liao, J. Chen, L. Peng, J. Han, H. Yi, F. Zheng, Y. Wu, Wenjiang Ding, Fabrication and Characterization of Magnesium Matrix Composite Processed by Combination of Friction Stir Processing and High-energy Ball Milling, *Materials Science & Engineering A*, 683 (2017) 207–214
- [2] S. Arokiasamy, B. Anand Ronald, Experimental Investigations on the Enhancement of Mechanical Properties of Magnesium-based Hybrid Metal Matrix Composites through Friction Stir Processing, *The International Journal of Advanced Manufacturing Technology* (2017), 1–11

- [3] M.E. Turan, H. Zengin, E. Cevik, Y. Sun, Y. Turen, H. Ahlatci, Wear Behaviors of B₄C and SiC Particle Reinforced AZ91 Magnesium Matrix Metal Composites, *International Journal of Chemical, Molecular, Nuclear, Materials and Metallurgical Engineering*, 10 (9) 2016
- [4] S. R. Bansal and S. Ray, Microstructure and Mechanical Properties of Cast Composite of Steel Wool Infiltrated by Magnesium and AZ91 Alloy, *Materials and Manufacturing Processes*, 26 (2011) 1173-1178.
- [5] E. Hajjari, M. Divandari and H. Arabi, Effect of Applied Pressure and Nickel Coating on Microstructural Development in Continuous Carbon Fibre-reinforced Aluminum Composites Fabricated by squeeze Casting, *Materials and Manufacturing Processes*, 26 (2011) 599-603.
- [6] A. Banerji, H. Hu, A. T. Alpas, Sliding Wear Mechanisms of Magnesium Composites AM60 Reinforced with Al₂O₃ Fibers under Ultra-mild Wear Conditions, *Wear*, 301 (2013) 626-635.
- [7] J. Lo, and R. Santos, Magnesium matrix composites for elevated temperature applications, 2007 Society of Automotive Engineers World Congress, Detroit, MI, 01 (2007) 1028.
- [8] Q. Zhang, and H. Hu, Development of Hybrid Magnesium-based composites, *Advances in Light Weight Materials-Aluminum, Casting Materials, Magnesium Technologies*, Society of Automotive Engineers World Congress, (2010) 107-114.
- [9] J. Zhou, X. Zhang, L. Fang, H. Hu, Processing and Properties of As-Cast Magnesium AM60-Based Composite Containing Alumina Nano Particles and Micron Fibres, *Magnesium Technology 2017*, Part of the series *The Minerals, Metals & Materials Series*, 573-578
- [10] S. Fida Hassan, A. M. Al-Qutub, S. Zabiullah, K. S. Tun, M. Gupta, Effect of Increasingly Metallized Hybrid Reinforcement on the Wear Mechanisms of Magnesium Nanocomposite, *Bulletin of Materials Science*, 39 (4) (2016) 1101–1107.

- [11] X. Zhang, Q. Zhang and H. Hu, Tensile Behavior and Microstructure of Magnesium AM60-based Hybrid Composite Containing Al₂O₃ Fibres and Particles. *Materials Science Engineering A*, 607 (2014) 269-276.
- [12] S.F. Hassan and M. Gupta, Development of High Performance Magnesium Nanocomposites Using Nano-Al₂O₃ As Reinforcement, *Material Science Engineering A*, 392 (2005) 163-168
- [13] L. Chen, J. Xu, H. Choi, M. Pozuelo, X. Ma, S. Bhowmick, J. Yang, S. Mathaudhu and X. Li., Processing and Properties of Magnesium Containing a Dense Uniform Dispersion of Nanoparticles, *Nature*. 528 (2015) 539-543.
- [14] W. L. E. Wong, M. Gupta, Enhancing the Tensile Response of Magnesium Through Simultaneous Addition of Aluminum and Alumina Nanoparticulates, *Magnesium Technology 2017*, Part of the series *The Minerals, Metals & Materials Series*, 253-257
- [15] Q. Zhang, H. Hu, and J. Lo, Solidification of Discontinuous Al₂O₃ Fiber Reinforced Magnesium (AM60) Matrix Composite. *Defect and Diffusion Forum*. 312-315 (2011) 277-282.
- [16] H. Hu, Grain Microstructure Evolution of Mg (AM50A)/ SiCp Metal Matrix Composites, *Scripta Materialia*, 39(8) (1998) 1015-1022.
- [17] L. Jiang, G. Wu, K. Norio, and S. Hideo, Effects of Sub-Micron Particles on the Matrix Microstructure of Al Based Composites, *Rare metal materials and engineering*, 36(6) 2007 1002-1004.

CHAPTER 5 Microstructure and Tensile Properties of Cast Magnesium AM60-Based Hybrid Nanocomposites Reinforced With Al₂O₃ Fibres and Al₂O₃ or AlN Nanoparticles

5.1. Introduction

Magnesium and its alloys, owing to their low density, approximately two-third of that of aluminium, and high specific strength as compared to other structural metals, have attracted widespread attention in commercial products as well as scientific research as demands for energy conservation and engineering performance are increasing [1, 2]. Especially, a significant rise has been witnessed in the magnesium-based engineering applications in the automotive industry. Due to their relatively low mechanical and high-temperature and corrosion and wear properties, magnesium alloys seem uncompetitive with aluminum alloys and steels. To improve mechanical properties of metallic materials, ceramic-based reinforcement is often introduced to a monolithic alloy to form a metal matrix composite (MMC). Consequently, considerably enhancement of engineering properties such as high strengths, high moduli and high-wear resistance, low coefficient of thermal expansion becomes achievable. The superior properties of MMCs over non-reinforced monolithic alloys provide a large variety of engineering designs. Therefore, magnesium-based composites, which are capable of meeting the demand for high-performance materials with lightweight features, have been receiving attention in the past decade for engineering applications in the automotive industry[3-5].

But, MMCs are often disadvantaged by relatively high cost of fabrication processes and reinforcement materials [6-9]. An economic process for the preparation of composite materials

is an essential element for expanding their applications. Recently, Zhang et al [10] and Zhou et al [11] demonstrated the success in the introduction of two or more reinforcements including short fibres and particles with different sizes into magnesium matrix alloy AM60 by using a preform-squeeze casting process. The hybrid reinforce Mg-based composites exhibited excellent properties as well as a high degree of freedom in materials design for magnesium [10, 11]. As the addition of several reinforcements, Mg-based hybrid composites show opportunities optimize the engineering performance of magnesium-based composites by emerging specific characteristics of reinforcements for various potential applications [12]. The study by Zhang et al [13] indicated that, with the introduction the micron-sized particle and fibres, magnesium hybrid composites have gained high tensile strengths and elastic modulus compared to the unreinforced matrix alloy. Meanwhile, it was observed a remarkable reduction in ductility. To minimize ductility reduction recently, nano-sized particles were highlighted for improvement of this situation. The addition of nano-sized particles into magnesium alloys by substituting micron-sized particles successfully increases the ductility of micron-sized reinforced MMCs significantly [3, 14-16]. However, studies on magnesium-based hybrid composites reinforced with both nano particles and micron fibres are limited in the open literature. In particular, the types and sizes of nano particles influence the mechanical properties of Mg-based nanocomposites. Also, because of high costs of fabricating processes such as evaporation, spray processing and ball milling compared with conventional approaches, i.e., stir casting and/or preform and squeeze casting, real engineering applications of magnesium-based composites are scarce in the highly competitive automotive industry.

In this study, magnesium alloy AM60-based hybrid nanocomposites (MHNC) incorporating nano Al_2O_3 or AlN particles with different sizes and micron alumina (Al_2O_3) fibre are prepared by a preform and squeeze casting technique. The microstructures of the MHNCs are analyzed by the Transmission Electron Microscopy (TEM), Scanning Electron Microscopy (SEM), and Optical Microscopy (OM) and compared with that of the base alloy. The mechanical properties of the MHNCs are determined by tensile testing. The effects of the microstructure characteristics and reinforcement types on the tensile behavior of the MHNCs are investigated. The SEM fractographic analyses of the MHNCs are performed.

5.2. Experimental Procedures

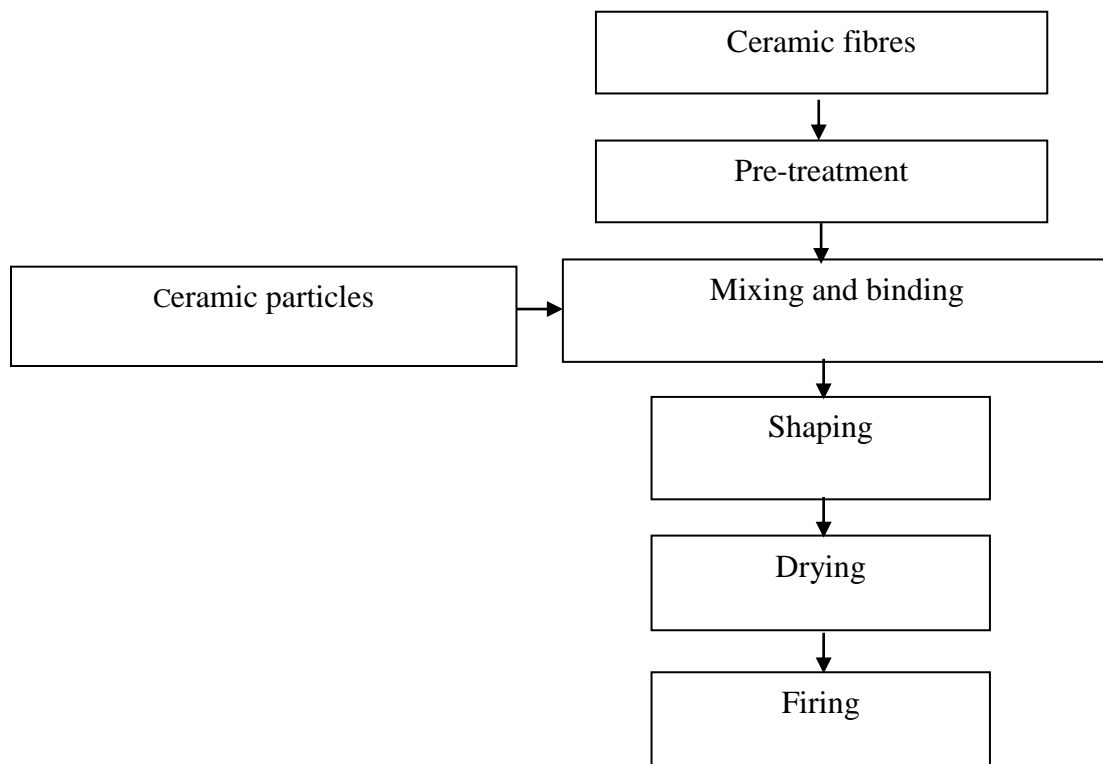
5.2.1. Materials

Magnesium alloy AM60 with a chemical composition (wt %) of 6.0Al-0.22Zn-0.4Mn-0.1Si-0.01Cu-0.004Fe-0.002Ni-Mg was chosen as matrix alloy. Nano-sized Al_2O_3 ceramic particles with an average particulate size of 100 nm (US Research Nanomaterials, Inc., USA), nano-sized AN ceramic particles with an average particulate size of 800 nm (US Research Nanomaterials, Inc., USA), and Al_2O_3 short fibres (Morgan Advanced Materials, United Kingdom) with an average diameter of 4 μm and length of 50 μm were employed as raw materials for the preparation of hybrid reinforcements since they are relatively inexpensive and possess adequate properties listed in Table 5.1.

Table 5.1 Mechanical properties of nano-sized ceramics particles

	Elastic Modulus (GPa)	Fracture Toughness (MPa/m ²)
Al ₂ O ₃	385 [17]	3.3-5 [19]
AlN	308 [18]	3-5.9 [20]

(a)



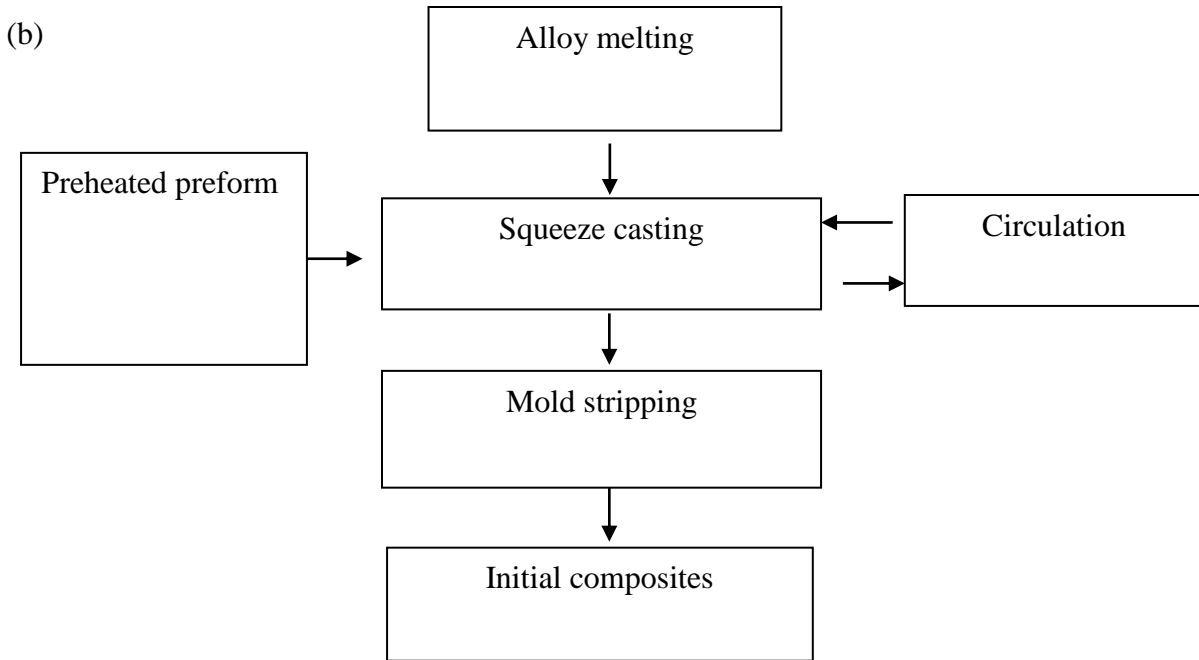


Figure 5.1. Flowchart showing the procedure for fabricating hybrid (a) preform and (b) composites.

5.2.2. Fabrication of hybrid preform

The preparation steps for fabrication of the hybrid preforms (Figure 5.1, a) involve mixing the ceramic short fibres and particles, introducing the binding compounds, forming the preform shape under a pressure, drying and sintering. In the hybrid preform, the fibres served as the skeleton for a cellular structure. The content level of the fibre was pre-determined based on the desired amount of porosity in the cellular solid. The particulate reinforcements were dispersed in the pores present in the cellular solid. The content, size and type of the ceramic reinforcements were adjusted to yield the required quantity, and shape of the preform. In addition, for the purpose of a comparative study of the hybrid preform characteristics; a pure fibre preform was also fabricated using the same process without adding particulate reinforcements.

5.2.3. Fabrication of composites

Figure 5.1 (b) shows the fabrication process for the composites in which a squeeze casting process was adopted. During fabrication, a hybrid preform was first preheated to 700 °C. Then, molten matrix alloy AM60 at 700 °C infiltrated into the preheated preform under an applied pressure of 90 MPa. The pressure was maintained at the desired level for 30 seconds. After squeeze casting, cylindrical disks of single or dual-phase reinforced composites with 3 vol.% of nano-sized Al₂O₃ or nano-sized AlN particles and 5 vol.% Al₂O₃ fibres, were obtained. In the hybrid composite, the particles constituted the primary reinforcement phase, and short fibres served as the secondary reinforcement phase. For the purpose of comparisons, three different types of composites, 5 vol.% Fibre/AM60, (5 vol.% Fibre + 3 vol.% nano-Al₂O₃-Particle)/AM60 and (5 vol.% Fibre+3 vol.% nano-AlN-Particle)/AM60 composites were prepared, which were also named the fibre-only composite, the MHNC-Al₂O₃, and the MHNC-AlN, respectively. More details on the process for fabricating the composites are given in references 10, 11 and 13.

5.2.4. Microstructure analysis

All specimens were cut from the center of the casting coupon. The type of heat treatment, T4, was conducted on both of the unreinforced alloy AM60 and fiber-reinforced composites to reveal the grain structure. Following the standard metallographic procedures, as-cast and T4-treated specimens were mounted and polished. To disclose the microstructural characteristics of the composites and alloys, samples were then polished and etched in a hybrid solution (60 ml 99% ethanol solution, 20 ml acetic acid, 19 ml dilute water, and 1 ml nitric acid) for microstructural analyses. The primary morphologic grain characteristics of the polished and

etched samples were investigated under optical microscopy (OM) (Buehler image analyzer 2002). The existence and distribution of the reinforcements were investigated by a JEOL JSM-5800LV scanning electron microscope (SEM) with an energy dispersive X-ray spectrometer (EDS). Samples for TEM (JOEL 2010F) were prepared by focus ion beam (FIB) (Zeiss NVision 40) using STEM modulus for investigation; electron energy loss spectroscopy (EELS) was applied for identification of non-conductive and negative element such as nitrogen. To prevent the fall-off of the tiny nano Al_2O_3 particle, a tungsten coating was applied to the cross-section surface of the MHNC foil prepared by the FIB before the TEM observation.

5.2.5. Tensile testing

Mechanical properties were evaluated via tensile testing (ASTM B557) at ambient temperature using specimens of $25 \text{ mm} \times 6 \text{ mm} \times 6 \text{ mm}$ (gauge length \times width \times thickness) on an Instron (Grove City, PA, USA) machine equipped with a computer data acquisition system. The tensile specimens were machined from the center of as-cast coupons. The tensile tests were performed at a strain rate of $5 \times 10^{-3} \text{ s}^{-1}$. The tensile properties, including 0.2% yield strength (YS), ultimate tensile strength (UTS), elongation to failure (ef), and elastic modulus (E) were obtained based on the average of three tests.

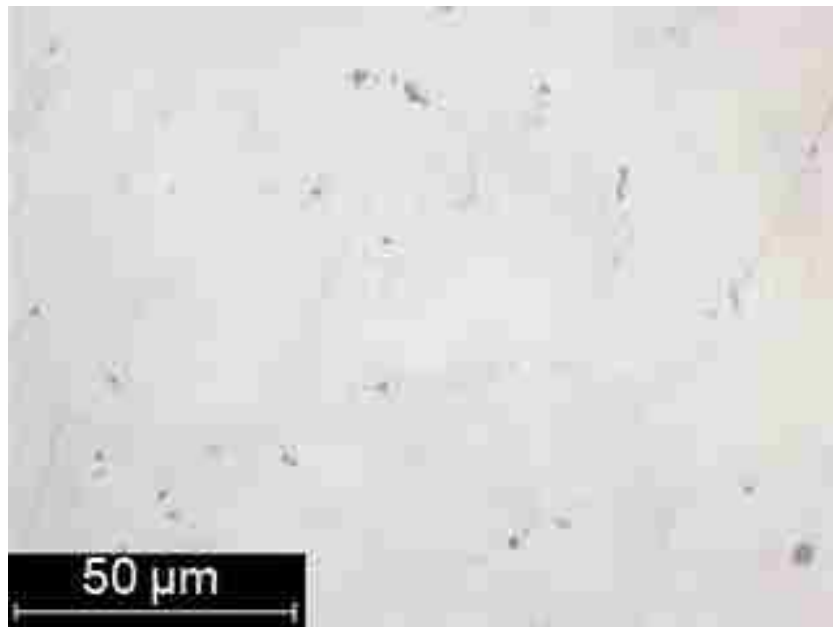
5.3. Results and Discussion

5.3.1. Microstructure

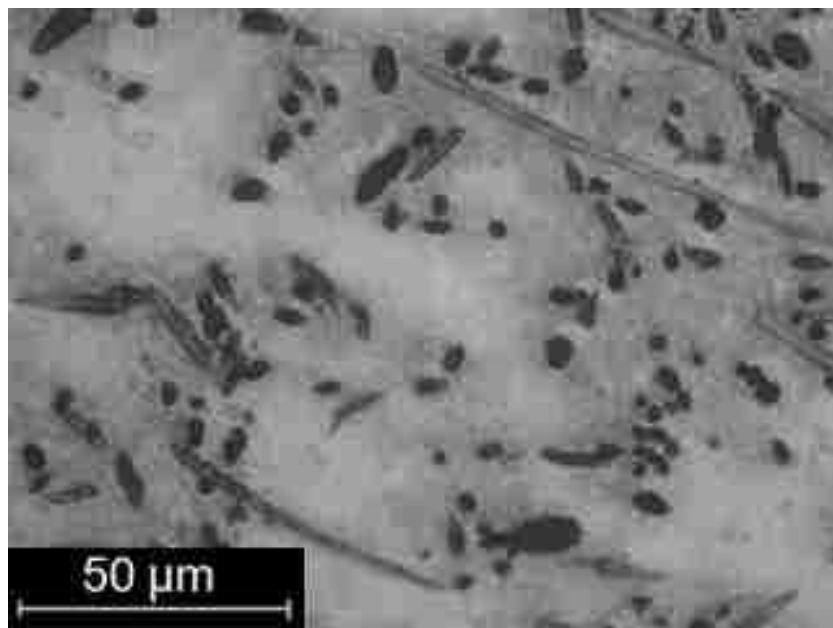
Optical micrographs given in Figure 5.2 show the unetched matrix alloy and the composites. Figure 5.2(a) reveals the divorced eutectic phases ($\beta\text{-Mg}_{17}\text{Al}_{12}$) is present along the grain boundaries of the unreinforced alloy. As shown in Figure 5.2(b), the short fibres are distributed in a random and isotropic orientation in the fibre-reinforced composite. Figures 5.2(c) and (d) presents the microstructures of the hybrid magnesium composites reinforced with nano-sized Al_2O_3 or AlN particles, respectively. It can be seen that the fibres and particles are uniformly distributed throughout the matrices in the fibre-only composite and the MHNCs. The introduction of either nano-sized Al_2O_3 or nano-sized AlN particles up to 3 vol% has almost no influence on the uniformity of fibres. Pores are barely found in the microstructure, suggesting the hybrid composites are well densified during fabrication due to a gradual application of the infiltration pressure. The pore-free microstructure of the composites also ascertains the success in the infiltration of the matrix alloy into the hybrid preform.

A non-uniform distribution of reinforcements could lead to a inhomogeneity of grain structure and induce the formation of defects, and consequently degrade mechanical properties of the composites. Despite the presence of the large difference in size between the particles and the fibres, it is observed from Figures. 5.2(c) and (d) that the nanoparticles and fibres are dispersed homogeneously without agglomeration and cave in the matrix alloy. The homogeneous microstructures of the composites reinforced with both the Al_2O_3 and/or AlN nanoparticles and micron fibres in the matrix meet the demand for the materials design by using ceramic particles as the main reinforcement to enhance the mechanical and wear properties of the composites, with

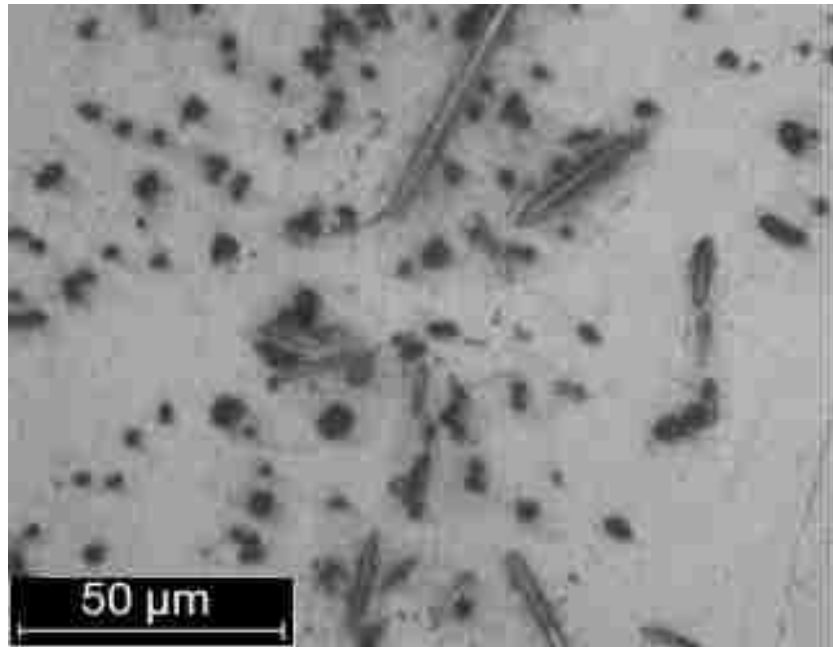
the fibres helping improve their toughness. The overall properties of the composites should be tailored and enhanced by the well-distributed reinforcements.



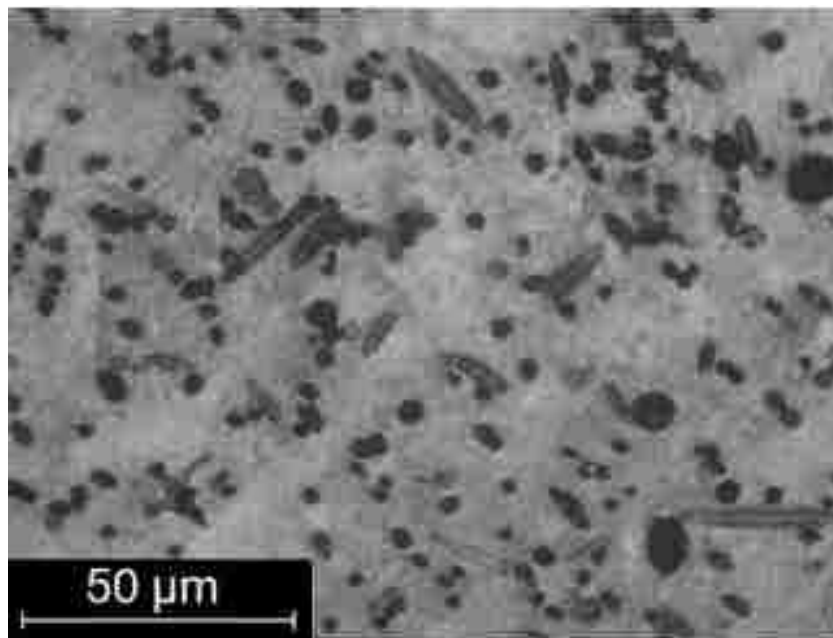
(a)



(b)



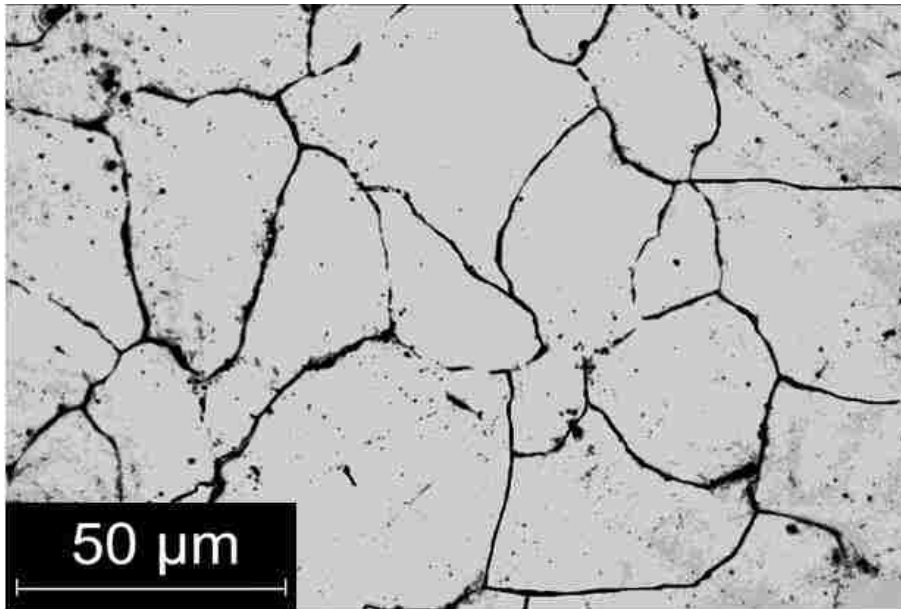
(c)



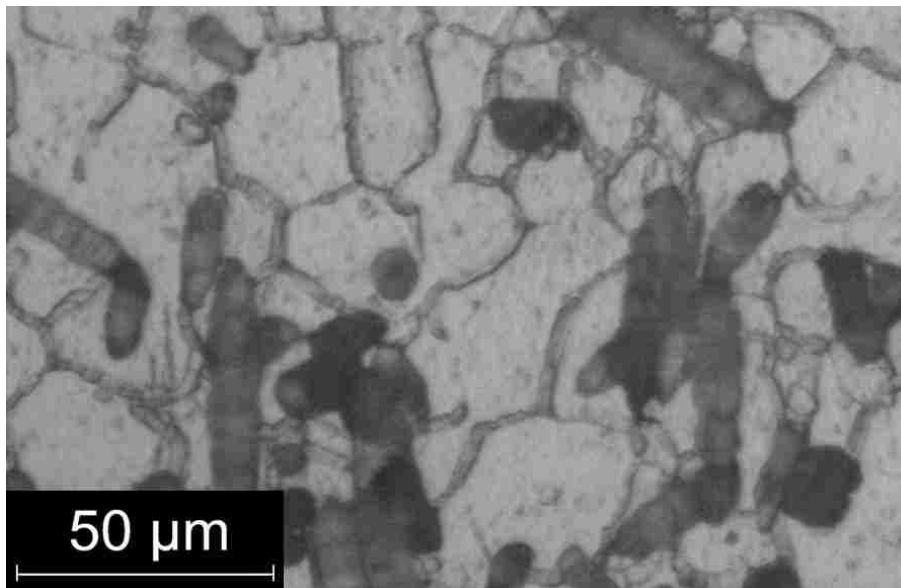
(d)

Figure 5.2. Optical photograph showing the microstructures of unetched as-cast matrix alloy and composites, (a) unreinforced matrix alloy AM60, (b) 5 vol% Fibre/ AM60, (c) (3 vol% nano Al_2O_3 particle +5 vol% fibre)/ AM60, and (d) (3 vol. % nano AlN particle +5 vol% fibre)/ AM60.

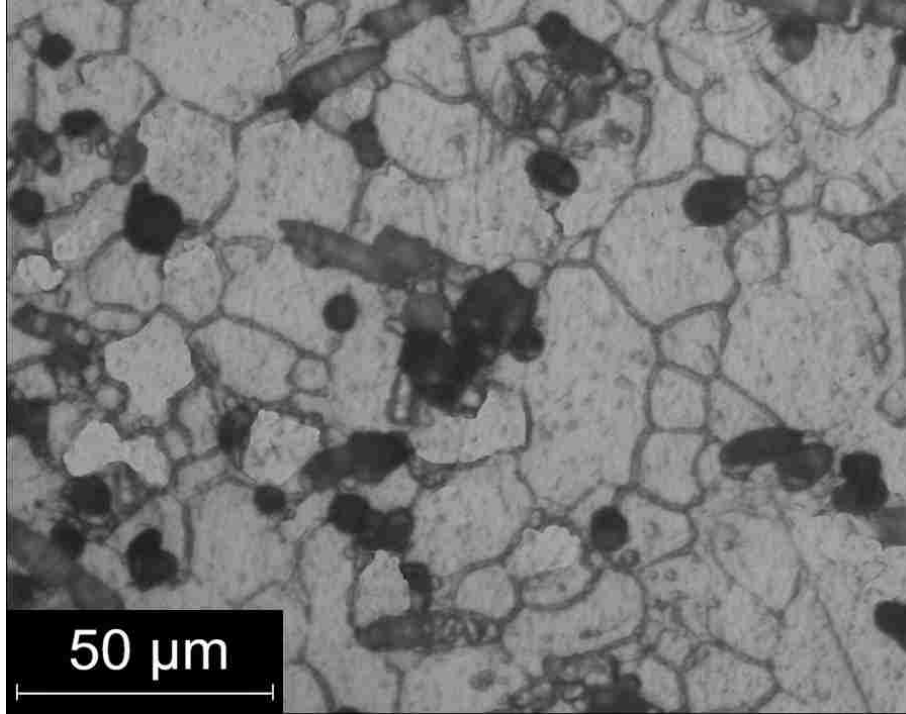
Figure 5.3 presents the grain structures of the etched matrix alloy and the composites. The grain size measurements for the composites and unreinforced AM60 matrix alloy are presented in Figure 5.4. With 5 vol% of micron-sized fibres, the grain size of the matrix alloy decreases from 68 to 45 μm by 34%. Qiang et al [21] reported that the restriction of grain growth by the limited cellular space formed in the skeleton of the fiber preform structure should be responsible for the refinement of grain structure in the fibre-only composite. The addition of 3 vol.% AlN nano particles to the hybrid composite further reduces the grain size of the matrix alloy from 45 to 34 μm by 24%. It was observed [22] that the grain refinement of as-cast Mg alloy AM50 with 5 vol% micron fibre was attributed to the coupled effect of the heterogeneous nucleation of the primary magnesium phase on particles and the restricted growth of magnesium crystals. The microstructural analysis of the nanocomposite reveals the similar effect of grain refinement by the addition of nano-sized particles. The replacement of the relatively large nano AlN particles with the fine nano Al₂O₃ particles further reduces the grain size of the matrix in the MHNC from 34 to 28 μm by 21%.



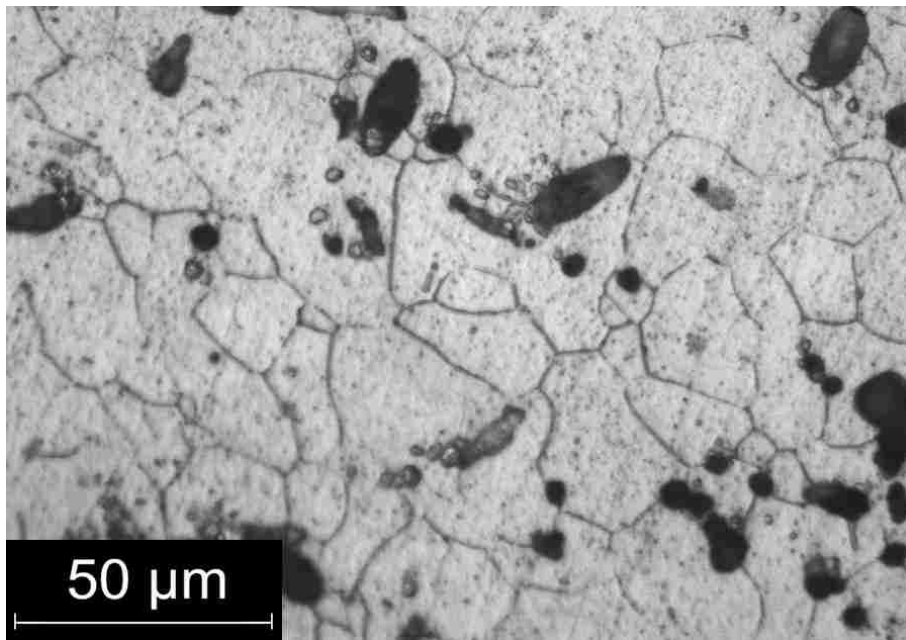
(a)



(b)



(c)



(d)

Figure 5.3. Optical micrographs showing grain structures of etched (a) unreinforced matrix alloy AM60, (b) 5 vol.% fibre/ AM60, (c) (3 vol% nano Al₂O₃ particle +5 vol.% fibre)/ AM60, and (d) (3 vol. % nano AlN particle +5 vol.% fibre)/ AM60.

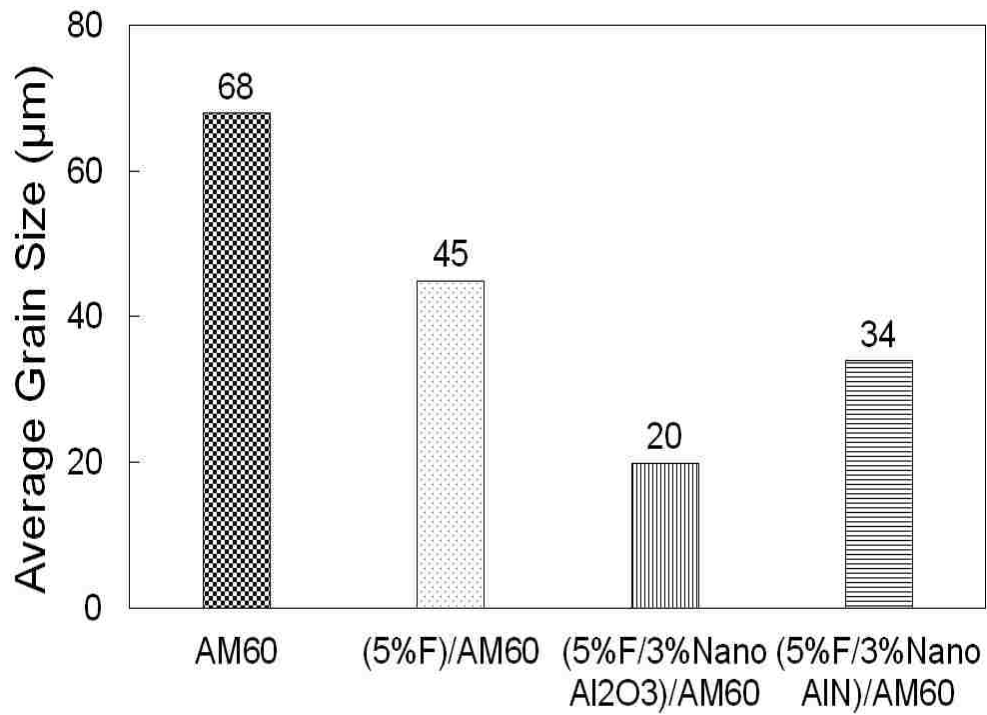
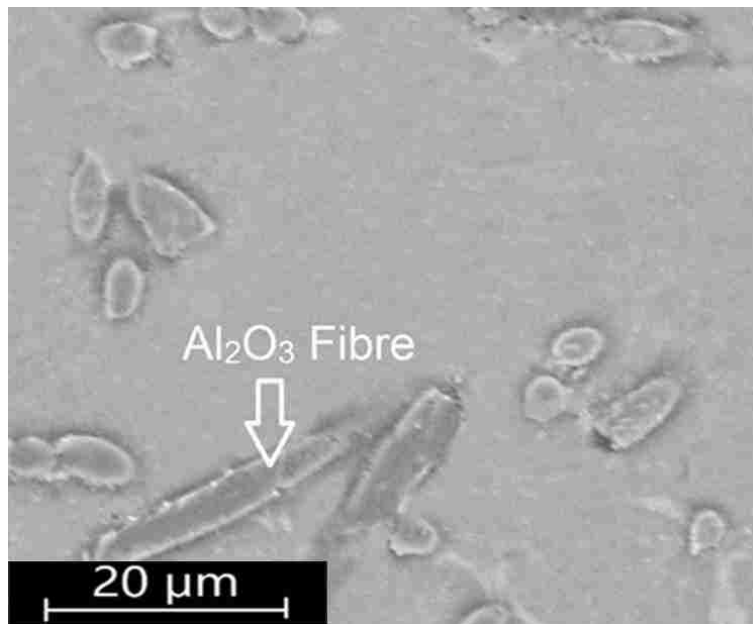
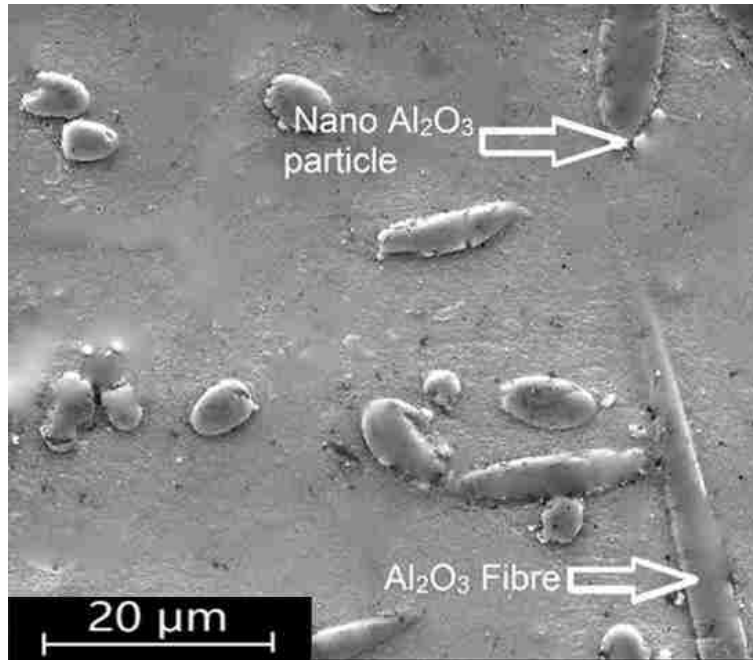


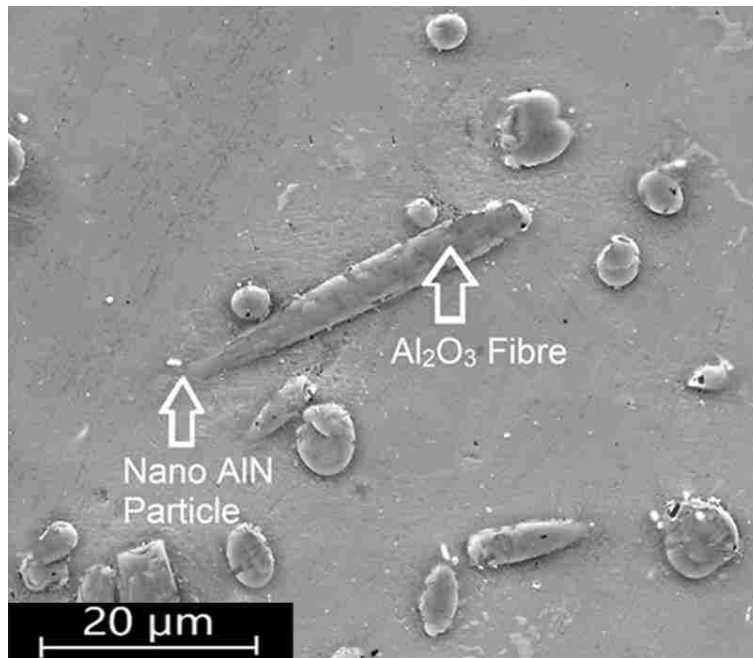
Figure 5.4. Measured grain sizes of the unreinforced matrix alloy AM60, 5 vol% fibre/ AM60, (3 vol% nano Al₂O₃ particle +5 vol% fibre)/ AM60, and (d) (3 vol. % nano AlN particle +5 vol% fibre)/ AM60.



(a)



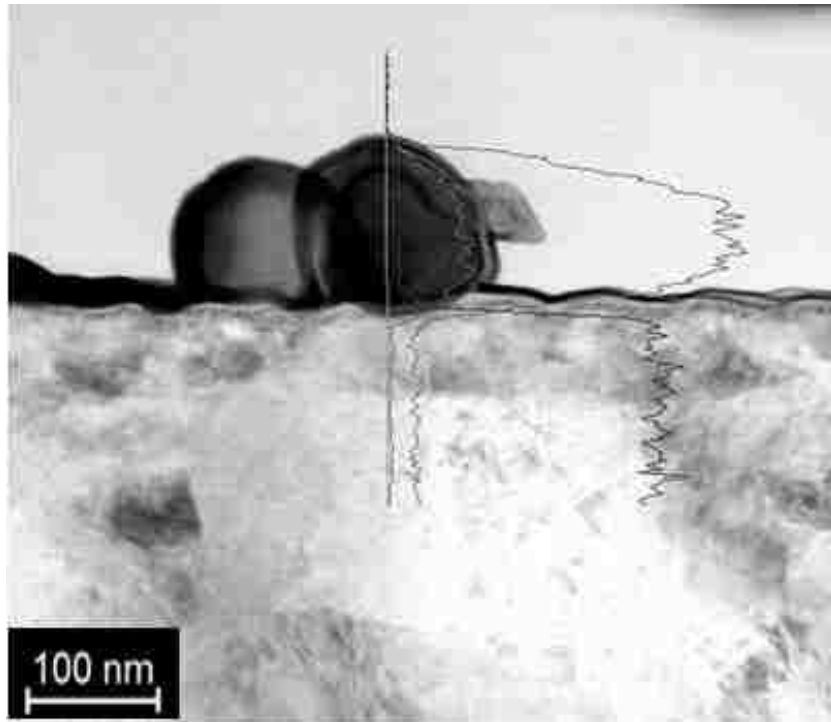
(b)



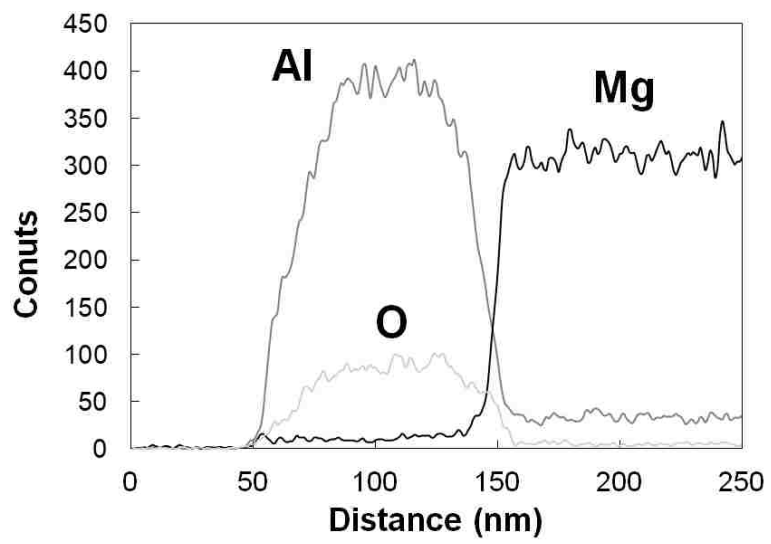
(c)

Figure 5.5. SEM micrographs in BSE mode showing the reinforcement distribution in (a) 5 vol% fibre/ AM60, (b) (3 vol% nano Al₂O₃ particle +5 vol% fibre)/ AM60, and (c) (3 vol. % nano AlN particle +5 vol% fibre)/ AM60.

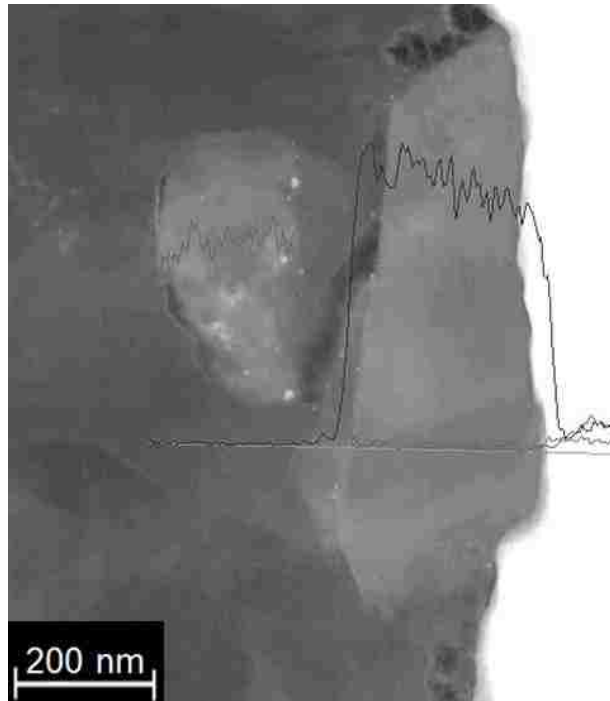
Figure 5.5 gives the reinforcement distribution in the microstructure of the unreinforced matrix alloy, the fibre-only composite and the hybrid composites by SEM micrographs in a backscattered electron (BSE) mode. As shown in Figure 5.5, the reinforced fibres and nano particles are well dispersed and placed individually with little agglomeration. The TEM and EDS analyses presented in Figure 5.6, confirm the presence of the nano particles in the MHNCs which further evidences the successful introduction of the nanoparticles in the composites (Figure 5.6(a) and (c)). The probe crossed an Al_2O_3 nano particle and the AlN nano particles along the white lines in Figures 5.6(b) and (d). When the probe went from the matrix to the nano-sized Al_2O_3 particle, a large sharp decrease in magnesium, and a rapid increase in aluminum and oxygen were found. For the nano AlN particle-reinforced MHNC, the probe detected a rapid increase in aluminum counts and a decrease in magnesium counts when crossing a nano AlN particle by EDS scanning, and a rapid increase in nitrogen by EELS scanning. This observation is consistent with the compositions of the matrix and particle reinforcements. Examination of the interfacial structure reveals a relatively clean and featureless surface of both the Al_2O_3 and AlN particles in the MHNCs. No particle/matrix reaction products are detected in either the nano Al_2O_3 -reinforced MHNC or the nano AlN-reinforced MHNC by TEM. This should be primarily due to the presence of inadequate reaction time between the particles and matrix alloy as a result of fast pressurized infiltration implemented during squeeze casting.



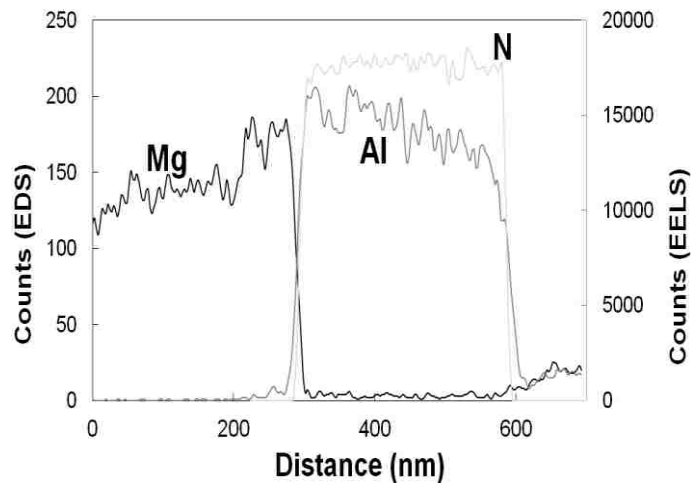
(a)



(b)



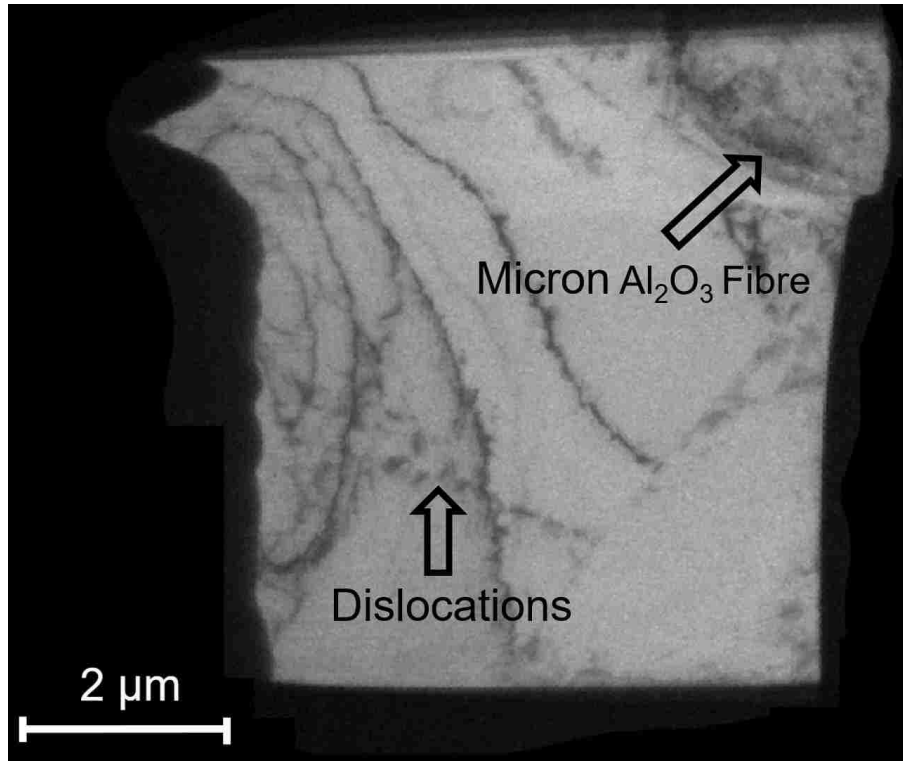
(c)



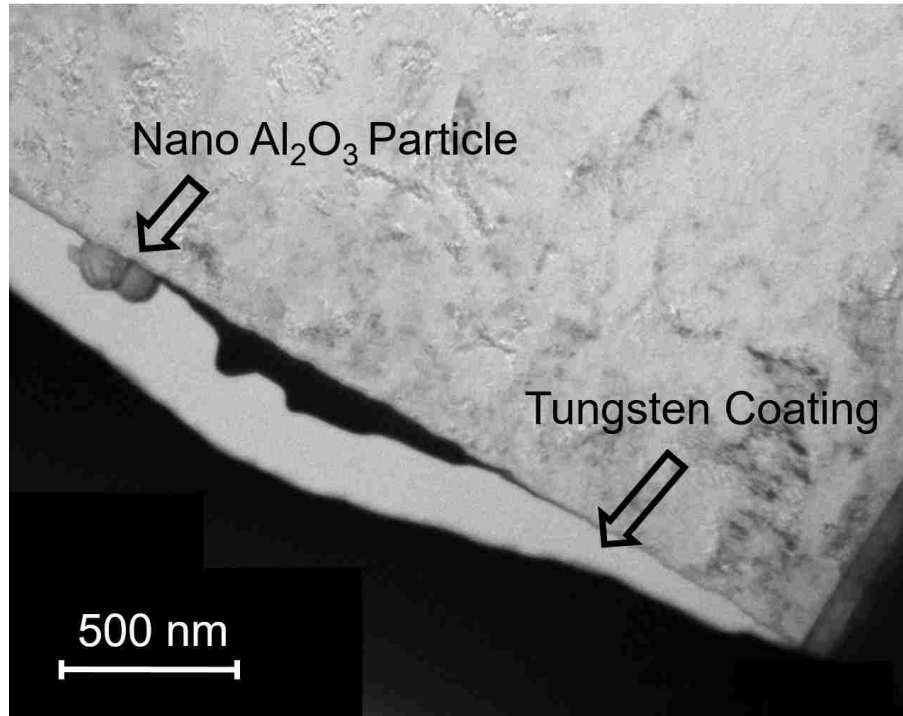
(d)

Figure 5.6. TEM micrographs (a) a nano Al_2O_3 particle in the (3 vol% nano Al_2O_3 particles + 5 vol% Fibres) /AM60 MHNC line scans and the corresponding line scanning pattern for the nano particle cross-section area (b) EDS pattern for the nano Al_2O_3 particle line scan (c) a nano AlN particle in the (3 vol% nano AlN particles + 5 vol% Fibres) /AM60 MHNC line scans and the corresponding line scanning pattern for the particle cross-section area (d) EDS and EELS patterns for the nano AlN particle line scan.

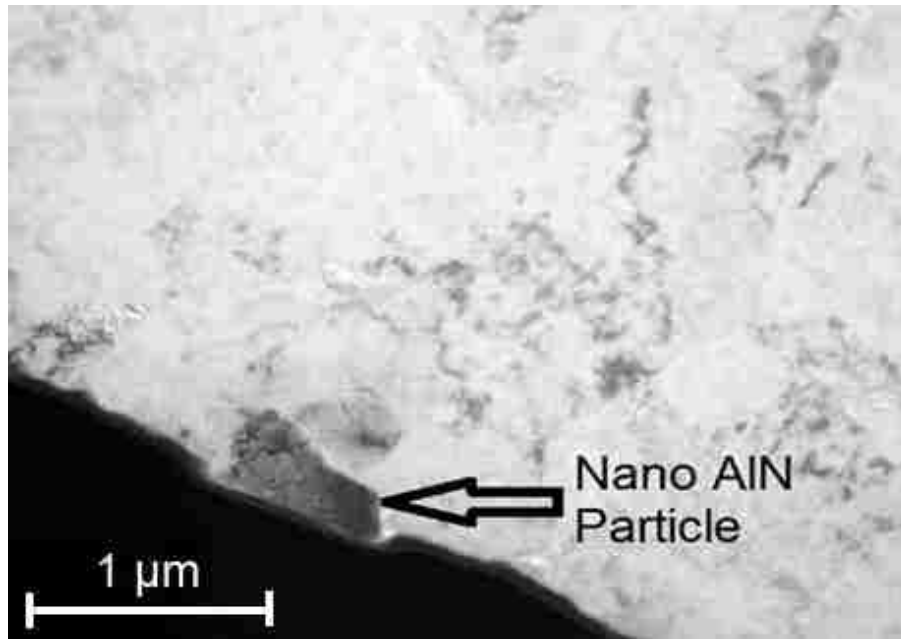
Figure 5.7 shows the TEM micrographs of the fibre-only composite, MHNC-Al₂O₃, and MHNC-AlN. As shown in Figure 5.7(a), the fibre-only composite contains high dislocation densities around a micron fibre. However, Figure 5.7(b) reveals that the MHNC-Al₂O₃ is almost free of dislocations under the applied condition of the electron diffraction pattern. The very low dislocation density in the MHNC-Al₂O₃ should primarily result from the fact that the nano particles are extremely tiny (100 nm), which are hard to generate sufficient strain by the thermal mismatch to induce dislocations during solidification. A moderate dislocation density exists in the MHNC-AlN (Figure 5.7(c)), which might be attributed to their relatively large size of 800 nm compared with that of the nano Al₂O₃ particles. The inherent difference in thermal expansion coefficients should be responsible for the formation of mismatch stress of the particles and matrix alloy, which results in a dislocation density to some extent. This observation is consistent with the results disclosed in references [14, 23]. However, by the addition of the nano AlN particles, nano-sized pores in a closed-cell structure are found, which is similar to a structure in metal foams at macroscopic scale. Shi et al [24] suggested that this type of the structure in nano scale formed during solidification rose from the wettability between the AlN and magnesium alloy. The presence of the nano pores might act like those cells in foam metal increases energy absorption, stiffness, and even ductility by extending the amount of plastic dissipation during mechanical loading.



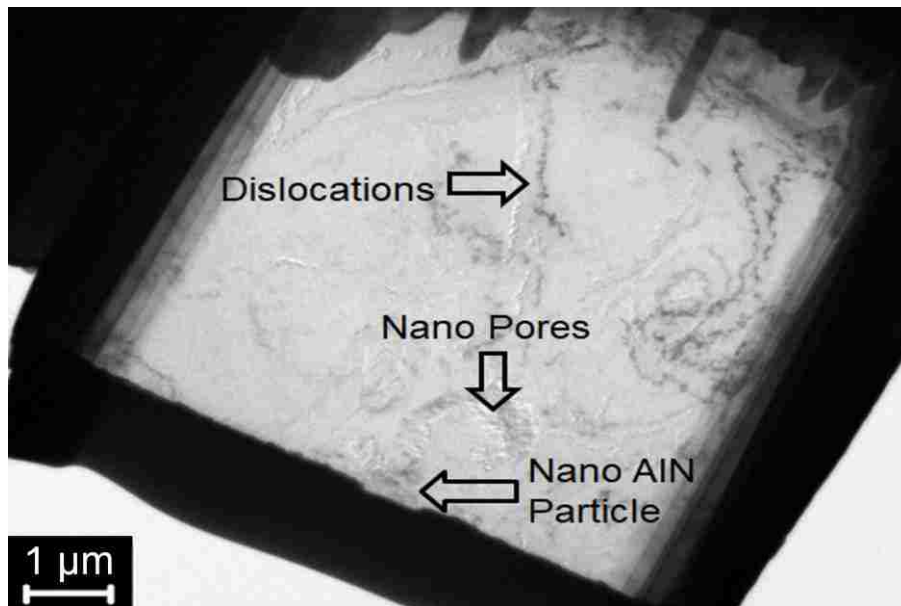
(a)



(b)



(c)



(d)

Figure 5.7. TEM micrographs showing (a) the micron fibre-only composites with dislocations, (b) the MHNC- Al_2O_3 with almost no dislocations, and MHNC-AlN with (c) AlN particle and (d) nano pores and dislocations ((c)zoomed out).

5.3.2. Tensile properties

The typical engineering stress-strain curves for AM60, the fibre-only composite (AM60 5%F), the the MHNC- Al_2O_3 (AM60 5%F-3%P nano Al_2O_3), and the MHNC-AlN (AM60 5%F-3%P nano AlN) are shown in Figure 5.8. The curves for the matrix alloy and the composites exhibit a similar pattern, where they deform elastically first. Upon the yield point is reached, the plastic deformation sets in. The introduction of fibers and/or particles lifts the yield points of the composites up to high stress levels. Consequently, the composites fractures at much higher stress and lower strain levels than that of the matrix alloy AM60. It can be seen from Figure 5.8 that, although the introduction of the reinforcements leads to an increase in the strengths, there is a significant reduction in elongation as micron fibres are added. But, the addition of the nano Al_2O_3 or AlN particles in the MHNC recovers the elongation significantly.

The tensile properties data given in Table 5.2 show that the as-cast matrix alloy has 171 MPa of its UTS, 81 MPa of its YS, 40 GPa of its elastic modulus and 6.0% failure elongation. The introduction of the micron fibre reinforcement, increases the UTS, YS and E to 189 MPa, 120 MPa and 50 GPa, by 11%, 48%, and 25%, respectively, but reduces the elongation from 6.0% to 2.2% by 63%. Additional 3 vol.% of nano Al_2O_3 particles further enhances the UTS, YS and E to 216 MPa, 140 MPa and 53 GPa by 14%, 17% and 6% over those of the fibre-only composite. Meanwhile, the MHNC-AlN composite possesses the UTS, YS and E of 210 MPa, 139 MPa, and 51 GPa, showing the increases of 11% in UTS, 16% in YS, 2% in E compared to those of the fibre-only composite. Furthermore, it should be pointed out that the introduction of nano-sized Al_2O_3 or AlN particles restores the elongation considerably from 2.2% of the fibre-only composite to 3.5% or 3.6% by 59% or 63%, respectively. The determined yield and tensile strengths of the tested materials are in line with the grain size measurements since the grain

refinement enhances the materials strengths. Since the tensile properties of the MHNC- Al₂O₃ and MHNC-AlN are very comparable, the sizes of the tested nano particles seems to have a limited effect on the tensile properties of the MHNC, although the nano AlN particles is eight times larger than the nano Al₂O₃ particles. Also, the TEM observation suggests that the presence of the moderate dislocation in the MHNC-AlN should be responsible for the resultant tensile strengths, which are comparable to the tensile properties of the MHNC-Al₂O₃, although the modulus of nano AlN particles is lower than that of nano Al₂O₃ particles. The existence of nano pores in the MHNC-AlN might be beneficial to the deformation for extra strains, while its dislocation density is only at a moderate level which might have a limited effect on ductility. Overall, by taking into consideration of engineering performance and materials cost, the nano Al₂O₃ particles with a relatively low price of appears attractive to the development of automotive applications.

Table 5.2 UTS, YS, ef and E of the Matrix Alloy AM60, the Composites of 5 vol. % Fibre/AM60, (5 vol.% Fibre+3 vol.% nano Al₂O₃ particles)/AM60, (5 vol.% Fibre+3 vol.% nano AlN particles)/AM60

	YS (MPa)	UTS (MPa)	ef (%)	E (GPa)
AM60	81±6	171±8	6.0±1.3	40±4
Fibre-only	120±5	189±12	2.2±1.7	50±2
MHNC nano Al ₂ O ₃	140±14	216±5	3.5±1.2	53±3
MHNC nano AlN	139±12	210±7	3.6±0.6	51±4

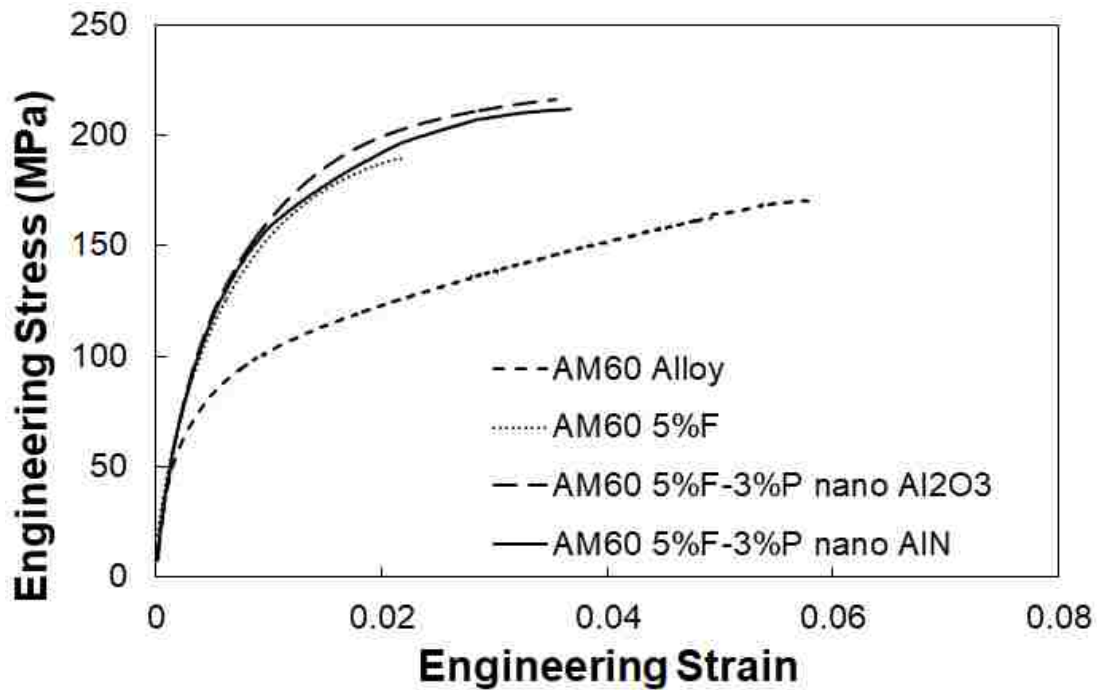


Figure 5.8. Engineering stress vs. strain curves for the matrix alloy AM60, 5 vol% Fibre/AM60, (5 vol.% Fibre+3 vol% nano Al₂O₃ particles)/AM60, and (5 vol.% fibre+3 vol.% nano AlN particles)/AM60.

The observed ductility recovery is evidently supported by the results of the TEM analysis. A high dislocation density provides more tough obstacles to overcome, which increases the strength and toughness of materials. With a low dislocation density, however, materials are capable of carrying more strain during deformation. Also, Hassan and Gupta[14] have also observed that the addition of micron-sized reinforcements leads to an improvement in the elastic modulus and the strengths, but results in a marked diminishment in elongation. However, the addition of nano-sized particles results in a significant improvement in the elastic modulus and the strengths as well as a restoration of ductility. This is because the sites provided by nano-particles where cleavage cracks are opened ahead of the advancing crack front are capable of

dissipating stress concentration from crack tips and altering local effective stress state from plane strain to plane stress in the neighborhood of the crack tip. Overall, the high strengths and moderate elongation of the MHNC should result from the combined strengthening effect: homogeneous distribution of nano particles, matrix grain structure refinement, good interfacial bonding between the matrix and the nano particles and micron fibres[15].

5.3.3. Strain hardening

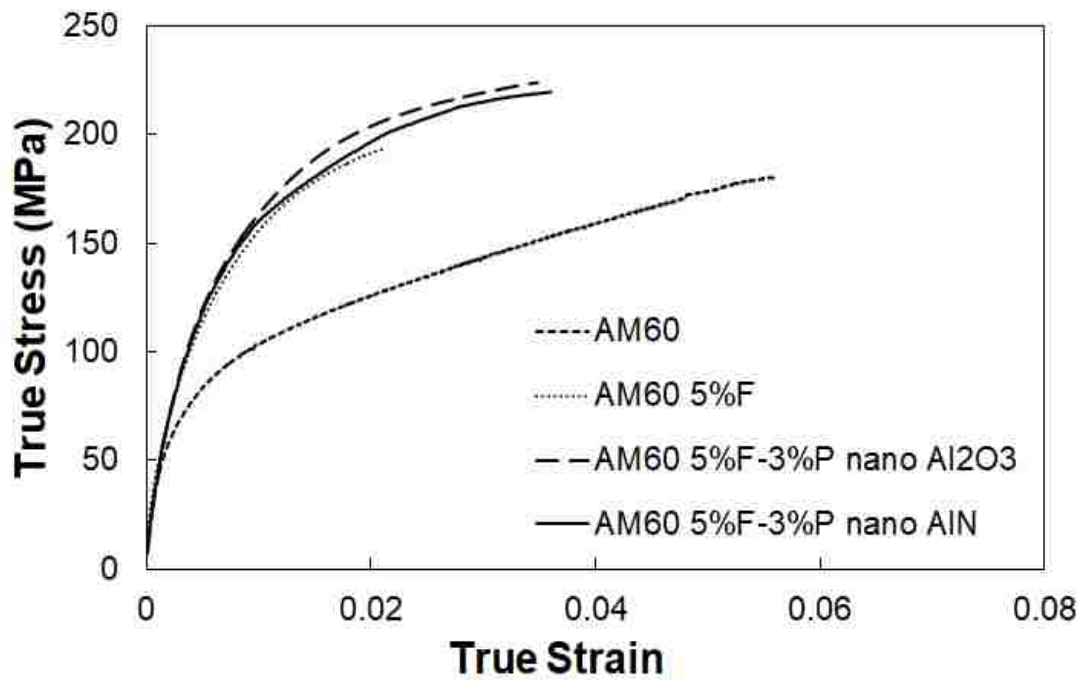


Figure 5.9. True stress vs. strain curves for the matrix alloy AM60, 5 vol% Fibre/AM60, (5 vol.% Fibre+3 vol% nano Al₂O₃ particles)/AM60, and (5 vol.% fibre+3 vol.% nano AlN particles)/AM60.

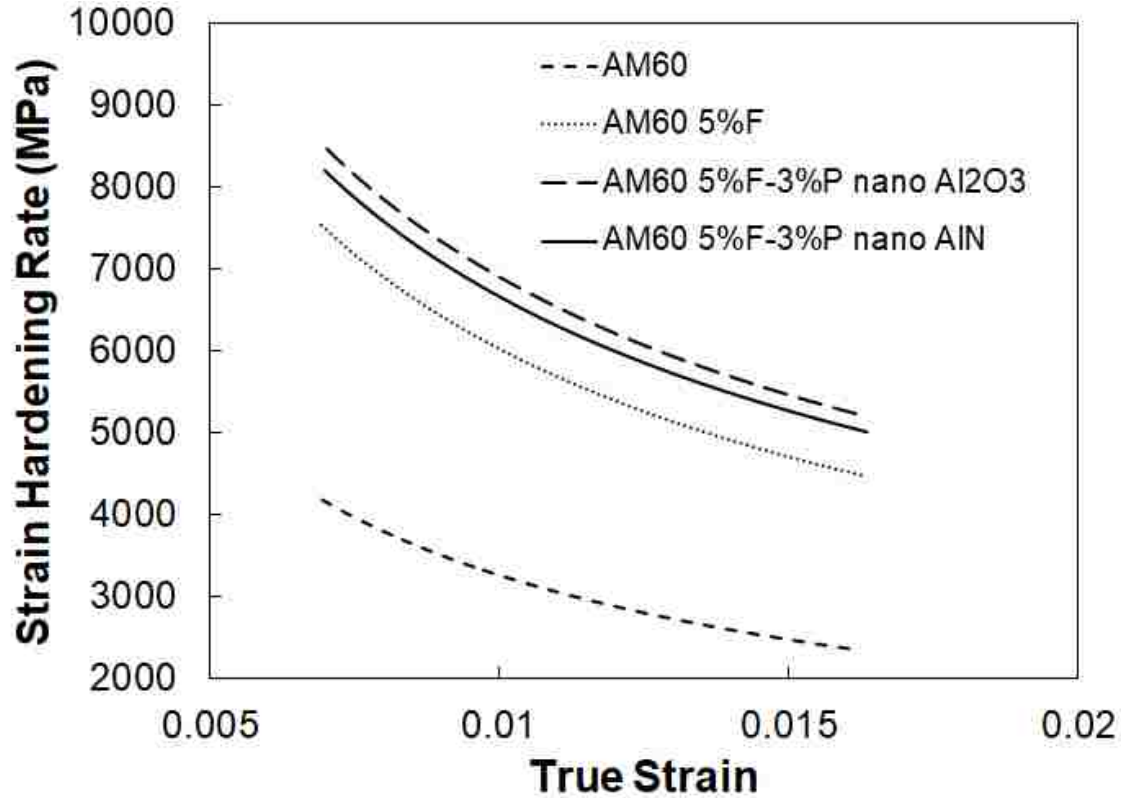


Figure 5.10. Strain hardening curves for the matrix alloy AM60, 5 vol% Fibre/AM60, (5 vol.% Fibre+3 vol% nano Al_2O_3 particles)/AM60, and (5 vol.% fibre+3 vol.% nano AlN particles)/AM60, upon the commencement of plastic deformation.

The true stress and strain can be calculated from the engineering stress and strain by applying the following equations:

$$\sigma_t = \sigma_e (1 + \epsilon_e) \quad (\text{Eq. 5.1})$$

$$\epsilon_t = \ln (1 + \epsilon_e) \quad (\text{Eq. 5.2})$$

where σ_t is the true stress, ϵ_t is the true strain, σ_e is the engineering stress, and ϵ_e is the engineering strain. Figure 5.9 shows the true stress vs. strain curves for the matrix alloy AM60, 5 vol% Fibre/AM60, (5 vol.% Fibre+3 vol% nano Al_2O_3 particle)/AM60, and (5 vol.% fibre+3 vol.% nano AlN particle)/AM60.

The true stress-strain curve for engineering materials can be described by the power law relationship for plastic deformation [13]:

$$\sigma = K \varepsilon^n \quad (\text{Eq.5.3})$$

where K is the strength index, ε is the plastic strain and n is the strain hardening exponent.

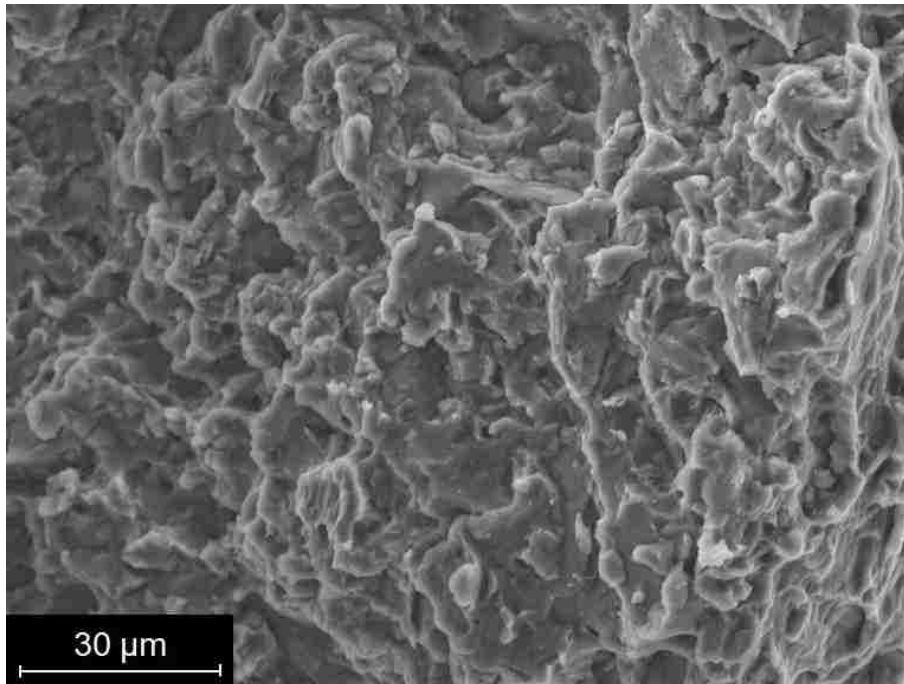
Table 5.3 Best fit parameters of power equation

Materials	K (MPa)	n	R ²
AM60	444±10	0.3187±0.0074	0.9957±0.0019
AM60 5%F	932±11	0.3908±0.0052	0.9946±0.0021
AM60 5%F-3%P nano Al ₂ O ₃	1143±15	0.4223±0.0098	0.9992±0.007
AM60 5%F-3%P- nano AlN	1097±10	0.4201±0.0102	0.9907±0.0032

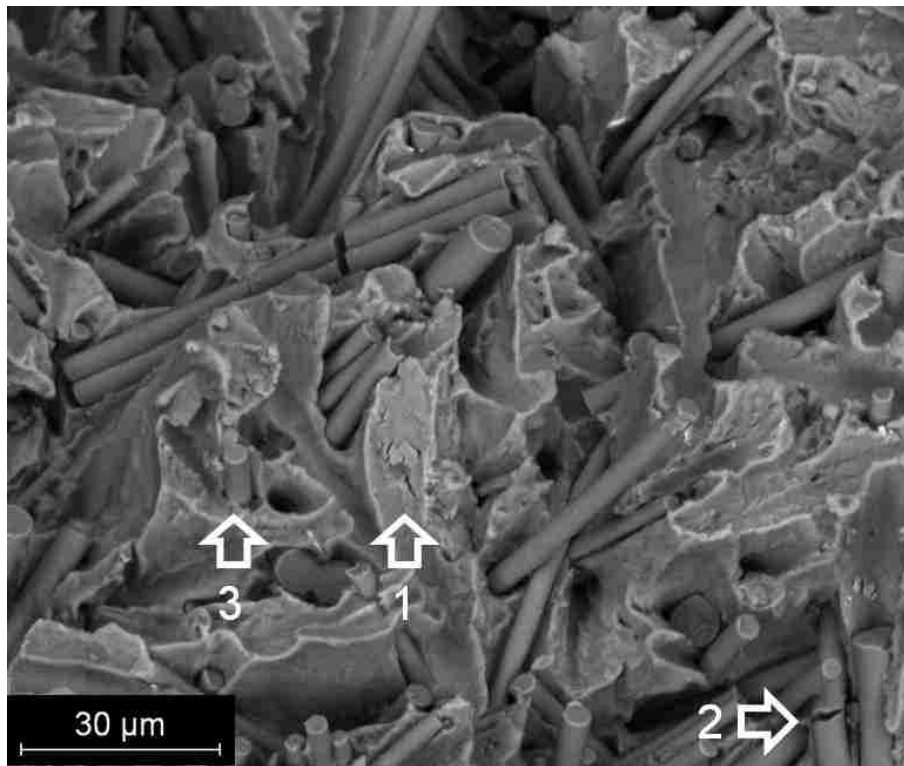
Table 5.3 lists the numerical values of the constants in Eq. 5.3 with the regression coefficients. The strain hardening rate ($d\sigma/d\varepsilon$) can be obtained from the differentiation of the Eq. 5.3. The strain hardening behaviors of the matrix alloy and composites are shown in Figure 5.10, which was derived from Figure 5.9. Figure 5.10 presents the strain hardening rates at the beginning of the plastic deformation for the matrix alloy AM60, 5 vol% Fibre/AM60, (5 vol.% Fibre + 3 vol.% nano Al₂O₃ particle)/AM60, and (5 vol.% fibre + 3 vol.% nano AlN particle)/AM60. All the tested materials exhibit the similar trend, in which the strain hardening rates decrease with increasing the true strain. At the beginning of the plastic deformation, the matrix alloy shows a strain hardening rate of only 4085.2 MPa. The ceramics fibre introduction increases the strain hardening rate to 7453.5 MPa. The strain hardening rate rises to 8418.6 MPa

after the addition of the nano Al_2O_3 particles to the fibre-only composite. The substitution of the nano AlN particles for the nano Al_2O_3 particles leads to a minor decrease in the strain hardening rate to 8201.9 MPa. Among all the tested materials, the MHNC- Al_2O_3 has the highest strain hardening rate. The MHNC- AlN has the strain hardening rate slight lower than, but comparable to that of the MHNC- Al_2O_3 . With the relatively high YS, UTS and ϵ_f , the MHNC- AlN is capable of absorbing large amount of energy before fracture. Both the MHNC- Al_2O_3 and MHNC- AlN are capable of spontaneously strengthening themselves increasingly to a large extent, in response to plastic deformation before the final fracture. It seems that the variation of the nano particle type and sizes has a limited effect on the strain hardening rate of the MHNCs.

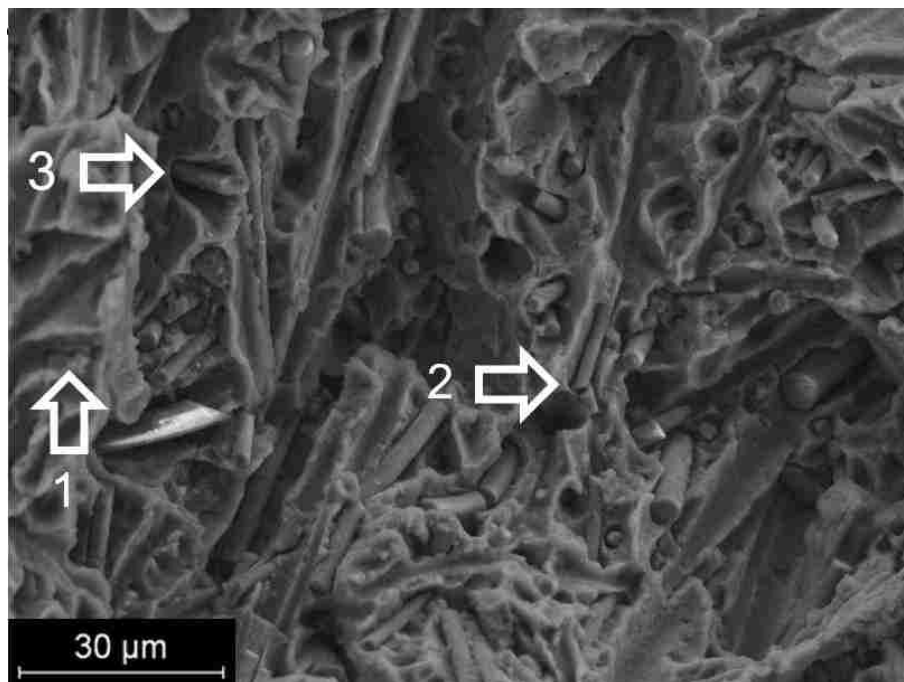
5.3.4. Fractography



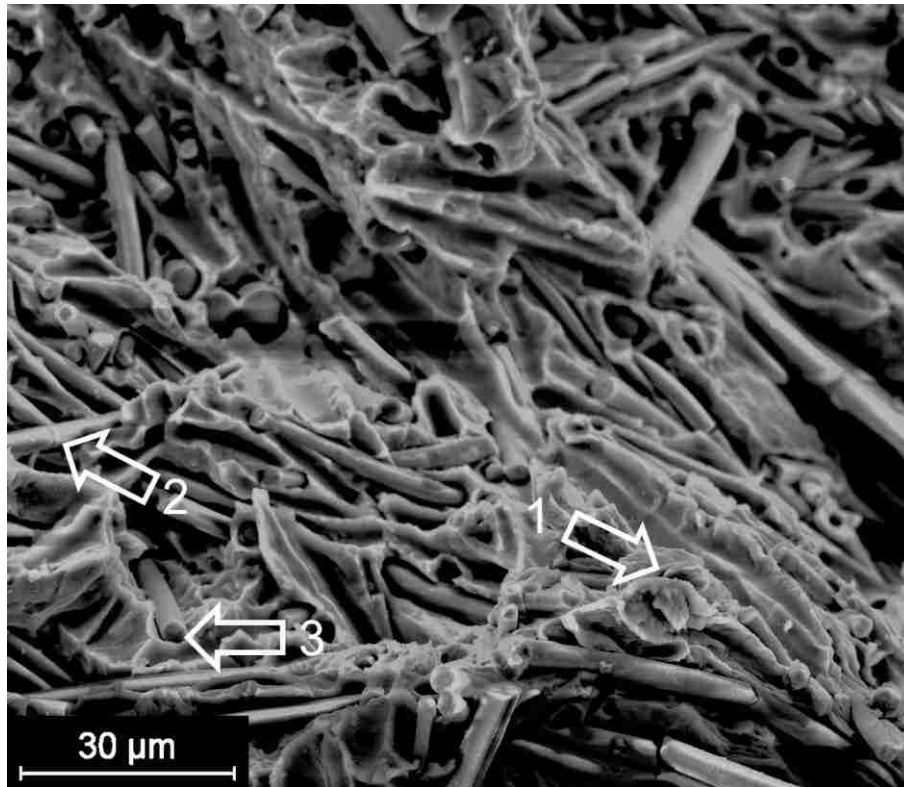
(a)



(b)



(c)



(d)

Figure 5.11. Fractures of AM60, AM60 composites with Al_2O_3 fibres particles (a) AM60 alloy (b) AM60 alloy with 5% fibre (c) AM60 alloy with 5% fibre/ 3% nano Al_2O_3 particles, and (d) AM60 alloy with 5% fibre/ 3% nano AlN particles (arrow 1- matrix crack; arrow 2- fibre crack; arrow 3- debonding).

The SEM fractographs given in Figure 5.11 depict the difference in the fracture modes of the matrix alloy, the fibre-only composite, and the MHNCs. With SEM high magnifications, detailed features of the fracture surfaces are revealed and the fracture behaviours are determined with reference to the tensile properties of the composites reinforced with the different sizes and types of fibre and particles. A typical fracture surface of the matrix is presented in Figure 5.11 (a). The existence of shallow dimples on the surface generally displays ductile behavior, which implies the consumption of a considerable amount of energy in the process of the formation of

micronvoids. The coalescence of microvoids under high tensile loading gives rise to the formation of cracks, eventually leading to failure. The presence of fibre reinforcement and nano-sized particles enables certain amount of tensile loads to be transferred from the matrix alloy to fibre and nano-sized particles. The composites break in a brittle mode different from that of the unreinforced alloy. The final tensile fracture primarily was caused by fibre cracking, as shown in Figure 5.11(b), (c) and (d) due to the inherent nature of the high strength and brittleness of the ceramic fibres. The debonding at the interface between the fibre and matrix as well as the particle and matrix could be another crack initiation area of the composites, which might be attributed to the insufficient infiltration of the molten metal into the close packed network of fibres and particles. Few dimples are found on the fracture surfaces of the fibre-only composite in Figure 5.11 (b). Certain deformation of the matrix alloy is evidently present on the fracture surface of the MHNCs. In general, the results of the SEM observation on the fracture surfaces of the tested materials are in consistent with the tensile data.

5.4. Conclusions

Mg alloy AM60-based hybrid nanocomposites (MHNC) incorporating nano Al_2O_3 or AlN particles with different sizes and micron alumina (Al_2O_3) fibre were successfully prepared by a preform and squeeze casting technique. The optical microstructure analyses of the composites reveal the random orientation and the homogeneous distribution of fibres in the matrix and the refinement of matrix grain structure. It is shown by the SEM observation that both types of nano-sized Al_2O_3 or AlN particles disperse homogenously in the matrix alloy without agglomeration. The TEM analyses indicate that, compared with the micron fibre-only composite, the MHNCs possesses a low or moderate dislocation density, which results from the deficient

thermal strain during matrix solidification due to the presence of nano-sized particles. Among the three types of tested composites, the MHNC- Al_2O_3 exhibits the highest UTS (216 MPa), YS (140 MPa), E (53 GPa), strain hardening rate (8418.6 MPa). The addition of 3 vol.% Al_2O_3 or AlN nano particles restores the elongation of the hybrid composite from 1.6% to 3.5% or 3.6%, respectively. The presence of a low or moderate dislocation density in the MHNCs should be primarily responsible for ductility restoration by nano-sized reinforcements. Due to their high engineering performance and low materials cost, the application of nano Al_2O_3 particles should be considered for the development of advanced automotive components.

5.5. Acknowledgments

The author would like to take this opportunity to thank the Natural Sciences and Engineering Research Council of Canada and the University of Windsor for supporting this work.

5.6. References

- [1] S. Nimityongskul, M. Jones, H. Choi, R. Lakes, S. Kou and X. Li, Grain refining mechanisms in Mg–Al alloys with Al_4C_3 microparticles, *Materials Science and Engineering: A*, 527 (2010) 2104-2111.
- [2] M. Habibnejad-Korayem, R. Mahmudi and W.J. Poole, Enhanced properties of Mg-based nano-composites reinforced with Al_2O_3 nano-particles, *Materials Science and Engineering: A*, 519 (2009) 198.
- [3] H. Liao, J. Chen, L. Peng, J. Han, H. Yi, F. Zheng, Y. Wu, Wenjiang Ding, Fabrication and characterization of magnesium matrix composite processed by combination of friction stir processing and high-energy ball milling, *Materials Science & Engineering A*, 683 (2017) 207–214

- [4] S. Arokiasamy, B. Anand Ronald, Experimental investigations on the enhancement of mechanical properties of magnesium-based hybrid metal matrix composites through friction stir processing, *The International Journal of Advanced Manufacturing Technology* (2017) 1–11
- [5] M.E. Turan, H. Zengin, E. Cevik, Y. Sun, Y. Turen, H. Ahlatci, Wear behaviors of B₄C and SiC particle reinforced AZ91 magnesium matrix metal composites, *International Journal of Chemical, Molecular, Nuclear, Materials and Metallurgical Engineering* , 10 (9) (2016)
- [6] Ramalingaiah, S. Bansal and S. Ray, Microstructure and mechanical properties of cast composite of steel wool infiltrated by magnesium and AZ91 alloy, *Materials and Manufacturing Processes*, 26 (2011) 1173-1178.
- [7] E. Hajjari, M. Divandari and H. Arabi, Effect of applied pressure and nickel coating on microstructural development in continuous carbon fibre-reinforced aluminum composites fabricated by squeeze casting, *Materials and Manufacturing Processes*, 26 (2011) 599-603.
- [8] A. Banerji, H. Hu, A. T. Alpas, Sliding wear mechanisms of magnesium composites AM60 reinforced with Al₂O₃ fibers under ultra-mild wear conditions. *Wear*. 301 (2013) 626-635.
- [9] J. Lo, and R. Santos, Magnesium matrix composites for elevated temperature applications, 2007 Society of Automotive Engineers World Congress, Detroit, MI, 01 (2007) 1028.
- [10] Q. Zhang, and H. Hu, Development of hybrid magnesium-based composites, *Advances in Light Weight Materials-Aluminum, Casting Materials, Magnesium Technologies*, Society of Automotive Engineers World Congress, (2010) 107-114.
- [11] J. Zhou, X. Zhang, L. Fang, H. Hu, Processing and properties of as-cast magnesium AM60-based composite containing alumina nano particles and micron fibres, *Magnesium Technology 2017*, Part of the series *The Minerals, Metals & Materials Series*, 573-578.

- [12] S. Fida Hassan, A. M. Al-Qutub, S. Zabiullah, K. S. Tun, M. Gupta, effect of increasingly metallized hybrid reinforcement on the wear mechanisms of magnesium nanocomposite, *bulletin of materials science*, 39 (4) (2016) 1101–1107
- [13] X. Zhang, Q. Zhang and H. Hu, Tensile behavior and microstructure of magnesium AM60-based hybrid composite containing Al₂O₃ fibres and particles. *Materials Science Engineering A*, 607 (2014) 269-276.
- [14] S.F. Hassan and M. Gupta, Development of high performance magnesium nano-composites using nano-Al₂O₃ as reinforcement, *Material Science Eng. A*, 392 (2005) 163-168
- [15] L. Chen, J. Xu, H. Choi, M. Pozuelo, X. Ma, S. Bhowmick, J. Yang, S. Mathaudhu and X. Li., Processing and properties of magnesium containing a dense uniform dispersion of nanoparticles, *Nature*, 528 (2015) 539-543.
- [16] W. L. E. Wong, M. Gupta, Enhancing the tensile response of magnesium through simultaneous addition of aluminium and alumina nanoparticulates, *Magnesium Technology 2017*, Part of the series, *The Minerals, Metals & Materials Series*, 253-257
- [17] P. J. Karditsas, and M. Baptiste, Thermal and structural properties of fusion related materials, United Kingdom Atomic Energy Authority, Government Division (1995)
- [18] D. Gerlich, S.L. Dole, and G.A. Slack, Elastic properties of aluminum nitride, *Journal of Physics and Chemistry of Solids*, 47(5) (1986) 437-441
- [19] Alumina - Aluminium Oxide - Al₂O₃ - A refractory ceramic oxide, Retrieved August 09, 2017, from <https://www.azom.com/article.aspx?ArticleID=52>
- [20] Properties: Aluminium Nitride / Aluminum nitride (AlN) - properties and applications. (n.d.). Retrieved August 09, 2017, from <https://www.azom.com/properties.aspx?ArticleID=610>

- [21] Q. Zhang, H. Hu, and J. Lo, Solidification of discontinuous Al_2O_3 fiber reinforced magnesium (AM60) matrix composite, *Defect and Diffusion Forum*, 312-315 (2011) 277-282.
- [22] H. Hu, Grain Microstructure evolution of Mg (AM50A)/ SiCp metal matrix composites, *Scripta Materialia*, 39(8) (1998) 1015-1022.
- [23] L. Jiang, G. Wu, K. Norio, and S. Hideo, Effects of sub-micron particles on the matrix microstructure of Al-based composites, *Rare metal materials and engineering*, 36(6) (2007) 1002-1004.
- [24] W. Shi, M. Kobashi, T. Choh, Wettability of molten magnesium on carbon and AlN, *Journal of the Japan Institute of Metals and Materials*, 64 (5) (2000) 335-338.

CHAPTER 6 Conclusions

The conclusions drawn from this study are summarized as follows:

A preform-squeeze casting process has been developed and applied to effectively fabricate magnesium-based fibre and nano-sized particle-reinforced hybrid composites. The preform infiltration method improves the volume fraction limitation of nano-sized particles in the magnesium hybrid nano composites without agglomeration compared to traditional stirring casting method.

The SEM observation on the microstructure reveals that, in the prepared hybrid preform composites, the ceramic fibre and micron/nano particles are homogeneously dispersed. The microstructure analysis of the composites also indicates that both particles and fibres are free of agglomeration, and fibres orientate randomly in the matrix.

The investigation of grain refinement demonstrates that the nano-sized particles could be served as heterogeneous nucleation sites for the primary α -Mg phase, and both fibres and particles could become the heterogeneous nucleation substrate of the eutectic phase of the matrix alloy, which resultantly, decreases the grain size of composite matrix. For the comparison of hybrid composites, nano-sized Al_2O_3 particles shows superior grain size refinement effect than micron-sized Al_2O_3 particles.

The TEM microscopy analysis accompanying by EDS and EELS detection demonstrates that the interfaces between micron-sized Al_2O_3 particles, nano-sized Al_2O_3 particles, nano-sized AlN particles are clean without reinforcement agglomeration and reaction products. The mechanism of the ductility restore phenomena is investigated under high magnification TEM observation. There is almost no dislocation observed in the hybrid composite reinforced with

nano-sized Al_2O_3 particles compared to the micron-sized Al_2O_3 particle-reinforced hybrid composite. With the addition of AlN nano-sized particles, the dislocation is observed in the MHNC owing to their relatively large size, but with a low density. The resultant strength and ductility of the hybrid nano composite with nano-sized AlN particles are similar to those of hybrid nano-sized Al_2O_3 particles composite. The similar tensile results should be attributed to the presence of the low dislocation contribution and the nano-sized pores formed between the nano-sized AlN particles and magnesium matrix alloy due to the relatively poor wettability. However, the inferior high cost of nano AlN particles makes it less attractive than nano-sized Al_2O_3 particles.

The hybrid composite reinforced with 3 vol. % nano-sized Al_2O_3 particles and 5 vol. % Al_2O_3 fibres exhibits improved tensile strengths over those of the matrix alloy. In particular, the yield strength (140 MPa) of the hybrid composite is 73% higher than that of the matrix alloy. The elastic modulus of the micron hybrid composite (54 GPa) shows 33 % improvement over the matrix alloy (40 GPa). Compared with the 6% elongation of the matrix alloy, the composite reinforced by 5 vol.% of the Al_2O_3 micron fibre exhibits only the elongation of 2.2%.

The addition of 3 vol.% of the Al_2O_3 nano particles restores the elongation of the composite from 1.3% to 3.5%. The MHNC- Al_2O_3 gives the UTS of 216 MPa showing an increase of 13% in UTS over the hybrid composite as its YS (140 MPa) and E (53 GPa) are maintained. The MHNC-AlN composite possesses the UTS, YS and E of 210 MPa, 139 MPa, and 51 GPa. It should be pointed out that the substitution of nano-sized Al_2O_3 or AlN particles for the micron ceramic particles restores the elongation considerably from 1.6% of the micron hybrid composite to 3.5% or 3.6% by almost 120% or 125%, respectively.

The determined yield and tensile strengths of the tested materials are in line with the grain size measurements since the grain refinement enhances the materials strengths. Since the tensile properties of the MHNC- Al_2O_3 and MHNC-AlN are very comparable, the sizes of the tested nano particles seems to have a limited effect on the tensile properties of the MHNC, although the nano AlN particles are eight times larger than the nano Al_2O_3 particles. Also, the TEM observation suggests that the presence of the low dislocation density in the MHNC-AlN should be responsible for the resultant tensile strengths, which are comparable to the tensile properties of the MHNC- Al_2O_3 , although the modulus of nano AlN particles is lower than that of nano Al_2O_3 particles. The existence of nano pores in the MHNC-AlN might be beneficial to the deformation for extra strains, while its dislocation density is only at a moderate level which might have a limited effect on ductility. Overall, by taking into consideration of engineering performance and materials cost, the nano Al_2O_3 particles with a relatively low price of appears attractive to the development of automotive applications.

Compared to the ductile fracture of the matrix alloy, the SEM fractography reveals that the fracture of the micron-sized hybrid composites is in brittle mode, and the nano-sized hybrid composites is in relatively ductile mode. The localized damages, i.e., reinforcement cracking, matrix cracking and interface debonding, could be responsible for the tensile fracture of the Mg-based hybrid composites.

CHAPTER 7 Future Work

Because the size of reinforcement for both particle and fibre has a significant influence on the engineering performance and microstructure development of composites, the future work for this study can be classified into the following research areas:

Investigation in corrosion behaviors nano-sized hybrid composite with coating;

Detailed studies on solidification and characterization of the hybrid composites reinforced with nano-sized particles and fibres;

Investigation in wear behaviors of hybrid composites for potential engineering applications;

Development of thermal treatment schemas (T4 and T6), in which the tensile properties of the hybrid composites are optimized.

APPENDIX A

COPYRIGHT RELEASES FROM PUBLICATIONS

Chapter 3

 **Junxiang Zhou** <zhou11m@uwindsor.ca> 2 Jun ☆  

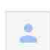


to Permissions ▾

Hello Matt,

The thesis will be produced in hard copy format, and the university will post my thesis online on their website either. Please let me know if I can use my posted paper to my graduation thesis. Thank you very much.

Best Regards,
Junxiang Zhou

...

 **Permissions** <permissions@tms.org> 2 Jun ☆  

to me ▾

Dear Junxiang,

You may include the pre-publication version of your TMS2017 paper in your thesis. This would be the final accepted manuscript, not the published version that is available through Springer. Please be sure to include a footnote with a full citation that indicates where the paper was eventually published.

Let me know if you have any other questions about this.

Best regards,
Matt Baker



Matt Baker | Content Senior Manager
The Minerals, Metals & Materials Society
5700 Corporate Drive Suite 750, Pittsburgh, PA 15237
Direct: [1-724-814-3176](tel:1-724-814-3176) | Fax: [1-724-776-3770](tel:1-724-776-3770) | Toll Free: [1-800-759-4867](tel:1-800-759-4867) (Ext. 280)
mbaker@tms.org | <http://www.tms.org>

Chapter 4

From: eesserver@eesmail.elsevier.com <eesserver@eesmail.elsevier.com> on behalf of MSEA <eesserver@eesmail.elsevier.com>
Sent: August 21, 2017 10:38 AM
To: Henry Hu
Subject: Your Submission MSEA-D-17-03716

Ms. Ref. No.: MSEA-D-17-03716
Materials Science & Engineering A

Dear Professor Hu,

Your manuscript, "As-cast Magnesium AM60-Based Hybrid Nanocomposite Containing Alumina Fibres and Nanoparticles: Microstructure and Tensile Behavior", is being returned to you with a mandatory revision recommendation. It will be considered for publication in MSE A provided that it is revised in accord with any below comments of the reviewer or any additional comments and or corrections in the "Reviewer Attachments".

If you choose to revise your manuscript it will be due into the Editorial Office by the Oct 20, 2017. Please note that this is a strict deadline. Any papers outstanding in the system after this deadline has expired will be withdrawn unless you have contacted the Editorial Office regarding your revised manuscript.

Please submit your revised paper files as well as the "Detailed Responses to the reviewer comments" file, which incorporates all the reviewer comments and your detailed responses to such, at: <https://eeslive.elsevier.com/msea/>

Elsevier Editorial System™

eeslive.elsevier.com

Full-Function Web-Enabled Manuscript Submission and Tracking System for Peer Review

Your username is: huh@uwindsor.ca

If you need to retrieve password details, please go to: http://ees.elsevier.com/msea/automail_query.asp

NOTE: Upon submitting your revised manuscript, please upload the source files for your article. For additional details regarding acceptable file formats, please refer to the Guide for Authors at: <http://www.elsevier.com/journals/materials-science-&-engineering-a/0921-5093/guide-for-authors>

When submitting your revised paper, we ask that you include the following items:

Response to Reviewers (mandatory)

This should be a separate file labeled "Response to Reviewers" that carefully addresses, point-by-point, the issues raised in the comments appended below. You should also include a suitable rebuttal to any specific request for change that you have not made. Mention the page, paragraph, and line number of any revisions that are made.

Manuscript and Figure Source Files (mandatory)

We cannot accommodate PDF manuscript files for production purposes. We also ask that when submitting your revision you follow the journal formatting guidelines. Figures and tables may be embedded within the source file for the submission as long as they are of sufficient resolution for Production. For any figure that cannot be embedded within the source file (such as *.PSD Photoshop files), the original figure needs to be uploaded separately. Refer to the Guide for Authors for additional information.

<http://www.elsevier.com/journals/materials-science-&-engineering-a/0921-5093/guide-for-authors>

When submitting your revised paper, please ensure that the item uploaded as "manuscript" is a clean file which incorporates all the revisions/changes and this should be the final version of the main manuscript text. Please do not include the previous (old) version of your manuscript.

Please ensure that the item uploaded as the "marked up manuscript" is the revised file which contains all the revisions/changes made in highlighted font so that one can easily view the revisions/changes made to your revision.

Click on [Author Login]

On your Main Menu page is a folder entitled "Submissions Needing Revision". You will find your submission record there. Click on 'View Reviewer Attachments' (if present) to access any files uploaded by the reviewers.

Kindly use the above manuscript reference number with all correspondence concerning this paper.

Please note that this journal offers a new, free service called AudioSlides: brief, webcast-style presentations that are shown next to published articles on ScienceDirect (see also <http://www.elsevier.com/audioslides>). If your paper is accepted for publication, you will automatically receive an invitation to create an AudioSlides presentation.

Materials Science & Engineering A features the Interactive Plot Viewer, see: <http://www.elsevier.com/interactiveplots>. Interactive Plots provide easy access to the data behind plots. To include one with your article, please prepare a .csv file with your plot data and test it online at <http://authortools.elsevier.com/interactiveplots/verification> before submission as supplementary material.

Yours sincerely,

Jian Ku Shang
Editor
Materials Science & Engineering A

APPENDIX B

Microstructure Analysis Figures

AM60 (3 vol% micron Al_2O_3 particle +5 vol% fibre)

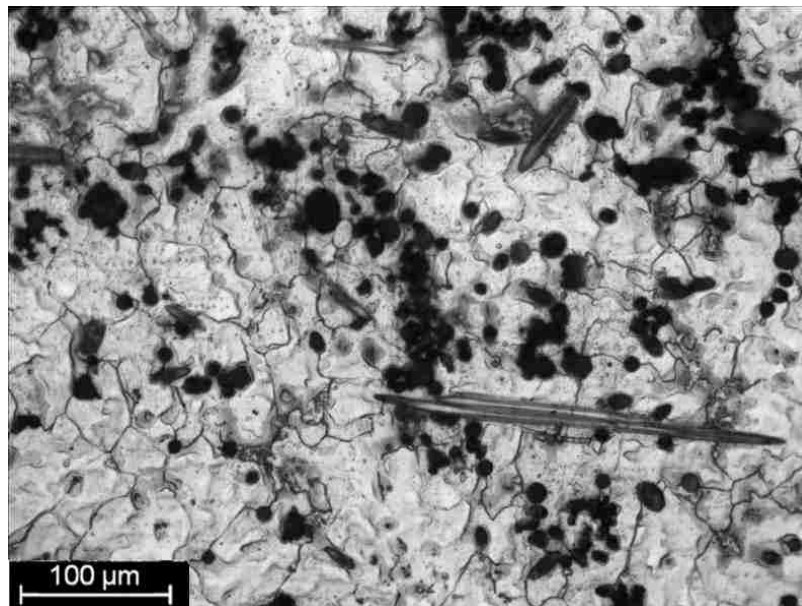
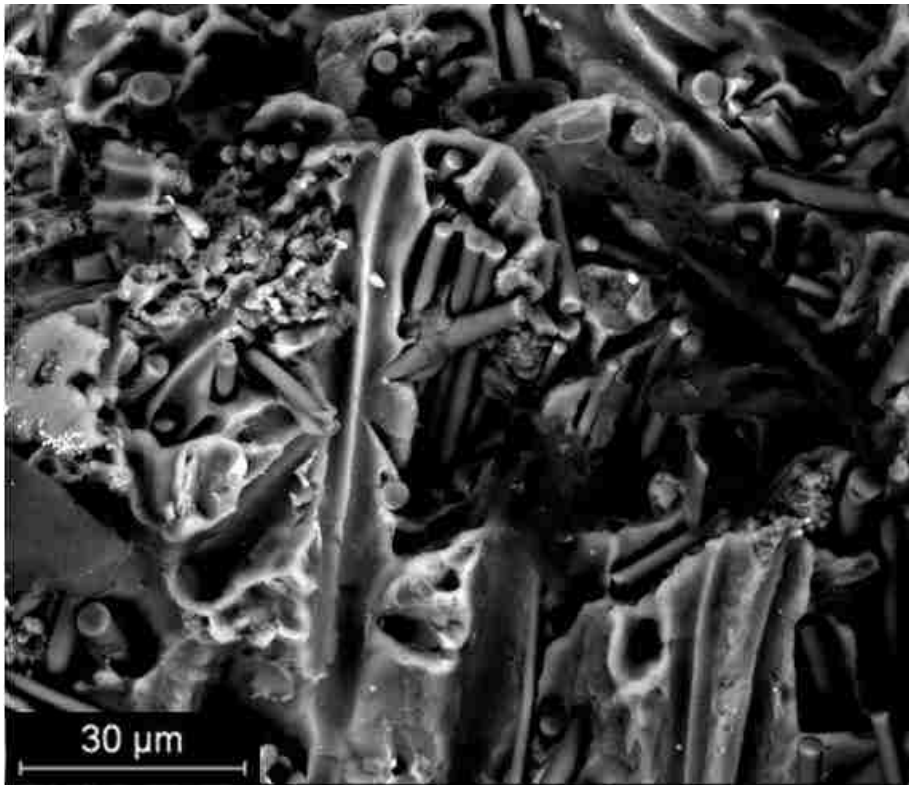
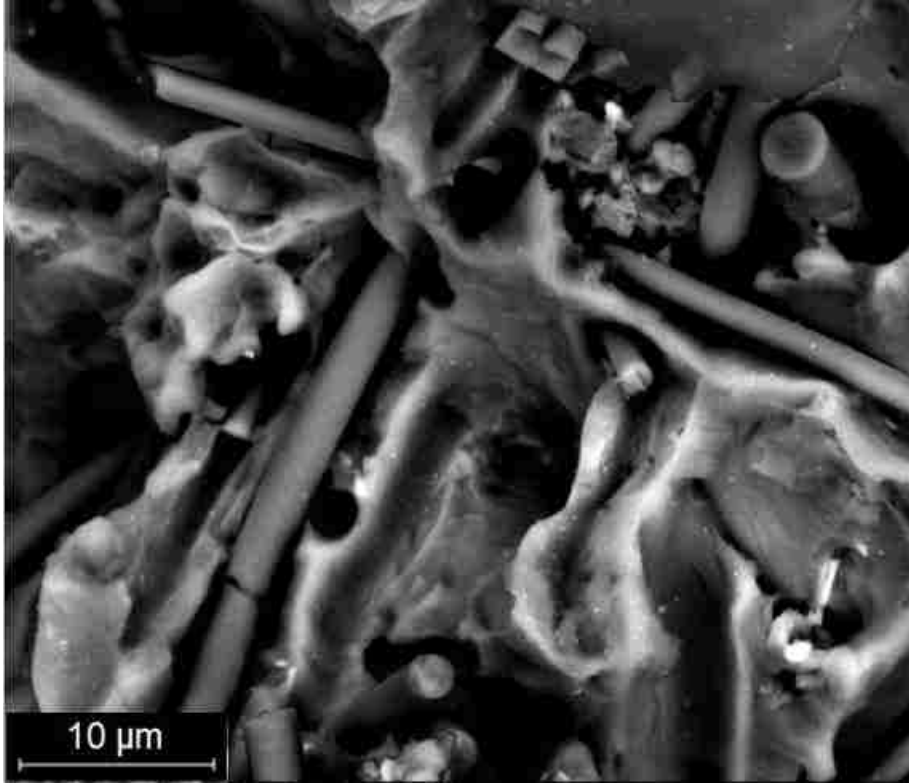


Figure B.1. OM micrographs of (3 vol% micron Al_2O_3 particle +5 vol% Al_2O_3 fibre)/ AM60 composite



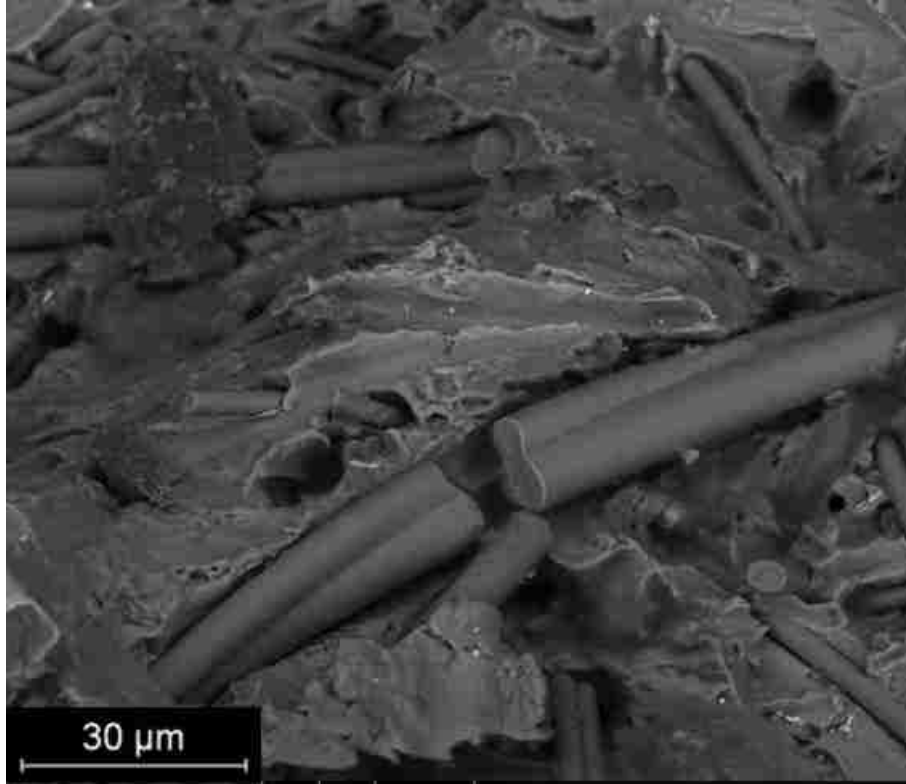
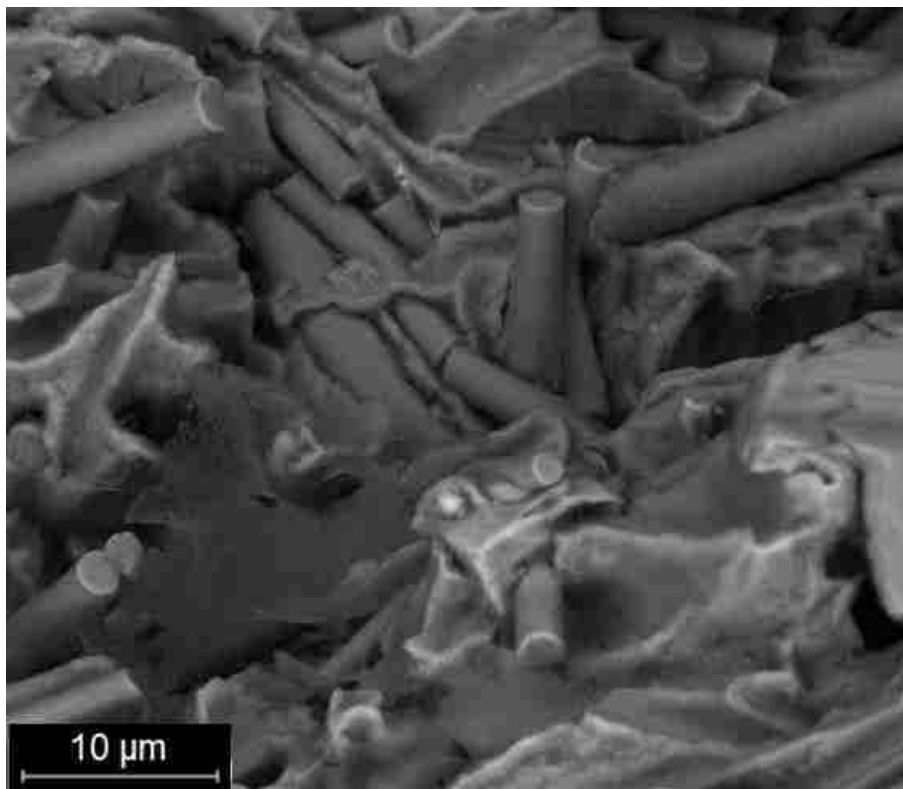
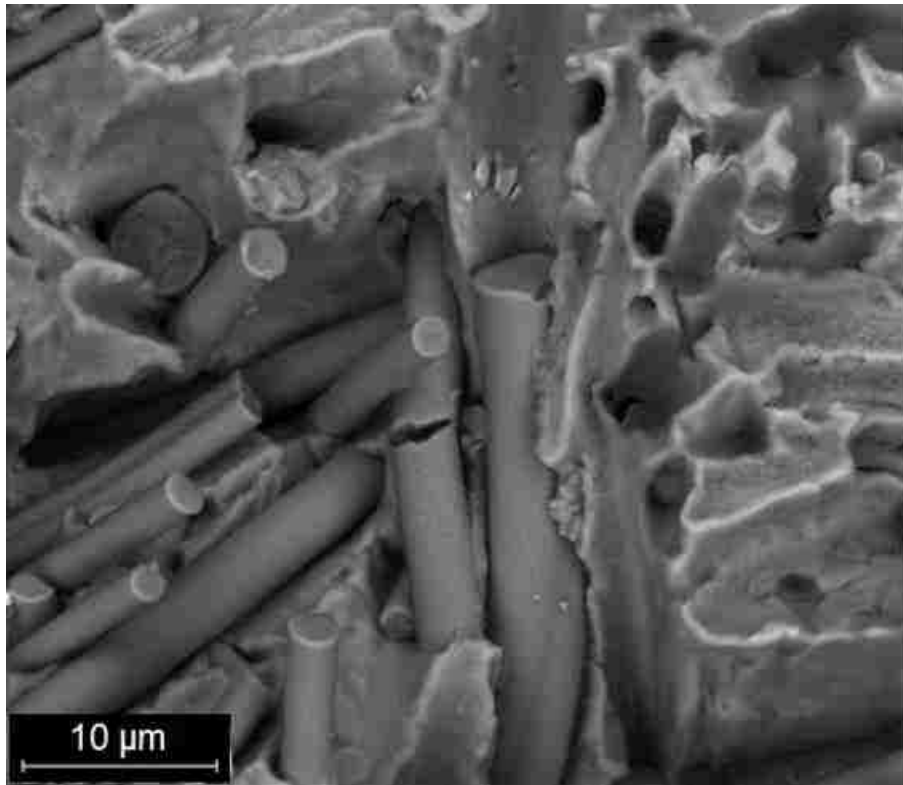


Figure B.2. Fracture of AM60-based composite with 5 vol% Al₂O₃ Fibre + 3 vol% micron Al₂O₃ particle



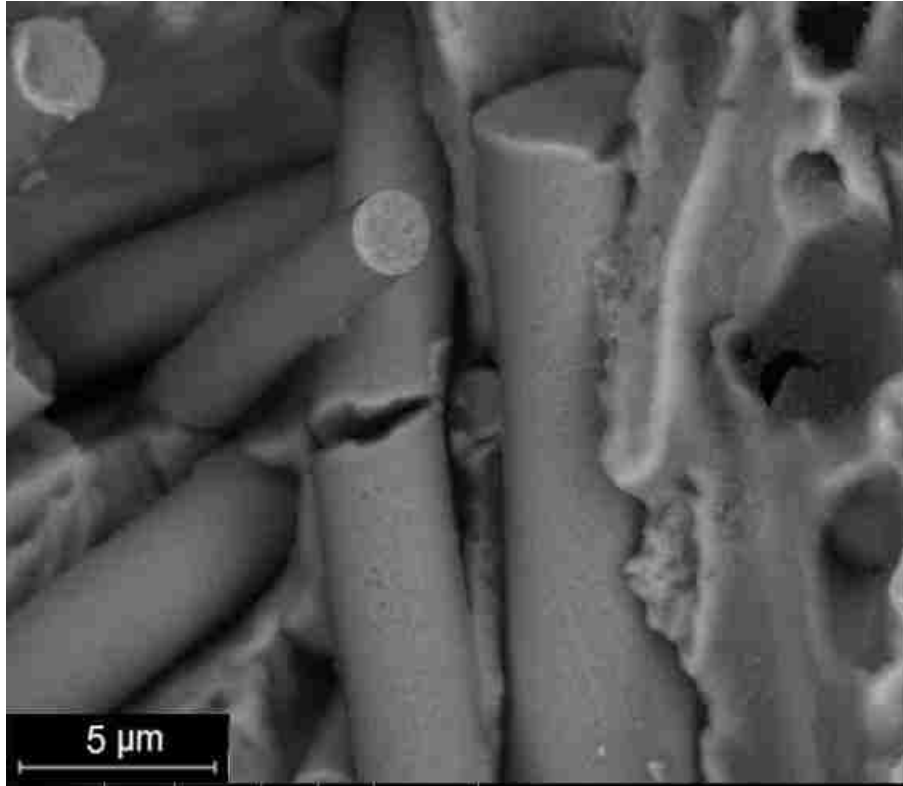


Figure B.3. High magnification fracture of AM60-based composite with 5 vol% Al₂O₃ fibre

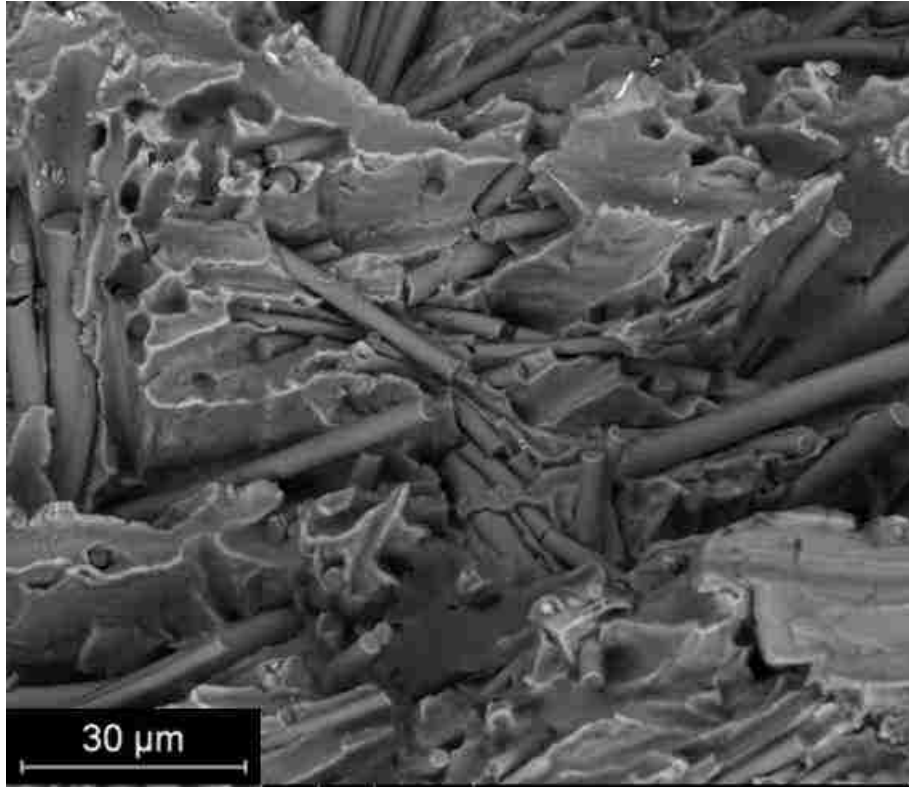


Figure B.4. Fracture of AM60-based composite with 5 vol% Al₂O₃ fibre (Brittle Area)

AM60 (3 vol% nano AlN particle +5 vol% fibre)

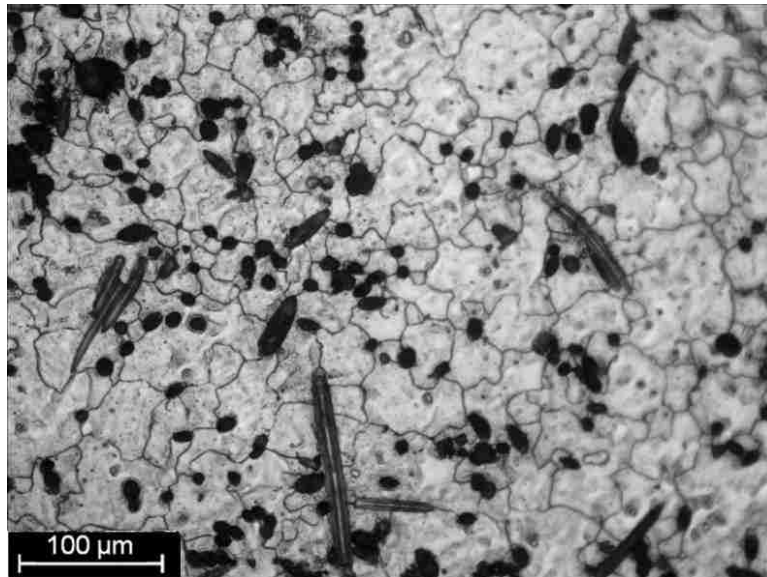


Figure B.5. OM micrographs of (3 vol% nano AlN particle +5 vol% Al₂O₃ fibre)/ AM60 composite

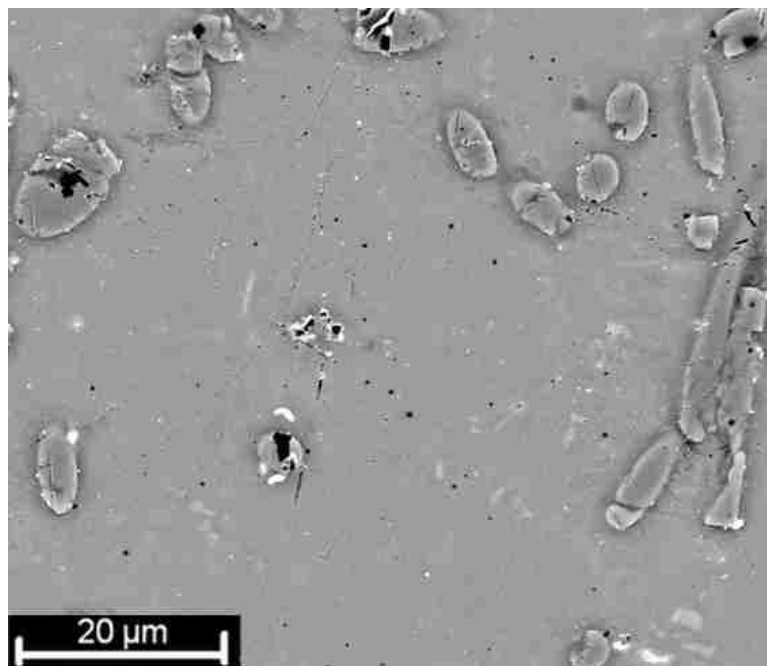


Figure B.6. SEM micrographs in BSE mode showing the reinforcement distribution in (3 vol% nano AlN particle +5 vol% fibre)/ AM60 composite

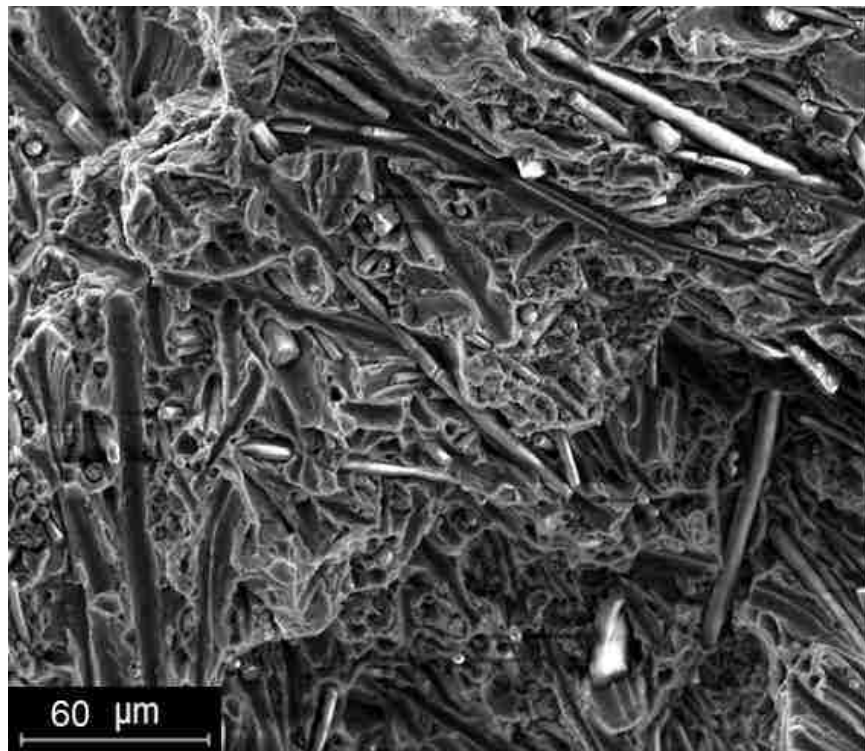
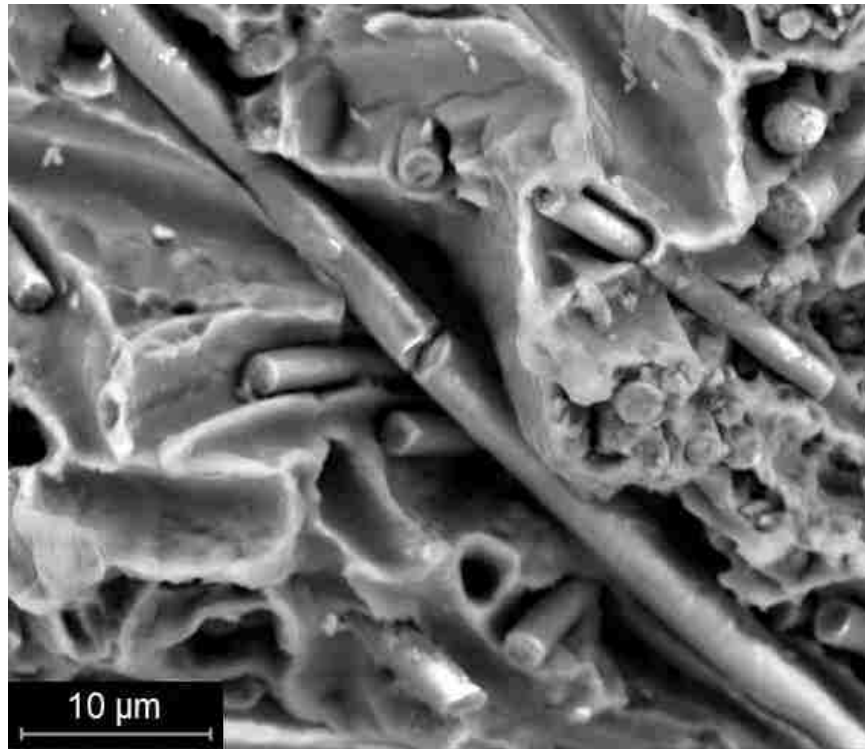


Figure B.7. Fractures of AM60-based composites with 5 vol% Al₂O₃ fibre and 3 vol% nano AlN particles

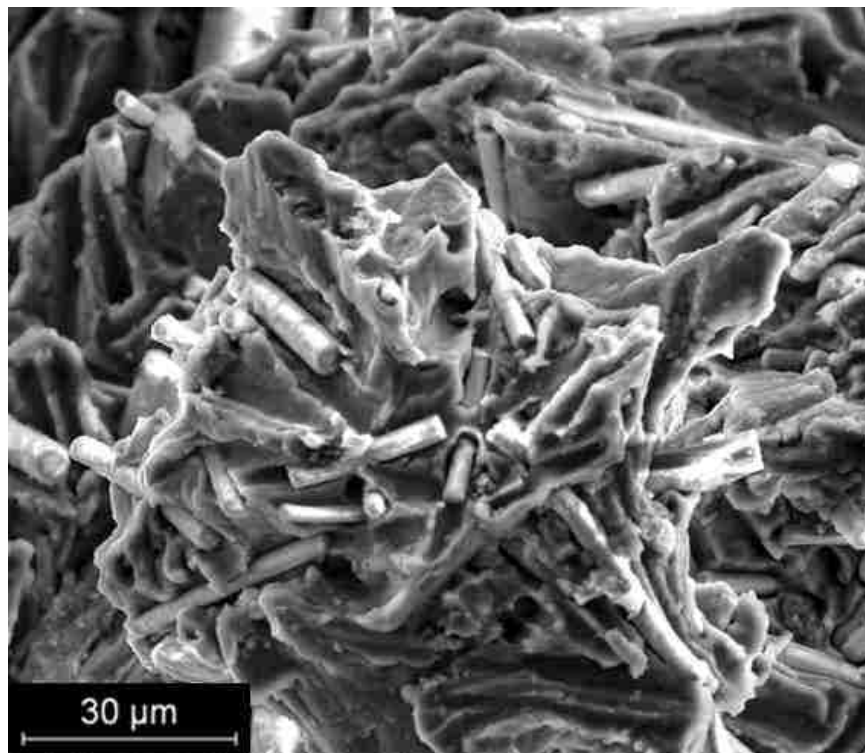
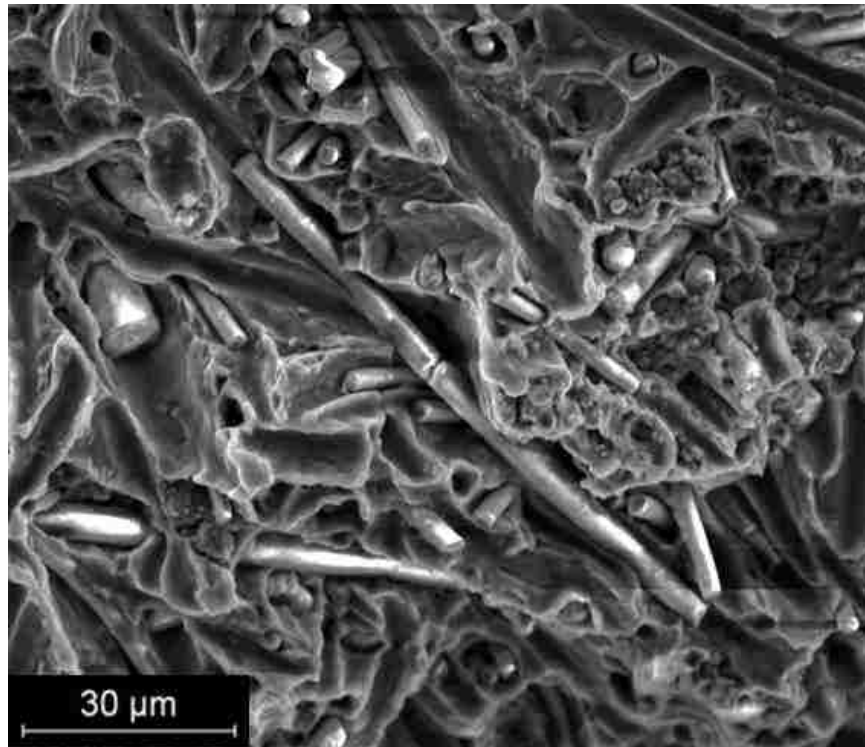


Figure B.8. Fractures of AM60-based composites with 5 vol% Al₂O₃ fibre and 3 vol% nano AlN particles

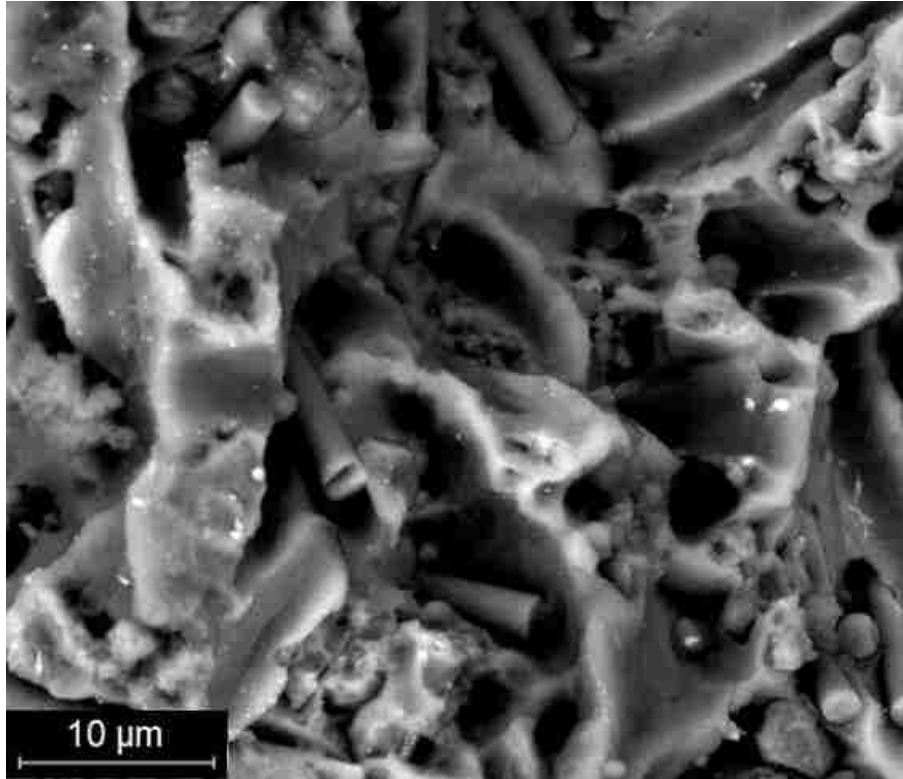


Figure B.9. Fractures of AM60-based composites with 5 vol% Al₂O₃ fibre and 3 vol% nano AlN particles

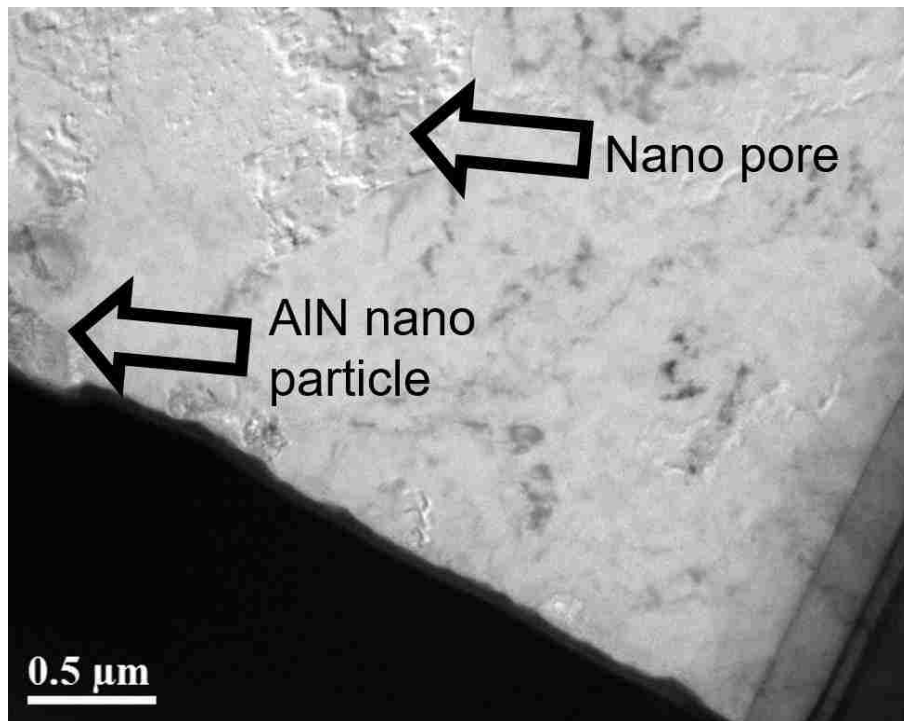
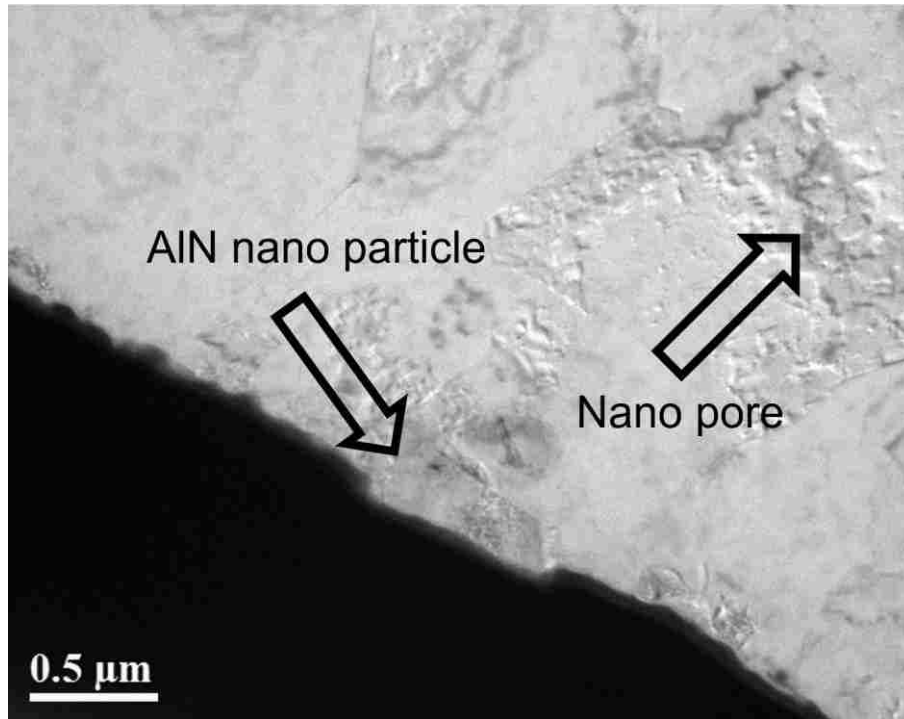


Figure B.10. TEM showing the nano-pores structure in (3 vol% nano AlN particle +5 vol% Al_2O_3 fibre)/ AM60 composite

AM60 (3 vol% nano Al₂O₃ particle +5 vol% fibre)

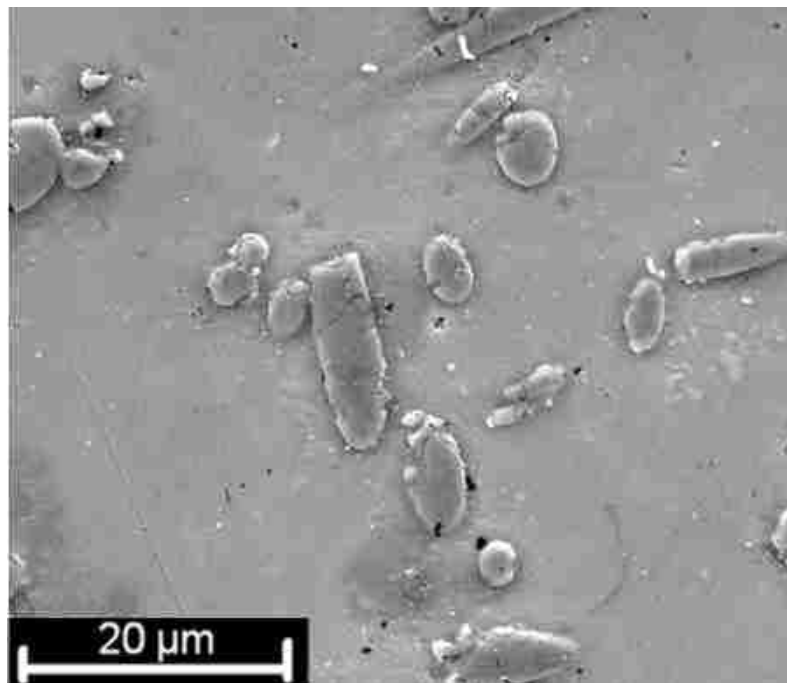
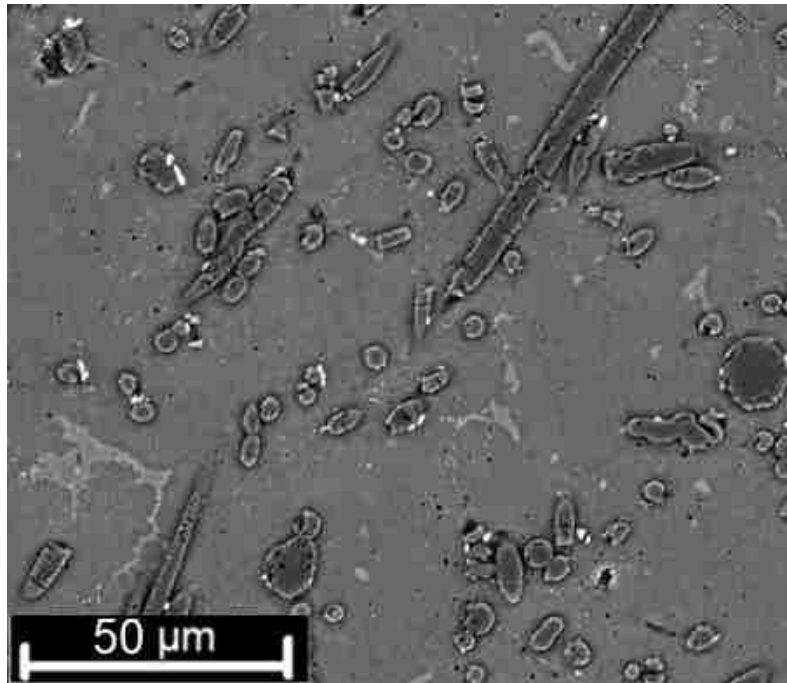


Figure B.11. SEM micrographs in BSE mode showing the reinforcement distribution in (3 vol% nano Al₂O₃ particle +5 vol% Al₂O₃ fibre)/ AM60 composite

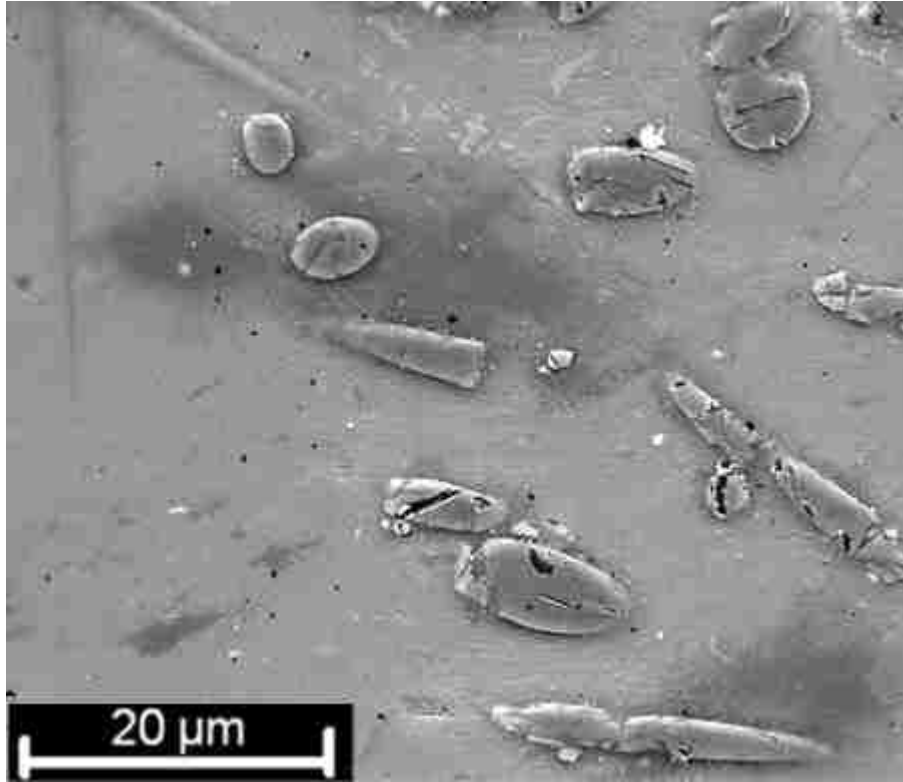


Figure B.12. SEM micrographs in BSE mode showing the reinforcement distribution in (3 vol% nano Al₂O₃ particle +5 vol% Al₂O₃ fibre)/ AM60 composite

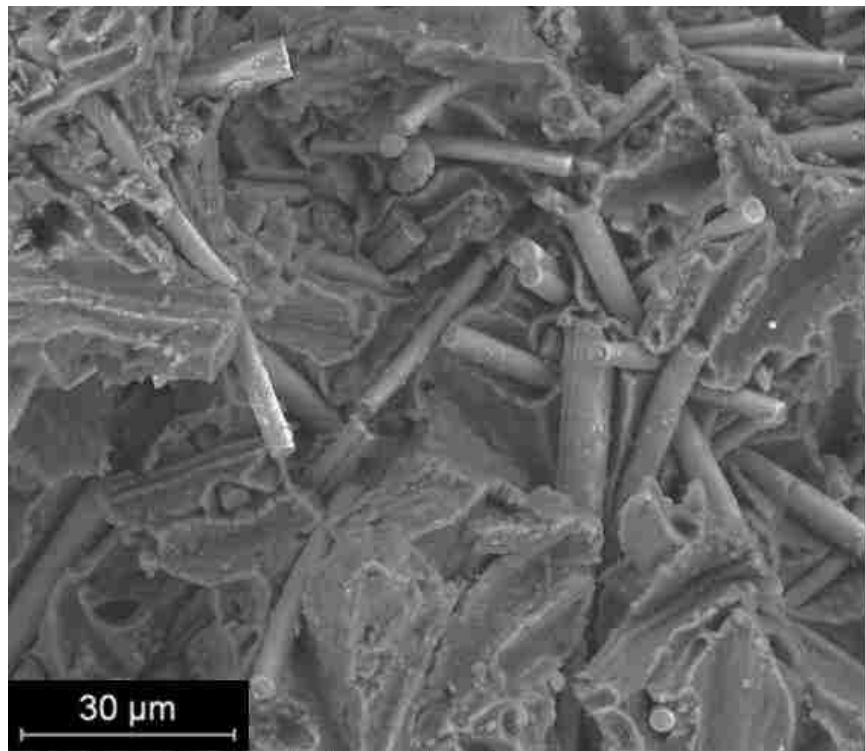
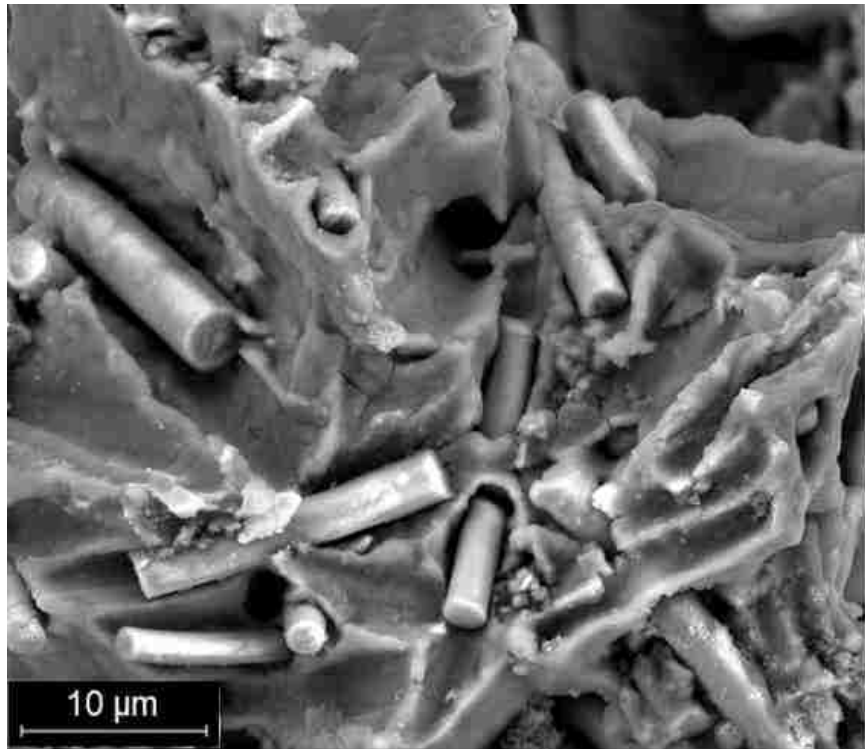


Figure B.13. Fracture of AM60-based composite with 5 vol% Al₂O₃ fibre + 3 vol% nano Al₂O₃ particle

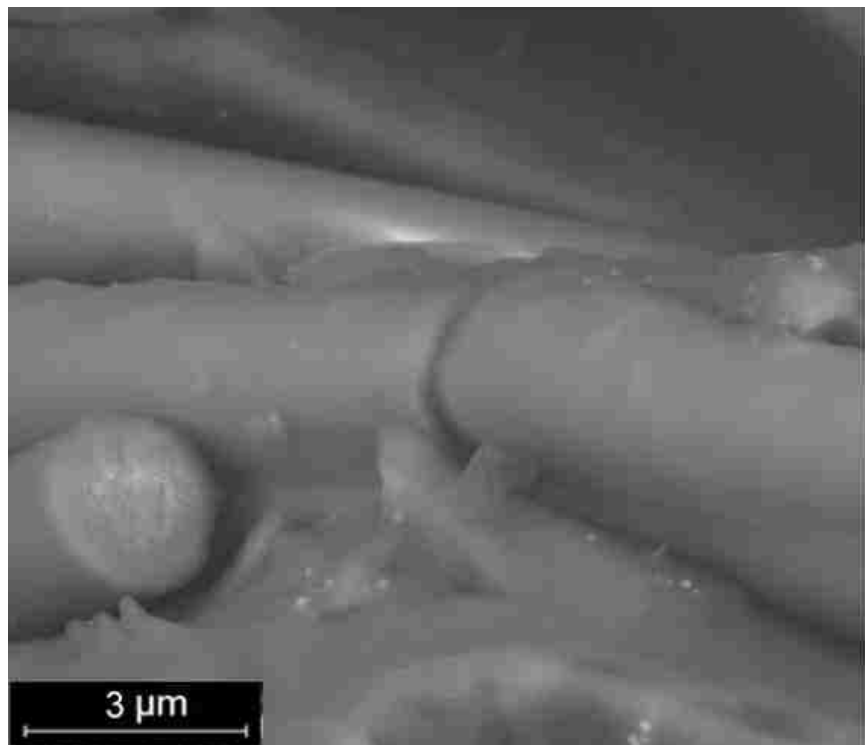
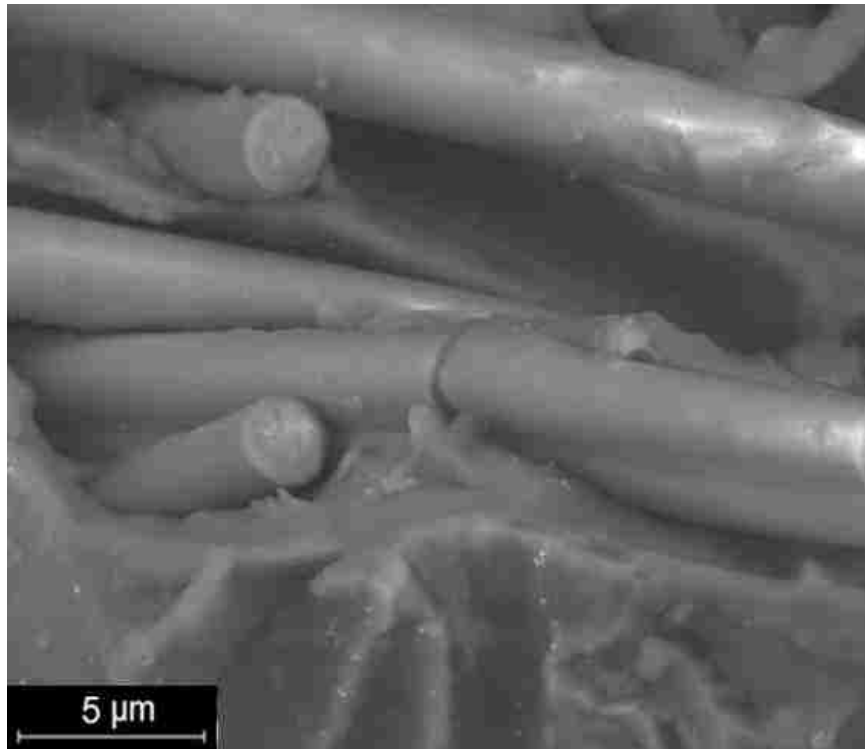


Figure B.14. High magnification fracture of AM60-based composite with 5 vol% Al₂O₃ fibre + 3 vol% nano Al₂O₃ particle

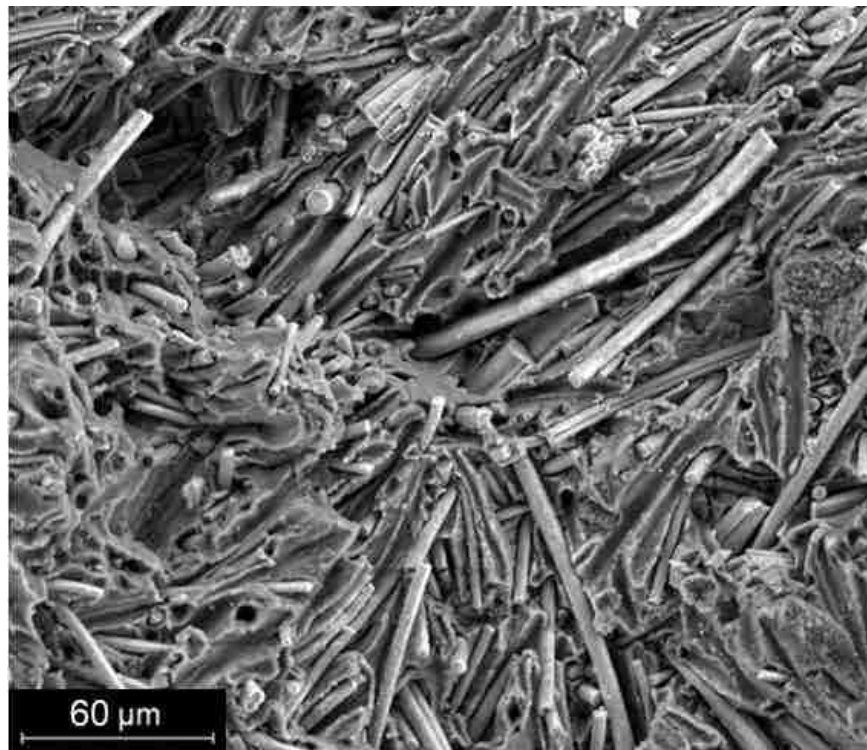
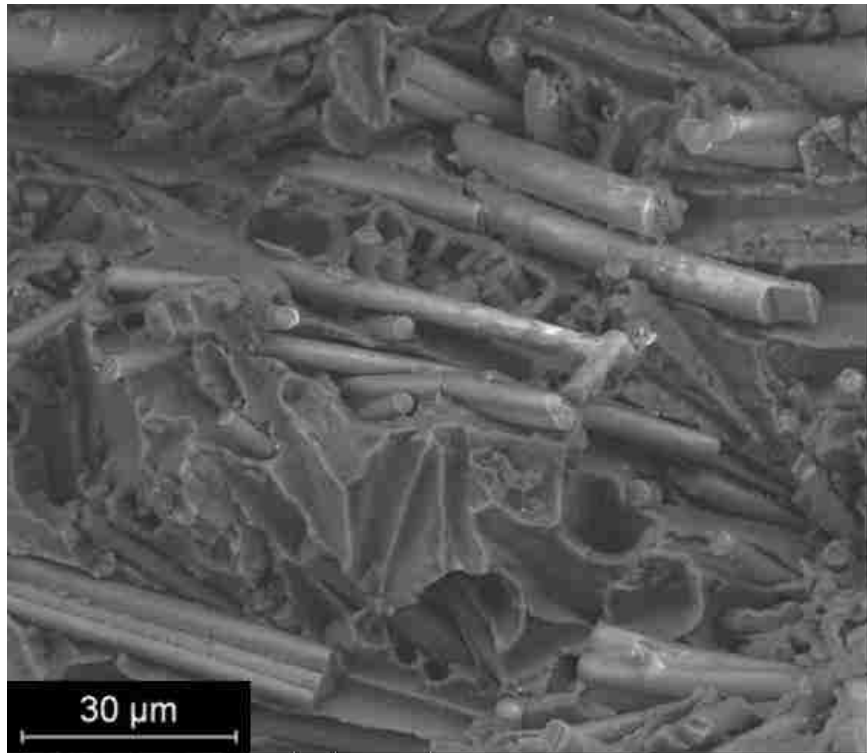


Figure B.15. Fracture of AM60-based composite with 5 vol% Al₂O₃ fibre + 3 vol% nano Al₂O₃ particle

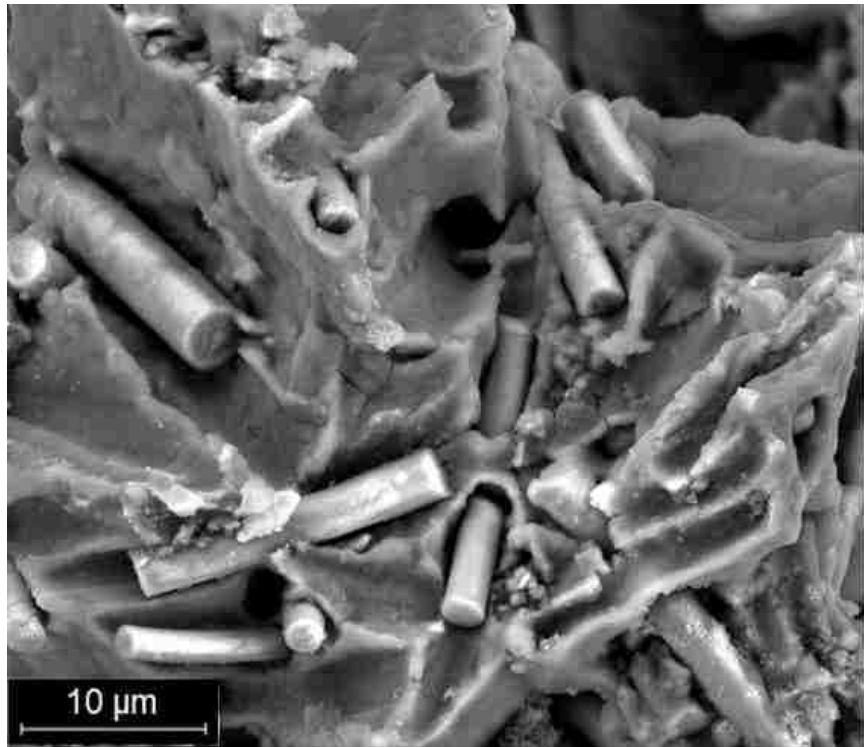


Figure B.16. High magnification fracture of AM60-based composite with 5 vol% Al₂O₃ fibre + 3 vol% nano Al₂O₃ particle

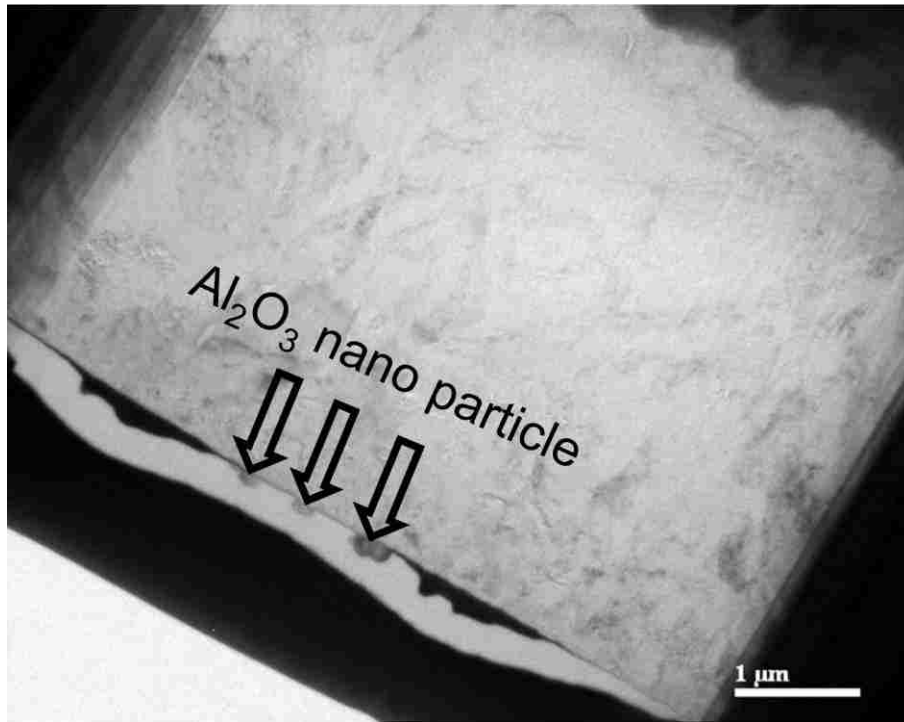


Figure B.17. TEM showing the dislocation-free phenomena in (3 vol% nano Al₂O₃ particle +5 vol% fibre)/ AM60

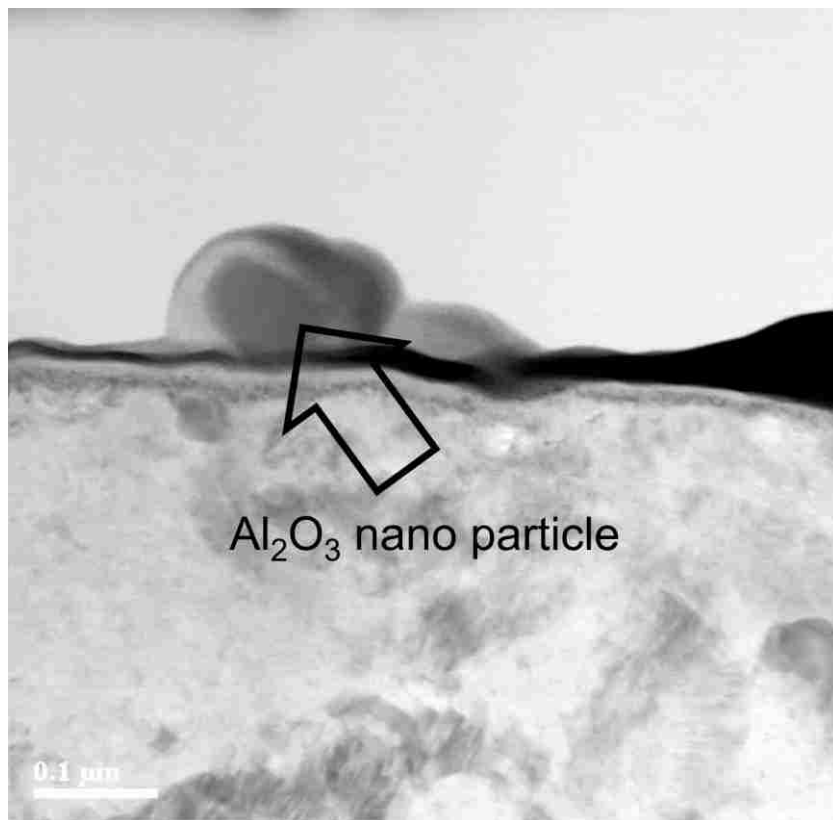
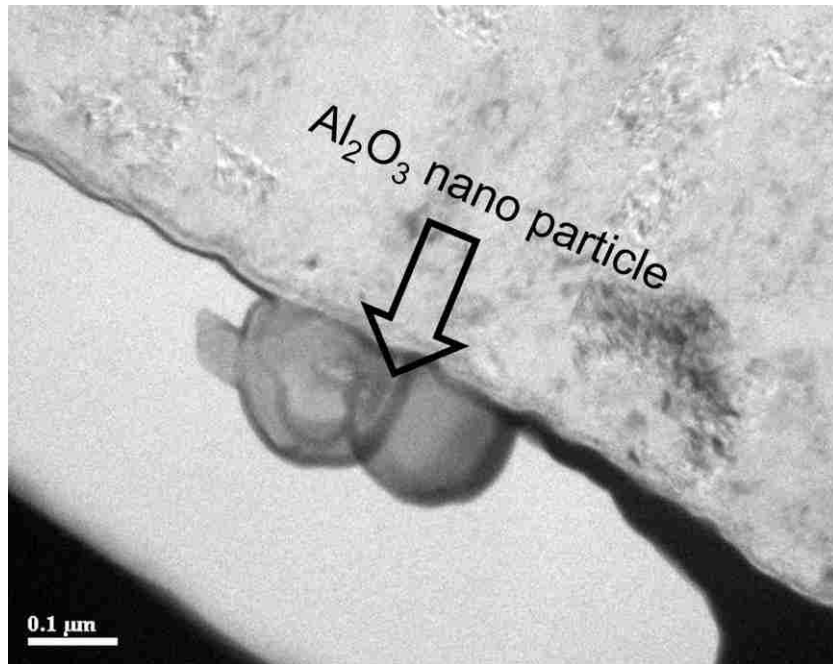


Figure B.18. TEM showing the presence in (3 vol% nano Al₂O₃ particle +5 vol% fibre)/ AM60

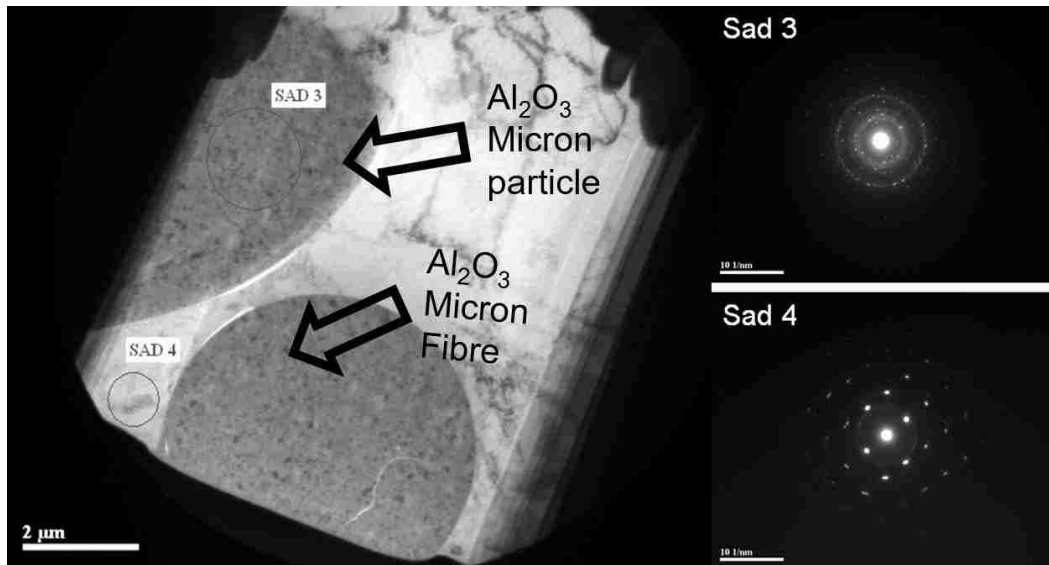


Figure B.19. TEM diffraction pattern showing the difference between the metal matrix AM60 and the micron Al₂O₃ particle

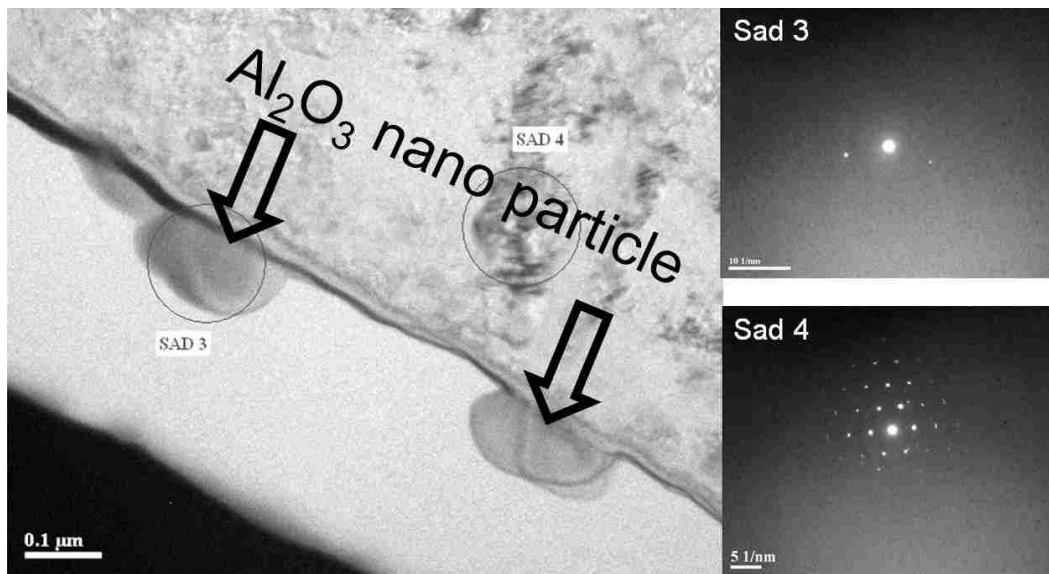
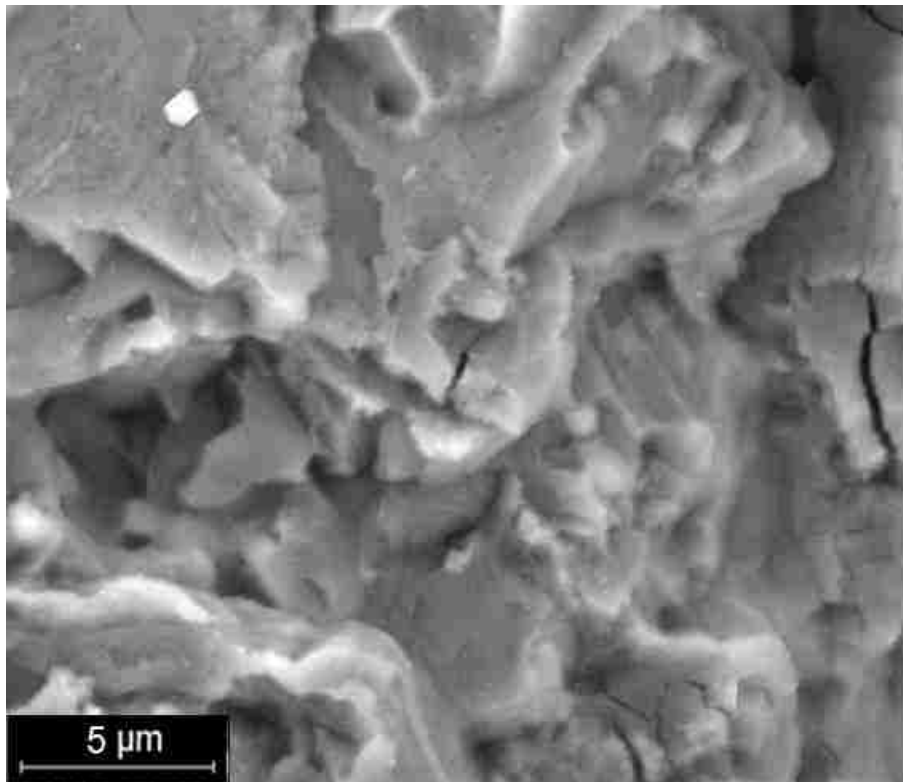
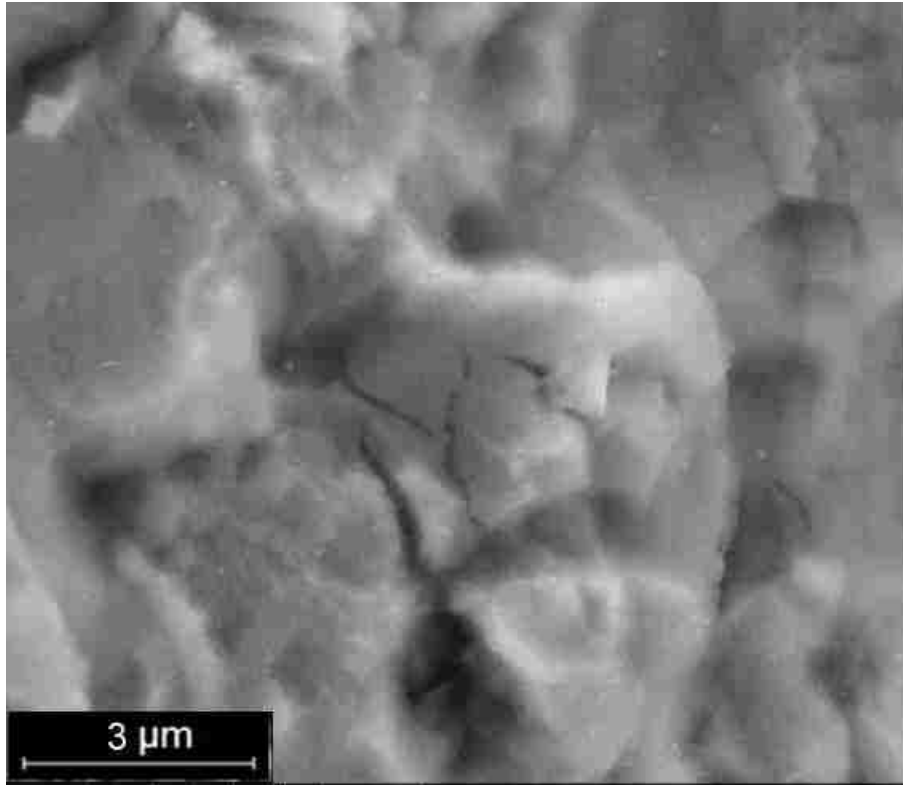
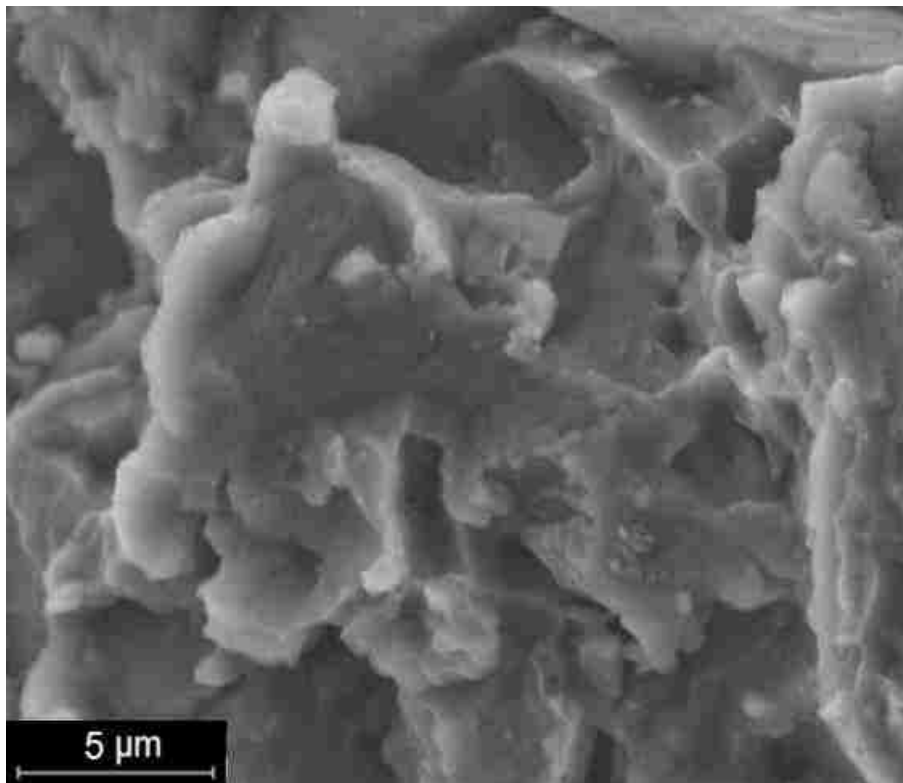
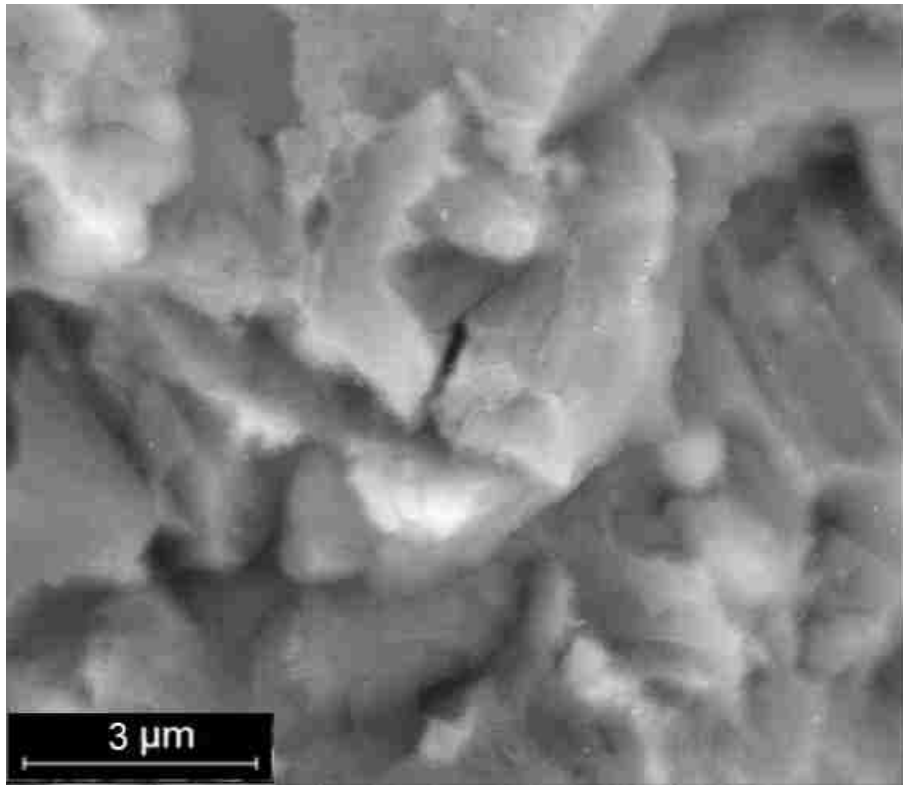


Figure B.20. TEM diffraction pattern showing the difference between the metal matrix AM60 and the nano Al₂O₃ particle

AM60 Alloy





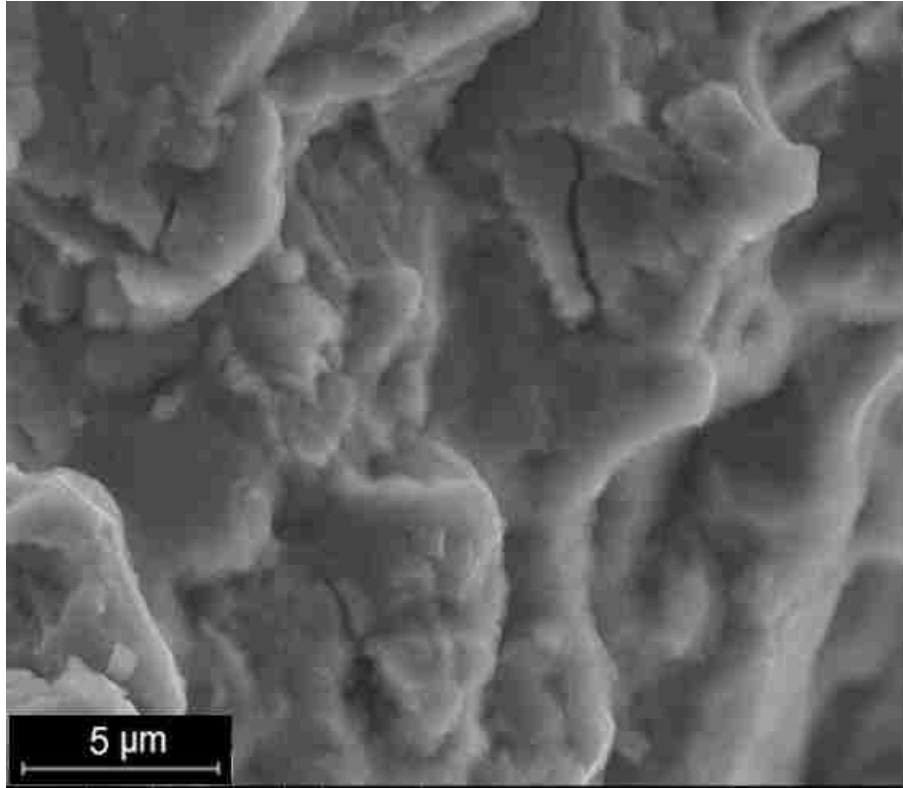


Figure B.21. High Magnification Fracture of AM60 Alloy

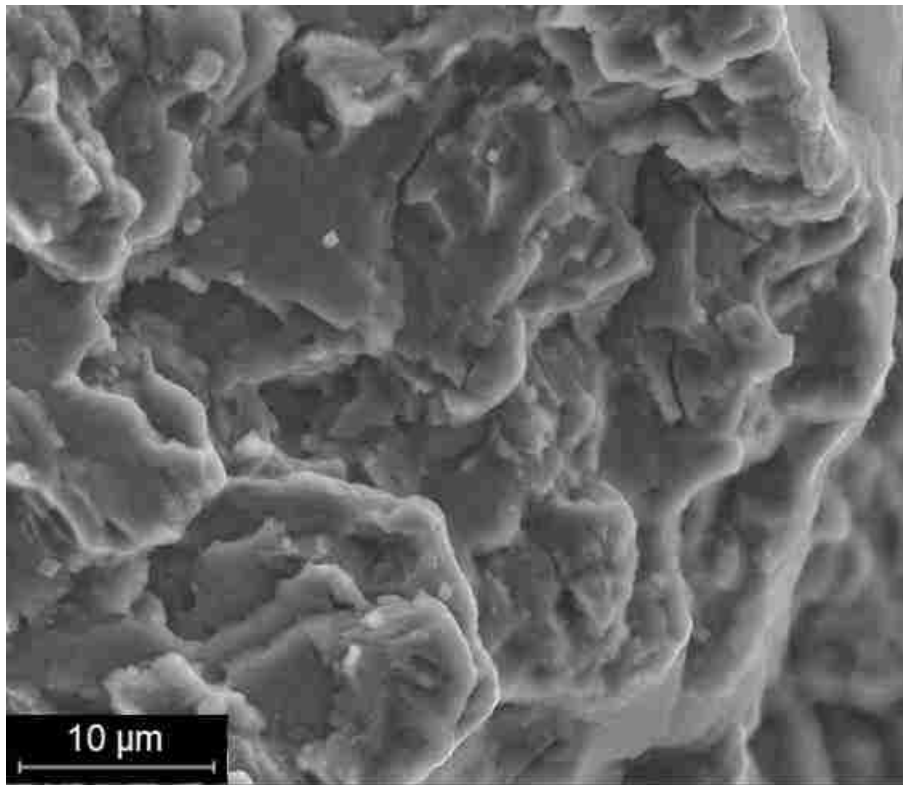
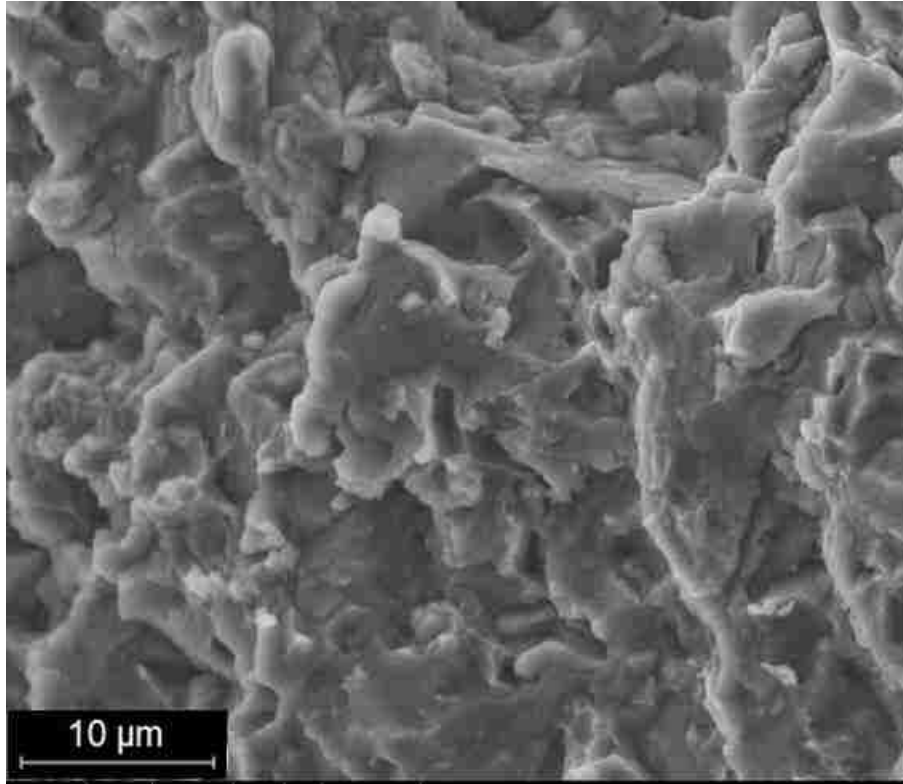


Figure B.22. Fracture of AM60 Alloy

VITA AUCTORIS

NAME: JUNXIANG ZHOU

COUNTRY OF BIRTH: CHINA

DATE OF BIRTH: 1992

EDUCATION: University of Windsor, Windsor, Ontario, Canada

Department of Mechanical, Automotive and Materials Engineering

2011-2015, B.Sc. Honors

University of Windsor, Windsor, On, Canada

Department of Mechanical, Automotive and Materials Engineering

2015-2017, M.Sc.